Sun-Earth Kinematics, the Equation of Time, Insolation and the Solar Analemma

Phil Lucht
Rimrock Digital Technology, Salt Lake City, Utah 84103
last update: January 8, 2013
rimrock@xmission.com

Maple code is available upon request. Comments and errata are welcome.

The graphics look ratty in Windows Adobe PDF viewers when not scaled up, but look just fine in this excellent freeware viewer: http://www.tracker-software.com/pdf-xchange-products-comparison-chart .

Overview

This paper gives an elementary presentation of the kinematics of the earth-sun system with a few basic applications. An interested reader would do well to read the Summary first, to acquire a familiarity with the general thread of the paper and with the symbols used for the variables involved.

The term kinematics refers to the set of variables used to describe the mechanics of the sun-earth system. Much of this paper is concerned with finding expressions for and relations among these variables. One might refer to the way the variables vary in time ("motion") as the dynamics of the earth-sun system characterized by the kinematics.

The paper is almost completely self-contained and derives from scratch precise mathematical expressions for all quantities of interest. The only math required is trigonometry, some geometry, the use of 3x3 matrices, and a basic knowledge of spherical coordinates. A small handful of derivatives and simple one-dimensional integrals are encountered along the way. One first-order differential equation appears in Section 4.

Due to the high historical cost of creating and printing graphics, authors of technical books often short-changed their readers with regard to "figures", having to replace proper detailed drawings with complicated text descriptions of what those drawings would look like. The author of this paper, though hardly an artist, benefits greatly from reasonably precise and well-labeled drawings, and for that reason has produced many of them for this document, even though that increased the file size to several megabytes. Most were quickly created in Visio, though some were cribbed from the web (with reference always given). Our drawings are "line drawings", rather than elaborate renderings of intersecting curved surfaces. A particular graphic trick used several times is the superposition of two screen-clip images in Visio where the front one is made partially transparent, allowing us to compare one of our graphs with another graph found elsewhere.

Finally we come to Maple. The author uses a 1995 version of the Maple computer algebra system that works beautifully and is unencumbered with GUI enhancements. The internal Maple system is deep and powerful and one gets a lot done with a few lines of code (see author's Maple User's Guide). Maple code is readable by a person familiar with any programming language. The main use of Maple in this paper is to graphically display how interesting quantities vary with respect to one or maybe two parameters. The analemmas in the last section were created by generating time-strobed data arrays for analemma coordinates and having Maple plot the data with its pointplot routine. Our Maple code is freely available by email to any interested party (it is presented only in screen-clip form in this document). It will run in the worksheet of the current Maple release, or can be translated into Mathematica, MATLAB, Octave (freeware), etc. It is hard to imagine how "those who went before" investigated things with only hand calculations. It does generate a sense of respect.

- Equation numbers for equations which are repeats of the original equation are italicized.

- Unit vectors are usually marked with a "hat", as in $\hat{\mathbf{x}}$. Exceptions are the $\mathbf{e_n}$ and $\mathbf{e'_n}$ unit vectors.

Summary

This is an abnormally detailed summary which the author feels is useful to introduce the names of the many kinematic variables, and to make visible the meandering thread of the paper.

Section 1 presents the basic facts of the earth's orbit around the sun, then shows how this picture is transformed into one in which the sun apparently orbits the earth. These are the heliocentric and geocentric views of the earth-sun relationship. Three different angular velocities are involved, called $\Omega_{\mathbf{0}}$, ω and $\omega_{\mathbf{s}}$. The earth's rotation axis is tilted by $\theta_{\mathbf{tmax}} \approx 23^{\mathbf{o}}$ relative to the plane of its slightly elliptical orbit which has eccentricity $e \approx .017$ and whose major and minor axes are rotated by an angle $\varphi_{\mathbf{per}} \approx 13^{\mathbf{o}}$ relative to another pair of axes associated with seasonal moments of the year known as solstices and equinoxes. The equation of the ellipse is stated and Kepler's "anomalies" are described.

The basic heliocentric picture is this (Fig 1.3),

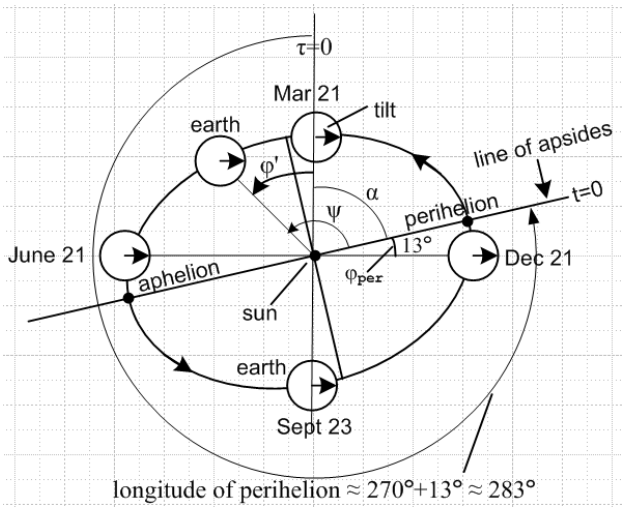

which shows two azimuthal angles φ' and ψ for the earth's position, and another angle α. Angle φ' is measured from March equinox, where time $\tau = 0$, while ψ is measured from the point of closest approach (perihelion) where a different time $t = 0$. The figure shows that

$$\alpha = \pi/2 - \varphi_{\mathbf{per}} \qquad (1.9)$$

$$\varphi' = \psi - \alpha \ . \qquad (1.10)$$

$$t = \tau + t_{\mathbf{Me}} \qquad (7.2)$$

where $t_{\mathbf{Me}}$ is the time it takes for the earth to move from perihelion to March equinox.

Section 2 describes the sun's apparent daily path in the sky at the two solstice and two equinox days of the year, as viewed by an observer at the North Pole. The two equinox paths are the same, so these paths form three circles in the sky which are parallel to the earth's equatorial plane. On any day of the year, there is one circle on which the sun rides, and it lies somewhere between the extremal solstice circles.

Section 3 introduces the celestial sphere as a visualization tool for describing the angular location (declination = latitude, right ascension = longitude) of distant astronomical objects as well as local objects

like the sun and planets whose projections move on this sphere. The three special circular *daily* paths of the sun (solstices and equinox) are projected onto this celestial sphere and also onto the earth, where they become the Tropics of Cancer and Capricorn and the Equator. These three projected celestial sphere paths of the sun are later plotted from the point of view of inhabitants of the earth at different latitudes, using a few lines of Maple code. These abstract circles, when clipped to the local tangent plane of the earth, become the familiar sun paths of everyday life. After a brief discussion of the radius of the celestial sphere, the *annual* path of the sun on the celestial sphere is described, a path known as the ecliptic. The earth's rotation axis precesses slowly and this has implications which are duly noted. Finally, the significance of the Arctic and Antarctic Circles is explained.

Section 4 shows how the angular velocity $\Omega = \dot{\psi}$ of the sun along its elliptical path (and along its circular projected ecliptic path on the celestial sphere) *varies* slightly with sun position due to orbital eccentricity (Kepler's second law). This causes the angular position ψ of the sun to differ slightly from the position of a circular-orbit sun. The azimuthal position $\psi(t)$ is given approximately by (t=0 is perihelion Jan 3),

$$\psi(t) = \Omega_0 t + 2e \sin(\Omega_0 t) + (5/4)e^2 \sin(2\Omega_0 t) \qquad (4.31)$$

which is one of two principle ingredients in the so-called "equation of time".

Section 5 discusses the way the earth's tilt angle toward the sun, called θ_t, varies during the year between $\theta_{tmax} = 23^o$ at June solstice and -23^o at December solstice. At either equinox, $\theta_t = 0$. A physical interpretation of θ_t is developed in which θ_t really is the angle of "earth's tilt toward the sun". This same angle θ_t is in fact the declination of the sun on the celestial sphere ecliptic and is shown to be

$$\theta_t(t) = \sin^{-1}\{ \sin\theta_{tmax} \sin(\varphi')\} = \sin^{-1}\{ \sin\theta_{tmax} \sin(\psi-\alpha)\} . \qquad (5.5)$$

Section 6 obtains expressions for the sun's position on the ecliptic first in Cartesian coordinates $\mathbf{r} = x,y,z$ and then in spherical coordinates R,θ,φ where R is the radius of the celestial sphere and θ,φ are the sun's polar and azimuthal angles on the celestial sphere. Since θ_t is the sun's declination (latitude), $\theta = \pi/2 - \theta_t$. This angle φ (the sun's right ascension) is measured from a certain point on the celestial sphere (March equinox) where $\tau = 0$. Since the ecliptic is tilted on the celestial sphere, angle φ and the angle φ' of Section 1 are not the same and we find that,

$$\varphi(t) = \tan^{-1}[\cos\theta_{tmax} \tan\varphi'(t)] = \tan^{-1}[\cos\theta_{tmax}\tan(\psi-\alpha)] . \qquad (6.13)$$

A "mean fictitious sun" is imagined to exist in the sky which operates with $\theta_t = 0$ (no tilt) and e = 0 (circular orbit). The azimuth of this fictitious sun is shown to be

$$\varphi_f(t) = \Omega_0 t - \alpha . \qquad (6.14)$$

The difference

$$\Delta\varphi = \varphi(t) - \varphi_f(t) \qquad (6.15)$$

is called "the equation of time", which then includes the azimuthal variation effects of both the tilt θ_{tmax} and the eccentricity e. Since $\varphi_f(t)$ is a simple linear function of time t, it can be regarded as time on a clock, and then $\Delta\varphi$ describes the variation of "sun time" from "clock time", which is the real meaning of the phrase "the equation of time" -- it is a temporal correction. Sundials follow $\varphi(t)$, whereas mechanical or electronic clocks follow $\varphi_f(t)$.

Section 7 considers an observer's reference Frame S' which is located on the surface of the earth at colatitude (polar angle) θ_1 and longitude φ_1 east of Greenwich. In the celestial sphere frame of reference, the location of the earth's Frame S' origin is described by a vector **b**(t) which moves (on a cone) because the earth rotates. The polar angle of **b** is θ_1 and its azimuth is $\varphi_b(t)$. This azimuth $\varphi_b(t)$ can be projected out onto the celestial sphere where it becomes in effect the right ascension of the observer site. Since the earth rotates at sidereal rate ω_s, one has

$$\varphi_b(\tau) = \omega_s\tau + \varphi_{b0} \qquad (7.3)$$

where then φ_{b0} is the right ascension the observer site had at the last March equinox $\tau = 0$. The value of φ_{b0} is given by $\varphi_{b0} = \varphi_1 + \varphi_{G0}$ where φ_{G0} is the right ascension that Greenwich had at $\tau = 0$, and this in turn can be obtained from the published GMT time of March equinox. We mention all this detail just to get all the symbols laid out on the table. The sun's position in Frame S' is computed first in Cartesian coordinates **r'** = x',y',z' and then in spherical coordinates R,θ',φ' :

$$\begin{aligned} x' &= R\cos\theta_t \sin(\varphi - \varphi_b) \\ y' &= R\,[\sin\theta_t \sin\theta_1 - \cos\theta_t \cos\theta_1 \cos(\varphi - \varphi_b)\,] \\ z' &= R\,[\sin\theta_t \cos\theta_1 + \cos\theta_t \sin\theta_1 \cos(\varphi - \varphi_b)] \end{aligned} \qquad (7.14)$$

and

$$\begin{aligned} \theta' &= \cos^{-1}[\sin\theta_t \cos\theta_1 + \cos\theta_t \sin\theta_1 \cos(\varphi - \varphi_b)] \\ \varphi' &= \tan^{-1}\left([\sin\theta_t \sin\theta_1 - \cos\theta_t \cos\theta_1 \cos(\varphi - \varphi_b)\,] / [\cos\theta_t \sin(\varphi - \varphi_b)] \right) . \end{aligned} \qquad (7.29)$$

In these equations, θ_t and φ are given by (5.5) and (6.13) quoted above.

Section 8 replaces the azimuth φ' in (7.29) with $\Phi' = \pi/2 - \varphi'$ so the second of equations (7.29) describing the sun's azimuthal position in Frame S' becomes

$$\begin{aligned} \Phi' &= \pi + \tan^{-1}\left([\cos\theta_t \sin(\varphi_b - \varphi)] / [-\sin\theta_t \sin\theta_1 + \cos\theta_t \cos\theta_1 \cos(\varphi_b - \varphi)\,]\right) \\ \Phi'_f &= \pi + \tan^{-1}\left([\sin(\varphi_b - \varphi_f)] / [\cos\theta_1 \cos(\varphi_b - \varphi_f)\,]\right) \quad . \end{aligned} \qquad (8.3)$$

where the second line is for the fictitious sun. For northern hemisphere observers at latitude above 23^o, Φ' is an azimuth that "runs with the sun" at all times of the year, and solar noon always occurs at $\Phi' = \pi$ which is "due south" in Frame S'. At the North Pole ($\theta_1 = 0$), we find

$$\Delta\Phi'^{NP} \equiv \Phi'^{NP} - \Phi_f'^{NP} = -(\varphi - \varphi_f) = -\Delta\varphi \quad . \qquad (8.6)$$

At the north pole, Φ' "runs with the sun" while $\Phi_{\mathbf{f}}$ "runs with the clock" and their difference is again the equation of time, albeit negated. The notions of Local Mean Time (LMT) and Local Sundial Time (LST) are defined, and we arrive then at our version of the "official" equation of time,

$$EOT(t) \equiv [LST - LMT]^{\mathbf{minutes}} = -(720/\pi)\{\tan^{-1}[\cos\theta_{\mathbf{tmax}}\tan(\psi-\alpha)] - (\Omega_{\mathbf{0}}t-\alpha)\}. \qquad (8.16)$$

LST varies from LMT by a maximum of about 15 minutes during the year.

Section 9 uses the equations developed above to compute the Local Mean Time (LMT) of (actual sun) noon and midnight in Frame S' on any day of the year. Similarly, the times of sunrise ($t'_{\mathbf{sr}}$) and sunset ($t'_{\mathbf{ss}}$) are obtained relative to noon, so the nominal length of day equals $t'_{\mathbf{ss}} - t'_{\mathbf{sr}}$, with time of day*light* being up to 8 minutes longer (ball park). The Frame S' azimuth for sunrise ($\varphi'_{\mathbf{sr}}$) is computed and plotted for different latitudes and days of the year. Finally, an expression is found for the noontime elevation of the sun. These results are:

$$LMT(\text{noon}) = [12{:}00 + (720/\pi)\Delta\varphi] \bmod 24 \qquad (9.5)$$
$$LMT(\text{midnight}) = [00{:}00 + (720/\pi)\Delta\varphi)] \bmod 24\ . \qquad (9.6)$$

$$t'_{\mathbf{sr}} = -(1/\omega)\cos^{-1}[-\tan\theta_{\mathbf{t}}\cot\theta_{\mathbf{1}}] \quad < 0 \quad \text{// sunrise}$$
$$t'_{\mathbf{ss}} = +(1/\omega)\cos^{-1}[-\tan\theta_{\mathbf{t}}\cot\theta_{\mathbf{1}}] \quad > 0 \quad \text{// sunset} \qquad (9.15)$$
$$t_{\mathbf{day}} = 2\,t'_{\mathbf{ss}} = (24/\pi)\cos^{-1}[-\tan\theta_{\mathbf{t}}\cot\theta_{\mathbf{1}}] \text{ hours} \qquad (9.16)$$

$$\tan\varphi'_{\mathbf{sr}} = (\tan\theta_{\mathbf{t}}/\sin\theta_{\mathbf{1}}) / \sqrt{1 - \tan^2\theta_{\mathbf{t}}\cot^2\theta_{\mathbf{1}}} \qquad (9.17)$$

$\theta_{\mathbf{1}}+\theta_{\mathbf{t}}$ range:	0	$\pi/2$	π	
$\theta^{\mathbf{el}}_{\mathbf{noon}} =$:	no noon	$\theta_{\mathbf{1}}+\theta_{\mathbf{t}}$	$\pi - (\theta_{\mathbf{1}}+\theta_{\mathbf{t}})$	no noon

(9.20)

These expressions are approximations which assume (correctly) that $\theta_{\mathbf{t}}(t)$ and $\Delta\varphi(t)$ vary slowly during a day so one can approximate these functions at precision time t by their computed values at the start of a day of interest.

Section 10 is concerned with the amount of solar energy per second loaded into a square meter of black ground on the earth (insolation) as a function of latitude and time. If the solar power flux is S watts/m^2, then the amount captured by that black square meter of ground is Scosθ', a fairly trivial fact known as Lambert's Law (θ' is the polar angle of the sun given by the first of equations (7.29) above). Daily insolation is Scosθ' averaged over a day, while annual insolation is this same quantity averaged over a year. Various plots are generated by Maple code and are then compared with other references. The same approximation mentioned in the previous paragraph is used in this insolation work.

Section 11 introduces an imaginary sphere called the sun sphere which is a version of the celestial sphere which rotates once a year such that the mean fictitious sun remains at a fixed point on the sun sphere all year long. The actual sun then moves in a pattern in the neighborhood of this fixed point on a path that is called the solar analemma. A qualitative description of the analemma viewed from various locations is presented. The analemma path can be exposed by the use of stroboscopic photography of the real sun wherein a multiple exposure image is accumulated over the period of a year by taking a heavily filtered

exposure at the same time each day (or every n^{th}day) in the general direction of the fictitious sun's fixed point. The path that is the analemma is computed in a few dozen lines of Maple code in both angle-space (θ',Φ') and in the screen-space (x_s,y_s) of the film in the camera. An analemma "gallery" then presents Maple-computed images of the analemma as it would appear shot from various positions in the northern hemisphere. The final section treats a certain Crimean-shot analemma as a case study, and the computed analemma is compared with the one captured on film.

Appendix A describes a special arctangent function implementation which returns a well-defined result in the range 0 to 2π and introduces the special notation $\tan^{-1}([y] / [x])$. This notation is used in the second line of (7.29) above and the corresponding function is implemented in Maple for evaluation of φ'. Several other arctangent functions are also considered and are then compared on a branch diagram.

Appendix B discusses the active and passive views of the rotation of a vector.

Appendix C studies the shape of the analemma for a circular-orbit earth. It is shown to be symmetric in both directions, and in the limit of small θ_{tmax} it becomes a curve known as the lemniscate of Gerono.

Appendix D develops a chart to show how much a photographed analemma will be tipped left or right on the film, assuming a camera platform whose pointing direction is set by certain tilt and pan angles.

The final section contains a few **References**.

1. Geometry of the Earth's Orbit

(a) The Heliocentric Picture

The following "heliocentric" (sun-centered) camera view of the earth's orbit is taken from above the earth's orbital plane, in the sense that the earth's north pole is up, and the camera is elevated perhaps 30 degrees above that plane. Note the basic fact that the earth rotates about its axis in the same sense that the earth rotates around the sun: both rotations are counterclockwise viewed from above. This is why the noon-to-noon day is a little longer than the sidereal (relative to stars) day. Starting at noon, after rotating one sidereal day the earth has to rotate an extra 4 minutes to reach noon again because the earth has moved ahead a bit in its orbit. The average noon-to-noon day (mean solar day) is exactly 24 hours (by definition), whereas the sidereal day is about 23 hours and 56 minutes (≈ 23.93447). A sidereal year is 365.25 mean solar days long (365.256363004 in 2000), and is the time for the earth to completely traverse its orbit, returning to its starting point relative to the distant stars. Since time is now based on an atomic standard, and since the earth has tiny variations in its rotational speed, the mean solar day might vary from 24 hours by 1 second per year (called a leap second), but we ignore this 10^{-8} fine detail.

The sun is located at one of the two focal points of the earth's elliptical orbit. The distances for closest approach (perihelion) and farthest (aphelion) are stated in millions of km.

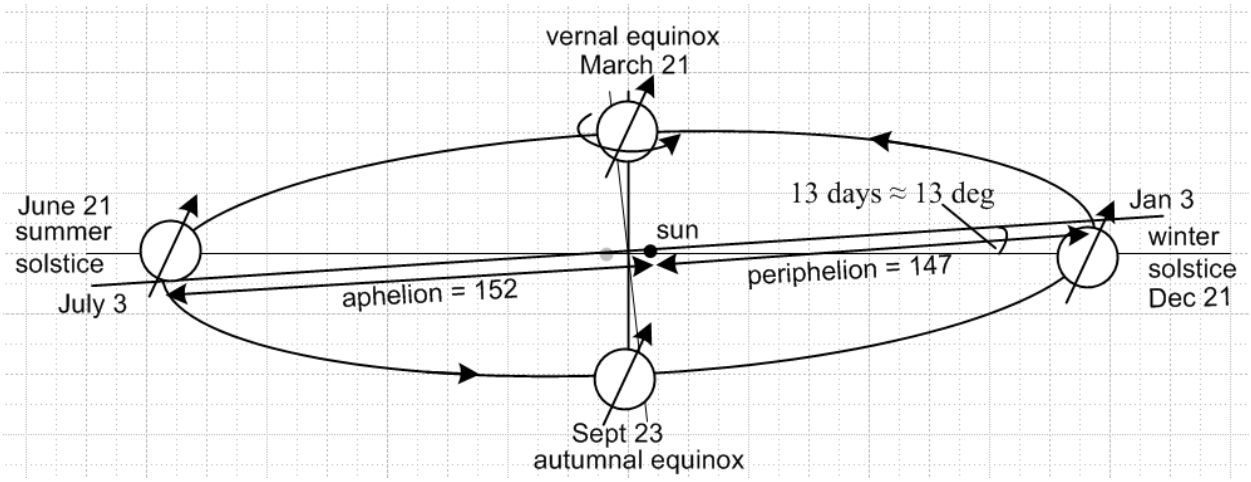

Fig 1.1

The slanted arrows indicate the angular momentum vector of the rotating earth. The times of the year when this tilt arrow points toward or away from the sun are called solstices, and the times at which the arrow points neither toward nor away from the sun are called equinoxes. When the arrow tilts toward the sun, earth inhabitants in the northern hemisphere experience "summer". At the summer solstice, the mean daily insolation reaches a maximum (but not close to the equator), as we show in some detail in Section 10. This is basically due to the fact that the sun is close to overhead much of the time during the day. At the same time, the insolation reaches a minimum in the southern hemisphere, so Argentineans experience winter.

In hemisphere-neutral language, it is best to refer to "December solstice" and "June solstice", and as well "March equinox" and "September equinox". The term "vernal equinox" is heavily embedded into astronomy literature meaning the March equinox, though it is not verdant spring in Argentina at that time.

The plane of the earth's orbit around the sun is called "the ecliptic plane", but one more normally uses this term when thinking of the plane of the sun's apparent orbit around the earth. It is the same plane relative to the stars in either case, just viewed by different observers.

The plane of the earth's equator is tilted by an angle of about 23^{o} relative to the ecliptic plane of the earth's orbit. For reasons seen later, we refer to this angle as θ_{tmax}, and its official name is "the obliquity of the ecliptic". Here both planes are seen edge-on,

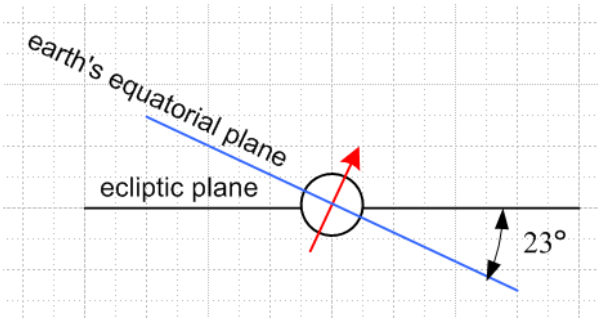

Fig 1.2

Viewed from directly above, the elliptical orbit would appear very close to circular, having eccentricity e = c/a = .0167. The ratio of the extremal earth-sun distances is about 152/147 ≈ 1.034, resulting in a solar energy flux ratio of $(1.034)^{2} = 1.069$ between the two solstices (ignoring the 13^{o} in Fig 1.1). Solar flux is therefore 6.9% greater at summer solstice in the southern hemisphere (Dec) than it is in the northern hemisphere (June).

To see more clearly the position of the earth at the equinoxes, we now swing the camera up and view the ecliptic plane from directly above (ellipse eccentricity exaggerated). The earth's angular position can be measured by angle φ' from March equinox (τ=0), or by angle ψ from perihelion (t=0) where τ and t are two different time variables with different zero points:

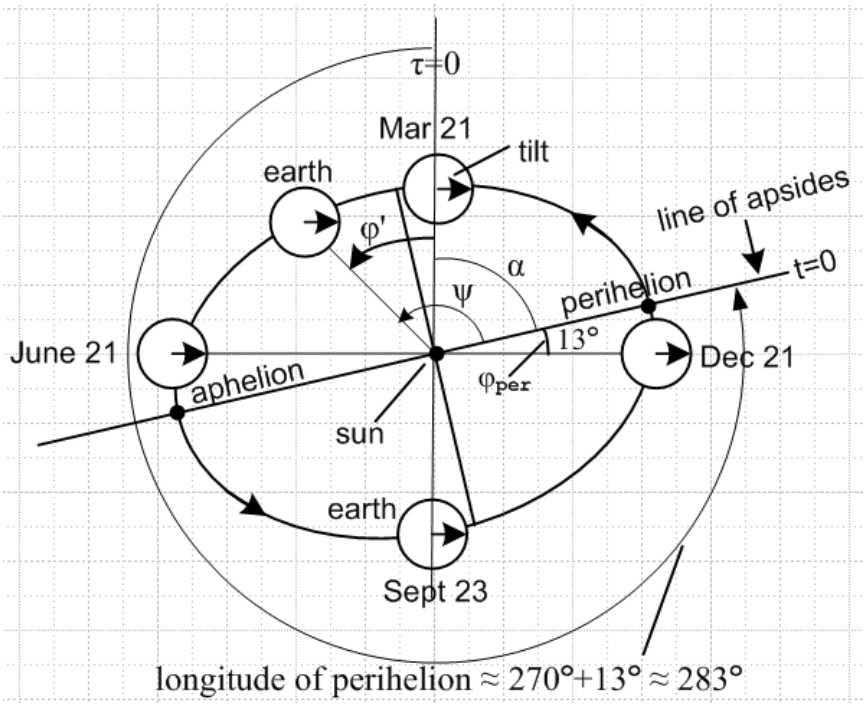

Fig 1.3

The official way of measuring the 13^{o} angle is shown below as the "longitude of perihelion" $\approx 283^{o}$. Here is some data from http://aom.giss.nasa.gov/srorbpar.html showing how this angle, the tilt angle and even eccentricity change over a small number of years: [$283^{o} = 270^{o} + 13^{o}$]

Year (A.D.)	Eccentricity	Obliquity (degrees)	Long. of Perihel. (degrees)
2000	0.016704	23.4398	282.895
2001	0.016703	23.4396	282.913
2002	0.016703	23.4395	282.930
2003	0.016702	23.4394	282.947
2004	0.016702	23.4392	282.964
2005	0.016702	23.4391	282.981
2006	0.016701	23.4390	282.998
2007	0.016701	23.4389	283.015
2008	0.016700	23.4387	283.033
2009	0.016700	23.4386	283.050
2010	0.016700	23.4385	283.067
2011	0.016699	23.4383	283.084
2012	0.016699	23.4382	283.101
2013	0.016698	23.4381	283.118
2014	0.016698	23.4379	283.135
2015	0.016698	23.4378	283.152
2016	0.016697	23.4377	283.170

Table 1.1

For 2012 the angle is therefore 13.101^{o}. Here is data at two larger time scales,

Year (A.D.)	Eccentricity	Obliquity (degrees)	Long. of Perihel. (degrees)
0	0.017466	23.6954	248.820
500	0.017285	23.6330	257.304
1000	0.017097	23.5693	265.811
1500	0.016904	23.5047	274.342
2000	0.016704	23.4398	282.895

Table 1.2

Year (A.D.)	Eccentricity	Obliquity (degrees)	Long. of Perihel. (degrees)
-50000	0.013761	24.2948	204.382
-45000	0.012600	24.4096	268.347
-40000	0.012764	23.9301	332.177
-35000	0.013997	23.0810	40.933
-30000	0.015732	22.3636	116.292
-25000	0.017451	22.2499	196.531
-20000	0.018800	22.7986	278.768
-15000	0.019557	23.6063	0.989
-10000	0.019605	24.1552	82.842
-5000	0.018900	24.1647	165.105
0	0.017466	23.6954	248.820

Table 1.3

The 13^{o} angle indicates a relationship between the earth's elliptical orbit and the direction of its tilt vector. This angle $\varphi_{per} \approx 13^{o}$ along with the tilt angle $\theta_{tmax} \approx 23^{o}$ and the eccentricity $e \approx .017$ all vary in time as part of the complicated solution of a gravitational N-body problem involving the earth, sun, moons, planets, and asteroids. In this solution, the total change in a parameter like φ_{per} can be

approximately viewed as being a sum of changes each associated with a certain physics "mechanism", some of which are long term and some short term relative to human time scales.

One such mechanism causing a change in $\varphi_{\mathbf{per}}$ (called astronomical precession, see Section 3 (d)) is that the earth's rotation axis precesses in a complete conical circle every 26,000 years. Although this precession does not affect $\theta_{\mathbf{tmax}}$, other mechanisms do, and $\theta_{\mathbf{tmax}}$ cycles between $22.0^{\mathbf{o}}$ and $24.5^{\mathbf{o}}$ with a period of 41,000 years. Another mechanism is that the ellipse of the earth's orbit is *itself* rotating in its plane relative to the stars, completing a rotation every 112,000 years. Each of the two extremal points of an ellipse is called an apsis (perihelion = periapsis, aphelion = apapsis, plural apsides), and the line connecting these points is the line of apsides, so it is this line that rotates relative to the stars (called apsidal or perihelion precession). Yet another mechanism is that the ecliptic plane of the earth's orbit wobbles back and forth with a similarly long period. Furthermore, the eccentricity of the orbit varies as well (range .005 to .058) with cycles of 413,000 years and 100,000 years. These "mechanisms" are all due to forces of the moon and other objects acting on the earth. They were studied by the Serbian geologist/climatologist Milutin Milankovic (1879-1958) who was interested in the effect of these changing orbital parameters on climate. His theory called orbital forcing shows how changing orbital parameters could cause ice ages on the earth.

Short term mechanisms also affect the parameters. As the earth's rotation axis precesses, it also nutates ±20 arc seconds with a 19 year cycle due the perihelion precession of the moon's elliptical orbit around the earth. Another form of nutation is associated with the "wander" of the earth's poles, such as the 433 day Chandler wobble which moves the poles ±15 feet. These effects are caused by the non-rigidity and non-roundness of the earth.

Ignoring all these effects due either to their long time scale or their small size, we may regard the earth's rotation axis as pointing in a direction which is fixed relative to the stars.

(b) Development of the Geocentric Picture

First, consider a scenario in which some object A moves counterclockwise in a closed path about object B which is at rest. Neither object is rotating about its own axis. Each object has a glued-on set of axes. This scenario appears on the left below (black) which is the view taken by an observer on object B in Frame S:

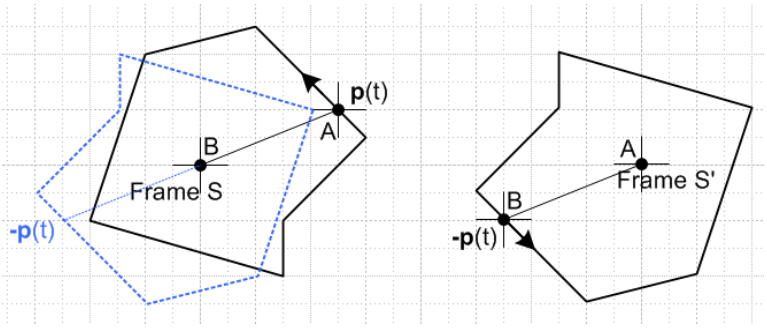

Fig 1.4

If we call the path **p**(t), t being time, then on the left we have in Frame S,

$\mathbf{r_B}(t) = 0$ // B is at rest

$\mathbf{r_A}(t) = \mathbf{p}(t)$. // A moves around the path **p**(t)

Now we go to a new frame of reference S' defined by a time-dependent translation by - **p**(t) relative to Frame S,

$$\mathbf{r}'(t) = \mathbf{r}(t) - \mathbf{p}(t) .$$

In this new frame of reference we find that the positions of A and B are given by,

$$\mathbf{r}_A'(t) = \mathbf{r}_A(t) - \mathbf{p}(t) = \mathbf{p}(t) - \mathbf{p}(t) = 0 \qquad \text{// A is at rest at the origin of Frame S'}$$
$$\mathbf{r}_B'(t) = \mathbf{r}_B(t) - \mathbf{p}(t) = \mathbf{0} - \mathbf{p}(t) = -\mathbf{p}(t) . \qquad \text{// B moves around the path } -\mathbf{p}(t)$$

In Frame S' the object A is now at rest, and object B is traversing a negated path – **p**(t) which is an inversion of the original path through the Frame S origin (blue dotted path). This situation is shown on the right above.

If we now assume that **p**(t) is a *planar* path, as suggested by the drawing, then inverting the original path is the same as rotating it 180 degrees about the Frame S origin in the plane of paper. This is so because then $R_z(\pi)\ \mathbf{p}(t) = -\mathbf{p}(t)$ since $p_z(t) = 0$.

The two points of this exercise are the following:

(1) To obtain the picture on the right, rotate the path **p**(t) 180 degrees about the Frame S origin on the left (to get the dotted blue path), then translate points A and B together by -**p**(t) which causes B to lie on the inverted path.

(2) If A is going counterclockwise around B on the left, then B is going counterclockwise around A on the right. The sense of the path motion is not reversed. The new path is -**p**(t), not **p**(-t).

Example. Suppose path **p**(t) is a tilted ellipse and suppose A lies at a focal point. Application of the above procedure takes the left picture below (A is at rest) into the right picture (B is at rest) :

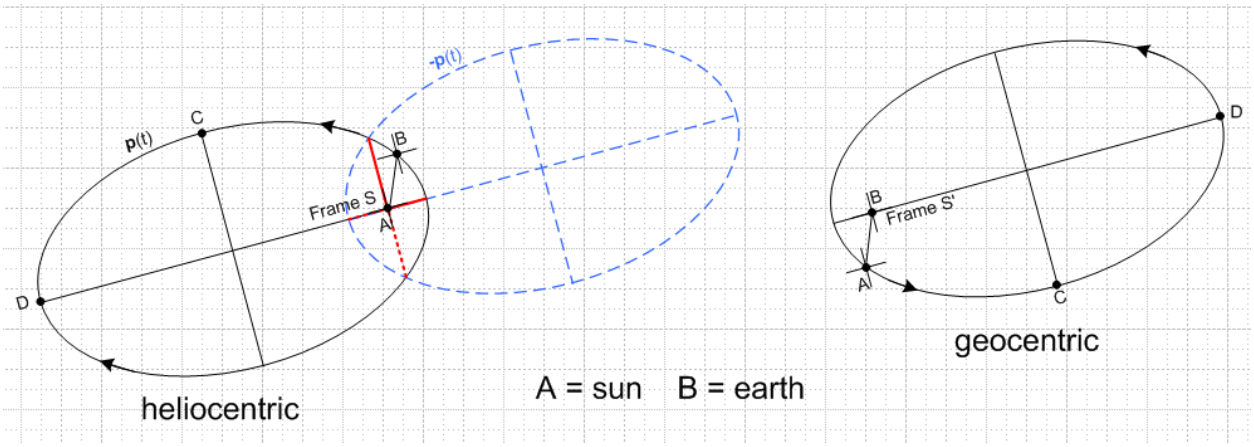

Fig 1.5

If A is the non-rotating sun and B is the non-rotating earth, then the left side picture is the heliocentric one and the right is the geocentric one. Of course for the earth-sun application the eccentricity is much less than shown here. Since the sun is so massive, it can be regarded as a fixed point A in the left picture. The

conclusions are that in the geocentric picture on the right, the earth lies at a focus of the elliptical sun orbit, and the sun moves counterclockwise around the earth. Notice where C and D end up on the right.

Without further ado, we now transform Fig 1.3 to the geocentric view :

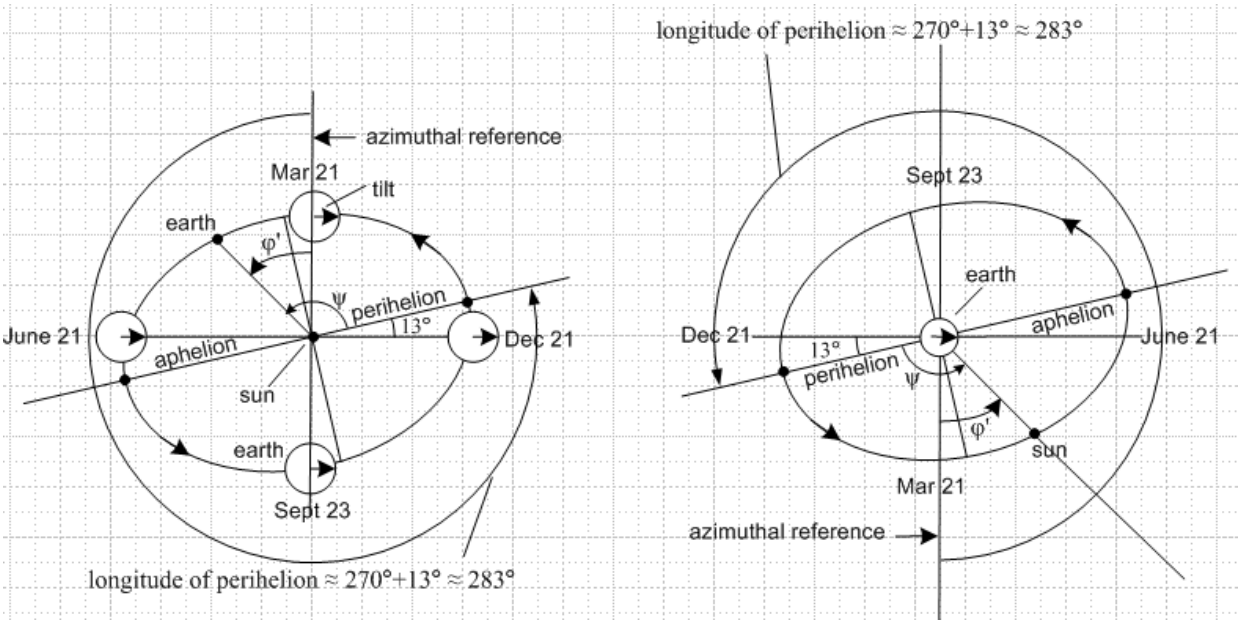

Heliocentric Picture Geocentric Picture

Fig 1.6

(c) Relation between the three angular velocities

Let diy = 365.256363004 be the number of days in a year. In one (sidereal) year's time, the earth experiences diy number of 24 hour periods, normally referred to as "mean solar days". But during this same time, the earth has in fact rotated diy+1 times relative to the stars. If a person faces the noon sun each day and is the subject of a stroboscope movie filmed from above the ecliptic, with a frame shot each day at that person's noon (shots are 24 hours apart), that movie will show that person making one complete revolution during the year. Had that movie shown a static person, one would say that the earth rotated exactly diy times during the year. But in fact the earth rotates a little more than 360^{o} each 24-hour day to keep that person facing the sun and then the total rotations is diy + 1. So we have

$T_{year} = diy*T$ T ≡ 24 hours, length of solar day

$T_{year} = (diy+1)*T_s$ T_s ≡ length of sidereal day (1.1)

Therefore,

$T_s = [diy/(diy+1)]\ T$ (1.2)

$= [365.256363004/366.256363004]*24 = 23.93447$ hours

which agrees with the number quoted above. The (mean) rotation rate of the earth around the sun is

$\Omega_0 \equiv 2\pi/T_{year}$ (1.3)

The solar-day angular frequency ω is, using (1.3) then (1.1),

$$\omega \equiv 2\pi/T = \Omega_0 (T_{year}/T) = \Omega_0 * \text{diy}$$

$$\Rightarrow \Omega_0 = \omega/\text{diy} . \qquad (1.4)$$

Inverting equation (1.2) then multiplying by 2π gives

$$2\pi/T_s = [1 + 1/\text{diy}]\, 2\pi/T$$

or

$$\omega_s = [1 + 1/\text{diy}]\, \omega \quad . \qquad (1.5)$$

Then using (1.4),

$$\omega_s = \omega + \Omega_0 \qquad (1.6)$$

which is the main result of this little section (ω_s is a little larger than ω). As for units, most often we shall use ω = π/12 radians/hr and Ω_0 = 2π radians/year.

(d) Equation of the ellipse

We refer to the 13^o angle in Fig 1.3 as φ_{per} (perihelion). Notice in this same figure another angle ψ which is the usual angle one uses when describing an ellipse in polar coordinates (a = semimajor axis, e = eccentricity)

$$r = a(1-e^2) / (1 + e \cos\psi) \qquad (1.7)$$

so that ψ = 0 gives the shortest (perihelion) value of r. The figure shows that

$$\psi - \varphi' = \pi/2 - \varphi_{per} \qquad \Rightarrow \varphi' = \psi + \varphi_{per} - \pi/2 \qquad (1.8)$$

To reduce symbol count later on, we define

$$\alpha \equiv \pi/2 - \varphi_{per} \qquad // \alpha \approx 77^o \text{ (2012)} \qquad (1.9)$$

and then

$$\varphi' = \psi - \alpha \quad . \qquad (1.10)$$

(e) The Anomalies

When Kepler wrote up his laws in 1609 and 1619, he used the term "anomaly" for an angle that exhibited some unusual behavior. As we shall find in Section 4, the angle ψ (and therefore φ') varies with time in a non-linear fashion; it is linear only when the elliptical orbit is circular. The angle ψ (Fig 1.3 or Fig 1.6) measured from perihelion is called "the true anomaly". Kepler's third law says that the period of an elliptical orbit (for two given objects) is a function only of the semimajor axis a ($T^2 \sim a^3$). One can circumscribe a circle of radius a around an ellipse and if the orbiting object had that circular orbit, the orbital period would be the same as that of the inscribed elliptical orbit. The angular position along this alternate circular orbit is linear in time and is sometimes called M(t), the "mean anomaly", so one has then $M(t) = 2\pi(t/T)$ where T is the orbital period. If the elliptically orbiting object's position is projected "vertically" to that circumscribed circle, a third angle appears, E(t), called "the eccentric anomaly". After time t elapses from perihelion, the three anomalies ψ, M and E all have different values.

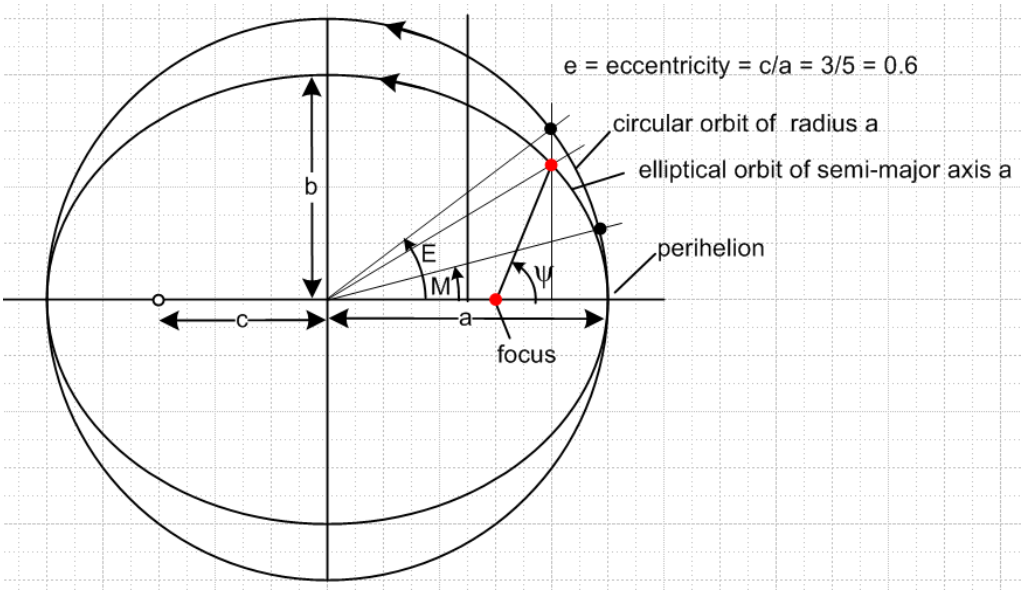

Fig 1.7

Kepler showed that $M = E - e \sin(E)$ and $\tan(\psi/2) = (\sqrt{1+e}/\sqrt{1-e})\tan(E/2)$, so this provided a numerical method of finding ψ(t) by first solving the transcendental equation for E. In Section 4 we shall calculate ψ(t) using an approximation method good for small e, and we shall make use only of this true anomaly ψ. Ref [1] Chap 3 (3-18) and (3-20) provides a general formal solution to the Kepler problem.

2. The Sun's Apparent Path in the Sky

As noted above, the earth tips toward the sun at June solstice, and away at December solstice. This figure shows a composite of three different earth positions relative to the sun,

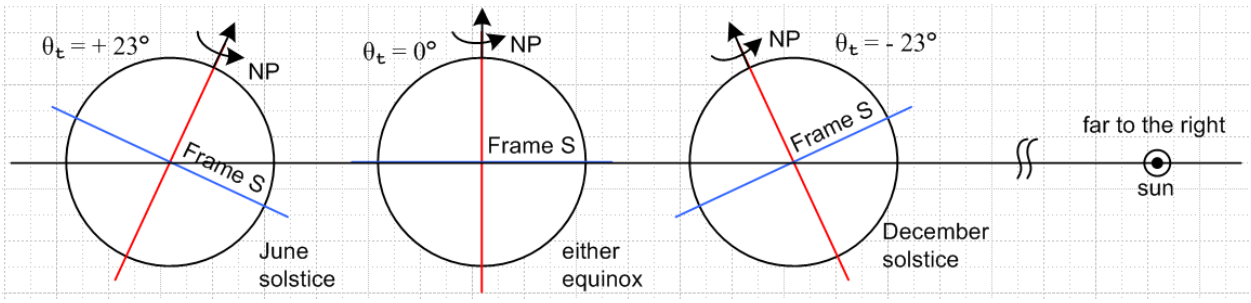

Fig 2.1

For the moment, let's call the maximum earth tilt 23^{o} (Table 1.1 shows 23.4382 for 2012). By the term "tilt" we mean "amount of tilt toward the sun" which is 0 in the middle image above. This tilt will later get the name θ_t, and the maximum value for θ_t is $23^{o} \equiv \theta_{tmax}$.

When the earth is in the orientation shown at the left, a *June solstice* observer on the north pole sees the sun elevated 23^{o} above the horizon. As the earth turns, that sun appears to sweep around in a circle, holding its 23^{o} elevation angle above the horizon. An *equinox* north pole observer instead sees the sun sweep right around *at* the horizon, with half the sun above the horizon and half below (the sun is very far away). A *December solstice* north pole observer never sees the sun, but if this observer had X-ray vision the sun would appear to be going in a circular path 23^{o} below the horizon.

In Fig 2.1 Frame S is a coordinate system: (1) whose origin is at the center of the earth; (2) whose axes are aligned with the earth but don't rotate with the earth; (3) whose axis directions are fixed relative to the stars; (4) whose z axis is along the red line and whose x and y axes lie in the blue equatorial plane. Since the earth moves slowly around the sun, it has some small acceleration relative to the stars, so Frame S is not quite an inertial frame. [The red lines in Fig 2.1 point in different directions only because the "camera" is attached to the earth-sun line and is at different orientations for the three earth images. See Fig 5.1 and discussion there.]

We now construct a rotating Frame S' glued to the north pole that rotates with the earth. Later we shall move Frame S' to other locations on the earth. If one hops aboard Frame S' which is rotating at rate $\boldsymbol{\omega}$ relative to Frame S, then objects which were at rest in Frame S appear to be rotating at rate $-\boldsymbol{\omega}$ relative to Frame S'. In each of the three different situations shown above, the $\boldsymbol{\omega}$ vector lies along the red line. What one sees from Frame S' in these three situations is shown below, where the earth's size is highly exaggerated relative to its distance from the sun (earth should really be a dot),

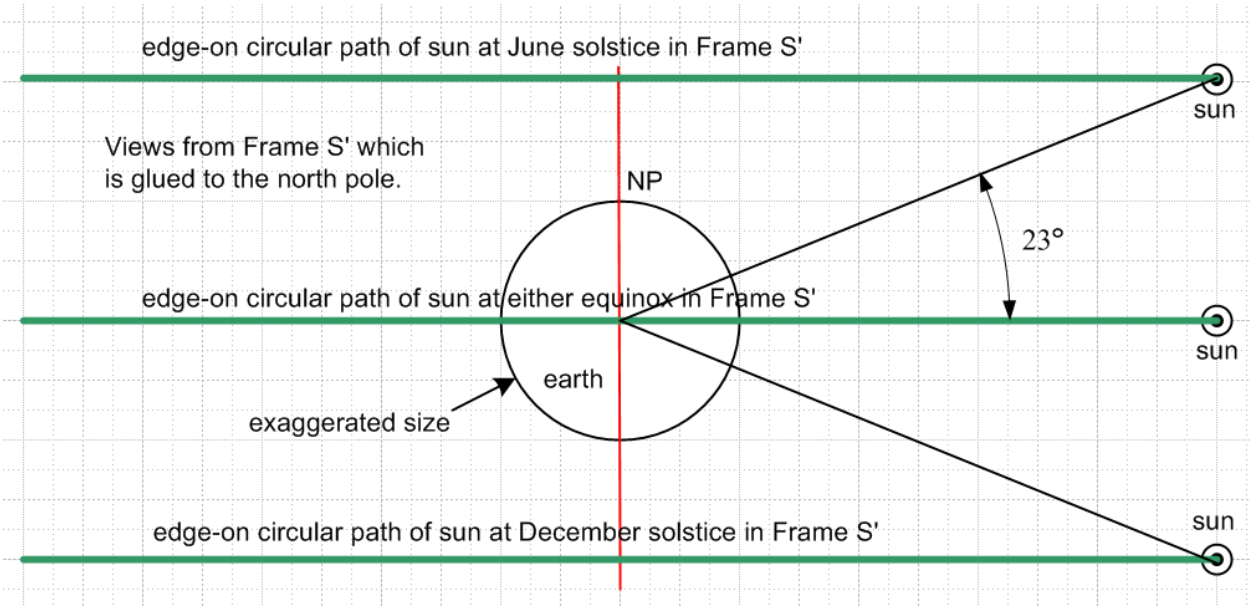

Fig 2.2

During the cycle of the year, the green daily circular sun path moves. If we start at a June solstice, it is the upper green circle (but the circle is viewed edge-on so appears as a green line segment). Moving toward September, that circle drops down and at September equinox becomes the middle green circle above. Moving toward December, the sun continues to move down until the December solstice when it follows the lower green circle. During the next 6 months the path of the sun reverses and next June it is at the top again. So all possible sun paths are *bounded* by the upper and lower green circles. The daily sun rotates clockwise as viewed from above the north pole (sun rises in the east). For the positions of the sun marked on the right, the sun is moving toward the observer. In reality, the green circular daily sun paths shown above are turns of a dense continuous green slinky spiral having 365.25 nearly-horizontal turns (half of the turns spiraling down, the other half spiraling back up), and we have drawn three of the spiral turns.

In the next Sections, we shall refine this brief qualitative description of the sun's apparent motion in the sky and shall provide appropriate equations describing this motion.

3. The Celestial Sphere and the Sun's Daily and Annual Paths Thereon

(a) The Celestial Sphere and the Tropics of Cancer and Capricorn

The celestial sphere is an imaginary spherical surface surrounding the earth at some unspecified radius R upon which one imagines that the sun and other astronomical objects are replaced by their *projections* onto this sphere. An infinite ray is drawn from the center of the earth through an astronomical object, and the projection point is the intersection of this ray with the celestial sphere. Astronomical objects could be inside or outside the celestial sphere. The "marked up" (with star projections) celestial sphere is at rest with respect to the distant stars (Frame S), and the earth rotates within it. Of course in our Frame S' glued to the north pole of the earth, the earth is at rest and the celestial sphere rotates clockwise around the earth causing stars to "rise in the east" and "set in the west".

We shall now draw the projections of the three green circular sun paths of Fig 2.2 onto both the earth and onto a celestial sphere. The projections of sun paths onto the earth are shown here in blue, while projections onto the celestial sphere are shown in red, and we slightly displace the equatorial projections just so they are visible :

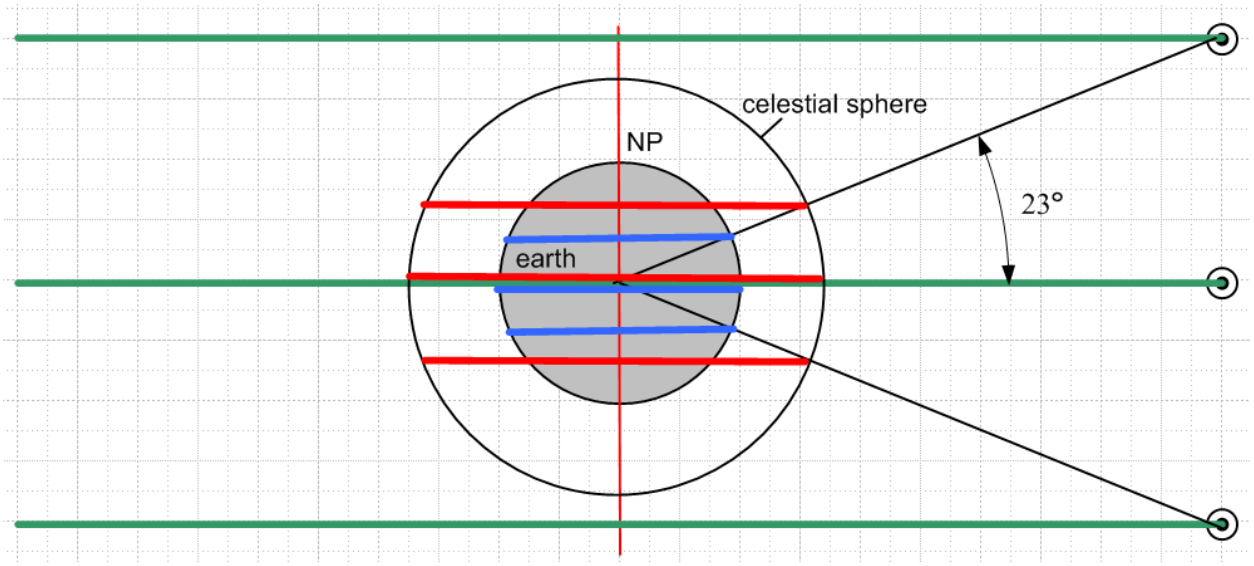

Fig 3.1

The two extremal blue circles on the earth are at latitude ± 23^{o}. These latitude circles have the special historical names Tropic of Cancer in the north, and Tropic of Capricorn in the south. The history of these names is obscure, but the word "tropic" indicates a "turning point", and indeed these extremal circles mark the turning points of the sun path (projected onto the earth) as the yearly cycle progresses, as described in the previous Section. The "tropics" lie between these bounding latitudes.

> [ad. L. *tropicus*, a. Gr. τροπικός pertaining to the 'turning' of the sun at the solstice, tropical (hence as . // OED2

The two extremal red circles on the celestial sphere are of course also at latitude ± 23^{o} on the celestial sphere. The radius of the celestial sphere (discussed below) is supposed to be much larger than the radius of the earth, so to make the above picture more accurate, we redraw it with the earth shrunk to a small dot.

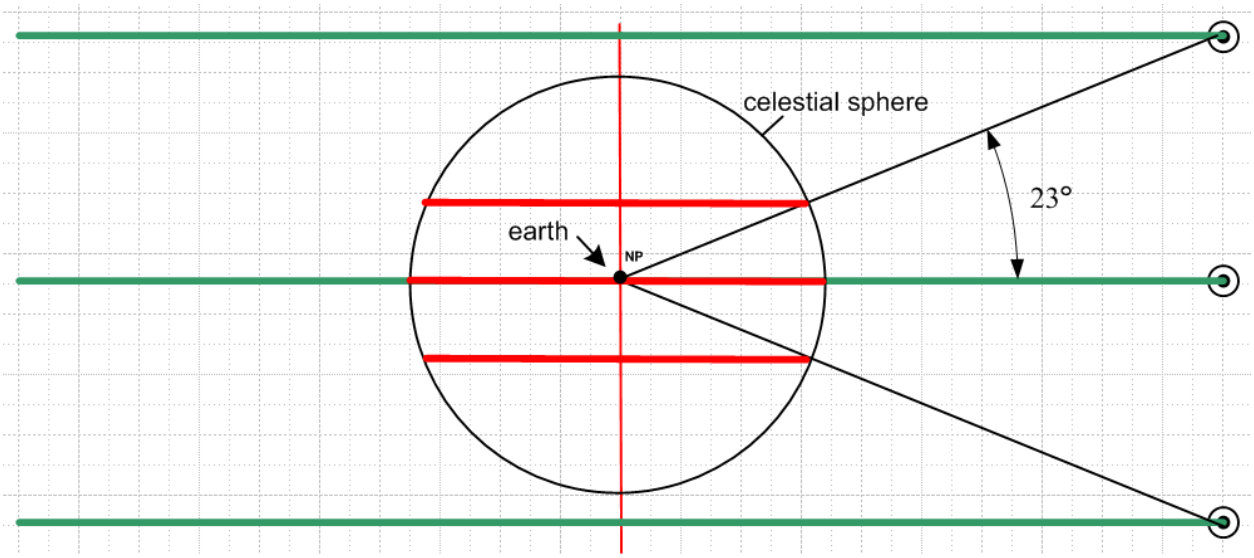

Fig 3.2

A very convenient model for thinking about the sun paths is to think of them as *being* those red circles on a celestial sphere (usually called *the* celestial sphere). In the above drawing, the radius R of the celestial sphere is perhaps 25 million miles, since the sun is 93 million miles away.

Below we are going to ask the question: What do the three red circles look like from various observation points on the earth? We want an exact answer to this question. For an observer on the north pole, the answer is clear and is represented by the left picture below (the winter circle is not visible to this observer), while for an observer on the equator the answer is also clear and is represented by the right picture below. In these two pictures, the vertical direction represents "up" for the observer, south is to the left and east is toward the viewer.

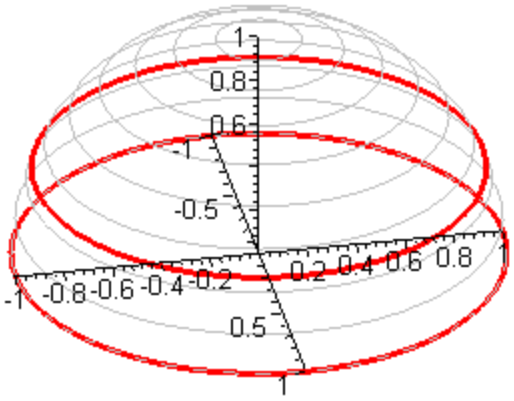

Observer at North Pole

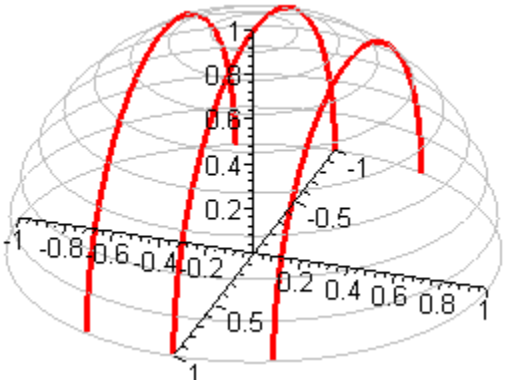

Observer at the equator

Fig 3.3

In these drawings the celestial sphere is suggested by the dim gray circles. These gray circles form a half sphere, and the flat bottom of the half sphere coincides with a plane tangent to the earth at the observer's location. This plane contains the observer's horizon, so portions of the red circles below this plane are not visible to the observer. The ending points of partial red circles (as on the right) are identified therefore with sunrises and sunsets (the near ones are sunrises since east is toward the viewer).

(b) Why is R >> R_{Earth} for the celestial sphere?

The celestial sphere construct simply does not "work" if it is very close to the earth. For example, suppose the celestial sphere were 500 feet above the surface of the earth. One could imagine for some observer the stars projected onto this sphere and their positions marked with paint dots on the otherwise transparent sphere. As the observer moves to a different location, those paint dots no longer align with the stars they represent. The projections of the stars for this celestial sphere are dependent on the location of the observer on the earth. On the other hand, if the mathematical celestial sphere is placed 100 earth radii out into space, then as the observer wanders from A to B, the paint dots made at A will be pretty close to the stars seen from location B. Maybe the maximum angular error will be 1/100th of a radian or about 1/2 degree (parallax error). As the celestial sphere is mentally moved further away, this error becomes smaller, and in the limit $R \to \infty$ the paint dots are in the same place for all observers on the earth (the stars are imagined to be infinitely far away). So we want R large to prevent parallax error for viewers on the earth, then a single celestial sphere map of the stars can be used by everyone.

A separate but related issue concerns the distance of observed objects from the earth. A balloon at 500 feet could be projected onto the celestial sphere, but its projection must be different for different observers, and the celestial sphere is pretty useless in this case. The moon is about 61 earth radii away, so if it were projected onto the celestial sphere, its position would be the same value for all earth observers with perhaps 1 degree of error or less. The sun is 24,000 earth radii from the earth, so the parallax error for any earth observer is then very small, perhaps .002 degrees.

Eventually we will set R = 1 unit and have mind perhaps R_{Earth} = .0000001 unit.

(c) Annual apparent motion of the sun around the earth: the ecliptic

Viewed from directly above the ecliptic plane, the path of the sun around the earth was shown on the right side of Fig 1.6, which we reproduce here as its own separate figure. The elliptical orbit of the sun lies in the plane of paper and the earth's tilt arrow points 23° out of the plane of paper and to the right.

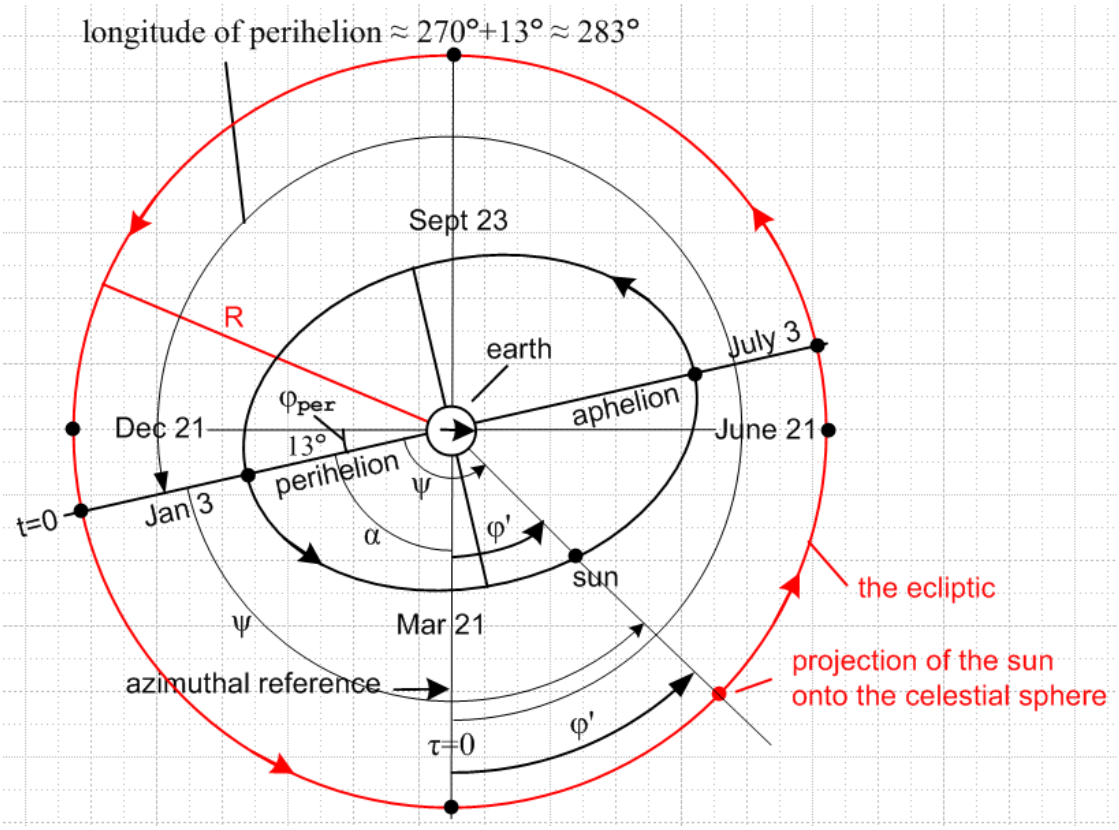

Fig 3.4

We have added in red the intersection of the sun's ecliptic plane with the celestial sphere, which sphere we now show being outside the sun's orbit. Since the earth lies at the center of the celestial sphere, this intersection is a great circle on the celestial sphere. This red circle lies in the plane of paper above and is commonly referred to as **the ecliptic**. The March equinox is the azimuthal reference point on both the ecliptic and on the earth's elliptical orbit. The angle φ' from the ecliptic reference point to the sun's projection on the ecliptic is the same as the angle φ' going from the elliptical orbit reference point to the actual sun (similarly for ψ). The elliptical orbit is thus projected onto the circular ecliptic.

If we now think of the red disk (with earth) as a flat damper disk hinged on the vertical axis, we can rotate that disk 23° so that the June solstice rises above the plane of paper, the December solstice drops behind the plane of paper, and the two equinoxes (being on the hinge) stay in the plane of paper. Such a rotation causes the angular momentum vector of the earth to point directly at the viewer. This situation would be precisely the view of the earth-sun system from the north pole of the celestial sphere.

Here then is a nice 3D representation of the celestial sphere and its red ecliptic, where June solstice is the high point on the ecliptic on the right. One now sees the abovementioned damper disk in its rotated position.

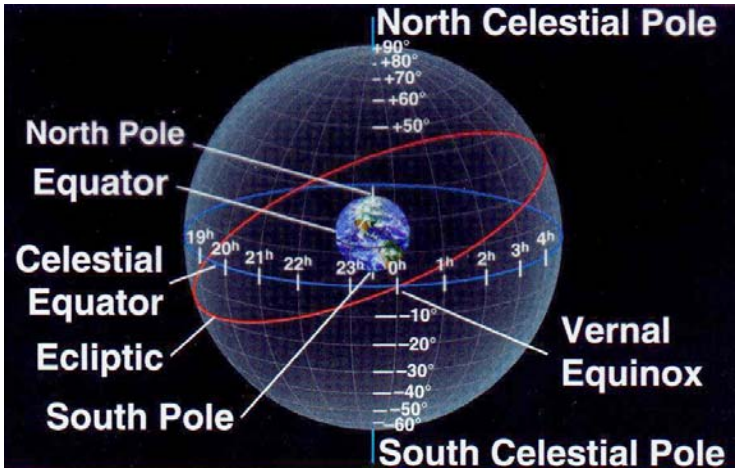

Fig 3.5

http://astro.wsu.edu/worthey/astro/html/lec-celestial-sph.html

The ecliptic circle intersects the celestial sphere equator at the two (hinge) equinox points on opposite sides of the celestial sphere. The March equinox (northern hemisphere's vernal equinox) is used as the azimuthal reference on the celestial sphere. This azimuth may be regarded as longitude on the celestial sphere, measured in the same sense that longitude is measured on the earth east of Greenwich. To avoid confusion with various other azimuths, the longitude or azimuth on the celestial sphere is called **right ascension**. It could be measured in degrees or hours, and in the latter case one refers to the "hour angle" of the azimuth, as in the picture above. Similarly, latitude on the celestial sphere is called **declination** and runs from $+90^{o}$ at the north pole to -90^{o} on the south pole with 0^{o} at the celestial equator.

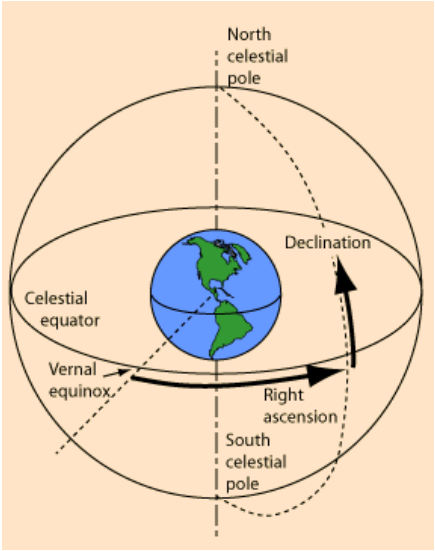

http://hyperphysics.phy-astr.gsu.edu/hbase/eclip.html

Fig 3.6

A star on the celestial sphere located at a certain right ascension will "ascend" from the eastern horizon into the night sky (as viewed from the earth) at a time associated with that star's right ascension. The term "right" has a historical meaning, but it is best to think of it meaning the angle is measured to the "right" of the vernal equinox as shown in the above figure.

If Fig 3.5 were "live", one would see the celestial sphere fixed, the earth rotating counter clockwise once per day (viewed from the north celestial pole), and the sun slowly traversing the red ecliptic circle counterclockwise once per year.

The sun traverses the ecliptic circle over a period of 12 months, and each month's segment of the ecliptic lies "in" one of the 12 constellations of the **zodiac** (circle of animals, like Leo the lion, but only half of the 12 constellations are animals). Roughly in February, for example, the sun is "in the house of Aquarius". The houses don't exactly align with official months.

One might wonder how the ancients knew where the sun was on the ecliptic since the bright sun makes the stars on the celestial sphere invisible. They might have done it this way: (1) observe the elevation of the noon sun (sun on meridian) and deduce from one's latitude the corresponding celestial sphere declination of the sun (Eq. 9.20); (2) at midnight, observe what stars are located at this same declination on the midnight meridian; (3) the sun must then be on that same declination on the opposite meridian; (4) consult a celestial sphere map to see where the sun must therefore be.

The mass-averaged plane of the planetary orbits is called the **invariable plane**. The orbits of the 8 major planets all lie fairly close to this invariable plane ($< \sim 6^{o}$). For that reason, the orbits of the planets all lie close to that of the ecliptic ($< \sim 7^{o}$). Therefore, one looking for the planets in the nighttime sky should look near the path in the sky the sun took that day. Since the moon's orbit is inclined only 5^{o} relative to the ecliptic, when visible the moon will be located in that same region of the sky. So the planets and the moon all wander through the houses of the zodiac.

Notice that the *annual* path of the sun shown in red in Fig 3.5 is very different from the *daily* paths of the sun which are red circles which align with lines of latitude on the celestial sphere as shown in Fig 3.2. When the sun on the above tilted red ecliptic circle is viewed from our north-pole Frame S' which is glued to the rotating earth, its path over a year is a red spiral (with 365.25 turns) which runs back and forth once between the two extremal daily red circles shown in Fig 3.2. Here is an illustration of that spiral where we draw 12 turns instead of 365.25 turns:

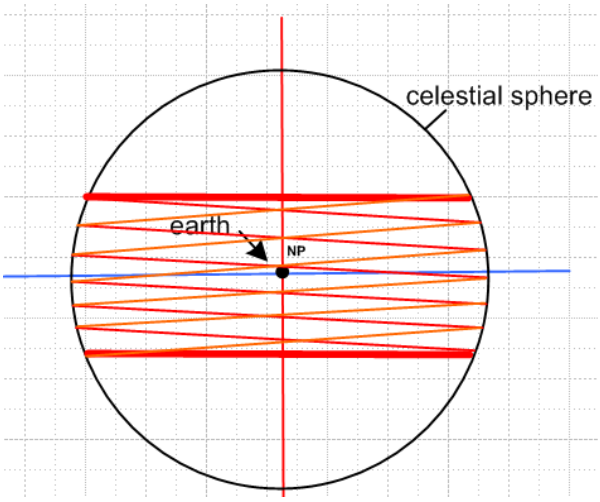

Fig 3.7

On any given day, that day's spiral turn is very close to lying on a fixed declination circle of the celestial sphere, and that spiral turn is then the sun path for that day.

Here is an $80 commercial celestial sphere with various stars, galaxies and the milky way projected onto its surface:

Fig 3.8

http://starlab.com/shop/Celestial-Globe-SKU1094.html

The yellow Milky Way shown in Fig 3.8 reflects the position and orientation of the earth relative to the galaxy as indicated in this Britannica picture (the earth is in the Orion Arm of the Milky Way) :

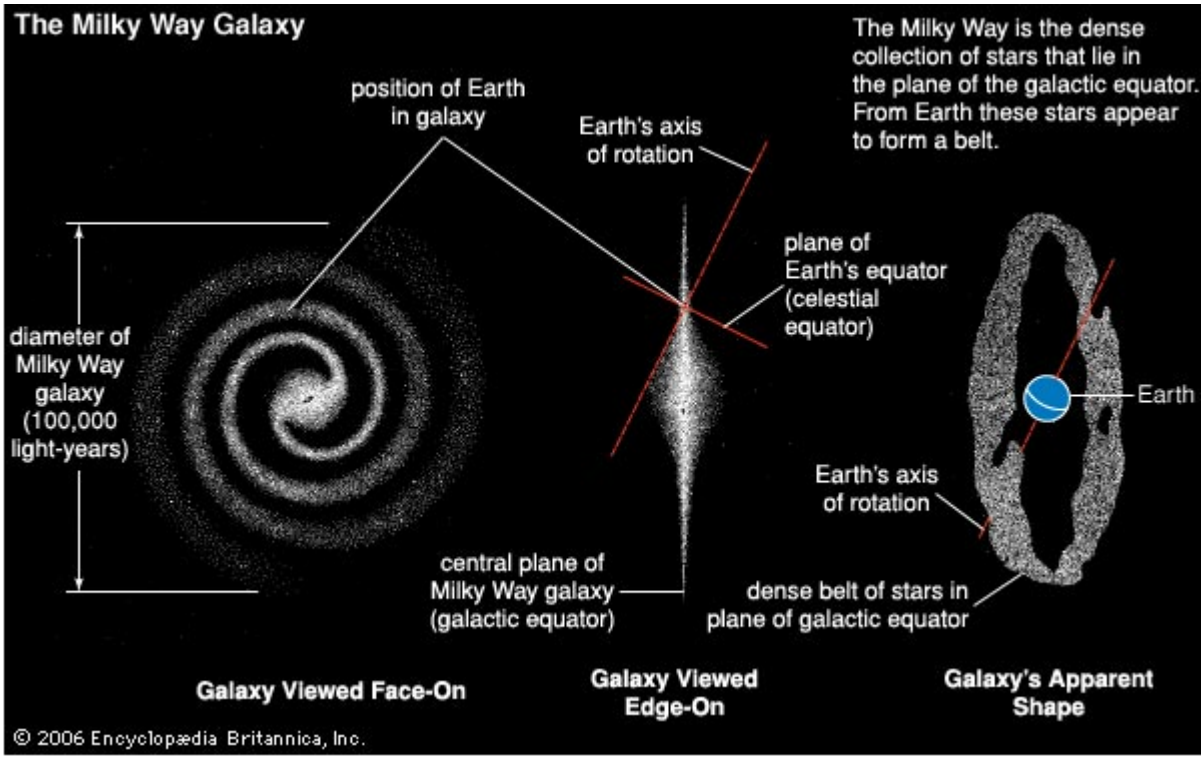

http://www.britannica.com/EBchecked/media/101407/Three-views-of-the-Milky-Way-Galaxy Fig 3.9

The picture shows that the ring of the Milky Way runs close to the north and south poles of the earth and one can then imagine its location on the celestial sphere (yellow in Fig 3.8).

Commercial celestial globe makers face a conundrum: if the sphere is accurate, then all constellations appear inverted when the sphere is viewed from the outside, which is where it is normally viewed from. Sometimes manufacturers transform the true celestial sphere so what one sees from the outside is what one would see on a true celestial sphere from the inside, which is immensely confusing. Transparent spheres at least allow the possibility of doing it right so one can view through the sphere. One could imagine a fancy celestial sphere with a tiny movable camera on the earth which one can hook to one's "PC". A simpler alternative is to just download the freeware Stellarium http://www.stellarium.org/ .

(d) Precession effects

The reason a tilted spinning top precesses is that gravity applies a torque $\mathbf{N} = \mathbf{r} \times m\mathbf{g}$ about the center of mass of the top, relative to the point of contact. This tangential torque causes a change $d\boldsymbol{\omega} = \mathbf{N}dt$ which is perpendicular to the rotation vector $\boldsymbol{\omega}$ of the top and causes the top to precess.

Since the earth rotates and is not rigid, it has a larger radius at the equator than at the poles (by about 21 km). The plane of the earth's fat equator makes some significant angle relative to the earth-moon line, as in this drawing which assumes a set of positions and orientations at some instant in time (the moon-earth line can be at most 5^{o} out of the ecliptic).

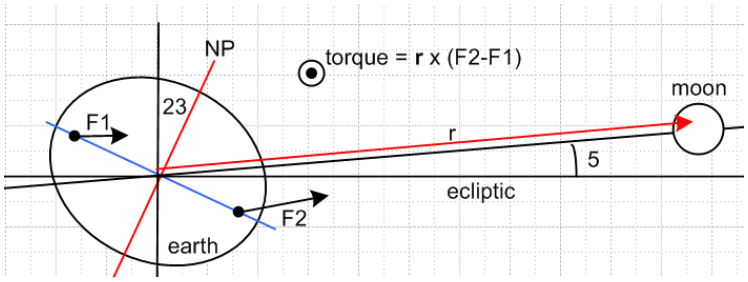

Fig 3.10

As a result, the moon exerts a net torque on the earth due to the gradient of its gravitational field at the earth (the same gradient which causes the bulging of the tides). This torque causes the earth to precess. If the earth were perfectly spherical and uniform, it would act as a point mass at its center upon which the moon could exert no torque.

The sun creates a torque in this same manner, but the torque is smaller because the sun's distance outweighs its larger mass. The net result is that the sun's effect is about half that of the moon, as is the case for earth tides.

The precession rate of the earth's rotation axis is about one degree every 72 years (25,800 year cycle). The earth's angular momentum vector $\boldsymbol{\omega}$ points from the center of the earth to its north pole. If one traces out the path of this vector, it rotates around a cone of half angle 23^{o} once every 25,800 years, as shown in Fig 5.1 below. One consequence of the earth's precession is that the time between March equinoxes is slightly less than a year. After the sun does exactly one revolution about the earth starting at a March equinox, it expects to be at the next March equinox where the earth is again tilted neither toward nor away from the sun. But the tilt axis has precessed 1/72 of one degree (50 arc sec), so the equinox is *early* (it turns out) by this amount of time :

$$\Delta t = (1/72)\ \text{deg} * [1\ \text{yr}/\ 360\ \text{deg}] * [\ 365.25\ \text{day/yr}] * [24*60\ \text{min/day}] = \ 20.3\ \text{minutes} \qquad (3.1)$$

This effect is called "the Precession of the Equinoxes", and of course the September equinox and the two solstices experience this same anomaly. The seasonal "year" between solstices is called "the tropical year". The sidereal year is "too long" and if it could be shortened a bit, it would match the seasonal year. But as it is, the seasons are slowly sliding backwards relative to a sidereal calendar and in fact slide entirely through the calendar every 25,800 years. The solstices are associated with the high and low points of the ecliptic circle on the celestial sphere, and those points in turn are associated with certain of those zodiac zoo animals, so the 12 members of the zodiac slide along with the seasons relative to the sidereal calendar.

But most people don't use a sidereal calendar. Instead, they use one that is on average 365.25 days long, since every 4th year (leap year) adds a day on Feb 29 (the Julian calendar). Now the sidereal year is 365.25 days + 9.17 min long, so the tropical year is then 365.25 days - 11.13 min long (taking off the 20.3 minutes in (3.1)). So the Julian calendar is too long by 11.13 minutes, which means the seasons are sliding backwards through the Julian calendar by 11.13 minutes every year. This adds up to one day after 129.4 years. A scheme was concocted to knock out 3 days every 400 years which is one day every 133.3 years, close enough for government work. The scheme is to not have a leap year every XX00 year, except when XX is a multiple of 4. This plan is called the Gregorian calendar and was set up in 1582 by Pope Gregory. Since Easter was associated with a certain seasonal date (first Sunday after full moon after vernal equinox) *and* with a certain calendar date (vernal equinox around March 20-21), the Pope didn't like the idea of these two associated dates drifting apart. It is all a very long story.

Since the north pole of the celestial sphere always aligns with that of the earth, one can think of this precession effect in terms of the earth's rotation axis staying fixed vertically and the celestial sphere (and all the stars attached to it) doing the precessing. This is a very difficult concept to illustrate with line drawings, but here is a crude attempt:

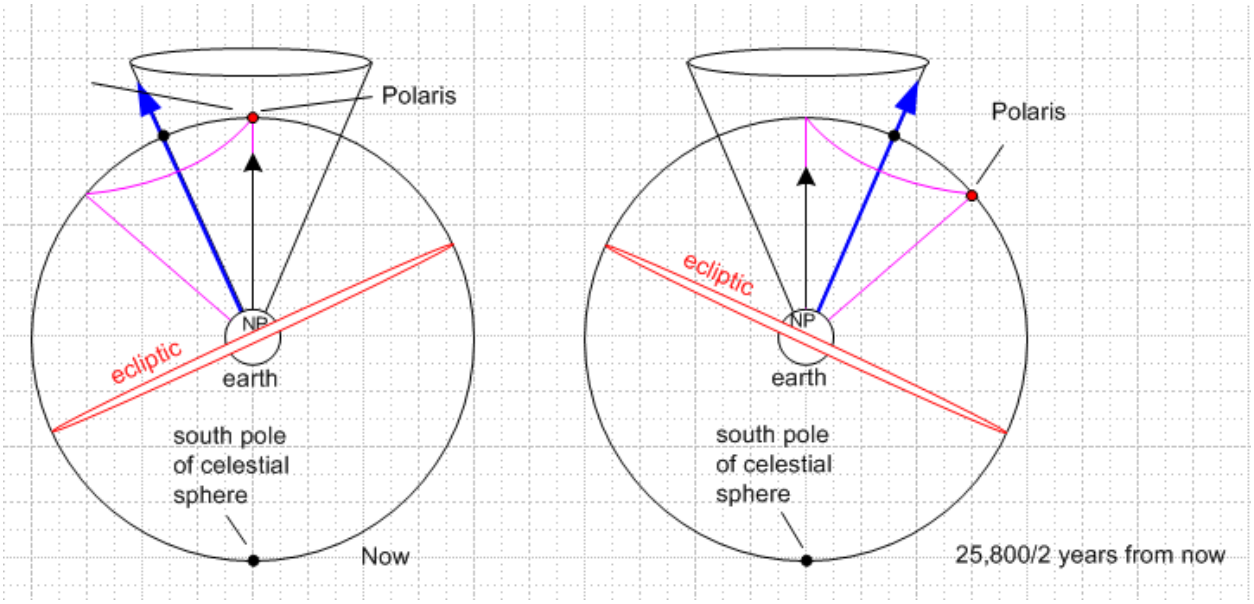

Fig 3.11

Think of the present celestial sphere on the left as a globe with all the stars and the sun's ecliptic painted on it. The usual axis of this globe is the vertical black arrow, but consider the blue arrow shown on the

left as another axis glued to the celestial sphere. As the celestial sphere precesses, this blue arrow traverses the large vertical cone (half angle 23^{o}), so that 25,800/2 years from now the blue arrow will be as shown on the right. The positions of all stars on our precessed globe are then transferred to the celestial sphere of that future time. Polaris which *was* the north star moves to the new location shown, 46^{o} down from the celestial north pole. The small black rotation axis of the earth meanwhile has moved on *its* cone, which is the pink cone of Fig 5.1. The red ecliptic circle wobbles around with the celestial sphere and after half a wobble ends up as on the right. Every point on the ecliptic, and in fact every point on the original celestial sphere, traverses a circle on the sphere of half angle 23^{o}, Polaris being an example. As the ecliptic wobbles around, its intersections with the celestial equator move, and these intersections are the equinoxes which are then moving 1/72nd of a degree per year on the celestial sphere. To understand this picture, one has to hold a physical globe in two hands, imagine a blue arrow sticking out, and then wobble the globe in such a way that the blue arrow traverses the cone.

During this precession of the celestial sphere, star charts have to be updated. Since any two orientations of a sphere are related by a specific rotation R, the coordinates (ephemerides, see below) of all stars at t = t can be obtained from those at t = 0 by applying some uniform rotation R(t) to their coordinates at t = 0.

Ephemeris. A table or book of computed future positions of astronomical objects on the celestial sphere as a function of time is called an ephemeris (< Gk. journal, diary, calendar). The positions themselves are called ephemerides, plural of ephemeris. The phrase "ephemeris time" (ET) refers to a certain precision time scale (of which there are now many) which is independent of the vagaries of the earth's (rotational) motion and which agrees exactly with the dynamical time variable "t" in Newton's Laws governing the motions of objects in the solar system, as based on observations of these objects. Ephemeris time was used in ephemeris tables circa 1950-1980, but is now replaced by more elaborate precision times based on atomic clocks, some of which take into account effects of special (time dilation) and general (gravitational curvature) relativity.

(e) Daily sun paths for various observation points

In Section 7 below we shall derive the equations used in this section to plot three red daily sun-path circles (two solstice paths, one equinox path) as viewed from various observation sites in the northern hemisphere. Here we just display the results for the reader's possible interest. Recall that "up" is up, south is to the left, and east is toward the viewer. For each picture both the polar angle and latitude of the observer site are given, where polar angle + latitude = 90^{o}. Representative cities near the indicated latitude are noted. Basically one sees here how the two pictures shown earlier are "interpolated" as we move from equator to north pole. The plane of any of the red curves shown makes an angle with the horizontal site tangent plane which is equal to the polar angle shown. We are just viewing the three red circles of Fig 3.1 or Fig 3.2 from various places on the earth.

To obtain the figures for the southern hemisphere, the images below should be mirror-reflected left to right, that is, in the east-west-up plane. Then the red curves all tip to the right.

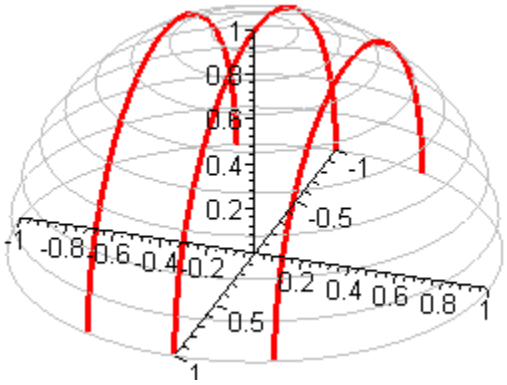

polar = 90 lat = 0 Singapore, Quito (equator)

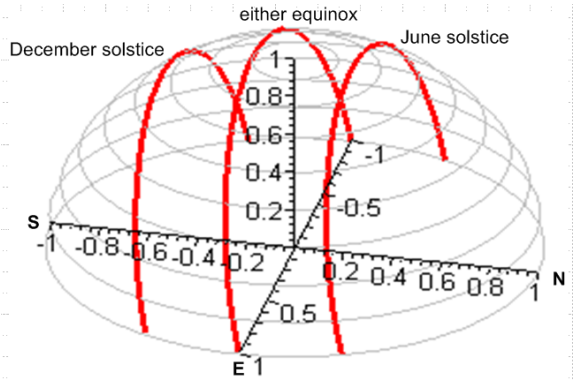

polar = 80 lat = 10 Caracas, Costa Rica

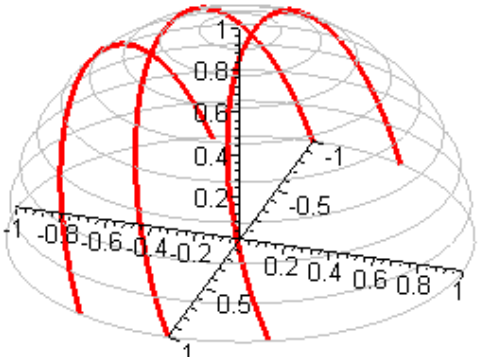

polar = 70 lat = 20 Honolulu, Mexico City, San Juan

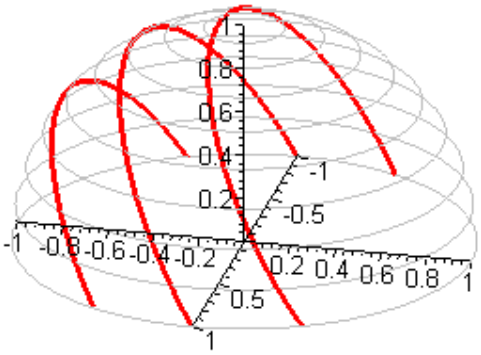

polar = 60 lat = 30 Cairo, Houston

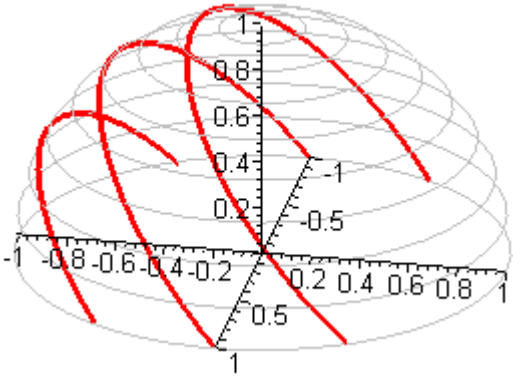

polar = 50 lat = 40 New York, Salt Lake City

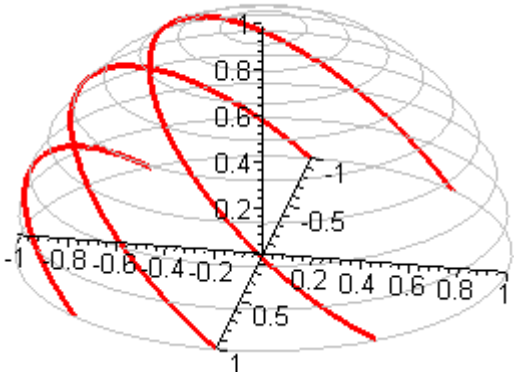

polar = 40 lat = 50 Brussels

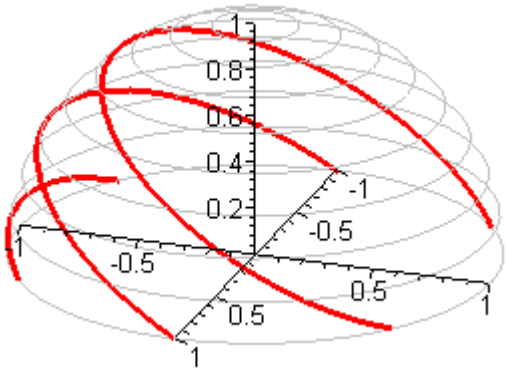

polar = 30 lat = 60 Helsinki

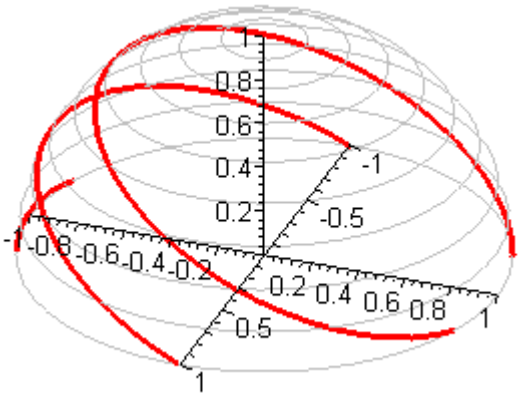

polar = 25 lat = 65 Reykjavik

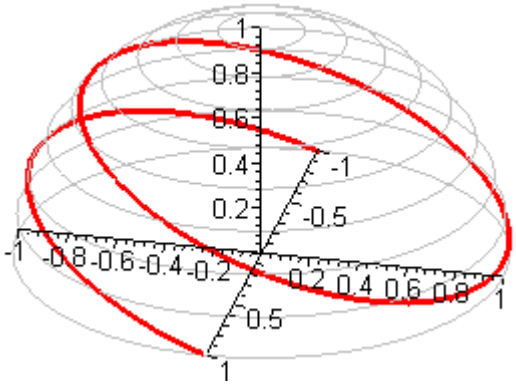

polar = 20 lat = 70 Barrow

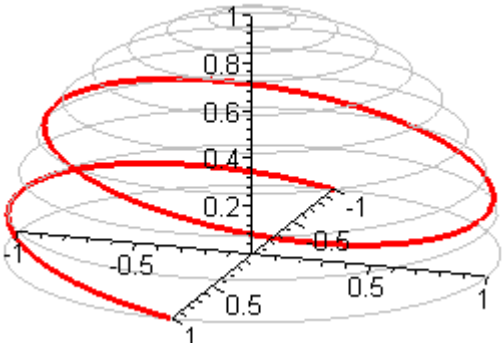

polar = 10 lat = 80 Eureka

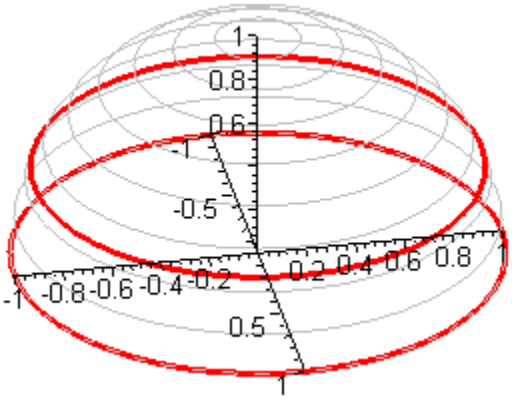

polar = 0 lat = 90 North Pole

Fig 3.12

Maple Code Notes

The code is based on equations (7.15) which are derived below in Section 7 (see notes there),

$$\begin{aligned} x' &= -R\cos\theta_t \sin(\omega t) \\ y' &= R\,[\sin\theta_t \sin\theta_1 - \cos\theta_t \cos\theta_1 \cos(\omega t)] \\ z' &= R\,[\sin\theta_t \cos\theta_1 + \cos\theta_t \sin\theta_1 \cos(\omega t)] \ . \end{aligned} \qquad (7.15)$$

The functions are first entered with R = 1 and we then verify that $x'^2+y'^2+z'^2 = 1$,

```
xp := -cos(thetat)*sin(omega*t);
```

$$xp := -\cos(thetat)\sin(\omega t)$$

```
yp := sin(thetat)*sin(theta1) - cos(thetat)*cos(theta1)*cos(omega*t);
```

$$yp := \sin(thetat)\sin(\theta 1) - \cos(thetat)\cos(\theta 1)\cos(\omega t)$$

```
zp := sin(thetat)*cos(theta1) + cos(thetat)*sin(theta1)*cos(omega*t);
```

$$zp := \sin(thetat)\cos(\theta 1) + \cos(thetat)\sin(\theta 1)\cos(\omega t)$$

```
evalf(xp^2+yp^2+zp^2): simplify(%);
```

$$1$$

Next, the plot library is activated and constants are set in,

```
with(plots):   omega := (2*Pi/24):
thtmax := 23.4382*(Pi/180): theta1 := 50*(Pi/180):
```

The Maple code generates one plot at a time, and for this plot $\theta_1 = 50^o$. The three red partial circles are generated in a display list p_1 :

```
p1 := spacecurve({seq([xp,yp,zp], thetat = [-thtmax,0,thtmax])}, t = -12..12,
axes=NORMAL, thickness=3, color=red,view=[-1..1,-1..1,0..1],scaling=CONSTRAINED  ):
```

Three values of θ_t are used here to make three red circles. The z part of the view option causes these circles to be plotted only for $z' \geq 0$ which means only for daytime. The grey half sphere latitude guide circles are generated using equations (6.7) with R = 1,

```
p2 := spacecurve({seq([sin(b*Pi/18)*cos(phi), sin(b*Pi/18)*sin(phi),cos(b*Pi/18)],b =
1..9)}, phi = -Pi..Pi, axes=NORMAL, thickness=1,
color=gray,view=[-1..1,-1..1,0..1],scaling=CONSTRAINED  ):
```

and then finally both the p1 and p2 plots are superposed, displayed and oriented by the last command,

```
display([p1,p2],orientation=[10,80]);
```

(f) The Arctic and Antarctic Circles

In going from the polar = 25 to the polar = 20 drawing in Fig 3.12, one notices that the winter solstice sun path has completely disappeared. In the following picture, we assume $\theta_t = -20^o$ which is not quite at December solstice (which would be -23.4^o).

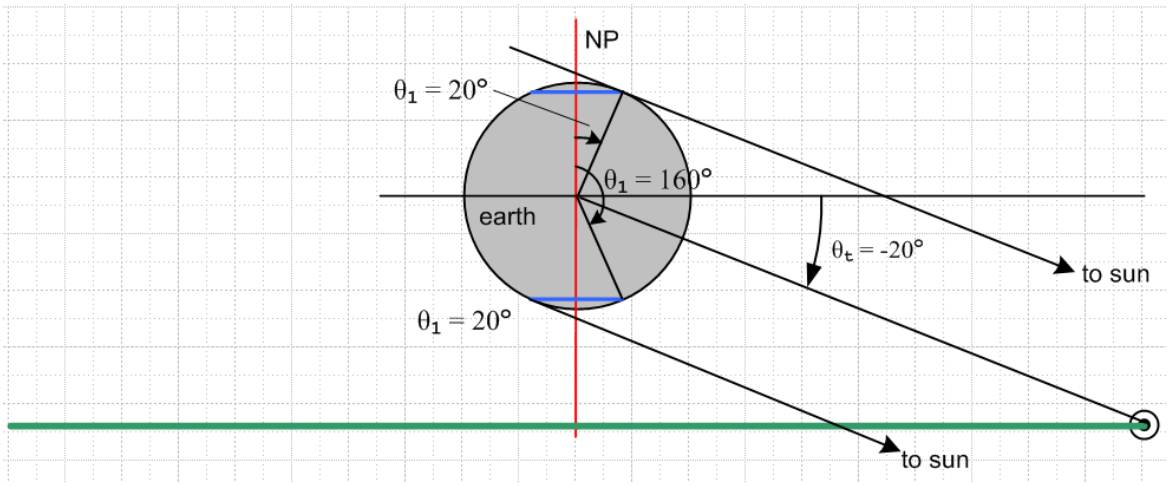

Fig 3.13

This picture is hard to draw because we really want the sun extremely far away. This is why the arrows which say "to sun" do not point to the close-in sun, but do point to the correct far-away sun. The bottom green line is the edge-on path of the close-in sun. The point here is that someone on the north pole cannot ever see the sun in this picture, no matter where it is on its green circular path. This is also true for any observer above the upper blue circle which is at $\theta_1 = 20^o$ polar angle. In general, the condition for 24 hour night near the north pole is this

$\theta_t < 0$ AND $\theta_1 < |\theta_t|$ // north pole region always night

The largest angle that θ_1 can be, with 24 hour darkness above it, is 23.4^o and this occurs at Dec solstice. The blue circle at this limiting point is called the Arctic Circle (not shown). Below that circle it can never be 24 hour night.

At the same time, an observer south of the mirror-image lower blue circle *always* sees the sun, as the lower arrow shows. The condition for 24 hour daylight here is

$\theta_t < 0$ AND $\pi - \theta_1 < |\theta_t|$ south pole region always day

The upper limit of the lower blue circle is called the Antarctic Circle. Above this circle it can never be 24 hour day.

Now consider the situation near June solstice

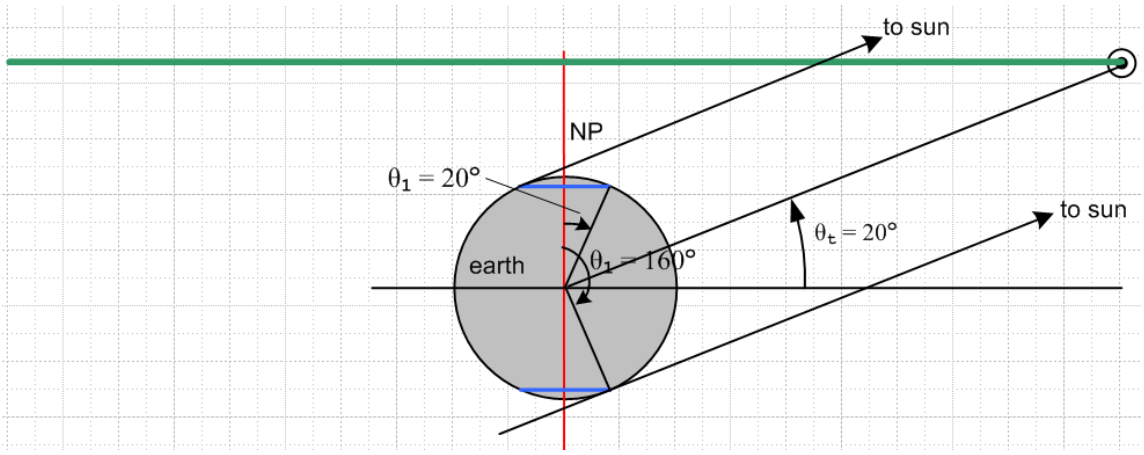

Fig 3.14

The conditions now for all night and all day are

$\theta_t > 0$ AND $\theta_1 < \lvert\theta_t\rvert$	north pole region always day
$\theta_t > 0$ AND $\pi - \theta_1 < \lvert\theta_t\rvert$	south pole region always night

We can then summarize these four conditions:

$\theta_t < 0$ AND $\theta_1 < \lvert\theta_t\rvert$	north pole region always night	
$\theta_t < 0$ AND $\pi - \theta_1 < \lvert\theta_t\rvert$	south pole region always day	
$\theta_t > 0$ AND $\theta_1 < \lvert\theta_t\rvert$	north pole region always day	
$\theta_t > 0$ AND $\pi - \theta_1 < \lvert\theta_t\rvert$	south pole region always night	(3.2)

4. How the Earth's Orbital Azimuthal Position ψ Varies with Time due to Eccentricity

(a) A simple solution for ψ(t)

Recall from Section 1 the equation of the elliptical orbit of the earth around the sun,

$$r(\psi) = a(1-e^2) / [1 + e\cos\psi] \ . \qquad (1.7)$$

Using 2012 data, a = 149.598261 million km and eccentricity e = .0167. Here a is the semi-major axis of the ellipse, and the semi-minor axis will be called b below.

Ignoring small external torques on the sun-earth system, the angular momentum L of the system is a conserved quantity. If m is the reduced mass of the system ($m \approx M_{Earth}$) then Kepler's second law of orbital motion states that (see for example Ref [1] p 60 Eq (3-8))

$$\dot{\psi}\, r^2 = L/m = \text{constant} \ . \qquad (4.1)$$

The area of a small triangular wedge of angle dψ is

$$dA = (1/2)r(rd\psi) = (1/2)r^2\dot{\psi}\, dt = (L/2m)\, dt \qquad (4.2)$$

and here we see (4.1) stated as the "equal areas swept out in equal times" rule. Integrating both sides around the entire ellipse then gives

$$A = (L/2m)T \ , \qquad (4.3)$$

where T is the period of the orbit. But we know that A = πab for an ellipse, and also that $b = a\sqrt{1-e^2}$, so the area is $A = \pi a^2\sqrt{1-e^2}$. Therefore,

$$(L/m) = 2A/T = 2\pi a^2\sqrt{1-e^2}\ /T \ . \qquad (4.4)$$

We define Ω_0 to be the mean angular velocity of the orbit,

$$\Omega_0 \equiv (2\pi/T) \qquad \text{// radians/time} \qquad (4.5)$$

and we then have

$$(L/m) = \Omega_0\, a^2\sqrt{1-e^2} \ . \qquad (4.6)$$

Then we can then rewrite (4.1) as

$$\dot{\psi}\, r^2 = \Omega_0 a^2\sqrt{1-e^2} \ . \qquad (4.7)$$

Combining this with (1.7), $r = a(1-e^2) / [1 + e\cos\psi]$, we get

$$\dot{\psi}\ \{a(1-e^2)/[1+e\cos\psi\ ]\}^2 = \Omega_0 a^2\sqrt{1-e^2}$$

or

$$\dot{\psi} = \Omega_0\,(1-e^2)^{-3/2}\,[1+e\cos\psi\ ]^2$$

or

$$d\psi/dt = C\,[1+e\cos\psi\ ]^2 \qquad C = \Omega_0\,(1-e^2)^{-3/2} \quad . \tag{4.8}$$

This equation can be integrated from t = 0 to t and ψ = 0 to ψ,

$$d\psi/[1+e\cos\psi\ ]^2 = C\,dt$$

$$I \equiv \int_0^{\psi} d\psi'/[1+e\cos\psi'\ ]^2 = C\,t \quad . \qquad //\ \psi(t=0) = 0 \tag{4.9}$$

Using the following integrals from p172 of Ref [2] with a = 1, b = e, A = 1, B = 0, and n = 2 :

3.* $$\int \frac{dx}{a+b\cos x} = \frac{2}{\sqrt{a^2-b^2}} \arctan\left(\frac{(a-b)\tan\left(\frac{x}{2}\right)}{\sqrt{a^2-b^2}}\right) \qquad \left[a^2 > b^2\right]$$

2.554

1. $$\int \frac{A+B\cos x}{(a+b\cos x)^n}\,dx = \frac{1}{(n-1)\,(a^2-b^2)}\left[\frac{(aB-Ab)\sin x}{(a+b\cos x)^{n-1}} + \int \frac{(Aa-bB)(n-1)+(n-2)(aB-bA)\cos x}{(a+b\cos x)^{n-1}}\,dx\right]$$

the integral I may be evaluated,

$$I = (1-e^2)^{-1}\ \{\ (2/\sqrt{1-e^2}\,)\tan^{-1}[\frac{\sqrt{1-e}}{\sqrt{1+e}}\tan(\psi/2)\ ] - \frac{e\sin\psi}{1+e\cos\psi}\ \}$$

$$= (1-e^2)^{-3/2}\ \{\ 2\tan^{-1}[\frac{\sqrt{1-e}}{\sqrt{1+e}}\tan(\psi/2)\ ] - \frac{e\sqrt{1-e^2}\,\sin\psi}{1+e\cos\psi}\ \}$$

Since $C = \Omega_0\,(1-e^2)^{-3/2}$ we then find that

$$\Omega_0 t = 2\tan^{-1}[\frac{\sqrt{1-e}}{\sqrt{1+e}}\tan(\psi/2)] - \frac{e\sqrt{1-e^2}\,\sin\psi}{1+e\cos\psi} \qquad //\ \text{radians} \tag{4.10}$$

Later we shall use years as the unit of time, so then $\Omega_0 = 2\pi$ radians/year and the time span of an orbit is from t = 0 at perihelion until t = 1 year at the next perihelion. Equation (4.10) appears in Ref [3] as (8).

Looking at Fig 1.3, we can identify these angles with the solstices and equinoxes,

$\psi = \pi/2-\varphi_{per} \equiv \alpha$	March equinox	// α was defined this way in (1.9)
$\psi = \pi-\varphi_{per}$	June solstice	
$\psi = 3\pi/2 - \varphi_{per}$	Sept solstice	
$\psi = 2\pi - \varphi_{per}$	Dec solstice	

Then using (4.10), we may compute the time (0-1) and day (0-365.25) at which these events occur :

```
t := (psi)->
(1/Omega0)*(2*arctan(sqrt(1-e)*tan(psi/2)/sqrt(1+e))-e*sqrt(1-e^2)*sin(psi)/
(1+e*cos(psi)));
```

$$t := \psi \to \frac{2\arctan\left(\frac{\sqrt{1-e}\,\tan\left(\frac{1}{2}\psi\right)}{\sqrt{1+e}}\right) - \frac{e\sqrt{1-e^2}\,\sin(\psi)}{1+e\cos(\psi)}}{\Omega 0}$$

```
Omega0 := 2*Pi:  e := .0167: phiper := (Pi/180)*13.101:
tMe := evalf(t(Pi/2-phiper));evalf(%*365.25);
```

$$tMe := .2084458064$$

$$76.13483079$$

```
tJs := evalf(t(Pi-phiper));evalf(%*365.25);
```

$$tJs := .4623885582$$

$$168.8874209$$

```
tSe := evalf(1+t(3*Pi/2-phiper));evalf(%*365.25);
```

$$tSe := .7188002563$$

$$262.5417936$$

```
tDs := evalf(1+t(2*Pi-phiper));evalf(%*365.25);
```

$$tDs := .9647987070$$

$$352.3927277$$

```
alpha := Pi/2-phiper: evalf(%);
```

$$1.342140742$$

(4.11)

In the case of a circular orbit, we expect to find that $\psi = \Omega_0 t$ and that is what (4.10) gives with e→ 0. In this case, keeping the "perihelion" at the same location, the time of the March equinox is determined by $\Omega_0 t_{Me} = \psi = \pi/2-\varphi_{per} \equiv \alpha$ so that

$$t_{Me} = \alpha/\Omega_0 = (\pi/2-\varphi_{per})/2\pi \qquad // \; e = 0 \qquad (4.12)$$

and then the four times or interest are close to, but different from, those shown above, and they are separated from each other by 1/4 orbit :

```
phiper := (Pi/180)*13.101:
tMe := (Pi/2-phiper)/(2*Pi);evalf(%*365.25);
                                        tMe := .2136083334
                                            78.02044377
tJs := tMe + 1/4;evalf(%*365.25);
                                        tJs := .4636083334
                                            169.3329438
tSe := tMe + 2/4;evalf(%*365.25);
                                        tSe := .7136083334
                                            260.6454438
tDs := tMe + 3/4;evalf(%*365.25);
                                        tDs := .9636083334
                                            351.9579438
```

(4.11)$_{e=0}$

Equation (4.10) gives t(ψ) which can be numerically inverted to obtain ψ(t). Since e is so small, it is much simpler to back up and use an approximation for ψ(t). Consider again (4.8),

$$d\psi/dt = C\,[1 + e\cos\psi\,]^2 \qquad (4.8)$$

$$\approx C\,[\,1 + 2\,e\cos\psi\,]. \qquad (4.13)$$

The fractional error in this approximation is $\sim e^2 = (.0167)^2 = 3 \times 10^{-4}$. Since the orbit is nearly circular, we approximate $\psi = \Omega_0 t$ inside the sine to get (another order e^2 error contribution)

$$d\psi/dt \approx C\,[\,1 + 2\,e\cos(\Omega_0 t)\,]\ . \qquad (4.14)$$

Taking the mean of the left hand side over a year gives $\langle d\psi/dt\rangle = C$, but in our approximation this must be $C = \Omega_o$, so defining $\Omega \equiv d\psi/dt$ as the instantaneous angular velocity of the orbit at time t we get

$$\Omega(t) = \Omega_o\,[\,1 + 2\,e\cos(\Omega_0 t)\,] \qquad . \qquad (4.15)$$

Here is a plot of $\Omega(t)/\Omega_0$ as in (4.15) which can be correlated with Fig 1.3. Starting at t = 0 (Jan 3 perihelion), Ω(t) first slows down, reaching a minimum value at aphelion, then speeds back up:

```
Omega0 := 2*Pi:  e := .0167:
Omega := Omega0 * (1 + 2*e*cos(Omega0*t)):
plot([Omega/Omega0,1,1.04],t=0..1,view = [0..1,.96..1.04], color = [red,
green,green],thickness = 2);
```

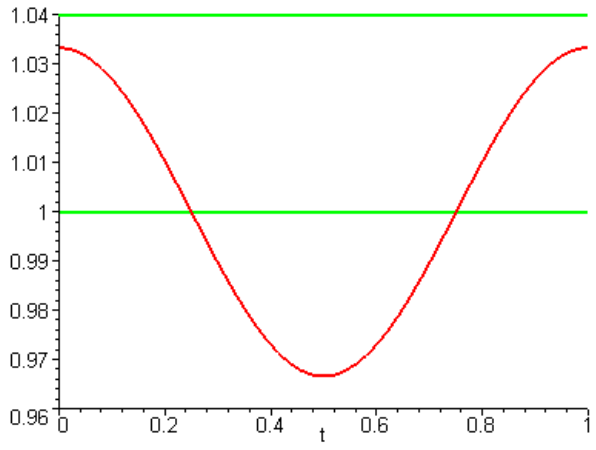

Fig 4.1

Alternatively, we can integrate (4.14) with C = Ω_o to get an expression for ψ(t),

$$d\psi/dt = \Omega_0 [\ 1 + 2e\cos(\Omega_0 t)\ ] \qquad (4.14)$$

$$\psi(t) - \psi(0) = \Omega_0 t + 2e\,\Omega_0 \int_0^t dt \cos(\Omega_0 t)$$

$$= \Omega_0 t + 2e\,\Omega_0 (1/\Omega_0)\,[\sin(\Omega_0 t)]|_0^t$$

$$= \Omega_0 t + 2e \sin(\Omega_0 t)\ . \qquad (4.16)$$

If we agree to start our clock at the instant the earth is at perihelion (Jan 3) , then ψ(0) = 0 as indicated in Fig 1.3. We already assumed this in writing ψ = Ω_0t inside the sine above. In this case,

$$\psi(t) = \Omega_0 t + 2e \sin(\Omega_0 t) \qquad \text{// radians} \qquad (4.17)$$

and using (1.9) and (1.10) we may express the angle φ' of Fig 1.3 this way,

$$\varphi'(t) = \Omega_0 t + 2e \sin(\Omega_0 t) + \varphi_{per} - \pi/2 \qquad (4.18)$$

where $\Omega_o = 2\pi$ rad/year. During a year the sine phase goes around once with a zero average value, so that

$$\langle \psi(t) - \Omega_0 t \rangle = 0\ .$$

This plot of ψ(t) - Ω_0t shows how ψ(t) in degrees deviates from straight-line clock time for t = (0,1) yr:

```
q := 2*e*sin(Omega0*t):
plot((180/Pi)*q, t = 0..1, deg = -2..2, thickness = 2, color = black);
```

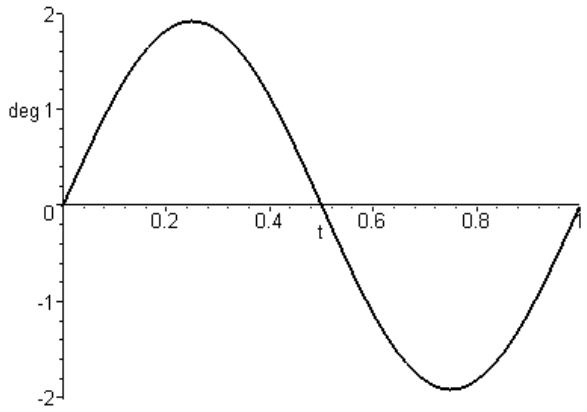

Fig 4.2

The above curve will reappear in Section 6 (e) in the discussion of the Equation of Time for the "black earth".

The preceding discussion addresses the variation in ψ due to eccentricity in the orbit of the earth around the sun. As shown in Fig 3.4, this same ψ applies to the projected sun's orbit around the ecliptic circle on the celestial sphere. However, when this red circle gets projected down onto the equator of the celestial sphere (Fig 3.5), a "tilt effect" arises which further affects azimuthal timing on that equator. This will be clarified in Section 5 below.

(b) A systematic solution for ψ(t) and estimate of error in using (4.17)

The exact (non-linear) differential equation for ψ shown in (4.8) is this

$$d\psi/dt = C\ [1 + e\cos\psi\ ]^2$$
$$= C\ [1 + 2e\cos\psi + e^2\cos^2\psi\ ]\ . \qquad (4.8)$$

One can expand ψ in a power series in smallness parameter $e \approx .0167$,

$$\psi(t) \approx \psi^{(0)}(t) + e\,\psi^{(1)}(t) + e^2\,\psi^{(2)}(t) + \ldots. \qquad (4.19)$$

where we require that for each order $\psi^{(n)}(0) = 0$, so that $\psi(0) = 0$. Now using

$$\cos(x+\varepsilon) \approx \cos(x) - \varepsilon\sin(x) + O(\varepsilon^2) \qquad (4.20)$$

we have

$$\cos\psi = \cos[\psi^{(0)}(t) + e\,\psi^{(1)}(t)] = \cos[\psi^{(0)}(t)] - e\,\psi^{(1)}(t)\sin[\psi^{(0)}(t)] + O(e^2)$$

$$\cos^2\psi = \cos^2[\psi^{(0)}(t)] + O(e)\ . \qquad (4.21)$$

Defining $c \equiv \cos[\psi^{(0)}(t)]$ and $s \equiv \sin[\psi^{(0)}(t)]$ this pair of equations becomes

$$\cos\psi = c - e\, s\, \psi^{(1)}(t) + O(e^2)$$

$$\cos^2\psi = c^2 + O(e) \ . \qquad (4.22)$$

Retaining only terms through order e^2, the right side of (4.8) becomes

$$= C\,[1+2e\{\, c - e\, s\, \psi^{(1)}(t)\} + e^2c^2]$$

$$= C\,[\ 1 +2ec - 2e^2 s\, \psi^{(1)}(t) + e^2c^2\ ]$$

$$= C\ + e\,[2Cc] + e^2[C(c^2-2s\, \psi^{(1)}(t)] \ . \qquad (4.23)$$

Balancing powers of e with the left side of (4.8) given by differentiating (4.19), we get then this set of equations,

$$d\psi^{(0)}/dt = C$$

$$d\psi^{(1)}/dt = 2Cc = 2C\cos[\psi^{(0)}(t)]$$

$$d\psi^{(2)}/dt = C\cos^2[\psi^{(0)}(t)]- 2C\sin[\psi^{(0)}(t)]\ \psi^{(1)}(t) \ . \qquad (4.24)$$

The solution to the first equation is just $\psi^{(0)}(t) = Ct$ and therefore $C = \Omega_0 = 2\pi$ radians/year,

$$\psi^{(0)}(t) = \Omega_0 t \ . \qquad \text{// solution for a perfectly circular orbit. e = 0} \qquad (4.25)$$

The remaining two equations are then

$$d\psi^{(1)}/dt = 2Cc = 2\Omega_0\cos(\Omega_0 t)$$

$$d\psi^{(2)}/dt = \Omega_0\cos^2(\Omega_0 t)- 2\,\Omega_0\sin(\Omega_0 t)\ \psi^{(1)}(t) \qquad (4.26)$$

The $\psi^{(1)}$ equation can be trivially integrated to give

$$\psi^{(1)}(t) = 2\,\sin(\Omega_0 t) \qquad (4.27)$$

so the third equation becomes

$$d\psi^{(2)}/dt = \Omega_0[\ \cos^2(\Omega_0 t)- 4\sin^2(\Omega_0 t)\ ]$$

$$= \Omega_0[\ (1/2)(1+\cos(2\Omega_0 t)) - 4(1/2)(1 - \cos(2\Omega_0 t))\ ]$$

$$= (1/2)\Omega_0[\ (1+\cos(2\Omega_0 t)) - 4\ (1 - \cos(2\Omega_0 t))\ ]$$

$$= (1/2)\Omega_0[\ (-3+5\cos(2\Omega_0 t)\ ]\ . \qquad (4.28)$$

The integral of interest in determining $\psi^{(2)}$ is

$$\int_0^t [-3+5\cos(2\Omega_0 t')\ ]\ dt' \ = \ -3t + 5/(2\ \Omega_0)\sin(2\Omega_0 t) \qquad (4.29)$$

so that

$$\psi^{(2)}(t) = \ -(3/2)\Omega_0 t\ + (5/4)\ \sin(2\Omega_0 t)\ . \qquad (4.30)$$

Therefore the solution ψ(t) through second order in eccentricity e is

$$\psi(t)\ = \ \Omega_0 t + 2e\ \sin(\Omega_0 t) + (5/4)e^2\ \sin(2\Omega_0 t)\ \ + \text{order}(e^3)\quad . \qquad (4.31)$$

The e^2 contribution is very small, being on the order of $(5/4)e^2 = (5/4)\ (.0167)^2 = 3.5 \times 10^{-4}$. Converting this from radians to degrees makes this term on the order of $1/50^{th}$ of one degree. Here is a plot of $\psi(t) - \Omega_0 t$ in degrees, with (red) and without (black) the e^2 term,

```
a := 2*e*sin(Omega0*t):
b := (5/4)*e^2*sin(2*Omega0*t):
plot(evalf((180/Pi))*[a+b,a], t= 0..1, color = [red,black]);
```

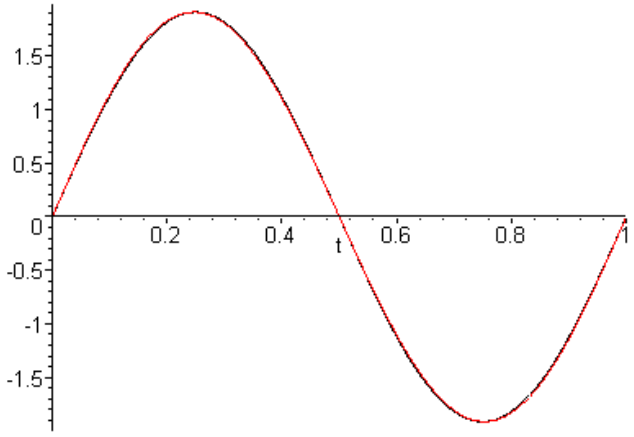

Fig 4.3

For our purposes in this document, such as plotting analemmas, there is no need to keep the e^2 term and we can use this simple approximation for ψ(t)

$$\psi(t)\ = \ \Omega_0 t + 2e\ \sin(\Omega_0 t)$$

which is the same as (4.17) obtained by our *ad hoc* method.

The result (4.31) is sometimes written this way,

$$\delta\ \equiv\ \psi(t) - \Omega_0 t\ \approx\ \ 2e\ \sin(\Omega_0 t) + (5/4)e^2\ \sin(2\Omega_0 t)\quad , \qquad (4.32)$$

where δ is then the difference between the true anomaly ψ and the mean anomaly $\Omega_0 t$ as discussed at the end of Section 1. This expression appears in the code shown in Ref [4] where the time scale is chosen so that a year is 2π units long, so t' = 2πt = $\Omega_0 t$. That code reads (kappa = e)

```
delta<-function(t,kappa) {
  return( 2*sin(t)*kappa+5/4*sin(2*t)*kappa^2 )
}
```

As a check on (4.31), let's use it to verify our earlier calculation of t_{Me} shown in (4.11) by setting t = t_{Me} in (4.31):

```
psi := Omega0*t + 2*e*sin(Omega0*t) + (5/4)*e^2*sin(2*Omega0*t);
```

$$\psi := \Omega 0\, t + 2\, e\, \sin(\Omega 0\, t) + \frac{5}{4} e^2 \sin(2\, \Omega 0\, t)$$

```
Omega0 := 2*Pi:  e := .0167:
t :=  .2084458064:
evalf(psi);
```

1.342145531

Thus, when we install t = t_{Me} = .2084458064 yrs from (4.11), we recover our $\psi_{Me} = \alpha$ as shown at the end of (4.11) to 6 decimal places accuracy. One could go on and find the e^3 and higher terms in the expansion (4.31) by the method outlined above.

5. How the Earth's Tilt Angle θ_t Varies with Time

In this section we think of θ_t as the angle of tilt of the earth's rotation axis toward or away from the sun. This angle varies between $-\theta_{tmax}$ and θ_{tmax} where θ_{tmax} is the earth's obliquity 23.4^o. This tilt θ_t is described below in a special frame of reference that rotates around the sun with the earth so that the sun and earth maintain their positions (earth on left, sun on right). Later in Section 6 (b) we show that θ_t is also the declination of the sun on the celestial sphere, its more conventional interpretation. This fact is implied by the inset in Fig 5.1 below.

We first replicate Fig 1.3 since it is closely related to the drawing we are about to present:

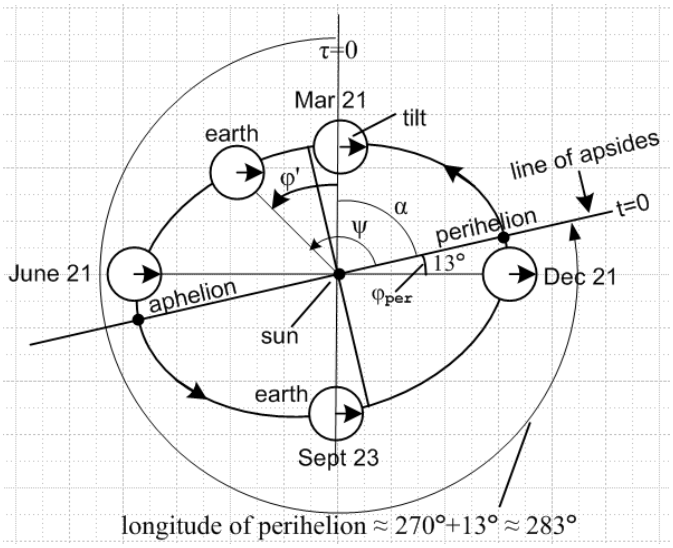

Fig 1.3

In Fig 1.3 angle φ' denotes the azimuthal position of the earth with respect to the March equinox. This angle φ' appears in the following picture, along with angle $\tilde{\varphi} = \pi - \varphi'$ and $\tilde{\theta} = \theta_{tmax}$:

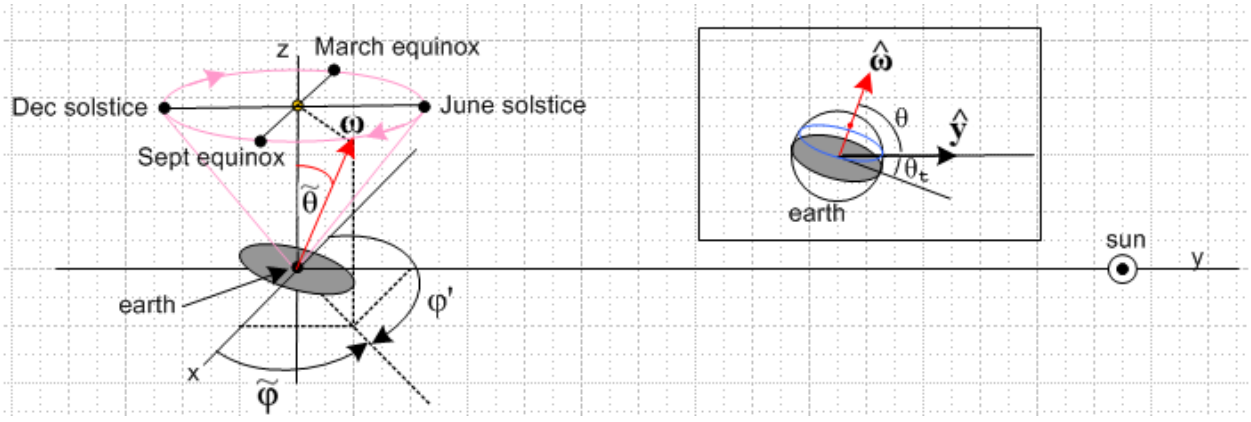

Fig 5.1

The earth is represented by the black origin dot on the left, and its equatorial plane by the gray disk. The red arrow **ω** is the angular momentum vector of the rotating earth. This vector's tip precesses clockwise

around the pink circle as the year progresses. The sun is on the right, "looking at the earth". The reader is invited to correlate this drawing and its markings with Fig 1.3. For example, when $\varphi' = 0$, in Fig 1.3 the sun sees the earth tilting to the right. The red vector on the cone in Fig 5.1 also tilts to the right as viewed from the sun when $\varphi' = 0$ (March equinox).

For the situation shown in Fig 5.1, we want to determine the location of the sun's path projected on the earth. We know that this path is a circle of constant latitude because the path is created by the earth rotating (see blue circles in Fig 3.1). We only need to find one point on this circle. The line from sun to earth-center penetrates the earth's surface at a point which must lie on this blue latitude circle of interest, since the circle is a projection of the sun's path (see Fig 5.1 inset in which $\hat{\boldsymbol{\omega}}$ is tilted toward the viewer as on the left).

First consider this standard expression for a spherical-coordinates radial unit vector in terms of the Cartesian basis vectors,

$$\hat{\mathbf{r}} = \sin\tilde{\theta}\cos\tilde{\varphi}\,\hat{\mathbf{x}} + \sin\tilde{\theta}\sin\tilde{\varphi}\,\hat{\mathbf{y}} + \cos\tilde{\theta}\,\hat{\mathbf{z}} \quad . \tag{5.1}$$

We can think of $\hat{\mathbf{r}} = \hat{\boldsymbol{\omega}}$, the direction of the red arrow. We know that $\hat{\boldsymbol{\omega}}$ is a unit vector normal to the equatorial plane of the earth. We know that $\hat{\mathbf{y}}$ points toward the sun. Therefore, the *co*latitude θ of our penetration point of interest is given by $\cos\theta = \hat{\boldsymbol{\omega}} \bullet \hat{\mathbf{y}}$ as shown in the Fig 5.1 inset**.** This colatitude θ is just the polar angle measured down from the north pole of the tilted earth to the $\hat{\mathbf{y}}$ vector. The corresponding latitude we shall call $\theta_t = \pi/2 - \theta$. Now,

$$\cos\theta = \cos(\pi/2 - \theta_t) = \sin\theta_t \quad . \tag{5.2}$$

Therefore,

$$\sin\theta_t = \cos\theta = \hat{\boldsymbol{\omega}} \bullet \hat{\mathbf{y}} = \sin\tilde{\theta}\sin\tilde{\varphi} = \sin\theta_{tmax}\sin(\pi - \varphi') = \sin\theta_{tmax}\sin\varphi' \tag{5.3}$$

and we obtain the key result which is

$$\sin\theta_t(t) = \sin\theta_{tmax}\sin\varphi'(t) \qquad \text{where } \theta_{tmax} = 23^o. \tag{5.4}$$

To check the result, at June solstice $\varphi' = \pi/2$ so $\sin\theta_t = \sin\theta_{tmax} * 1 \Rightarrow \theta_t = \theta_{tmax}$. Things check similarly at Dec solstice and the equinoxes. From Fig 3.4, $\varphi' = \psi - \alpha$, so using ψ from (4.31) we get

$$\varphi'(t) = \psi - \alpha = \Omega_0 t + 2e\sin(\Omega_0 t) + (5/4)e^2\sin(2\Omega_0 t) - \alpha \qquad // \ \alpha = \pi/2 - \varphi_{per}$$

so (5.4) becomes

$$\theta_t(t) = \sin^{-1}\{\sin\theta_{tmax}\sin(\psi - \alpha)\}$$

$$= \sin^{-1}\{\sin\theta_{tmax}\sin[\Omega_0 t + 2e\sin(\Omega_0 t) + (5/4)e^2\sin(2\Omega_0 t) - \alpha]\} \tag{5.5}$$

where $t = 0$ at perihelion Jan 3. The following black plot of $\theta_t(t)$ shows (5.5) with only its first term $\Omega_0 t$, while the red plot shows (5.5) with the first two terms. The e^2 term makes no visible difference so we don't bother with it.

```
Omega0 := 2*Pi:  e := .0167:
thtmax := (Pi/180)*23.4382:  phiper := (Pi/180)*13.101: alpha := Pi/2 - phiper:
thetat  := arcsin(sin(thtmax)*sin(Omega0*t + 2*e*sin(Omega0*t) - alpha)):
thetatapprox := arcsin(sin(thtmax)*sin(Omega0*t - alpha)):
plot(evalf(180/Pi)*[thetat,thetatapprox],t =0..1,thickness=2,color=[red,black]);
```

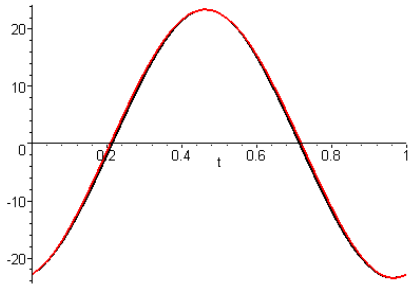

Fig 5.2

The extremes of the plot are $\theta_t \approx \pm 23^o$ at the solstices, while the zero crossings are the equinoxes $\theta_t = 0$. At t = 0 Jan 3 (left edge) we are just after December solstice where the sun was at - 23^o.

A geometric interpretation of θ_t.

It is possible to *interpret* θ_t as "the amount of tilt of the earth toward the sun" according to the following somewhat elaborate construction :

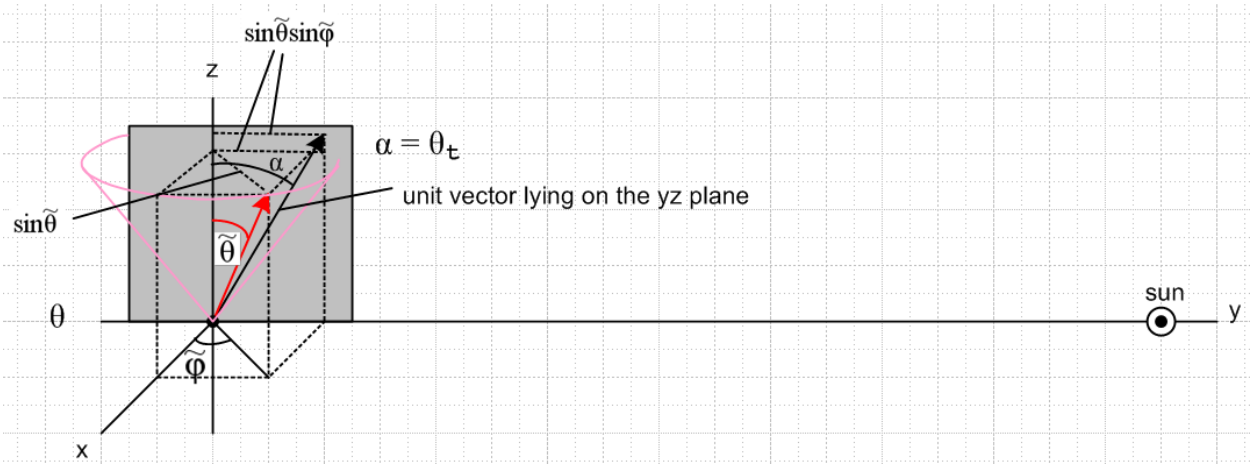

Fig 5.3

The distance from the z axis to the tip of the red unit vector is $\sin\tilde{\theta}$ as indicated. This distance can then be projected onto the gray wall (the yz plane) to get a distance $\sin\tilde{\theta}\sin\tilde{\varphi}$. We then create a black *unit* vector on the gray wall which has this distance $\sin\tilde{\theta}\sin\tilde{\varphi}$ as its y component. If we denote the angle of this black unit vector relative to the z axis as α, then $\sin\alpha = \sin\tilde{\theta}\sin\tilde{\varphi}$. But in (5.3) we had $\sin\tilde{\theta}\sin\tilde{\varphi} = \sin\theta_t$. Therefore, $\alpha = \theta_t$ and then we can interpret θ_t as the "amount of tilt of the earth toward the sun". Note that the black arrow is *not* the projection of the red one onto the wall, because the projected arrow would be too short to be a unit vector.

6. Coordinates of the Sun on the Celestial Sphere

(a) Cartesian coordinates x,y,z and velocity of the sun in Frame S

Consider this picture showing the tilted red ecliptic circle and the black equatorial circle on the celestial sphere (compare to Fig 3.5 above).

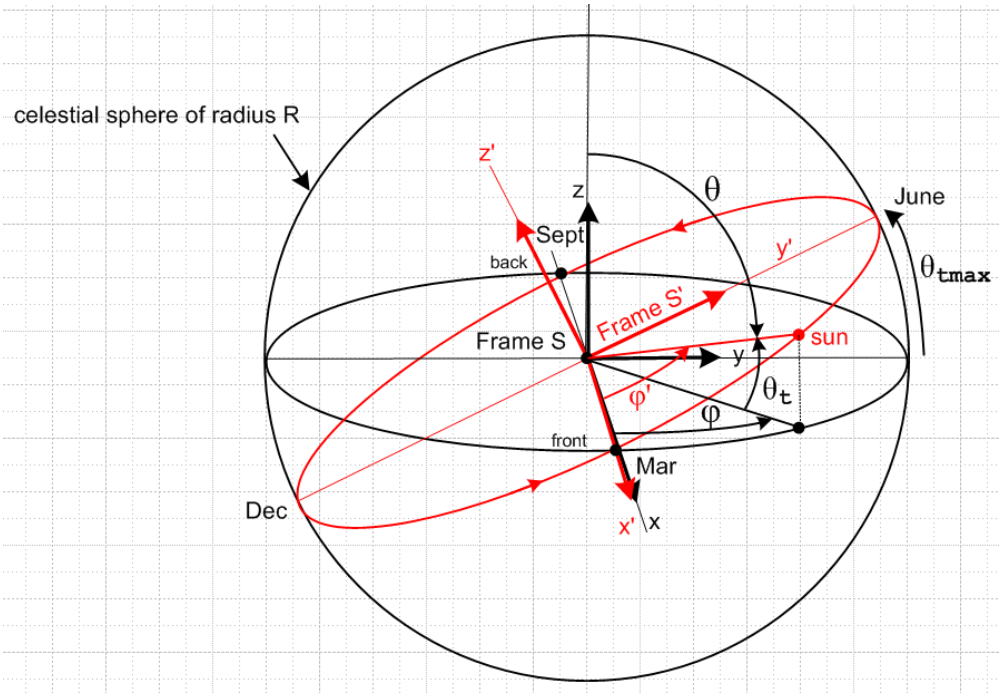

Fig 6.1

The black equatorial circle is associated with Frame S with x,y,z axes, while the ecliptic red circle is associated with Frame S' with x',y',z' axes. Staring at the figure one sees that

$$\hat{\mathbf{z}}' = R_{\mathbf{x}}(\theta_{\mathbf{tmax}})\,\hat{\mathbf{z}} \qquad \text{and} \qquad \hat{\mathbf{x}}' = \hat{\mathbf{x}} \;\Rightarrow\; x' = x$$
$$\hat{\mathbf{y}}' = R_{\mathbf{x}}(\theta_{\mathbf{tmax}})\,\hat{\mathbf{y}} \tag{6.1}$$

where $\theta_{\mathbf{tmax}} = 23^{\mathbf{o}}$. According to the rule that vectors rotate backwards from the unit vectors (see Appendix B), we then have in 2D that

$$\mathbf{r} = R_{\mathbf{x}}(\theta_{\mathbf{tmax}})\mathbf{r}' \quad \Rightarrow \quad \begin{pmatrix} y \\ z \end{pmatrix} = \begin{pmatrix} \cos\theta_{\mathbf{tmax}} & -\sin\theta_{\mathbf{tmax}} \\ \sin\theta_{\mathbf{tmax}} & \cos\theta_{\mathbf{tmax}} \end{pmatrix} \begin{pmatrix} y' \\ z' \end{pmatrix} \quad \Rightarrow$$

$$y = \cos\theta_{\mathbf{tmax}} y' - \sin\theta_{\mathbf{tmax}} z'$$
$$z = \sin\theta_{\mathbf{tmax}} y' + \cos\theta_{\mathbf{tmax}} z' \quad . \tag{6.2}$$

When $\theta_{\mathbf{tmax}} = 0$ this is clearly valid. When $\theta_{\mathbf{tmax}} = \pi/2$ we get $y = -z'$ and $z = y'$ which agrees with the picture -- just a validity check on the sign of the sine.

Now our interest is not so much in arbitrary points, but in points which lie on the red circle. For these points we have $z' = 0$ so the above becomes

$$x = x'$$
$$y = \cos\theta_{\mathbf{tmax}}\, y'$$
$$z = \sin\theta_{\mathbf{tmax}}\, y' \quad . \qquad (6.3)$$

In Frame S' we can define spherical coordinates r',θ',φ' related to x',y,'z' according to the usual equations,

$$x' = r'\sin\theta'\cos\varphi' \qquad y' = r'\sin\theta'\sin\varphi' \qquad z' = r'\cos\theta' \quad .$$

But again, for points on the red circle, $\theta' = \pi/2$ and $r' = R$ so

$$x' = R\cos\varphi' \qquad y' = R\sin\varphi' \qquad z' = 0 \quad .$$

Inserting these expressions into (6.3) then gives

$$x = R\cos\varphi'$$
$$y = R\cos\theta_{\mathbf{tmax}}\sin\varphi'$$
$$z = R\sin\theta_{\mathbf{tmax}}\sin\varphi' \; . \qquad (6.4)$$

Equations (6.4) give the Cartesian coordinates of the sun in Frame S. Recall that angle φ' appearing in (6.4) is given by,

$$\varphi' = \psi - \alpha \qquad \textit{(1.10)}$$
$$\psi = \Omega_{\mathbf{0}}t + 2e\sin(\Omega_{\mathbf{0}}t) + (5/4)e^{\mathbf{2}}\sin(2\Omega_{\mathbf{0}}t) \quad // + \text{order } e^{\mathbf{3}} \text{ which we ignore} \qquad \textit{(4.31)}$$
$$\alpha = \pi/2 - \varphi_{\mathbf{per}} \qquad \textit{(1.9)} \qquad (6.5)$$

where t = 0 is perihelion (Jan 3) and t = 1 is the next perihelion.

The velocity and acceleration of the sun's motion on the celestial sphere (as seen by our Frame S observer) can be obtained by differentiating (6.4). For example,

$$\dot{x} = -R\,\dot{\varphi}'\sin\varphi'$$
$$\dot{y} = R\,\dot{\varphi}'\cos\theta_{\mathbf{tmax}}\cos\varphi'$$
$$\dot{z} = R\,\dot{\varphi}'\sin\theta_{\mathbf{tmax}}\cos\varphi' \qquad (6.6)$$

where from (4.18) $\dot{\varphi}' = \dot{\psi} = \Omega_{\mathbf{0}}\,[1 + 2e\cos(\Omega_{\mathbf{0}}t) + (5/2)\cos(2\Omega_{\mathbf{0}}t)]$.

(b) Spherical coordinates θ, φ of the sun in Frame S

In Frame S, for points on the celestial sphere, we can define spherical coordinates R,θ,φ related to x,y,z according to the usual relations,

$$x = R\sin\theta\cos\varphi$$
$$y = R\sin\theta\sin\varphi$$
$$z = R\cos\theta \quad . \qquad (6.7)$$

Comparison of equations (6.7) with (6.4) shows that,

$$\begin{aligned} &\sin\theta\cos\varphi = \cos\varphi' \\ &\sin\theta\sin\varphi = \cos\theta_{\mathbf{tmax}}\sin\varphi' \\ &\cos\theta = \sin\theta_{\mathbf{tmax}}\sin\varphi' \quad . \end{aligned} \tag{6.8}$$

Dividing the second equation by the first gives

$$\tan\varphi = \cos\theta_{\mathbf{tmax}}\ \tan\varphi' \quad . \tag{6.9}$$

We then have from the last line in (6.8) and (6.9),

$$\begin{aligned} &\theta(t) = \cos^{-1}[\sin\theta_{\mathbf{tmax}}\sin\varphi'(t)] \\ &\varphi(t) = \tan^{-1}[\cos\theta_{\mathbf{tmax}}\ \tan\varphi'(t)] \\ &r(t) = R \end{aligned} \tag{6.10}$$

where φ' given by (6.5). Equation (6.10) gives the official Frame S spherical coordinates of the projection of the sun on the celestial sphere.

We now claim that our polar angle θ(t) is related to the tilt angle $\theta_{\mathbf{t}}(t)$ introduced in Section 5 (which was the angle of tilt of the earth toward the sun at some time t) by,

$$\theta(t) = \pi/2 - \theta_{\mathbf{t}}(t). \qquad \Rightarrow \qquad \sin\theta_{\mathbf{t}} = \cos\theta \quad . \tag{6.11}$$

If this were true, the last line of (6.8) would say

$$\sin\theta_{\mathbf{t}} = \sin\theta_{\mathbf{tmax}}\sin\varphi' \quad .$$

But this is the same as (5.4). Therefore (6.11) is correct and, since θ is the polar angle or colatitude of the sun on the celestial sphere, $\theta_{\mathbf{t}}$ must be the latitude or "declination" of the sun on the celestial sphere, as shown in Fig 6.1. Equations (6.10) can then be written as (the first equation then agrees with (5.5))

$$\begin{aligned} &\theta_{\mathbf{t}}(t) = \sin^{-1}[\sin\theta_{\mathbf{tmax}}\sin\varphi'(t)] \qquad \text{// latitude (declination) of sun on celestial sphere} \\ &\varphi(t) = \tan^{-1}[\cos\theta_{\mathbf{tmax}}\ \tan\varphi'(t)] \qquad \text{// longitude (right ascension) of sun on celestial sphere} \end{aligned} \tag{6.12}$$

where the sun azimuth φ', ψ and α as given by (6.5). Thus,

$$\begin{aligned} &\theta_{\mathbf{t}}(t) = \sin^{-1}[\sin\theta_{\mathbf{tmax}}\sin(\psi-\alpha)] \\ &\varphi(t) = \tan^{-1}[\cos\theta_{\mathbf{tmax}}\tan(\psi-\alpha)] \quad . \\ &\psi = \Omega_{\mathbf{0}}t + 2e\sin(\Omega_{\mathbf{0}}t) + (5/4)e^{\mathbf{2}}\sin(2\Omega_{\mathbf{0}}t) \quad \text{// + order } e^{\mathbf{3}} \text{ which we ignore} \qquad \textit{(4.31)} \\ &\alpha = \pi/2 - \varphi_{\mathbf{per}} \qquad \textit{(1.9)} \end{aligned} \tag{6.13}$$

These equations gives the declination $\theta_{\mathbf{t}}$ and right ascension φ of the sun on the celestial sphere during the year t = (0,1) where t = 0 is perihelion, Jan 3.

It is useful to think of a **fictitious sun** which orbits the earth in a perfectly circular orbit (e=0) and whose ecliptic lies in the equatorial plane of the celestial sphere ($\theta_{tmax} = 0$). For this sun the above equations are

$$\theta_{t,f}(t) = 0$$
$$\varphi_f(t) = \tan^{-1}[\tan(\psi_f - \alpha)] = \psi_f - \alpha = \Omega_0 t - \alpha$$
$$\psi_f = \Omega_0 t$$
$$\alpha = \pi/2 - \varphi_{per} \qquad \text{// fictitious sun} \qquad (1.9) \qquad (6.14)$$

Interpretation of the second equation of (6.12):

The equation in question and its time derivative are,

$$\varphi(t) = \tan^{-1}[\cos\theta_{tmax} \tan\varphi'(t)] \qquad (6.12)$$

$$\dot{\varphi}(t) = \{ \cos\theta_{tmax} / [\cos^2\varphi' + \cos^2\theta_{tmax}\sin^2\varphi']\} \dot{\varphi}' . \qquad (6.12)_{dot}$$

Near the equinoxes $\varphi' = 0$ and π one has $\cos^2\varphi' \approx 1$ and $\sin^2\varphi' \approx 0$ so then $\dot{\varphi} \approx \cos\theta_{tmax} \dot{\varphi}'$. The angular velocity $\dot{\varphi}$ at the equinoxes is *slower* than $\dot{\varphi}'$ by factor $\cos\theta_{tmax}$. The simple geometric reason for this, as Fig 6.1 shows, is that the two circular paths intersect at angle θ_{tmax} at the equinoxes, and the projection of speed on the ecliptic to speed on the equatorial circle is reduced by this factor at the equinoxes.

Near the solstices $\varphi' = \pi/2$ and $3\pi/2$ one has $\cos^2\varphi' \approx 0$ and $\sin^2\varphi' \approx 1$ so then $\dot{\varphi} \approx \dot{\varphi}'/ \cos\theta_{tmax}$. At these two points $\dot{\varphi}$ runs *faster* than $\dot{\varphi}'$ by factor $1/\cos\theta_{tmax}$. The geometric reason for this is slightly less obvious: at solstice an "orange slice" of the celestial sphere is thinner at the ecliptic than at the equator so the projection of a speed on the ecliptic gets magnified by factor $1/ \cos\theta_{tmax}$.

Both these situations are illustrated on the left of the following figure, where the red arrows indicate speed along the ecliptic and green arrows speed along the equatorial circle.

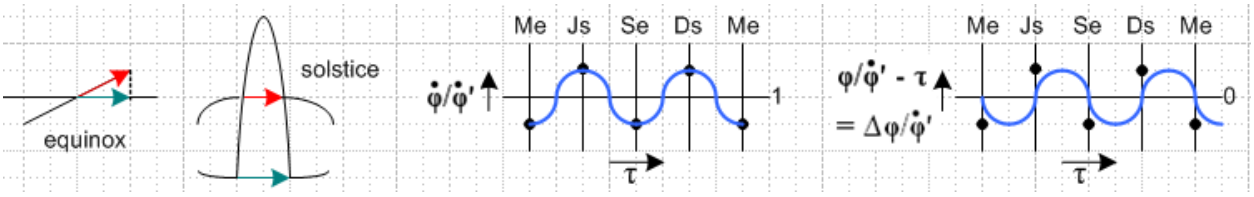

The first graph shows crudely how the ratio of angular speeds must therefore vary during the year where $\tau = 0$ is March equinox (Me). In the case that $\dot{\varphi}' =$ constant, φ must be generally as shown on the far right, since the derivative of this graph gives the first graph minus 1. This situation applies to "the blue earth" below where $e = 0$ so $\dot{\varphi}' = \Omega_0$. The actual plot is the blue curve in Fig 6.5 below, which begins at $t = 0$ which is the Jan 3 perihelion. Thus we have a physical interpretation of "the tilt effect" on azimuthal velocity of the sun. More generally, this interpretation explains why the full equation of time shown as the red curve in Fig 6.5 has two "cycles" during the year. The lower amplitude cycle and the higher amplitude cycle create the small and large lobes of the analemma in Section 11. Roughly the difference between the red curve and the blue curve in Fig 6.5 is the black curve which accounts for "the eccentricity effect" on azimuthal speed as studied in Section 4.

(c) The Equation of Time

The difference between the azimuth (right ascension) of the sun and that of the fictitious sun is known as "the Equation of Time" and is given by (6.13) and (6.14) above (using ψ and α as in (6.13) above)

$$\Delta\varphi(t) \equiv \varphi - \varphi_{\mathbf{f}} = \tan^{-1}[\cos\theta_{\mathbf{tmax}}\ \tan(\psi-\alpha)] - (\Omega_{\mathbf{0}}t-\alpha) \tag{6.15a}$$

$$= \tan^{-1}[\cos\theta_{\mathbf{tmax}}\ \tan(\psi-\alpha)] - \tan^{-1}[\ \tan(\Omega_{\mathbf{0}}t-\alpha)] \tag{6.15b}$$

$$= \tan^{-1}\left[\frac{\cos\theta_{\mathbf{tmax}}\ \tan(\psi-\alpha) - \tan(\Omega_{\mathbf{0}}t-\alpha)}{1 + \cos\theta_{\mathbf{tmax}}\ \tan(\psi-\alpha)\ \tan(\Omega_{\mathbf{0}}t-\alpha)}\right] \tag{6.15c}$$

where the last line follows from this identity from p 121 of Ref [5]

$$\textbf{4.24.15}\quad \operatorname{Arctan} u \pm \operatorname{Arctan} v = \operatorname{Arctan}\left(\frac{u \pm v}{1 \mp uv}\right) \quad . \tag{6.16}$$

There are other variations of (6.15). One can multiply top and bottom by $\cos(\psi-\alpha)\cos(\Omega_{\mathbf{0}}t-\alpha)$ to get

$$\Delta\varphi(t) = \tan^{-1}\left[\frac{-\sin(\Omega_{\mathbf{0}}t-\alpha)\cos(\psi-\alpha) + \cos\theta_{\mathbf{tmax}}\ \sin(\psi-\alpha)\cos(\Omega_{\mathbf{0}}t-\alpha)}{\cos(\psi-\alpha)\cos(\Omega_{\mathbf{0}}t-\alpha) + \cos\theta_{\mathbf{tmax}}\ \sin(\psi-\alpha)\sin(\Omega_{\mathbf{0}}t-\alpha)}\right] \ . \tag{6.15d}$$

A somewhat peculiar form is given in equation (21) of Ref [3] as

$$-\Delta\varphi(t) = \tan^{-1}\left[\frac{-\sin(\psi-\Omega_{\mathbf{0}}t) + \tan^{\mathbf{2}}(\theta_{\mathbf{tmax}}/2)\ \sin(\psi+\Omega_{\mathbf{0}}t-2\alpha)}{\cos(\psi-\Omega_{\mathbf{0}}t) + \tan^{\mathbf{2}}(\theta_{\mathbf{tmax}}/2)\ \cos(\psi+\Omega_{\mathbf{0}}t-2\alpha)}\right] \equiv \mu(t) \ . \tag{6.15e}$$

To verify (6.15e), comparing to (6.15c) we have to show that

$$(-1)\frac{\cos\theta_{\mathbf{tmax}}\ \tan(\psi-\alpha) - \tan(\Omega_{\mathbf{0}}t-\alpha)}{1 + \cos\theta_{\mathbf{tmax}}\ \tan(\psi-\alpha)\ \tan(\Omega_{\mathbf{0}}t-\alpha)} = \frac{-\sin(\psi-\Omega_{\mathbf{0}}t) + \tan^{\mathbf{2}}(\theta_{\mathbf{tmax}}/2)\ \sin(\psi+\Omega_{\mathbf{0}}t-2\alpha)}{\cos(\psi-\Omega_{\mathbf{0}}t) + \tan^{\mathbf{2}}(\theta_{\mathbf{tmax}}/2)\ \cos(\psi+\Omega_{\mathbf{0}}t-2\alpha)} \quad ?$$

Let $\theta_{\mathbf{tmax}} = x$, $\psi = y$, $\alpha = a$, $\Omega_{\mathbf{0}}t = c$, then we have to show that

$$\frac{\cos x\ \tan(y-a) - \tan(c-a)}{1 + \cos x\ \tan(y-a)\ \tan(c-a)} = (-1)\frac{-\sin(y-c) + \tan^{\mathbf{2}}(x/2)\ \sin(y+c-2a)}{\cos(y-c) + \tan^{\mathbf{2}}(x/2)\ \cos(y+c-2a)} \quad ?$$

$$\frac{A}{B} = -\frac{C}{D} \quad ?$$

$$AD + BC = 0 \quad ?$$

This is a job for Maple, and the conclusion is that we can remove all the question marks above :

```
unprotect('D'); unassign('D');
A := cos(x)*tan(y-a)-tan(c-a):
B := 1 + cos(x)*tan(y-a)*tan(c-a):
C := -sin(y-c) + tan(x/2)^2*sin(y+c-2*a):
D := cos(y-c) + tan(x/2)^2*cos(y+c-2*a):
E := (A*D+B*C):
E1 := simplify(E):
E2 := E1 * (cos(x)+1) * cos(y-a) * cos(c-a):
E3 := expand(E2):
simplify(E3);
                              0
```

Wiki provides a nice plot of the equation of time (see Ref [4] or Fig 6.8 below) which is based on the form (6.15e) above. Here is some of that code, where $\Omega_0 = 1$ (year = 2π time units) , $\delta \equiv \psi - t$, $\varepsilon \equiv \theta_{tmax}$, $\kappa \equiv e$. This δ is the same as our (4.32). [German Zähler = numerator, Nenner = denominator]

```
epsilon=23.45*2*pi/360
alpha  =78.5 *2*pi/360
kappa  =0.016722

mu<-function(t,epsilon,alpha,kappa) {
   zaehl= -sin(delta(t,kappa))+tan(epsilon/2)^2*sin(2*(t-alpha)+delta(t,kappa))
   nenn =  cos(delta(t,kappa))+tan(epsilon/2)^2*cos(2*(t-alpha)+delta(t,kappa))
   return( atan(zaehl/nenn) )
}
psi<-function(t) {
  return(t+delta(t))
}
delta<-function(t,kappa) {
   return( 2*sin(t)*kappa+5/4*sin(2*t)*kappa^2 )
}
```

Fig 6.2

(d) Plots of φ (right ascension of the sun) and Δφ (equation of time)

Note: For all plots in this section and the next, the left edge of the plot is t = 0, perihelion, Jan 3.

Defining q and s by

$$q \equiv 2e \sin(\Omega_0 t) + (5/4)e^2 \sin(2\Omega_0 t) \qquad // \psi - \Omega_0 t$$
$$s \equiv \Omega_0 t + \varphi_{per} - \pi/2 \qquad // \Omega_0 t - \alpha \;;\; s+q = \psi - \alpha \qquad (6.17)$$

we shall make four versions of equation (6.13), $\varphi(t) = \tan^{-1}[\cos\theta_{tmax}\tan(\psi - \alpha)]$, and we associate a color with each version (note that $\varphi_{red} = \varphi$ = right ascension of the actual sun)

$$\varphi_{red}(t) = \tan^{-1}[\cos\theta_{tmax}\ \tan(s+q)] \qquad // \text{the actual sun}$$
$$\varphi_{blue}(t) = \tan^{-1}[\cos\theta_{tmax}\ \tan(s)] \qquad // e = 0 \text{ so blue means tilt only}$$
$$\varphi_{black}(t) = \tan^{-1}[\tan(s+q)] = s+q \qquad // \theta_{tmax} = 0 \text{ so black is eccentricity only}$$
$$\varphi_{green}(t) = \tan^{-1}[\tan(s)] = s = \varphi_f(t) \qquad // e = 0 \text{ AND } \theta_{tmax} = 0 \text{ (green is fictitious sun)} \qquad (6.18)$$

Our first task is to enter the four functions with 2012 parameters,

```
t := n/diy:   diy := 365.25:
Omega0 := 2*Pi: e := .016708: tleft := 0:
thtmax := (Pi/180)*23.4382: phiper := (Pi/180)*13.101:
q := 2*e*sin(Omega0*t) + (5/4)*e^2*sin(2*Omega0*t) :
s := Omega0*t+phiper-Pi/2:
f_red   := arctan2Pis(cos(thtmax)*sin(s+q), cos(s+q)):
f_blue  := arctan2Pis(cos(thtmax)*sin(s), cos(s)):
f_black := arctan2Pis(sin(s+q), cos(s+q)):
f_green := arctan2Pis(sin(s), cos(s)):
```

The function arctan2Pis is a special version of $\tan^{-1}$ which causes the arctangent to be a continuous function even if it goes out of the nominal range $(0,2\pi)$. It keeps internal track of a certain winding number as discussed in Appendix A. The scale of the data is radians. The full ψ function is used in q, even though the e^2 term really makes no significant difference (see Section 4). Here then is a plot of the four functions,

```
winit(-1): s1 := plot(f_red,n = 0..diy, color = red):
winit(-1): s2 := plot(f_blue,n = 0..diy, color = blue):
winit(-1): s3 := plot(f_black,n = 0..diy, color = black):
winit(-1): s4 := plot(f_green,n = 0..diy, color = green):
display([s1,s2,s3,s4,s4]);
```

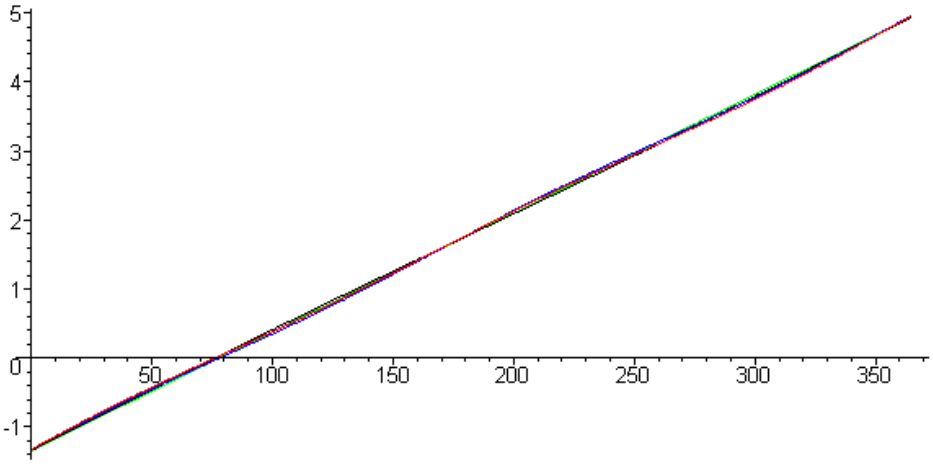

radians

Fig 6.3

It is far more interesting to plot the equations of time which are these differences,

$$\Delta\varphi_{red}(t) \equiv \varphi_{red}(t) - \varphi_{green}(t)$$
$$\Delta\varphi_{blue}(t) \equiv \varphi_{blue}(t) - \varphi_{green}(t) \quad // \; e = 0 \text{ so only tilt is active}$$
$$\Delta\varphi_{black}(t) \equiv \varphi_{black}(t) - \varphi_{green}(t) \quad // \; \theta_{tmax} = 0 \text{ so only eccentricity is active}$$
$$\Delta\varphi_{green}(t) \equiv \varphi_{green}(t) - \varphi_{green}(t) = 0 \qquad (6.19)$$

$$\Delta\varphi_{pink}(t) \equiv \Delta\varphi_{blue}(t) + \Delta\varphi_{black}(t) = \varphi_{blue}(t) + \varphi_{black}(t) - 2\,\varphi_{green}(t) \qquad (6.20)$$

where recall φ_{green} is for the fictitious sun:

```
d_red := f_red - f_green:
d_blue := f_blue - f_green:
d_black := f_black - f_green:
d_pink := f_black + f_blue - 2*f_green:
d_green := 0:
s1 := plot(d_red,n = 0..diy, color = red):
s2 := plot(d_blue,n = 0..diy, color = blue):
s3 := plot(d_black,n = 0..diy, color = black):
s4 := plot(d_pink,n = 0..diy, color = pink):
s5 := plot(d_green,n = 0..diy, color = green, thickness = 3):
display([s1,s2,s3,s4,s5], thickness = 2);
```

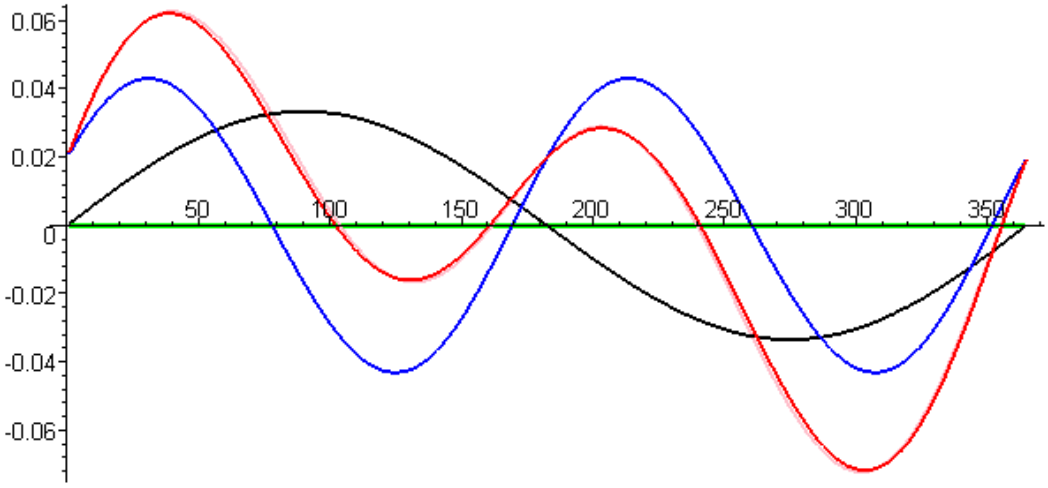

radians

Fig 6.4

Comment: The same plot is obtained with this single command (but see end of Appendix A)

```
plot([d_red,d_blue,d_black,d_pink,d_green],n=0..diy,thickness=2,
color = [red,blue,black,pink,green]);
```

Looking at the vertical scale (radians), one sees that these $\Delta\varphi$ differences are all quite small compared to the previous plot. Since the pink curve visibly deviates somewhat from the red curve, we see that the often assumed fact that $\Delta\varphi_{blue}(t) + \Delta\varphi_{black}(t) = \Delta\varphi_{red}(t)$ is only approximately true, and this is due to the relative smallness of angle θ_{tmax}. But qualitatively, we see that the red curve is roughly the sum of the blue curve and the black curve, so the effects of orbital tilt (blue curve) and eccentricity (black curve) are roughly additive. We shall dispense with the pink curve from now on.

By adding a factor of $180/\pi$ we can replot in degrees,

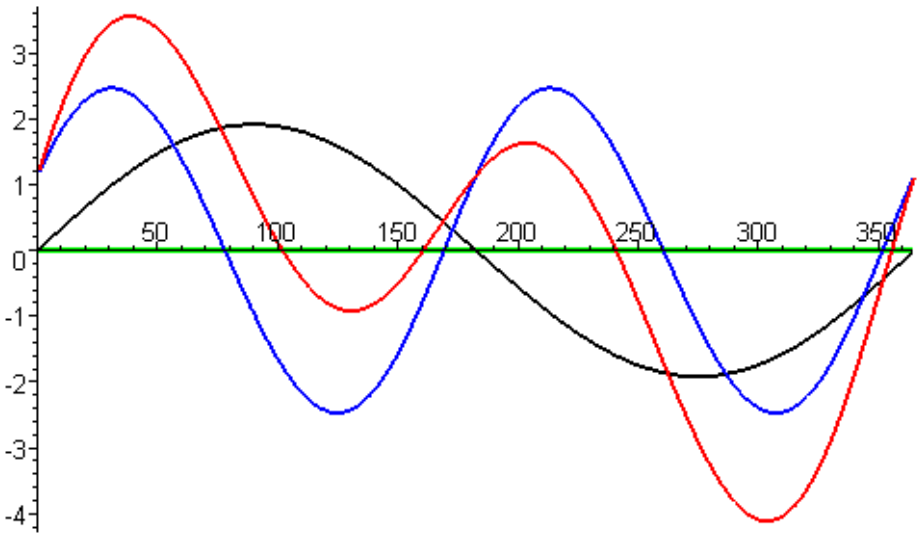

degrees

Fig 6.5

Since 15 degrees of azimuth corresponds to one hour of earth rotation time (1 degree = 4 minutes), one often sees the equation of time plotted with minutes as the vertical scale (factor now $4(180/\pi)$)

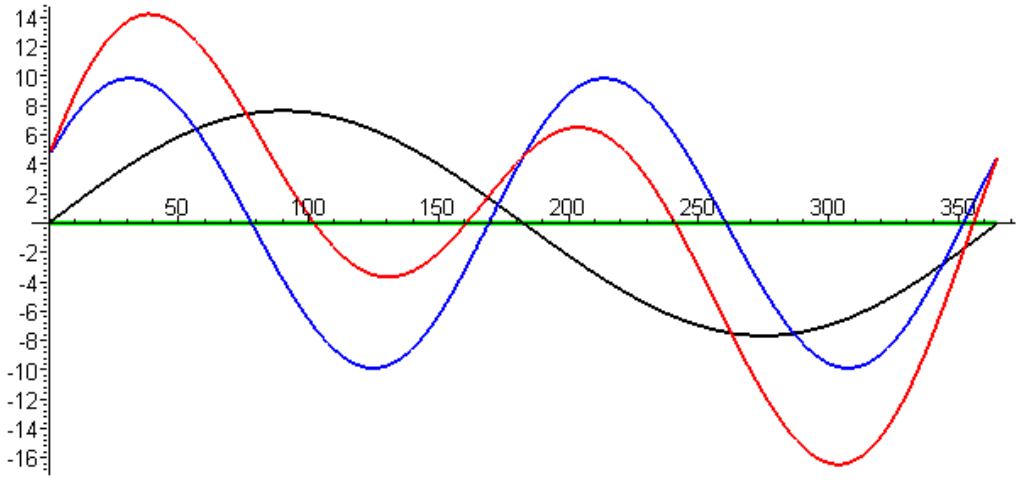

minutes

Fig 6.6

In these plots the left edge t = 0 corresponds to perihelion or Jan 3.

The actual expressions for the three $\Delta\varphi$ differences are

$$\Delta\varphi_{\mathbf{red}}(t) \equiv \varphi_{\mathbf{red}}(t) - \varphi_{\mathbf{green}}(t) = \tan^{-1}[\cos\theta_{\mathbf{tmax}}\ \tan(s+q)] - s$$
$$\Delta\varphi_{\mathbf{blue}}(t) \equiv \varphi_{\mathbf{blue}}(t) - \varphi_{\mathbf{green}}(t) = \tan^{-1}[\cos\theta_{\mathbf{tmax}}\ \tan(s)] - s$$
$$\Delta\varphi_{\mathbf{black}}(t) \equiv \varphi_{\mathbf{black}}(t) - \varphi_{\mathbf{green}}(t) = (s+q) - s = q \qquad (6.21)$$

$$q \equiv 2e\sin(\Omega_{\mathbf{0}}t) + (5/4)e^{2}\sin(2\Omega_{\mathbf{0}}t) \qquad // = \psi - \Omega_{\mathbf{0}}t$$
$$s \equiv \Omega_{\mathbf{0}}t + \varphi_{\mathbf{per}} - \pi/2 \qquad // = \Omega_{\mathbf{0}}t - \alpha\ ;\ s+q = \psi-\alpha \qquad (6.17)$$

It seems clear that the mean value of $\Delta\varphi_{\mathbf{black}}(t) = 2e\sin(\Omega_0 t) + (5/4)e^2\sin(2\Omega_0 t)$ will be zero over the year since it is an odd function of t (think of the year as running t = -1/2 to +1/2) and is periodic.

The mean of $\Delta\varphi_{\mathbf{blue}}(t)$ is also zero, but that fact is less obvious. One can write, using the trig identity (6.16) quoted above,

$$\Delta\varphi_{\mathbf{blue}}(t) = \tan^{-1}[\cos\theta_{\mathbf{tmax}}\ \tan(s)]\ - \tan^{-1}[\tan(s)]\ = \tan^{-1}\left[\frac{(\cos\theta_{\mathbf{tmax}} - 1)\tan(s)}{1 + \cos\theta_{\mathbf{tmax}}\tan^2(s)}\right], \qquad (6.22)$$

where $s = \Omega_0 t - \alpha = \Omega_0 t'$, where t' is a shifted time. Then the function is odd in t' and also periodic in t', so the blue mean is in fact 0. The mean of $\Delta\varphi_{\mathbf{pink}}(t) \equiv \Delta\varphi_{\mathbf{blue}}(t) + \Delta\varphi_{\mathbf{black}}(t)$ is then exactly 0 as well.

The above argument fails on the red mean,

$$\Delta\varphi_{\mathbf{red}}(t) = \tan^{-1}[\cos\theta_{\mathbf{tmax}}\ \tan(s+q)]\ - \tan^{-1}[\tan(s)]\ = \tan^{-1}\left[\frac{\cos\theta_{\mathbf{tmax}}\tan(s+q) - \tan(s)}{1 + \cos\theta_{\mathbf{tmax}}\tan(s)\tan(s+q)}\right]. \qquad (6.23)$$

Nevertheless, the red mean is very small and we can regard it as being zero to a few parts in a million. Here are the means computed by Maple by approximating each integral as a sum of diy = 365 rectangles (Maple cannot integrate a function which uses arctan2Pis)

```
diy := 365:   # need an integer here. Recall that t = n/diy, hence n := i.
for i from 1 to diy do n := i; del_black[i] := evalf(f_black-f_green); od:
for i from 1 to diy do n := i; del_red[i]   := evalf(f_red-f_green); od:
for i from 1 to diy do n := i; del_blue[i]  := evalf(f_blue-f_green); od:
mean_black := sum(del_black[j],j=1..diy)/diy;
mean_blue  := sum(del_blue[j], j=1..diy)/diy;
mean_red   := sum(del_red[j],  j=1..diy)/diy;
```

$$mean\_black := -.1178082192\ 10^{-10}$$

$$mean\_blue := .9013698630\ 10^{-10}$$

$$mean\_red := .3981059452\ 10^{-5}$$

Now replacing $\varphi_{\mathbf{red}}$ by its original symbol φ, and with $\varphi_{\mathbf{f}} = \Omega_0 t - \alpha$ as in (6.14), we have

red mean = 0 = $< \Delta\varphi_{\mathbf{red}} > = <\Delta\varphi> = <\varphi> - <\varphi_{\mathbf{f}}>$

so

$<\varphi_{\mathbf{f}}> = <\varphi>$.

This last equation says that during the year, the mean value of the azimuth of the fictitious sun is the same as the mean value of the azimuth of the actual sun. For this reason, the fictitious sun is often referred to as the **mean fictitious sun**. This fictitious sun is represented by the horizontal green line in the equation of time plots above, and the distance between the red curve and the green line is then the azimuthal distance between the actual sun and the mean fictitious sun at any instant of time t. As the plots show, the fictitious sun's right ascension matches that of the actual sun exactly four times per year (places where $\Delta\varphi = 0$).

Frequently the equation of time plot is shown in minutes with the vertical axis flipped (- 4 (180/π)),

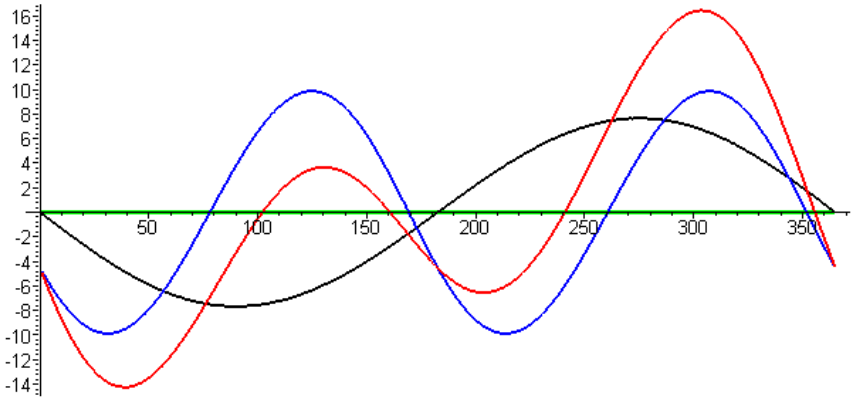

minutes

Fig 6.7

As a check on our plotting methods, if we temporarily set our orbital parameters to those quoted above in Ref [4] ,

e = .016722 $\theta_{tmax} = 23.45$ $\varphi_{per} = 11.5^{o}$ $\alpha = \pi/2 - \varphi_{per} = 78.5^{o}$

we can replot the flipped Fig 6.7 and then superpose that on this wiki plot of Ref [4],

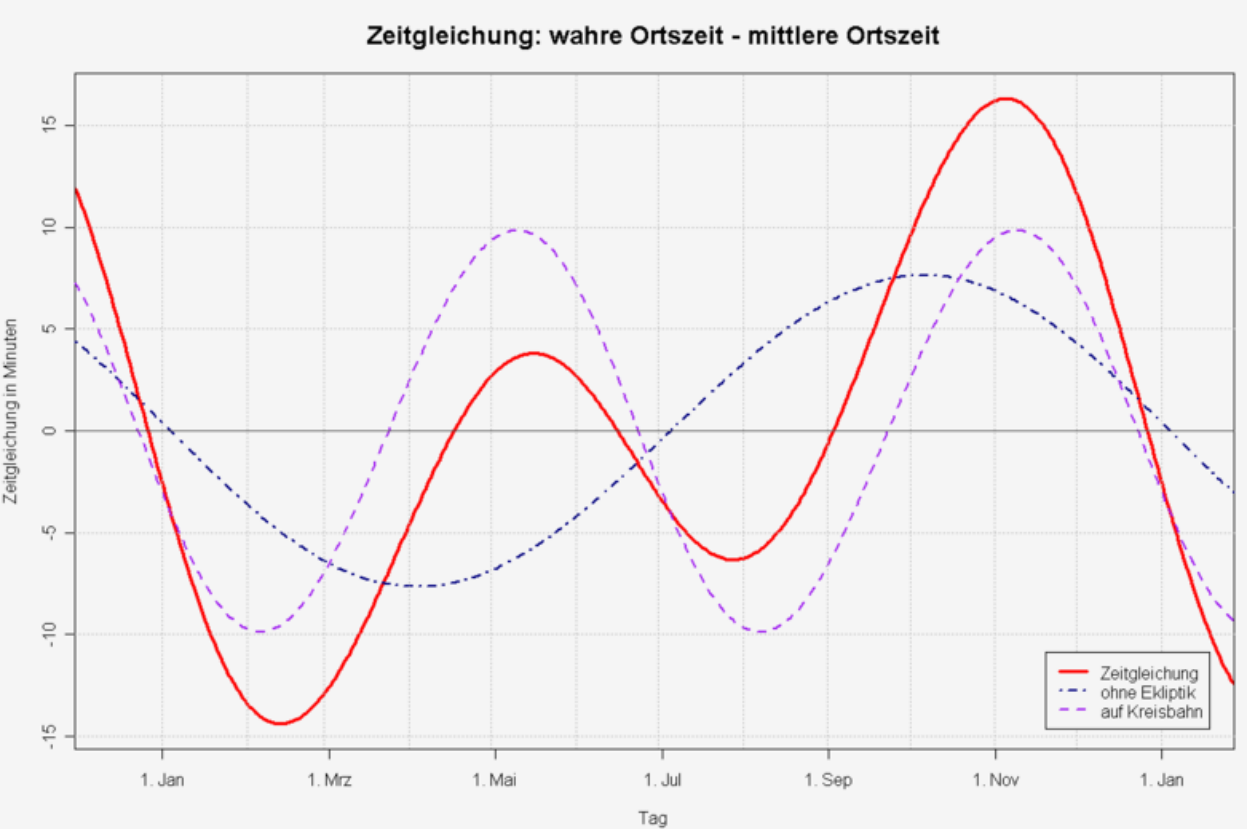

Fig 6.8

Here is the superposed result after axes are adjusted to match in both directions,

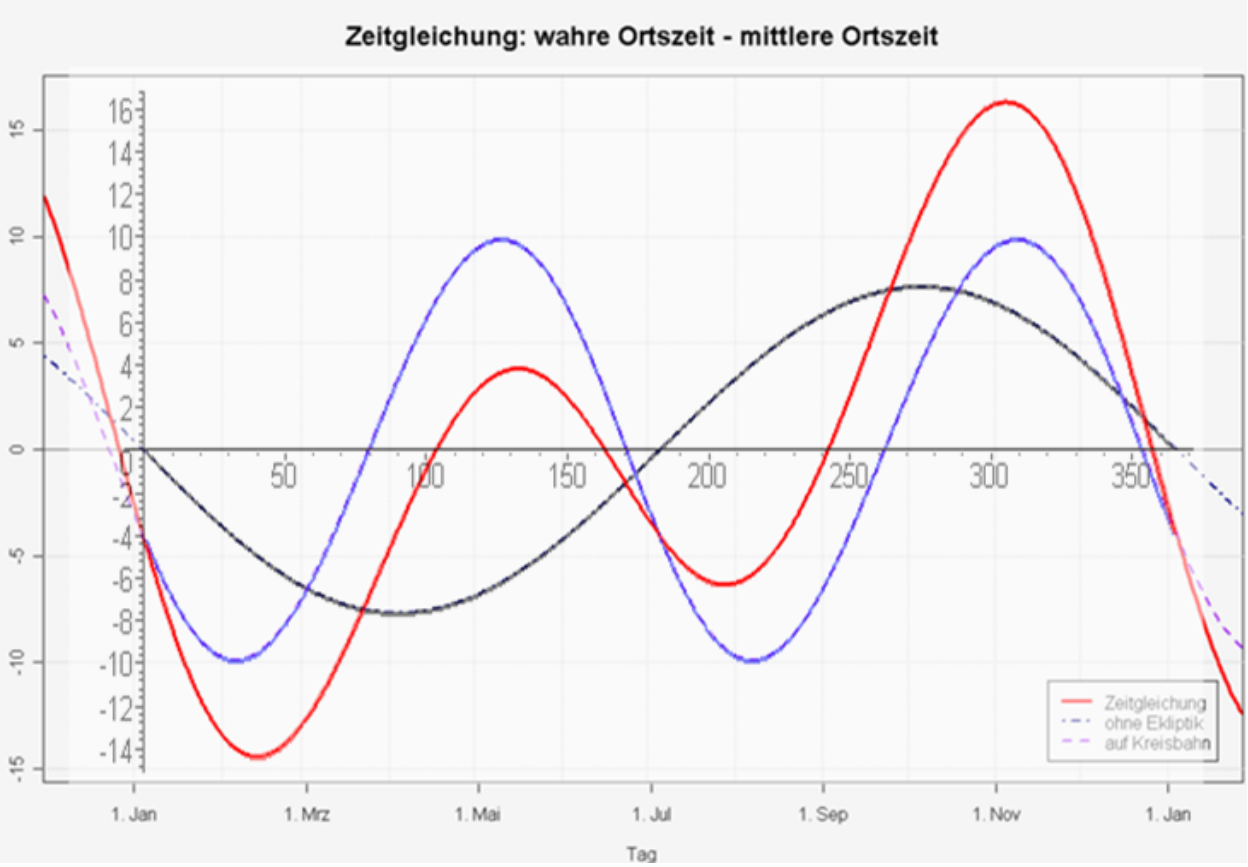

Fig 6.9

and the plots are basically identical. Their parameters seem to match the year 1919 according to the NASA source http://aom.giss.nasa.gov/srorbpar.html ,

Year (A.D.)	Eccentricity	Obliquity (degrees)	Long. of Perihel. (degrees)
1915	0.016738	23.4508	281.440
1916	0.016738	23.4507	281.457
1917	0.016737	23.4506	281.474
1918	0.016737	23.4504	281.491
1919	0.016736	23.4503	281.508
1920	0.016736	23.4502	281.525
1921	0.016736	23.4500	281.542
1922	0.016735	23.4499	281.560
1923	0.016735	23.4498	281.577
1924	0.016734	23.4497	281.594
1925	0.016734	23.4495	281.611

Table 6.1

In Section 8 we shall investigate the significance of these Δφ plots in terms of sundials and analemmas.

(e) Plots of θ_t (declination of the sun)

Using the same q and s shown in (6.17)

$$q \equiv 2e\sin(\Omega_0 t) + (5/4)e^2\sin(2\Omega_0 t) \quad // \psi - \Omega_0 t$$
$$s \equiv \Omega_0 t + \varphi_{per} - \pi/2 \quad // \Omega_0 t - \alpha \;;\; s+q = \psi-\alpha \qquad (6.17)$$

we can write the four "color" versions of the θ_t equation in (6.13) as

$$\theta_{t,red}(t) = \sin^{-1}[\sin\theta_{tmax}\sin(s+q)] \quad // \text{the actual sun}$$
$$\theta_{t,blue}(t) = \sin^{-1}[\sin\theta_{tmax}\sin(s)] \quad // e = 0 \text{ so blue means tilt only}$$
$$\theta_{t,black}(t) = 0 \quad // \theta_{tmax} = 0 \text{ so black is eccentricity only}$$
$$\theta_{t,green}(t) = 0 \quad // e = 0 \text{ AND } \theta_{tmax} = 0 \text{ (fictitious sun)} \qquad (6.24)$$

Having Maple plot the red and blue functions in the same manner as done above,

```
K := (180/Pi):
g_red := K*arcsin(sin(thtmax)*sin(s+q)):
g_blue := K*arcsin(sin(thtmax)*sin(s)):
plot([g_red,g_blue],n = 0..diy, color=[red,blue]);
```

we find that $\theta_{t,red}$ and $\theta_{t,blue}$ are nearly identical over the year, with the red being slightly above the blue near t = 75 and 275 days,

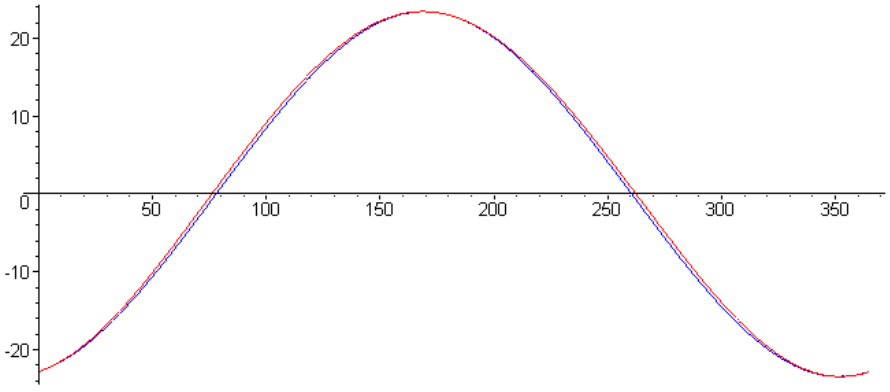

degrees Fig 6.10

We can plot $\theta_{t,red} - \theta_{t,blue}$ to see the small effect that eccentricity adds to the tilt-only curve:

```
plot(g_red - g_blue,n = 0..diy, color=[red,blue],thickness=2);
```

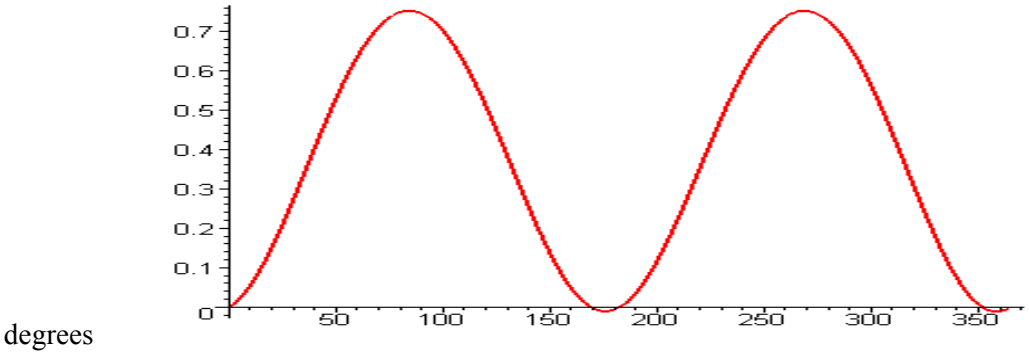

Fig 6.11

Since $\theta_{t,blue}(t)$ is an odd function of t and is periodic in t, we get $< \theta_{t,blue}(t)> = 0$. Since the difference plotted above is mostly positive, it must be that the mean of $<\theta_{t,red}(t)>$ is positive. Computing the means we find

```
mean_blue := evalf(Int(g_blue,n=0..diy)/diy);
mean_red := evalf(Int(g_red,n=0..diy)/diy);
```

$$mean\_blue := .1099775941\ 10^{-8}$$

$$mean\_red := .3786855627$$

7. Coordinates of the Sun in an Arbitrary Frame S' Glued to the Earth

(a) Setup: $\theta_1, \varphi_1, \varphi_b, \varphi_{b0}, \tau, t_{Me}$

Frame S of Fig 6.1 continues as Frame S in this new drawing, a frame fixed relative to the celestial sphere with $\mathbf{e_1} = \hat{\mathbf{x}}$, $\mathbf{e_2} = \hat{\mathbf{y}}$, $\mathbf{e_3} = \hat{\mathbf{z}}$. We discard Frame S' of Fig 6.1 and replace it with the one shown here, a new Frame S' glued to the rotating earth ("east" basis vector $\mathbf{e'_1}$ points mostly away from the viewer),

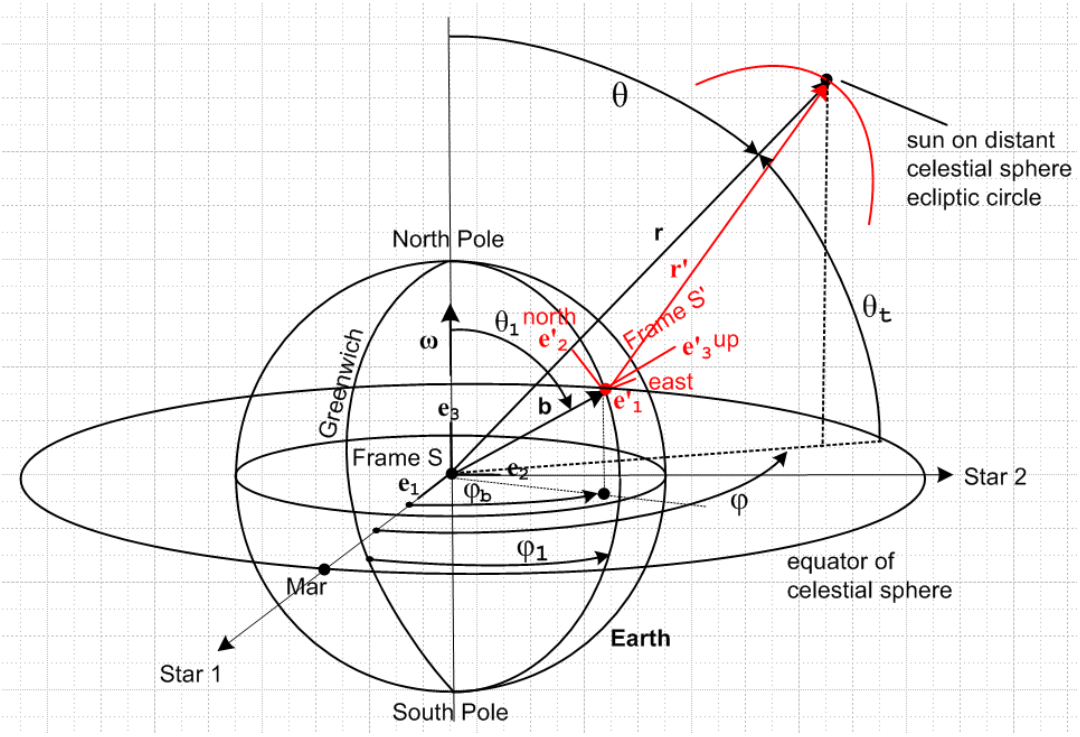

Fig 7.1

Star 1 is some star one sees looking from the earth through the March equinox point on the celestial sphere. In 2012 this happens to be somewhere in the Pisces constellation (but it is still called "the First Point of Aries" ♈, where it was 2000 years ago). Recall (Section 3(d)) that the equinox moves 1/72 degree along the ecliptic each year due to astronomical precession, causing it to also move on the celestial equator, so a new "Star 1" has to be found each year. Thus, Frame S very slowly rotates, a fact we ignore below.

A system of spherical coordinates for Frame S has these unit basis vectors at the observer's location **b** on the earth's surface,

$$\hat{\mathbf{r}} = \mathbf{e'_3} \qquad \hat{\boldsymbol{\theta}} = -\mathbf{e'_2} \qquad \hat{\boldsymbol{\varphi}} = \mathbf{e'_1} \ , \tag{7.1}$$

where we associate each of these unit basis vectors with a Frame S' unit basis vector.

Again, the earth is rotating counterclockwise in the above figure which is a snapshot at time t. The red Frame S' rotates with the earth, the black Frame S is essentially fixed relative to the stars.

The observation site is placed on the earth at polar coordinates (θ_1, φ_1) where as usual θ_1 is measured down from the north pole (colatitude), and φ_1 is the longitude measured east of the Greenwich meridian.

It is convenient now to define a shifted time coordinate $\tau \equiv t - t_{Me}$ where t_{Me} is the time from perihelion to March equinox as computed in (4.11). Then $\tau = 0$ at March equinox which is the basic azimuthal reference time in Fig 7.1. This distinction is very important:

t = time ranging 0 to 1 year where t = 0 at perihelion
τ = time ranging 0 to 1 year where $\tau = 0$ at March equinox

$$\tau = t - t_{Me} \ . \tag{7.2}$$

The time t was convenient for the work done in Section 4 concerning orbital eccentricity, while τ is convenient in our current context because $\tau = 0$ when the sun is at 0^o right ascension at March equinox, see Fig 3.5.

Let φ_{b0} be the right ascension that vector **b** had at $\tau = 0$. Then at any later time,

$$\varphi_b = \varphi_{b0} + \omega_s \tau \ = \varphi_{bo} + \omega_s t - \omega_s t_{Me}. \tag{7.3}$$

We use the sidereal rate ω_s because φ_b is relative to the celestial sphere which is at rest with respect to the stars. We use $+\omega_s$ because the earth is rotating counterclockwise causing φ_b to increase.

Therefore, the location of the observation point is given in Frame S spherical coordinates by

$$\mathbf{b}(\tau) = (R_E, \theta_1, \varphi_b(\tau)) \ . \tag{7.4}$$

The sun in Fig 7.1 is taken to be the projection of the sun on the celestial sphere. This sphere has a very large radius $R >> r_{S\text{-}E} >>> R_E$. The position of this sun projection in Frame S spherical coordinates is given by

$$\mathbf{r} = (R, \theta, \varphi) \ = \ (R, \pi/2 - \theta_t, \varphi) \tag{7.5}$$

where the two angles φ and θ_t are given by (6.13) and appear in Figs 6.1 and 7.1. Here φ is the right ascension and θ_t is the declination of the sun on the celestial sphere.

In Cartesian coordinates the sun position (7.5) is

$$\begin{aligned} x &= R \sin(\pi/2-\theta_t) \cos\varphi &&= R \cos\theta_t \cos\varphi \\ y &= R \sin(\pi/2-\theta_t) \sin\varphi &&= R \cos\theta_t \sin\varphi \\ z &= R \cos(\pi/2-\theta_t) &&= R \sin\theta_t \end{aligned} \tag{7.6}$$

$$\mathbf{r} = x\,\hat{\mathbf{x}} + y\,\hat{\mathbf{y}} + z\,\hat{\mathbf{z}} \ = x\,\mathbf{e_1} + y\,\mathbf{e_2} + z\,\mathbf{e_3}$$

where we have used $\sin(\pi/2-\beta) = \cos\beta$ and $\cos(\pi/2-\beta) = \sin\beta$. Equations (7.6) are the same as equations (6.7) since $\sin\theta = \cos\theta_t$ and $\cos\theta = \sin\theta_t$.

(b) Obtaining a value for φ_{b0} in terms of φ_{G0}

Let $\varphi_G(\tau)$ be the right ascension of the projected Greenwich meridian at time τ. We know that at any time

$$\varphi_b(\tau) - \varphi_G(\tau) = \varphi_1$$

where it is understood that everything is mod 2π. Therefore

$$\varphi_b(0) - \varphi_G(0) = \varphi_1$$

or

$$\varphi_{b0} = \varphi_1 + \varphi_{G0} \ . \qquad (7.7)$$

Here φ_{G0} is the right ascension of Greenwich on the last March equinox. This can be obtained from

$$\varphi_{G0} = [\ 12{:}00 - (\text{Greenwich mean time at March equinox})\ ] * 15^0 \ . \qquad (7.8)$$

For example, *if* at the March equinox (our $\tau = 0$) the Greenwich clock read exactly noon = 12:00, then the Greenwich meridian was exactly facing the sun so its projection onto the celestial sphere had right ascension 0^o. If the Greenwich clock instead read 11:00 = 11AM at equinox, then the projection of the Greenwich meridian onto the celestial sphere lay at right ascension + 15^o at $\tau = 0$.

Here is some data from http://aom.giss.nasa.gov/srver4x3.html ,

Orbital Events Tropical Year = 365.2425 (days) Greenwich Mean Time is used

Year	Vernal Equinox	Summer Solstice	Autumnal Equinox	Winter Solstice	Perihelion	Aphelion
2000	3/20 7:30	6/21 1:44	9/22 17:16	12/21 13:27	1/03 23:21	7/04 14:15
2001	3/20 13:19	6/21 7:32	9/22 23:05	12/21 19:16	1/03 5:35	7/04 20:29
2002	3/20 19:08	6/21 13:20	9/23 4:54	12/22 1:06	1/03 11:49	7/05 2:43
2003	3/21 0:58	6/21 19:08	9/23 10:42	12/22 6:56	1/03 18:03	7/05 8:57
2004	3/20 6:47	6/21 0:56	9/22 16:31	12/21 12:46	1/04 0:17	7/04 15:11
2005	3/20 12:36	6/21 6:44	9/22 22:20	12/21 18:35	1/03 6:31	7/04 21:25
2006	3/20 18:25	6/21 12:32	9/23 4:08	12/22 0:25	1/03 12:45	7/05 3:39
2007	3/21 0:14	6/21 18:21	9/23 9:57	12/22 6:15	1/03 18:59	7/05 9:53
2008	3/20 6:04	6/21 0:09	9/22 15:46	12/21 12:04	1/04 1:13	7/04 16:07
2009	3/20 11:53	6/21 5:57	9/22 21:34	12/21 17:54	1/03 7:27	7/04 22:21
2010	3/20 17:42	6/21 11:45	9/23 3:23	12/21 23:44	1/03 13:40	7/05 4:35
2011	3/20 23:31	6/21 17:33	9/23 9:12	12/22 5:34	1/03 19:54	7/05 10:49
2012	3/20 5:20	6/20 23:21	9/22 15:01	12/21 11:23	1/04 2:08	7/04 17:03
2013	3/20 11:10	6/21 5:09	9/22 20:49	12/21 17:13	1/03 8:22	7/04 23:17
2014	3/20 16:59	6/21 10:57	9/23 2:38	12/21 23:03	1/03 14:36	7/05 5:31
2015	3/20 22:48	6/21 16:46	9/23 8:27	12/22 4:53	1/03 20:50	7/05 11:45
2016	3/20 4:37	6/20 22:34	9/22 14:15	12/21 10:42	1/04 3:04	7/04 17:59

Table 7.1

For example, in 2012 the March equinox occurred at 05:20 GMT so we find

$$\varphi_{G0} = [\ 12{:}00 - 05{:}20\ ] * 15^0 = (12 - 5.33) * 15^0 = 100.05^o = 1.75 \text{ radians}$$

and then $\varphi_{b0} = \varphi_1 + \varphi_{G0}$ gives the constant φ_{b0} which appears in the various equations below.

(c) Cartesian coordinates x',y',z' and velocity of the sun in Frame S'

We wish to know **r'**, the position of the celestial sphere sun as viewed from rotating Frame S' . Our general relation is (see Fig 7.1)

$$\mathbf{r} = \mathbf{r}' + \mathbf{b} \, .$$

Since R >> b = R_E we have

$$\mathbf{r}' \approx \mathbf{r} \, . \tag{7.9}$$

As shown in Ref [6] Appendix A (A.13.c), at some arbitrary point r,θ,φ in Frame S the Cartesian unit vectors are given in terms of the spherical unit vectors according to

$$\begin{aligned}
\hat{\mathbf{x}} &= \cos\varphi\sin\theta\, \hat{\mathbf{r}} + \cos\varphi\cos\theta\, \hat{\boldsymbol{\theta}} - \sin\varphi\, \hat{\boldsymbol{\varphi}} \\
\hat{\mathbf{y}} &= \sin\varphi\sin\theta\, \hat{\mathbf{r}} + \sin\varphi\cos\theta\, \hat{\boldsymbol{\theta}} + \cos\varphi\, \hat{\boldsymbol{\varphi}} \\
\hat{\mathbf{z}} &= \cos\theta\, \hat{\mathbf{r}} - \sin\theta\, \hat{\boldsymbol{\theta}} \, .
\end{aligned} \tag{7.10}$$

We wish to apply these equations at our observation point $\mathbf{b} = (R_E,\theta_1,\varphi_b)$, and we wish to convert to the Frame S' basis vectors $\mathbf{e'}_n$, so we make these edits (using 7.1),

$$\theta \to \theta_1 \qquad \varphi \to \varphi_b \qquad \hat{\mathbf{r}} \to \mathbf{e'}_3 \qquad \hat{\boldsymbol{\theta}} \to -\mathbf{e'}_2 \qquad \hat{\boldsymbol{\varphi}} \to \mathbf{e'}_1$$

to get

$$\begin{aligned}
\hat{\mathbf{x}} &= \cos\varphi_b \sin\theta_1\, \mathbf{e'}_3 - \cos\varphi_b \cos\theta_1\, \mathbf{e'}_2 - \sin\varphi_b\, \mathbf{e'}_1 \\
\hat{\mathbf{y}} &= \sin\varphi_b \sin\theta_1\, \mathbf{e'}_3 - \sin\varphi_b \cos\theta_1\, \mathbf{e'}_2 + \cos\varphi_b\, \mathbf{e'}_1 \\
\hat{\mathbf{z}} &= \cos\theta_1\, \mathbf{e'}_3 + \sin\theta_1\, \mathbf{e'}_2 \quad .
\end{aligned} \tag{7.11}$$

Therefore

$$\begin{aligned}
\mathbf{r}' \approx \mathbf{r} &= x\, \hat{\mathbf{x}} + y\, \hat{\mathbf{y}} + z\, \hat{\mathbf{z}} \\
&= x\,(\cos\varphi_b\sin\theta_1\, \mathbf{e'}_3 - \cos\varphi_b\cos\theta_1\, \mathbf{e'}_2 - \sin\varphi_b\, \mathbf{e'}_1) \\
&\quad + y\,(\sin\varphi_b\sin\theta_1\, \mathbf{e'}_3 - \sin\varphi_b\cos\theta_1\, \mathbf{e'}_2 + \cos\varphi_b\, \mathbf{e'}_1) \\
&\quad + z\,(\cos\theta_1\, \mathbf{e'}_3 + \sin\theta_1\, \mathbf{e'}_2) \\
&= [-x\sin\varphi_b + y\cos\varphi_b]\mathbf{e'}_1 \\
&\quad + [-x\cos\varphi_b\cos\theta_1 - y\sin\varphi_b\cos\theta_1 + z\sin\theta_1]\mathbf{e'}_2 \\
&\quad + [\, x\cos\varphi_b\sin\theta_1 + y\sin\varphi_b\sin\theta_1 + z\cos\theta_1]\mathbf{e'}_3
\end{aligned} \tag{7.12}$$

$$= x' \mathbf{e'_1} + y' \mathbf{e'_2} + z' \mathbf{e'_3}$$

so that the Cartesian sun location coordinates in Frame S' are given by

$$\begin{aligned} x' &= -x \sin\varphi_b + y \cos\varphi_b \\ y' &= -x \cos\varphi_b \cos\theta_1 - y \sin\varphi_b \cos\theta_1 + z \sin\theta_1 \\ z' &= x \cos\varphi_b \sin\theta_1 + y \sin\varphi_b \sin\theta_1 + z \cos\theta_1 . \end{aligned} \tag{7.13}$$

Next, into these three expressions we insert our previous results (7.6),

$$\begin{aligned} x &= R \cos\theta_t \cos\varphi \\ y &= R \cos\theta_t \sin\varphi \\ z &= R \sin\theta_t \end{aligned} \tag{7.6}$$

to get: :

$$\begin{aligned} x' &= -x \sin\varphi_b + y \cos\varphi_b \\ &= -R \cos\theta_t \cos\varphi \sin\varphi_b + R \cos\theta_t \sin\varphi \cos\varphi_b \\ &= R \cos\theta_t [\sin\varphi \cos\varphi_b - \cos\varphi \sin\varphi_b] \\ &= R \cos\theta_t \sin(\varphi - \varphi_b) \end{aligned}$$

$$\begin{aligned} y' &= -x \cos\varphi_b \cos\theta_1 - y \sin\varphi_b \cos\theta_1 + z \sin\theta_1 \\ &= -R \cos\theta_t \cos\varphi \cos\varphi_b \cos\theta_1 - R \cos\theta_t \sin\varphi \sin\varphi_b \cos\theta_1 + R \sin\theta_t \sin\theta_1 \\ &= R [\sin\theta_t \sin\theta_1 - \cos\theta_t \cos\theta_1 (\cos\varphi \cos\varphi_b + \sin\varphi \sin\varphi_b)] \\ &= R [\sin\theta_t \sin\theta_1 - \cos\theta_t \cos\theta_1 \cos(\varphi - \varphi_b)] \end{aligned}$$

$$\begin{aligned} z' &= x \cos\varphi_b \sin\theta_1 + y \sin\varphi_b \sin\theta_1 + z \cos\theta_1 \\ &= R \cos\theta_t \cos\varphi \cos\varphi_b \sin\theta_1 + R \cos\theta_t \sin\varphi \sin\varphi_b \sin\theta_1 + R \sin\theta_t \cos\theta_1 \\ &= R [\cos\theta_t \sin\theta_1 (\cos\varphi \cos\varphi_b + \sin\varphi \sin\varphi_b) + \sin\theta_t \cos\theta_1 \\ &= R [\cos\theta_t \sin\theta_1 \cos(\varphi - \varphi_b) + \sin\theta_t \cos\theta_1] \\ &= R [\sin\theta_t \cos\theta_1 + \cos\theta_t \sin\theta_1 \cos(\varphi - \varphi_b)] \end{aligned}$$

The last three results may be summarized ($\mathbf{r'} \approx x' \mathbf{e'_1} + y' \mathbf{e'_2} + z' \mathbf{e'_3}$) ,

$$\begin{aligned} x' &= R \cos\theta_t \sin(\varphi - \varphi_b) \\ y' &= R [\sin\theta_t \sin\theta_1 - \cos\theta_t \cos\theta_1 \cos(\varphi - \varphi_b)] \\ z' &= R [\sin\theta_t \cos\theta_1 + \cos\theta_t \sin\theta_1 \cos(\varphi - \varphi_b)] \end{aligned} \tag{7.14}$$

where θ_t and φ are given by (6.13) and φ_b by (7.3).

Equations (7.14) give the Cartesian coordinates of the sun's location on the celestial sphere in Frame S' which rotates with the earth.

As shown in Fig 7.1, the phase $(\varphi_b - \varphi)$ takes all values in the range $0,2\pi$ during a 24 hour day, with φ_b doing most of the moving (in the positive direction). If we are only interested in using (7.14) to plot the daily trajectory of the sun, we can treat $p \equiv (\varphi_b - \varphi)$ as a generic parametric argument p which runs 0 to 2π

during the day. Such an argument can then be written p = ωt as t runs 0 to 24 hours(ω = 2π/24 rad/hr). We then obtain this version of (7.14) suitable for plotting the daily trajectory of the sun :

$$x' = -R\cos\theta_{\mathbf{t}}\sin(\omega t) \qquad \text{// valid only for making trajectory plots}$$
$$y' = R\,[\sin\theta_{\mathbf{t}}\sin\theta_{\mathbf{1}} - \cos\theta_{\mathbf{t}}\cos\theta_{\mathbf{1}}\cos(\omega t)]$$
$$z' = R\,[\sin\theta_{\mathbf{t}}\cos\theta_{\mathbf{1}} + \cos\theta_{\mathbf{t}}\sin\theta_{\mathbf{1}}\cos(\omega t)] \quad . \qquad (7.15)$$

One might wonder now about the location of the mean fictitious sun in Frame S'. Recall from (7.3) the right ascension of the observer site (projected onto the celestial sphere)

$$\varphi_{\mathbf{b}}(\tau) = \varphi_{\mathbf{b0}} + \omega_{\mathbf{s}}\tau \quad . \qquad \textit{(7.3)}$$

For the mean fictitious sun we have from (6.14) that

$$\varphi_{\mathbf{f}} = \Omega_{\mathbf{0}}t - \alpha \qquad \textit{(6.14)}$$

but we want this in terms of time τ, so using (7.2) and $t_{\mathbf{Me}}$ as in (4.12),

$$\varphi_{\mathbf{f}} = \Omega_{\mathbf{0}}(\tau + t_{\mathbf{Me}}) - \alpha \;= \Omega_{\mathbf{0}}\tau + [\Omega_{\mathbf{0}}\,t_{\mathbf{Me}} - \alpha] \;= \Omega_{\mathbf{0}}\tau + k$$
$$k \equiv [\Omega_{\mathbf{0}}\,t_{\mathbf{Me}} - \alpha] = -.032437114 \text{ rad (2012)} . \qquad (7.16)$$

Angle k is thus the right ascension of the mean fictitious sun at March equinox τ = 0. Then the fictitious sun is described by

$$\varphi_{\mathbf{f}}(\tau) = \Omega_{\mathbf{0}}\tau + k \qquad \text{// radians} \qquad k = -.032437114 \text{ rad (2012)}$$
$$\theta_{\mathbf{t,f}}(\tau) = 0 \qquad \text{// } \theta_{\mathbf{tmax}} = 0 \qquad (7.17)$$

so that, using the fact (1.6) that $\omega_{\mathbf{s}} - \Omega_{\mathbf{0}} = \omega$, for the mean fictitious sun we get

$$(\varphi_{\mathbf{f}} - \varphi_{\mathbf{b}}) = \Omega_{\mathbf{0}}\tau + k - [\varphi_{\mathbf{b0}} + \omega_{\mathbf{s}}\tau] = -\omega\tau + (k - \varphi_{\mathbf{b0}}) \qquad (7.18)$$

and then (7.14) for the fictitious sun position in Frame S' reads,

$$x'_{\mathbf{f}} = -R\sin(\omega\tau - k + \varphi_{\mathbf{b0}})$$
$$y'_{\mathbf{f}} = R\,[-\cos\theta_{\mathbf{1}}\cos(\omega\tau - k + \varphi_{\mathbf{b0}})]$$
$$z'_{\mathbf{f}} = R\,[\sin\theta_{\mathbf{1}}\cos(\omega\tau - k + \varphi_{\mathbf{b0}})] \quad . \qquad \text{// mean fictitious sun} \qquad (7.19)$$

Viewing the fictitious sun from the north pole one gets

$$x'_{\mathbf{f}} = -R\sin(\omega\tau - k + \varphi_{\mathbf{b0}})$$
$$y'_{\mathbf{f}} = -R\cos(\omega\tau - k + \varphi_{\mathbf{b0}})]$$
$$z'_{\mathbf{f}} = 0 \qquad \text{// mean fictitious sun, North Pole} \qquad (7.20)$$

As τ increases, these equations describe the fictitious sun rotating clockwise around the north pole, so as usual the sun rises in the east,

```
plot([-sin(t),-cos(t),t = 0..4], scaling=CONSTRAINED);
```

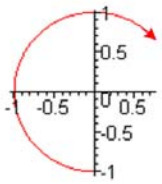

Fig 7.2

The velocity and acceleration of both the actual and fictitious sun's apparent motions on the celestial sphere (as seen by our Frame S' observer) can be obtained by differentiating (7.14) and (7.19). The velocity requires expressions for $\dot{\theta}_t$ and $\dot{\varphi}$ ($\dot{\varphi}_b = \omega_s$) obtained from (6.13), and then acceleration requires $\ddot{\theta}_t$ and $\ddot{\varphi}$. The results are easily obtained in Maple and then approximations can be made as needed.

(d) Spherical coordinates θ',φ' of the sun in Frame S'

Warning: The angle φ' here is totally unrelated to the angle called φ' which appears in Figs 1.3, 3.4 and 6.1 and which is used throughout Section 6.

We can convert the above equations to a spherical coordinate system (r',θ',φ') which has its origin at the Frame S' observation point on the surface of the earth with the z' axis pointing up:

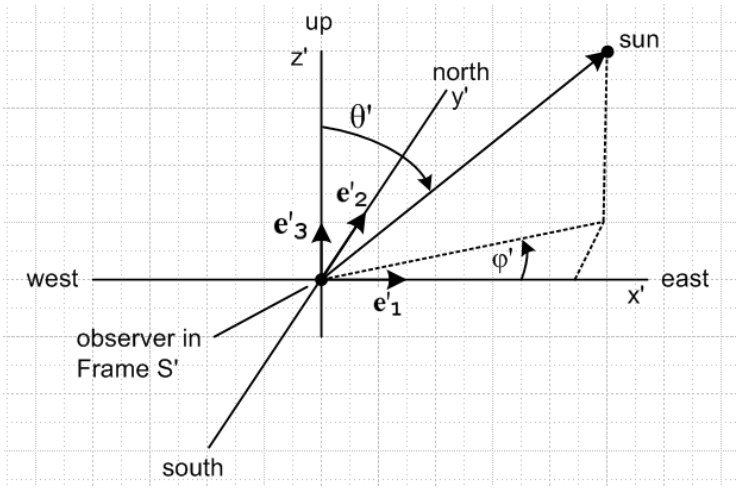

Fig 7.3

In this system, azimuth φ' = 0 is the east, and increases positively to the north. The noon sun always has φ' = ± π/2. At equinox, the sun rises at φ' = 0 and sets at φ' = π.

The general plan for converting to spherical coordinates starts as follows :

$$\rho'^2 = x'^2 + y'^2$$
$$r'^2 = x'^2 + y'^2 + z'^2 \quad . \tag{7.21}$$

Since **r'** lies on a celestial sphere of radius R, we know ahead of time that r' = R and can confirm that in Maple using the x',y',z' expressions given in (7.14). On the other hand, ρ' is a bit messy,

$$(\rho'/R)^2 = (x'/R)^2 + (y'/R)^2 = [\cos\theta_t \sin(\varphi - \varphi_b)]^2 + [\sin\theta_t \sin\theta_1 - \cos\theta_t \cos\theta_1 \cos(\varphi - \varphi_b)]^2$$

$$= \cos^2\theta_t \sin^2(\varphi - \varphi_b) + \cos^2\gamma \tag{7.22}$$

where

$$\cos\gamma \equiv \sin\theta_t \sin\theta_1 - \cos\theta_t \cos\theta_1 \cos(\varphi - \varphi_b) \; . \tag{7.23}$$

The relation between Cartesian and spherical coordinates is

$$x' = r'\sin\theta'\cos\varphi' \qquad y' = r'\sin\theta'\sin\varphi' \qquad z' = r'\cos\theta'$$

where sinθ' is always positive since θ' lies in (0,π). Meanwhile,

$$\rho'^2 = x'^2 + y'^2 = r'^2\sin^2\theta' \quad \Rightarrow \quad \rho' = r'\sin\theta' \; , \tag{7.24}$$

so that

$$x' = \rho'\cos\varphi' \qquad y' = \rho'\sin\varphi' \qquad z' = r'\cos\theta' \tag{7.25}$$

and we end up with

$$\cos\theta' = z'/r' \qquad \cos\varphi' = x'/\rho' \qquad \tan\varphi' = y'/x'$$
$$\sin\theta' = \rho'/r' \qquad \sin\varphi' = y'/\rho' \qquad r' = R \tag{7.26}$$

Installing the expressions (7.14) we then find that

$$\cos\theta' = [\sin\theta_t \cos\theta_1 + \cos\theta_t \sin\theta_1 \cos(\varphi - \varphi_b)]$$
$$\sin\theta' = \rho'/r' = \sqrt{\cos^2\theta_t \sin^2(\varphi - \varphi_b) + \cos^2\gamma} \tag{7.27}$$

$$\cos\varphi' = x'/\rho' = [\cos\theta_t \sin(\varphi - \varphi_b)] \,/\, \sqrt{\cos^2\theta_t \sin^2(\varphi - \varphi_b) + \cos^2\gamma}$$
$$\sin\varphi' = y'/\rho' = [\sin\theta_t \sin\theta_1 - \cos\theta_t \cos\theta_1 \cos(\varphi - \varphi_b)] \,/\, \sqrt{\cos^2\theta_t \sin^2(\varphi - \varphi_b) + \cos^2\gamma}$$
$$\tan\varphi' = y'/x' = [\sin\theta_t \sin\theta_1 - \cos\theta_t \cos\theta_1 \cos(\varphi - \varphi_b)] \,/\, [\cos\theta_t \sin(\varphi - \varphi_b)] \tag{7.28}$$

Therefore, we may write

$$\theta' = \cos^{-1}[\sin\theta_t \cos\theta_1 + \cos\theta_t \sin\theta_1 \cos(\varphi-\varphi_b)]$$
$$\varphi' = \tan^{-1}\left([\sin\theta_t \sin\theta_1 - \cos\theta_t \cos\theta_1 \cos(\varphi-\varphi_b)] / [\cos\theta_t \sin(\varphi-\varphi_b)] \right) . \quad (7.29)$$

In the above equations, the following objects appear:

$\theta_t = \sin^{-1}[\sin\theta_{tmax} \sin(\psi - \alpha)]$ *(6.13)*

$\varphi = \tan^{-1}[\cos\theta_{tmax} \tan(\psi - \alpha)]$. *(6.13)*

$\psi = \Omega_0 t + 2e \sin(\Omega_0 t) + (5/4)e^2 \sin(2\Omega_0 t)$ // + order e^3 which we ignore *(4.31)*

$\alpha = \pi/2 - \varphi_{per}$ *(1.9))*

$t = \tau + t_{Me}$ *(7.2)*

$\varphi_b = \varphi_{b0} + \omega_s \tau = \varphi_1 + \varphi_{G0} + \omega_s \tau$. *(7.3),(7.7)*

As the sun moves in the sky, equations (7.29) give the position of the sun in Frame S' spherical coordinates based at an observation point located at (θ_1,φ_1), where θ_1 is the polar angle from the north pole (colatitude) and φ_1 is the longitude east of the Greenwich meridian. Angle φ_{G0} is the right ascension of Greenwich at the last March equinox.

8. The Equation of Time Revisited

(a) Definition of new azimuths Φ' and Φ'_s

Recall the depiction of the Frame S' coordinate system given in Fig 7.3 which we replicate here with the addition of two new azimuthal angles Φ' and Φ'_s,

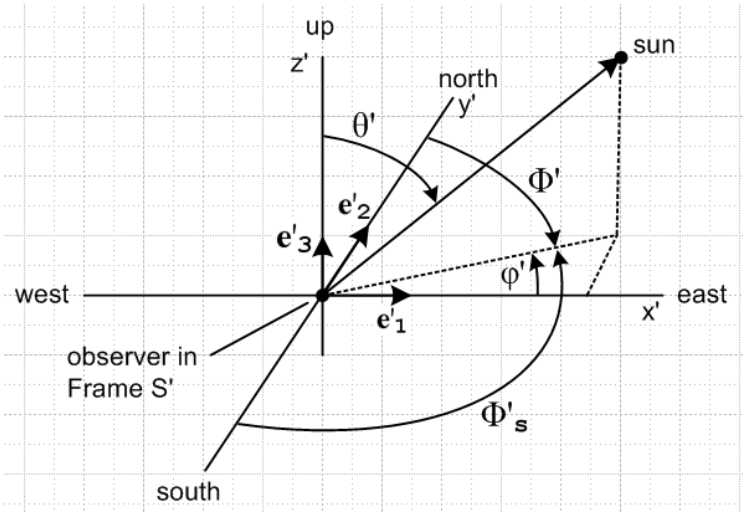

Fig 8.1

For an observer in the southern hemisphere below latitude - 23°, the azimuth φ' of the sun follows a regular pattern all year long: the sun rises generally in the east at φ' = 0 ± Δ, reaches noon in the north at φ' = π/2, sets generally in the west at φ' = π ∓ Δ, and hits midnight at φ' = 3π/2 = -π/2. The size of Δ varies with latitude and the time of year and is zero at equinoxes and maximal at solstices, as shown in Fig 9.5 below. For such an observer we might define a shifted azimuth in order to place midnight at the discontinuity point where 2π → 0,

$$\Phi'_s \equiv \pi/2 + \varphi' \ . \tag{8.1}$$

The sun rises in the east at $\Phi'_s = \pi/2 \pm \Delta$, reaches noon in the north at $\Phi'_s = \pi$, sets in the west at $\Phi'_s = 3\pi/2 \mp \Delta$, and hits midnight in the north at $\Phi'_s = 2\pi = 0$.

For an observer in the northern hemisphere above latitude 23°, the appropriate *sun-tracking* azimuth would be this,

$$\Phi' \equiv \pi/2 - \varphi' \ . \qquad // \ \Phi'_s = \pi - \Phi' \tag{8.2}$$

The sun rises in the east at $\Phi' = \pi/2 \mp \Delta$, reaches noon in the south at $\Phi' = \pi$, sets in the west at $\Phi' = 3\pi/2 \pm \Delta$, and hits midnight in the north at $\Phi' = 2\pi = 0$.

For viewers in the tropic region between -23° and +23°, the "sun tracking azimuth" is Φ'_s for part of the year, and Φ' for another part of the year. For example, the Honolulu image in Fig 3.12 shows that Φ' is

appropriate for most of the year when the sun is in the south, but for part of the year near June solstice the Φ'_s azimuth is appropriate.

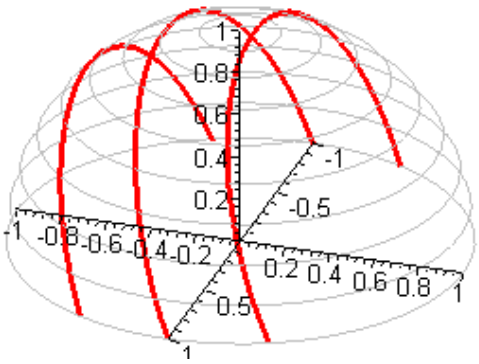

polar = 70 lat = 20 Honolulu, Mexico City, San Juan Fig 8.2

As we shall see in Section 11, it is *not* very useful to study the analemma for a tropical viewer using Frame S' polar coordinates θ',φ' using any of the three azimuths, but the direct calculation of the analemma "on film" using Cartesian coordinates x',y',z' always works.

We continue now assuming a northern hemisphere observer above 23^o latitude, mainly because we shall be interested in the limiting case of the North Pole, and because we shall be studying analemmas photographed by such observers.

Using equation (7.29),

$$\varphi' = \tan^{-1}\left[\sin\theta_t \sin\theta_1 - \cos\theta_t \cos\theta_1 \cos(\varphi - \varphi_b)\right] / \left[\cos\theta_t \sin(\varphi - \varphi_b)\right], \qquad (7.29)$$

we may relate Φ' to the position of the actual sun on the ecliptic this way, using (8.2),

$$\Phi' = \pi/2 - \tan^{-1}\left(\left[\sin\theta_t \sin\theta_1 - \cos\theta_t \cos\theta_1 \cos(\varphi_b - \varphi)\right] / \left[-\cos\theta_t \sin(\varphi_b - \varphi)\right]\right).$$

Then using the identity (A.12),

$$\pi/2 - \tan^{-1}([y]/[x]) = \pi + \tan^{-1}([-x]/[-y]) \qquad (A.12)$$

this becomes, for the actual and fictitious suns,

$$\Phi' = \pi + \tan^{-1}\left([\cos\theta_t \sin(\varphi_b - \varphi)] / [-\sin\theta_t \sin\theta_1 + \cos\theta_t \cos\theta_1 \cos(\varphi_b - \varphi)]\right)$$
$$\Phi'_f = \pi + \tan^{-1}\left([\sin(\varphi_b - \varphi_f)] / [\cos\theta_1 \cos(\varphi_b - \varphi_f)]\right) \quad . \qquad (8.3)$$

Using the fact that $\Phi'_s = \pi - \Phi'$, and the second line of (A.4) inverted,

$$\tan^{-1}([y]/[x]) = \pi - \tan([y]/[-x]), \qquad (A.4)$$

and the fact that -π and π represent the same angle, we can write for southern observers below -23^o,

$$\Phi'_{\mathbf{s}} = \pi + \tan^{-1}([\cos\theta_{\mathbf{t}} \sin(\varphi_{\mathbf{b}}-\varphi)] / [\sin\theta_{\mathbf{t}} \sin\theta_{\mathbf{1}} - \cos\theta_{\mathbf{t}} \cos\theta_{\mathbf{1}} \cos(\varphi_{\mathbf{b}}-\varphi)])$$
$$\Phi'_{\mathbf{s,f}} = \pi + \tan^{-1}([\sin(\varphi_{\mathbf{b}}-\varphi_{\mathbf{f}})] / [-\cos\theta_{\mathbf{1}} \cos(\varphi_{\mathbf{b}}-\varphi_{\mathbf{f}})]) \quad (8.4)$$

where the difference from (8.3) is that both bottom brackets are negated.

At the north pole (8.3) becomes (on the second line, $\tan^{-1}(\tan(\varphi_{\mathbf{b}}-\varphi_{\mathbf{f}})) = (\varphi_{\mathbf{b}}-\varphi_{\mathbf{f}})$)

$$\Phi'^{\mathbf{NP}} = \pi + \tan^{-1}([\cos\theta_{\mathbf{t}} \sin(\varphi_{\mathbf{b}}-\varphi)] / [\cos\theta_{\mathbf{t}} \cos(\varphi_{\mathbf{b}}-\varphi)]) = \pi + (\varphi_{\mathbf{b}}-\varphi)$$
$$\Phi'_{\mathbf{f}}{}^{\mathbf{NP}} = \pi + \tan^{-1}([\sin(\varphi_{\mathbf{b}}-\varphi_{\mathbf{f}})] / [\cos(\varphi_{\mathbf{b}}-\varphi_{\mathbf{f}})]) = \pi + (\varphi_{\mathbf{b}}-\varphi_{\mathbf{f}}) \quad (8.5)$$

Taking the difference, we find that

$$\Phi'^{\mathbf{NP}} - \Phi_{\mathbf{f}}'^{\mathbf{NP}} = -(\varphi - \varphi_{\mathbf{f}})$$

or

$$\Delta\Phi'^{\mathbf{NP}} = -\Delta\varphi . \quad \Rightarrow \quad \Phi'^{\mathbf{NP}} = \Phi_{\mathbf{f}}'^{\mathbf{NP}} - \Delta\varphi \quad (8.6)$$

where $\Delta\varphi$ is the "equation of time" shown in (6.15a),

$$\Delta\varphi(t) \equiv \varphi - \varphi_{\mathbf{f}} = \tan^{-1}[\cos\theta_{\mathbf{tmax}} \tan(\psi-\alpha)] - (\Omega_{\mathbf{0}}t-\alpha) \quad \textit{(6.15a)}$$
$$\psi = \Omega_{\mathbf{0}}t + 2e \sin(\Omega_{\mathbf{0}}t) + (5/4)e^{\mathbf{2}} \sin(2\Omega_{\mathbf{0}}t) \quad // + \text{order } e^{\mathbf{3}} \text{ which we ignore} . \quad \textit{(4.31)}$$

Recalling now that

$$\varphi_{\mathbf{f}}(\tau) = \Omega_{\mathbf{0}}\tau + k \qquad k = -.032437114 \text{ rad (2012)} \quad \textit{(7.17)}$$

$$\varphi_{\mathbf{b}}(\tau) = \varphi_{\mathbf{b0}} + \omega_{\mathbf{s}}\tau . \quad \textit{(7.3)}$$

We can write the second line of (8.5) as

$$\Phi'_{\mathbf{f}}{}^{\mathbf{NP}} = \pi + (\varphi_{\mathbf{b}}-\varphi_{\mathbf{f}}) = \pi + [\varphi_{\mathbf{b0}} + \omega_{\mathbf{s}}\tau] - [\Omega_{\mathbf{0}}\tau + k] = \pi + (\omega_{\mathbf{s}} - \Omega_{\mathbf{0}})\tau + (\varphi_{\mathbf{b0}}-k)$$

$$= \pi + \omega\tau + (\varphi_{\mathbf{b0}}-k) \qquad // \text{ using (1.6)} \quad (8.7)$$

(b) Local Time, Sundial Time and the Equation of Time

GMT. For our purposes here, we make no distinction between the various kinds of precision global time indicated by the letters GMT, UT, UT0, UT1, UTC and so on, so we will just use GMT. We are not concerned about tiny differences between these times due to things like the Chandler wobble mentioned at the end of Section 1 (a).

GMT means Greenwich Mean Time which is a 24 hour time system set so that the mean fictitious sun always passes over the Greenwich meridian (the prime meridian, longitude = $0^{\mathbf{0}}$) at GMT = 12:00. At this instant, the entire world experiences the same "day", perhaps Thursday. At GMT = 12:01 the world is still doing Thursday, except a tiny strip on the meridian opposite Greenwich has moved to Friday, and then Friday "grows" as time moves on. This meridian at $\varphi_{\mathbf{1}} = 180^{\mathbf{o}}$ is the GMT international date line, though

the actual date line has a deviation in the southern hemisphere. Thus it is that Samoa rings in the new year Jan 1 while it is still GMT noon Dec 31 in London (and 4AM in California).

LMT. The corresponding time at an arbitrary Frame S' observer site is LMT meaning Local Mean Time, and it is given by

$$\text{LMT} = [\ \text{GMT} + (\varphi_1/15)\ ] \mod 24\ . \tag{8.8}$$

where φ_1 is the site's longitude east of Greenwich, measured in degrees. At our observer site, the mean fictitious sun always crosses the local meridian at LMT = 12:00. So GMT is just LMT for Greenwich.

This LMT should not be confused with time zone times which are binned every 15^o (more or less).

Our observer can set a local clock to his LMT using the above equation and obtaining live GMT from a website displaying GMT, from a GMT "clock app", or from a WWV broadcast (where GMT is called "coordinated universal time" or UTC).

We know from (8.7) that $\Phi'_f{}^{NP}$ advances at the linear rate $\omega\tau$, so it can be related to LMT which advances at that same linear rate, albeit scaled to hours instead of degrees. We claim in fact that

$$\text{LMT} = 12(\Phi'_f{}^{NP}/\pi) \qquad \text{// Local Mean Time} \tag{8.9}$$

We know that $\Phi'_f{}^{NP} = \pi$ when the *fictitious* sun crosses the noon meridian, and there LMT = 12 = 12:00. Midnight occurs when $\Phi'_f{}^{NP} = 0$ which is then LMT = 0. Since Φ'_f is linear, (8.9) is thus proved.

Let us now define another time LST based on the azimuth of the *actual* sun,

$$\text{LST} \equiv 12(\Phi'^{NP}/\pi) \qquad \text{// Local Sundial Time} \tag{8.10}$$

This LST clock reads 12:00 when the *actual* sun crosses the local meridian, $\Phi'^{NP} = \pi$. This is the time when a local sundial vane shows no shadow to either side, hence the name "local sundial time".

Building an electronic LST clock: One could imagine constructing an electronic clock to display LST by having a feedback servo system which very slowly slews the clock rate so that it stays in daily sync with the event of the actual sun crossing the meridian every noon time (LST = 12:00). The design might be sophisticated in that it can remain in "lock" through some number of completely overcast days due to prediction based on recent past history. The clock rate is uneven because, during the year, the actual sun slowly wanders back and forth in right ascension relative to the mean fictitious sun by about ±15 minutes as indicated by the Equation of Time shown as the red curve in Fig 6.6. Our electronic LST clock is "better" than an actual sundial only because it displays time at all times, day and night, and even works on overcast days.

Using (8.9), (8.10) and (8.6), we find that

$$\text{LST} - \text{LMT} \ = \ 12(\Delta\Phi'^{NP}/\pi) \ = \ -\,12(\Delta\varphi/\pi)\ . \qquad \text{// hours and radians} \tag{8.11}$$

Here are four ways to write this last equation

$$[\text{LST} - \text{LMT}]^{\mathbf{hrs}} = -12(\Delta\varphi^{\mathbf{rad}}/\pi) \tag{8.12}$$

$$[\text{LST} - \text{LMT}]^{\mathbf{hrs}} = -12(\Delta\varphi^{\mathbf{deg}}/180) \tag{8.13}$$

$$[\text{LST} - \text{LMT}]^{\mathbf{min}} = -60*12(\Delta\varphi^{\mathbf{rad}}/\pi) = -(720/\pi)\Delta\varphi \tag{8.14}$$

$$[\text{LST} - \text{LMT}]^{\mathbf{min}} = -60*12(\Delta\varphi^{\mathbf{deg}}/180) = -4\,\Delta\varphi^{\mathbf{deg}} = -\Delta\varphi^{\mathbf{min}} \ . \tag{8.15}$$

It is most common to express the equation of time in minutes, and from (8.14) and (6.15a) we write

$$\text{EOT}(t) \equiv [\text{LST} - \text{LMT}]^{\mathbf{min}} = -(720/\pi)\Delta\varphi^{\mathbf{rad}} = -4\,(180/\pi)\,\Delta\varphi \quad \textbf{(6.15a)}$$

$$= -(720/\pi)\,\{\tan^{-1}[\cos\theta_{\mathbf{tmax}}\,\tan(\psi-\alpha)] - (\Omega_{\mathbf{0}}t-\alpha)\}\ . \tag{8.16}$$

A plot of this EOT(t) ~ $-\Delta\varphi = \varphi_{\mathbf{f}}-\varphi$ was already shown in Fig 6.7. Here we replicate that plot adding some horizontal gridlines

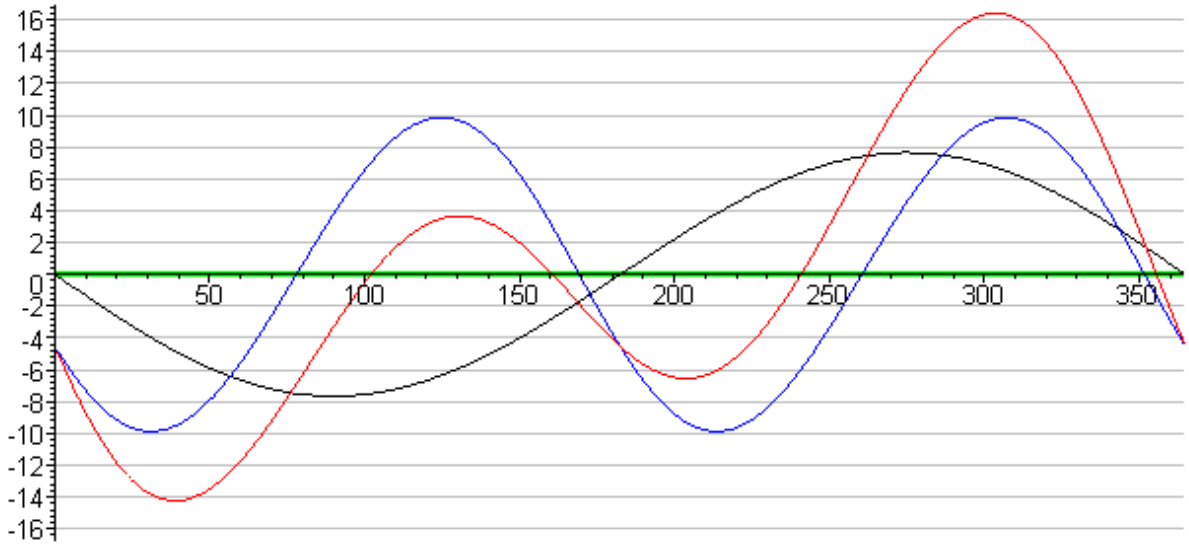

Fig 8.3

The EOT(t) plot for the actual sun is of course the red curve, while the green line represents the fictitious sun. Recall that the left edge corresponds to t = 0, Jan 3, perihelion. On the upper half of this plot, we have $-\Delta\varphi > 0$ so LST > LMT which means the sundial time is ahead of LMT, the sundial is "running fast", and the actual sun is ahead of the fictitious sun on the celestial sphere, $\varphi_{\mathbf{f}} > \varphi$. The opposite of course is true for the lower half of the plot.

9. Noon and Midnight, Sunrise and Sunset

Angle θ_1 continues here to be the *colatitude* of the Frame S' observation site. Letting θ_{LAT} be the corresponding *latitude*, so that $\theta_{LAT} = \pi/2 - \theta_1$, one can write all the equations below with these simple changes,

$$\sin\theta_1 \rightarrow \cos\theta_{LAT} \qquad \cos\theta_1 \rightarrow \sin\theta_{LAT} \qquad \cot\theta_1 \rightarrow \cot\theta_{LAT} .$$

(a) Conditions for Noon and Midnight

The path of the sun in local Frame S' coordinates is given by

$$\theta' = \cos^{-1}[\sin\theta_t \cos\theta_1 + \cos\theta_t \sin\theta_1 \cos(\varphi-\varphi_b)]$$
$$\varphi' = \tan^{-1}[\sin\theta_t \sin\theta_1 - \cos\theta_t \cos\theta_1 \cos(\varphi-\varphi_b)]/[\cos\theta_t \sin(\varphi-\varphi_b)] \qquad (7.29)$$

where

$$\theta_t = \sin^{-1}[\sin\theta_{tmax} \sin(\Omega_0 t + 2e\sin(\Omega_0 t) - \pi/2 + \varphi_{per})]$$
$$\varphi = \tan^{-1}[\cos\theta_{tmax} \tan(\Omega_0 t + 2e\sin(\Omega_0 t) - \pi/2 + \varphi_{per})] \qquad (6.13)$$
$$\varphi_b = \varphi_{b0} + \omega_s\tau = \varphi_1 + \varphi_{G0} + \omega_s\tau \text{ with } \tau = t - t_{Me} \qquad (7.3), (7.7), (7.2)$$

and here is the picture showing the observer site Frame S' coordinates,

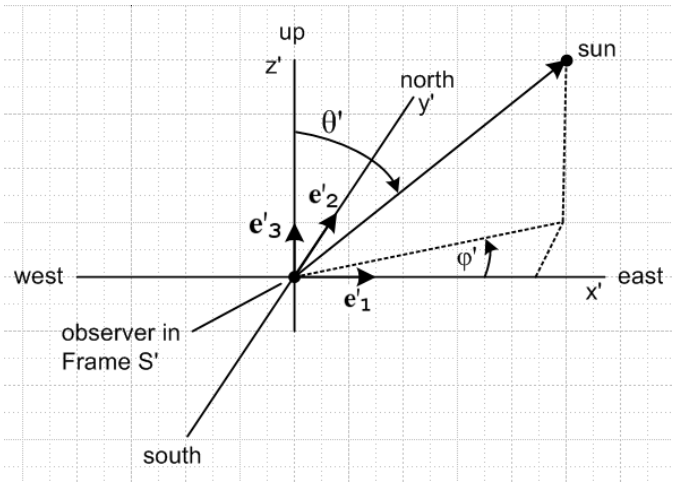

Fig 7.3

Noon occurs when the local polar angle θ' assumes its smallest value during the day; the sun is as much "overhead" as it will be for that day; it is at its closest to the zenith z' axis.

Looking at the first of equations (7.29) quoted above,

$$\cos\theta' = [\sin\theta_t \cos\theta_1 + \cos\theta_t \sin\theta_1 \cos(\varphi-\varphi_b)] , \qquad (9.1)$$

we naively ask: what is the value of $(\varphi-\varphi_b)$ at noon? The quantities $\cos\theta_t$ and $\sin\theta_1$ are always positive, so $\cos\theta'$ is maximum when $\cos(\varphi-\varphi_b) = 1$. Pondering the shape of $\cos\theta'$ for θ' in $0,\pi$ (its legal range), one concludes that θ' is minimal when $\cos\theta'$ is maximal. Therefore:

noon:	$\cos(\varphi-\varphi_b) = 1$	$\varphi = \varphi_b$	φ = (6.13) quoted above
midnight:	$\cos(\varphi-\varphi_b) = -1$	$\varphi = \varphi_b + \pi$	(9.2)

These both imply that $\sin(\varphi-\varphi_b) = 0$. Looking at the second of equations (7.29),

$$\tan\varphi' = [\sin\theta_t \sin\theta_1 - \cos\theta_t \cos\theta_1 \cos(\varphi - \varphi_b)] / [\cos\theta_t \sin(\varphi - \varphi_b)] \qquad (7.29)$$

we conclude that at noon, $\tan\varphi' = \pm\infty$ so $\varphi' = \pm\pi/2$. According to the figure above, this means that at noon the sun lies on the local meridian, a north-south line of longitude passing through the observation site.

Having "done the math", we now peruse Fig 7.1 where things are completely obvious :

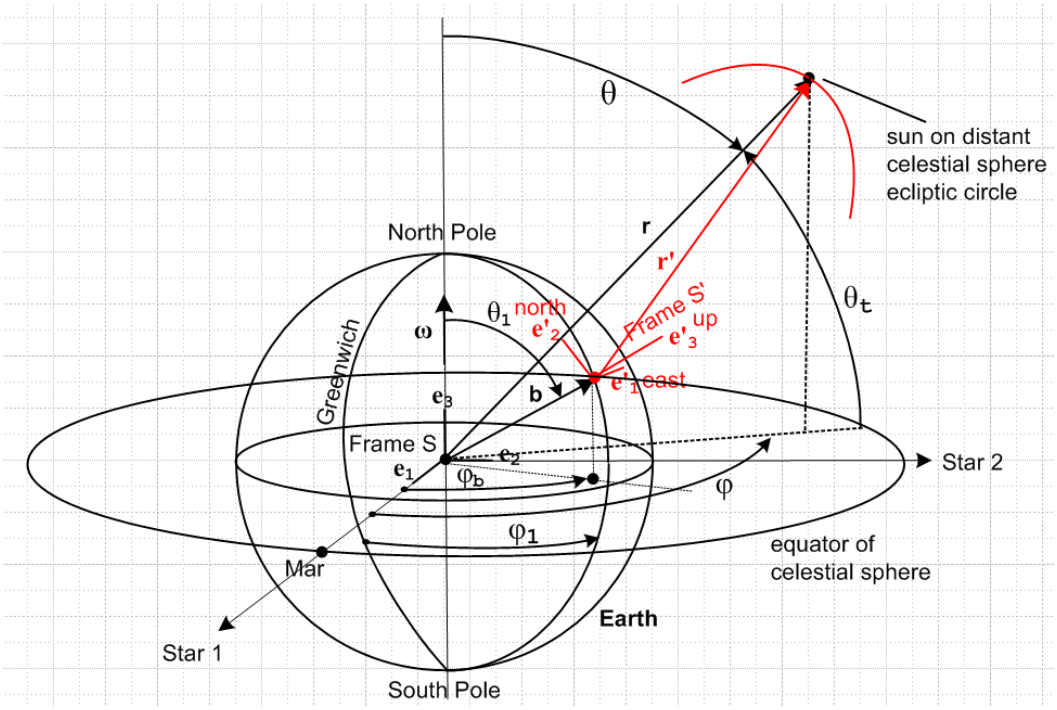

Fig 7.1

When $\varphi_b = \varphi$, the Frame S' origin on the earth and the sun on the celestial sphere have the same azimuth angle, so this is noon. Midnight occurs when $\varphi_b = \varphi + \pi$ and therefore $\cos(\varphi-\varphi_b) = -1$.

The conditions for noon and midnight of the mean *fictitious* sun are given by

fictitious noon:	$\cos(\varphi_f-\varphi_b) = 1$	$\varphi_f = \varphi_b$
fictitious midnight:	$\cos(\varphi_f-\varphi_b) = -1$	$\varphi_f = \varphi_b + \pi$ (9.3)

where

$\varphi_{\mathbf{f}} = \Omega_{\mathbf{0}}t - \alpha = \Omega_{\mathbf{0}}t - \pi/2 + \varphi_{\mathbf{per}} = \Omega^{\mathbf{o}}\tau + k$ with $k = [\ \Omega_{\mathbf{0}}t_{\mathbf{Me}} - \alpha\ ]$ *(6.14),(7.16)*

$\varphi_{\mathbf{b}} = \varphi_{\mathbf{b0}} + \omega_{\mathbf{s}}\tau = \varphi_{\mathbf{1}} + \varphi_{\mathbf{G0}} + \omega_{\mathbf{s}}\tau$ with $\tau = t - t_{\mathbf{Me}}$ *(7.3), (7.7), (7.2)*

(b) Local time of Noon and Midnight : approximations

From (8.12) we know that local mean time and local sundial time are related by

$$LMT = [LST + (12/\pi)\Delta\varphi] \bmod 24 \quad , \tag{9.4}$$

where $\Delta\varphi$ is the Equation of Time (in the form (6.15a)),

$$\Delta\varphi = -\varphi_{\mathbf{f}} + \varphi$$

$$= -\Omega_{\mathbf{0}}t + \alpha + \tan^{-\mathbf{1}}[\cos\theta_{\mathbf{tmax}} \tan(\psi-\alpha)] \ . \tag{6.15a}$$

Noon means the sundial has no side shadow and so LST = 12:00. From (9.4) this occurs at local time,

$$LMT(noon) = [12{:}00 + (12/\pi)\Delta\varphi] \bmod 24 \tag{9.5}$$

and we know this LMT will lie in the general range 11:45 to 12:15. Similarly,

$$LMT(midnight) = [00{:}00 + (12/\pi)\Delta\varphi)] \bmod 24 \ . \tag{9.6}$$

These results can be converted to GMT using (8.8) written as

$$GMT = [\ LMT - (\varphi_{\mathbf{1}}/15)] \bmod 24 \tag{9.7}$$

where $\varphi_{\mathbf{1}}$ is the observer's longitude east of Greenwich in degrees.

For 2012 parameters, here is a plot of the LMT(noon) from (9.5) and (6.15a) above

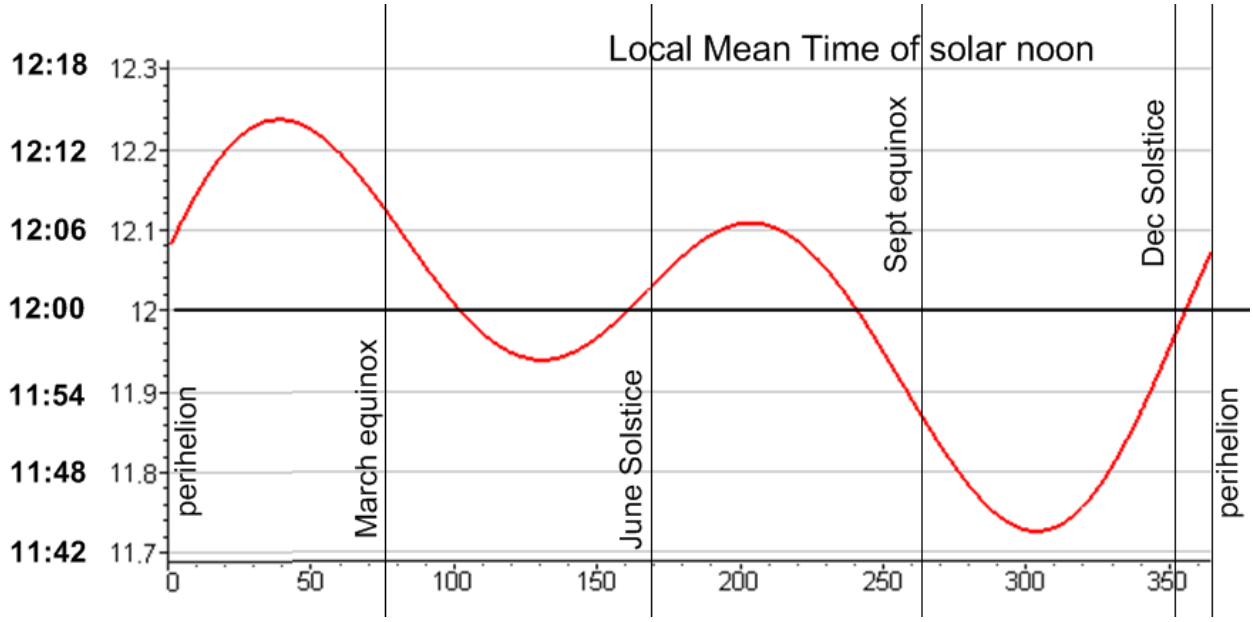

Fig 9.1

The vertical lines were placed using days computed in (4.11). Note that 0.1 hour = 6 minutes.

This is just a restatement of the equation of time Fig 6.6 with some LMT clock times added on the left. On September equinox, at solar noon the LMT clock reads 11:52 AM so "the sundial is running fast".

Precision calculation of solar noon. In the discussion just above, one can roughly look up on the graph $\Delta\varphi$ for a day of interest and use that to compute LMT(noon) using (9.5). To get a more precise result, one would use equation (6.15a) above to compute $\Delta\varphi$, but the question arises: exactly what t should one use in (6.15a)? If one knew the exact t of solar noon on our day of interest, *that* would be the right t to use, but of course one doesn't know the exact t of solar noon! We then have to make an approximation.

In $\Delta\varphi(t=\tau+t_{Me})$ we might set τ = 24d hours for day "d" of the year starting at March equinox. This approach corresponds to the left drawing below,

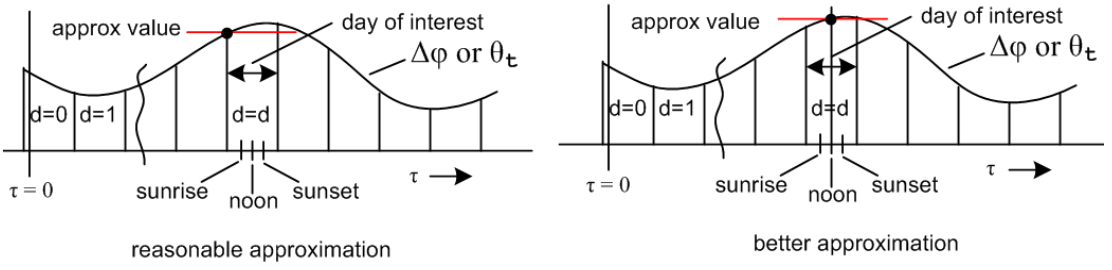

Fig 9.2

where the red line shows how we approximate $\Delta\varphi$ as being a constant for the entire day d. In this approach, things are a little hazy at the left end of the graph near τ = 0, but since $\Delta\varphi$ is a slowly varying function over a range of a few days, this approximation will work pretty well.

A better approximation (right drawing) is to set τ in $\Delta\varphi(t=\tau+t_{Me})$ to be the time of noon for the mean fictitious sun, which we know is going to be ± 15 min from the noon of the actual sun. This occurs according to (9.3) when $\varphi_f = \varphi_b + 2\pi d$ which from (7.1) tell us $-\omega\tau + (k - \varphi_{b0}) = 2\pi d$. This then gives

the time of fictitious sun noon to be $\tau = 12\ (k - \varphi_{b0})/\pi + 24d$ hours, where $\varphi_{b0} = \varphi_1 + \varphi_{G0}$ as in (7.7) and constant k is given in (7.16) as -.03243 radians for year 2012. Quantity φ_{G0} is the right ascension of Greenwich at $\tau = 0$. Setting d = 0, we find that the time of fictitious sun noon on day 0 occurs at $\tau_0 = 12(k - \varphi_{b0})/\pi$. For the picture as drawn, this would be a positive number. If the $\tau = 0$ line falls in the right half of day d = 0, then this τ_0 is a negative number.

Finally, one could find a numerically exact solution for t of actual solar noon on day d by solving a transcendental equation for a value of t on each day. That equation is just (9.2),

$$\varphi = \varphi_b \qquad (9.2)$$

Replacing φ from (6.13) and φ_b from (7.3), and with t_{Me} from (4.12), the above becomes

$$\tan^{-1}[\cos\theta_{tmax}\ \tan\{\ \Omega_0 t + 2e\ \sin(\Omega_0 t) + (5/4)e^2\ \sin(2\Omega_0 t) - \pi/2 + \varphi_{per}\}] = \varphi_{b0} + \omega_s t - \omega_s t_{Me}$$

or

$$\cos\theta_{tmax}\ \tan\{\ \Omega_0 t + 2e\ \sin(\Omega_0 t) + (5/4)e^2\ \sin(2\Omega_0 t) - \pi/2 + \varphi_{per}\} = \tan(\varphi_{b0} + \omega_s t - \omega_s t_{Me})$$

where one sees t appearing on both sides ($t = \tau + t_{Me}$ from (7.2)).

(c) Another approach to noon

As noted above, noon occurs when $(\varphi - \varphi_b) = 0$. We can write an expression for $(\varphi - \varphi_b)$ as follows, using the facts that $\varphi = \varphi_f + \Delta\varphi$, $\varphi_b = \varphi_{b0} + \omega_s\tau$ (7.3) and $\varphi_f = \Omega_0\tau + k$ (7.17) :

$$(\varphi - \varphi_b) = \varphi_f + \Delta\varphi - \omega_s\tau - \varphi_{b0} = \Omega_0\tau + k + \Delta\varphi - \omega_s\tau - \varphi_{b0}$$

$$= -\omega\tau + k + \Delta\varphi - \varphi_{b0} \qquad \text{// since } \omega_s = \omega + \Omega_0 \text{ as in (1.6)}$$

$$= -\omega\tau - [\varphi_{b0} - k - \Delta\varphi]]$$

$$= -\omega\tau - \kappa\omega \qquad \text{// } \kappa \equiv [\varphi_{b0} - k - \Delta\varphi]/\omega$$

$$= -\omega(\tau + \kappa)$$

$$= -\omega t' \qquad (9.8)$$

where we define a shifted time t' according to

$$t' = \tau + \kappa \qquad \kappa = [\varphi_{b0} - k - \Delta\varphi]/\omega\ . \qquad (9.9)$$

In this shifted time t', which is specific to our selected day (since $\Delta\varphi$ is specific), noon occurs at

$$t' = 0 \qquad \text{// noon} \qquad (9.10)$$

since this makes $\varphi = \varphi_b$. This fact is not very exciting, but becomes useful in the next section.

(d) Sunrise and Sunset, Length of Day, Noon Elevation of the Sun

Sunrise and Sunset

Looking at Fig 7.3 above, the condition for nominal sunrise and sunset on a perfectly smooth spherical earth is

$$\theta' = \pi/2 \; . \qquad \Rightarrow \qquad \cos\theta' = 0 \; . \tag{9.11}$$

Nominal means that the center of the sun passes through the horizon plane $\theta' = \pi/2$. Looking then at the first equation of (7.29) we obtain the condition (sr = sunrise, ss = sunset)

$$[\sin\theta_{\mathbf{t}} \cos\theta_{\mathbf{1}} + \cos\theta_{\mathbf{t}} \sin\theta_{\mathbf{1}} \cos(\varphi-\varphi_{\mathbf{b}})_{\mathbf{sr,ss}}] = 0 \tag{9.12}$$

so that

$$\cos(\varphi-\varphi_{\mathbf{b}})_{\mathbf{sr,ss}} = -\sin\theta_{\mathbf{t}} \cos\theta_{\mathbf{1}} / (\cos\theta_{\mathbf{t}} \sin\theta_{\mathbf{1}}) = -\tan\theta_{\mathbf{t}} \cot\theta_{\mathbf{1}} \; . \tag{9.13}$$

Since φ and $\theta_{\mathbf{t}}$ are both complicated functions of time t, as shown in (6.13), this is a transcendental equation one would have to solve numerically for the times of sunsets and sunrises.

We can, however, use either of the approximation methods discussed in section (b) above. The first method would just set $\tau = 24$d to evaluate $\theta_{\mathbf{t}}(t=\tau+t_{\mathbf{Me}})$. As for the second method, using the fact that (9.13) says $\cos(\varphi_{\mathbf{f}}-\varphi_{\mathbf{b}})_{\mathbf{sr,ss}} = 0$ for the fictitious sun, and the fact that $(\varphi_{\mathbf{f}}-\varphi_{\mathbf{b}}) = -\omega\tau + (k - \varphi_{\mathbf{b0}})$ from (7.18), one finds that $(\varphi_{\mathbf{f}}-\varphi_{\mathbf{b}})_{\mathbf{sr,ss}} = \pm \pi/2 - 2\pi d$ where d = days, and then $\tau_{\pm} = 12(k - \varphi_{\mathbf{b0}})/\pi \mp 6 + 24d$ where the - is for sunrise and the + for sunset. This then just says $\tau_{\pm} = \tau_{\mathbf{noon}} \mp 6$ hours, which seems pretty reasonable (all for the fictitious sun).

So, for our selected day, we compute $\theta_{\mathbf{t}}(t=\tau+t_{\mathbf{Me}})$ from (6.13) and then sunrise and sunset occur when

$$\cos(\varphi-\varphi_{\mathbf{b}})_{\mathbf{sr,ss}} = -\tan\theta_{\mathbf{t,sr,sr}} \cot\theta_{\mathbf{1}} \tag{9.13}$$

or, using (9.8),

$$\cos(\omega t'_{\mathbf{sr,ss}}) = -\tan\theta_{\mathbf{t,sr,ss}} \cot\theta_{\mathbf{1}} \; . \tag{9.14}$$

If we assume the simpler approximation $\tau = 24$d, then $\theta_{\mathbf{t}}$ is the same for sunrise and sunset so that

$$\begin{aligned}
&t'_{\mathbf{sr}} = -(1/\omega) \cos^{-1}[-\tan\theta_{\mathbf{t}} \cot\theta_{\mathbf{1}}] \quad < 0 \quad \text{// sunrise} \quad \theta_{\mathbf{1}} = \text{colatitude} \\
&t'_{\mathbf{ss}} = +(1/\omega) \cos^{-1}[-\tan\theta_{\mathbf{t}} \cot\theta_{\mathbf{1}}] \quad > 0 \quad \text{// sunset} \\
&\text{or} \\
&t'_{\mathbf{sr}} = -(1/\omega) \cos^{-1}[-\tan\theta_{\mathbf{t}} \tan\theta_{\mathbf{LAT}}] \quad < 0 \quad \text{// sunrise} \quad \theta_{\mathbf{LAT}} = \text{latitude} \\
&t'_{\mathbf{ss}} = +(1/\omega) \cos^{-1}[-\tan\theta_{\mathbf{t}} \tan\theta_{\mathbf{LAT}}] \quad > 0 \quad \text{// sunset}
\end{aligned} \tag{9.15}$$

where $\omega = 2\pi$ rad/day = $(\pi/12)$ rad/hr. These times are *relative to* t' = 0 as noon. We know the LMT of noon from (9.5) and then (9.15) tells us the displacement from that noon time of sunrise and sunset. In an exact numerical solution (or using the more accurate approximation discussed above), one would find that these displacements are not quite the same because θ_t changes slightly between sunrise and sunset, but we ignore this fact in our simple approximation as illustrated in Fig 9.2.

Looking at (9.14), one sees there is no solution t' for sunrise or sunset when $|\tan\theta_t \cot\theta_1| > 1$. This occurs in the northern hemisphere for observers with $\theta_1 < \theta_t$. For them the sun is either up all the time or down all the time so there *are* no sunrises or sunsets. The corresponding condition in the southern hemisphere is $\theta_1 > \pi - \theta_t$.

Here is a plot of t'_{ss} for a selection of northern hemisphere latitudes which uses (9.15) for t'_{ss} and (6.24) for θ_t [tp_ss = t'_{ss}, phip_sr = φ'_{sr} for making Fig 9.4 below]

```
restart; with(plots): tMe := .2084458064:
thtmax := (Pi/180)*23.4382:    e := 0.016699:
phiper := (Pi/180)*13.101:     Omega0 := 2*Pi:
thLAT := thLAT_deg*(Pi/180):
phip_sr := arctan(tan(thetat)*sec(thLAT)/sqrt(1 - (tan(thetat)*tan(thLAT))^2)):
tp_ss := (12/Pi)* arccos(-tan(thetat)*tan(thLAT)):
q := 2*e*sin(Omega0*t):  # ignore order e^2 term
s := Omega0*t + phiper - Pi/2:
t := tau + tMe:
thetat := arcsin(sin(thtmax)* sin(s + q)):    # (6.24)
p1 := plot([seq(tp_ss,thLAT_deg =
[0,10,20,30,40,50,60,65,66.5,70,80,85])],tau=0..1, color = red):display(p1):
p2 := plot([seq(N,N=0..12)],tau=0..1,color = green):
display(p1,p2);
```

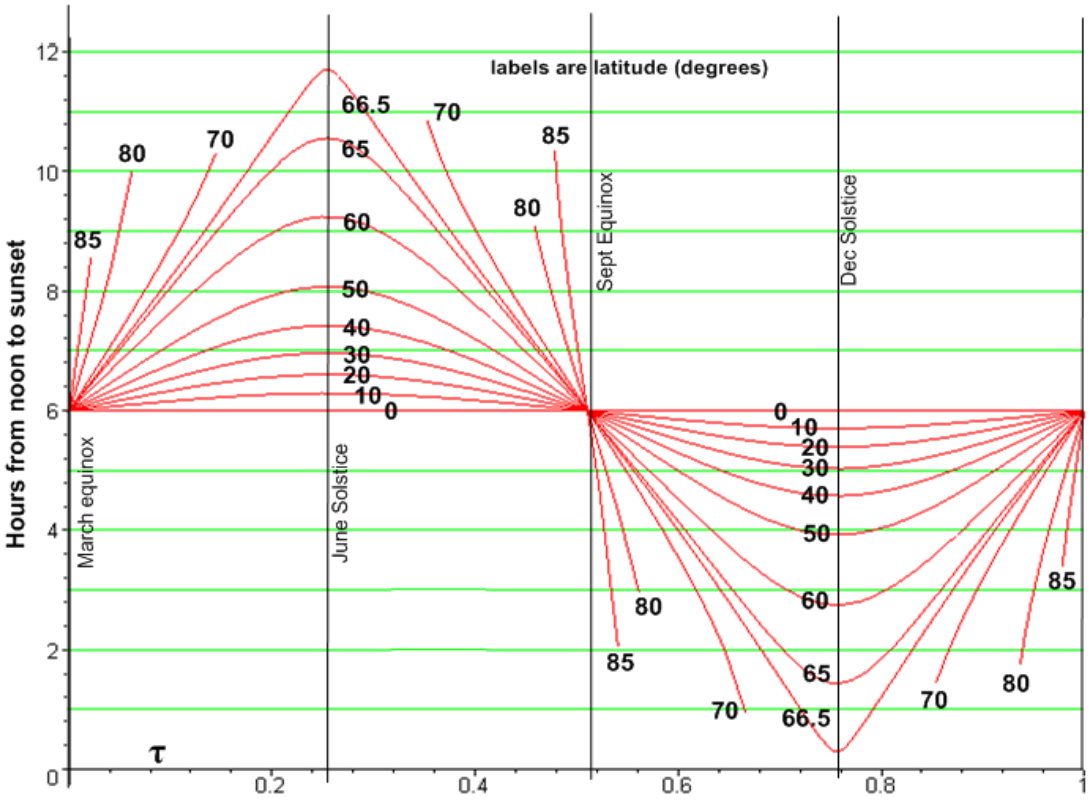

Fig 9.3

For the southern hemisphere, negate latitude labels in Fig 9.3 and reflect all curves vertically through the horizontal line at t_{ss} = 6 hours. This follows from (9.15) and the rule $\cos^{-1}(-x) = \pi - \cos^{-1}(x)$.

Example: In London (θ_{LAT} = 51.5°) at June solstice, $t'_{ss} \approx 8.2$ = 8:12. From Fig 9.1, noon occurs at LMT = 12:02, so nominal sunset would then be at about 8:14 PM. Since London is on daylight savings time, clock time of nominal sunset would then be 9:14PM. The official value is 9:21 PM, about 7 minutes later. Sunrise time would be 12:02 - 8:12 = 3:50 AM, but DST moves this to 4:50 AM. The official number is 4:43 AM, about 7 minutes earlier (see comments in next section). http://www.sunrisesunset.com/England/

Length of Day

The nominal length of day is given by,

$$t_{day} = 2\, t'_{ss} = (24/\pi) \cos^{-1}[-\tan\theta_t \cot\theta_1] \quad . \qquad (9.16)$$

Here we have assumed that "day" is twice the noon-to-sunset time, where sunset means the point at which the center of the sun passes through the horizon. Various adjustments are usually made to this result: (1) sunrise is usually defined as occurring when the upper limb of the sun first appears, and sunset when the upper limb disappears, since this controls "daylight". This correction is a function of the angle the sun makes with vertical at the horizon when it rises and sets (see below); (2) when the sun is just below the horizon, it appears above the horizon due to refraction in the atmosphere. The diameter of the sun is about a half degree (~ 30 arc minutes) and the refraction effect is about the same size. Both these effects make the official "daylight" longer than our nominal value t_{day}. As a ballpark estimate, these effects might add 2 degrees to daylight or 8 minutes to the nominal value given above.

Example: At summer solstice, an observer at θ_{LAT} = 40° north latitude would have,

$$t_{day} = (24/\pi)\cos^{-1}[-\tan(+23.4382^o)\tan(40^o)]$$

```
(24/Pi)*arccos(-tan(23.4382*Pi/180)*tan(40*Pi/180)): evalf(%);
                                                  14.84429702
```

= 14.844 hours = 14 hr 51 min

$$t_{daylight} \approx t_{day} + 8 \text{ min} \approx 15 \text{ hrs}$$

This would be the longest daylight of the year for this observation site.

Sunrise azimuth

We can install $\cos(\varphi-\varphi_b)_{sr}$ of (9.13) into (7.29) to find the sun's azimuth at sunrise. From (9.8) we know that $(\varphi-\varphi_b)_{sr} = -\omega t'_{sr} > 0$ so $\sin(\varphi-\varphi_b)_{sr} > 0$. Then,

$$\tan\varphi'_{sr} = [\sin\theta_t \sin\theta_1 - \cos\theta_t \cos\theta_1 \cos(\varphi - \varphi_b)_{sr}] / [\cos\theta_t \sin(\varphi - \varphi_b)_{sr}]$$

$$= [\sin\theta_t \sin\theta_1 + \cos\theta_t \cos\theta_1 \tan\theta_t \cot\theta_1] / [\cos\theta_t \sqrt{1 - \tan^2\theta_t \cot^2\theta_1}]$$

$$= [\sin\theta_t \sin\theta_1 + \cos\theta_t \cos\theta_1 (\sin\theta_t/\cos\theta_t)(\cos\theta_1/\sin\theta_1)] / [\cos\theta_t \sqrt{1 - \tan^2\theta_t \cot^2\theta_1}]$$

$$= [\sin\theta_t \sin\theta_1 + \sin\theta_t \cos^2\theta_1/\sin\theta_1] / [\cos\theta_t \sqrt{1 - \tan^2\theta_t \cot^2\theta_1}]$$

$$= \tan\theta_t[\sin\theta_1 + \cos^2\theta_1/\sin\theta_1] / \sqrt{1 - \tan^2\theta_t \cot^2\theta_1}$$

$$= (\tan\theta_t/\sin\theta_1) / \sqrt{1 - \tan^2\theta_t \cot^2\theta_1}$$

$$= (\tan\theta_t \sec\theta_{LAT}) / \sqrt{1 - \tan^2\theta_t \tan^2\theta_{LAT}} \qquad \theta_{LAT} = \text{latitude} = \pi/2 - \theta_1 \qquad (9.17)$$

Notice that φ'_{sr} is an odd function of θ_t. This fact appears in the red circle pictures of Fig 3.12 where the azimuth of sunrise at winter and summer solstice are equal and opposite. For example, with $\theta_{LAT} = 40^o$,

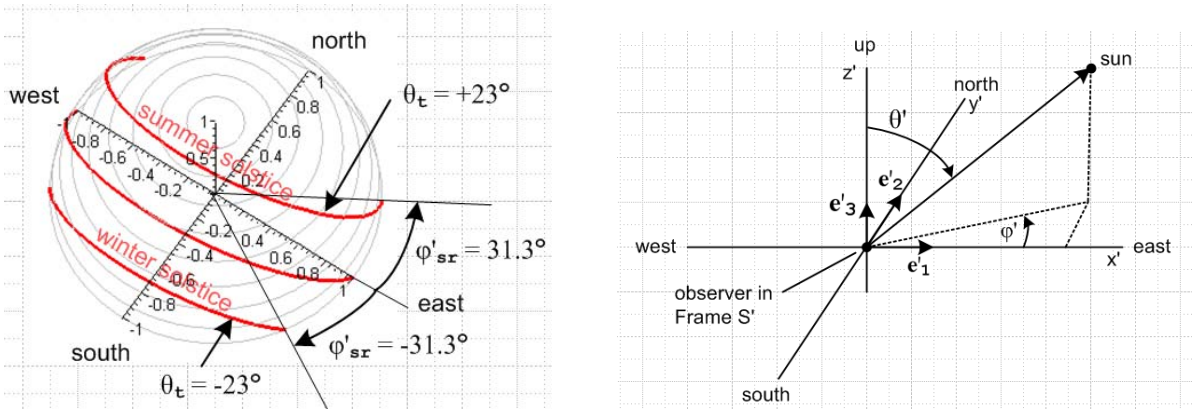

Fig 9.4

In this particular case the φ' sunrise azimuth at summer solstice is $+31.3^o$ north of east,

```
thetat := 23.4382*(Pi/180):  thLAT := 40*(Pi/180):
phip_sr := arctan(tan(thetat)*sec(thLAT)/sqrt(1 - (tan(thetat)*tan(thLAT))^2)):
evalf(% *(180/Pi));
```

31.28117809

and therefore the sunrise azimuth at winter solstice is -31.3^o.

Here is plot of sunrise azimuth as a function of time of year for a set of northern hemisphere latitudes, using equation (9.17) for φ'_{sr} and (6.13) for θ_t. The code is as shown above Fig 9.3 with the addition of these lines [phip_sr = φ'_{sr}],

```
p1 := plot([seq((180/Pi)*phip_sr,thLAT_deg =
[10,20,30,40,50,60,65,66.5,70,80,85])],tau=0..1, color = red):
p2 := plot([seq(10*N,N=-9..9)],tau=0..1,color = green):
display(p1,p2);
```

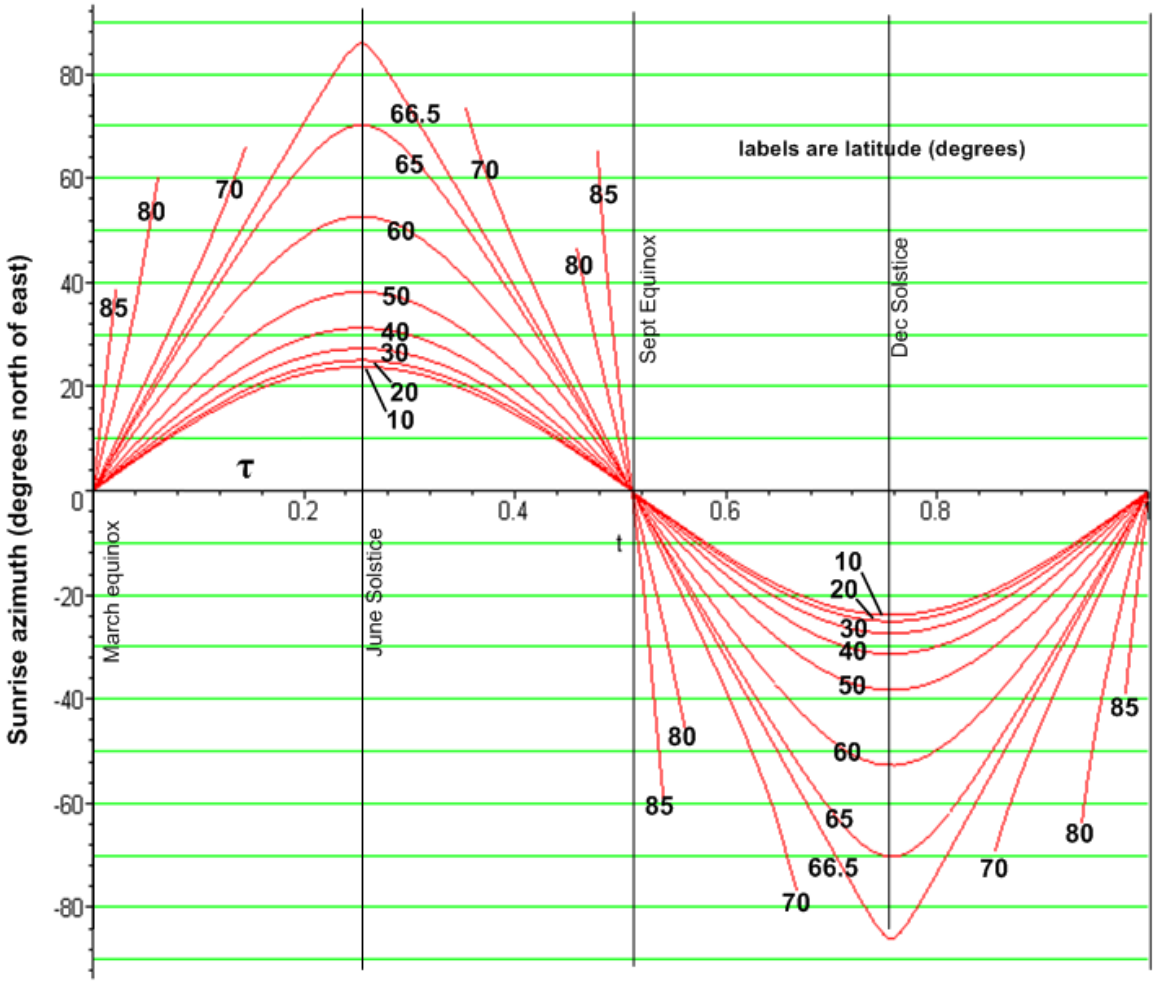

Fig 9.5

The curve for $\theta_{LAT} = 40^{o}$ latitude peaks at ~31^{o} at June solstice, in agreement with the calculation just done above. For latitudes in the arctic, the curves end where there is no daily sunrise. In the plotting mechanism, the curves end because the function goes complex.

The graphs are exactly the same for southern hemisphere latitudes, just negate the latitude labels. This follows from (9.17) which is even under $\theta_{LAT} \rightarrow - \theta_{LAT}$.

Sunset azimuths are the same numbers, but are measured north of west instead of north of east.

Noon Elevation of the Sun

The elevation of the sun above the horizon in terms of the sun's polar angle is given by

$$\theta^{\mathbf{el}} = \pi/2 - \theta' \,. \tag{9.18}$$

Then using (9.1) with (9.2), $\varphi = \varphi_{\mathbf{b}}$, one finds

$$\sin(\theta^{\mathbf{el}}_{\mathbf{noon}}) = \cos\theta'_{\mathbf{noon}} = [\sin\theta_{\mathbf{t}} \cos\theta_{\mathbf{1}} + \cos\theta_{\mathbf{t}} \sin\theta_{\mathbf{1}}] = \sin(\theta_{\mathbf{t}}+\theta_{\mathbf{1}}). \tag{9.19}$$

The correct solution of $\sin(\theta^{\mathbf{el}}_{\mathbf{noon}}) = \sin(\theta_{\mathbf{t}}+\theta_{\mathbf{1}})$ for $\theta^{\mathbf{el}}_{\mathbf{noon}}$ in this situation is as follows:

$\theta_{\mathbf{1}}+\theta_{\mathbf{t}}$ range:	0	$\pi/2$	π	
$\theta^{\mathbf{el}}_{\mathbf{noon}} =$:	no noon	$\theta_{\mathbf{1}}+\theta_{\mathbf{t}}$	$\pi - (\theta_{\mathbf{1}}+\theta_{\mathbf{t}})$	no noon

(9.20)

For example, if $\theta_{\mathbf{1}}+\theta_{\mathbf{t}} < 0$ or $\theta_{\mathbf{1}}+\theta_{\mathbf{t}} > \pi$ there is no noon because the sun never rises. If $\theta_{\mathbf{1}}+\theta_{\mathbf{t}}$ lies between 0 and $\pi/2$, then $\theta^{\mathbf{el}}_{\mathbf{noon}} = \theta_{\mathbf{1}}+\theta_{\mathbf{t}}$.

Examples:

$\theta_{\mathbf{1}} = 50^{\mathbf{o}}$ ($40^{\mathbf{o}}$ north latitude)	$\theta_{\mathbf{1}}+\theta_{\mathbf{t}}$	$\theta^{\mathbf{el}}_{\mathbf{noon}}$	
June solstice ($\theta_{\mathbf{t}} = 23.4^{\mathbf{o}}$)	$73.4^{\mathbf{o}}$	$73.4^{\mathbf{o}}$	high in sky
equinoxes ($\theta_{\mathbf{t}} = 0$)	$50^{\mathbf{o}}$	$50^{\mathbf{o}}$	
Dec solstice ($\theta_{\mathbf{t}} = -23.4^{\mathbf{o}}$)	$26.6^{\mathbf{o}}$	$26.6^{\mathbf{o}}$	low in sky

$\theta_{\mathbf{1}} = 130^{\mathbf{o}}$ ($40^{\mathbf{o}}$ south latitude)	$\theta_{\mathbf{1}}+\theta_{\mathbf{t}}$	$\theta^{\mathbf{el}}_{\mathbf{noon}}$	
June solstice ($\theta_{\mathbf{t}} = 23.4^{\mathbf{o}}$)	$153.4^{\mathbf{o}}$	$26.6^{\mathbf{o}}$	low in sky
equinoxes ($\theta_{\mathbf{t}} = 0$)	$130^{\mathbf{o}}$	$50^{\mathbf{o}}$	
Dec solstice ($\theta_{\mathbf{t}} = -23.4^{\mathbf{o}}$)	$106.6^{\mathbf{o}}$	$73.4^{\mathbf{o}}$	high in sky

10. Insolation

(a) The t_{ss} function and hours of daylight

In (9.15) the time t_{ss} from noon to sunset is given by (we drop the prime on t_{ss})

$$t_{ss} = (12/\pi)\cos^{-1}[-\tan\theta_t \cot\theta_1] \qquad (10.1)$$

where $\cos^{-1}$ is in radians and t_{ss} in hours. Here θ_t is the declination (on the celestial sphere) of the sun at some time of year as shown in Fig 6.1, and θ_1 is the colatitude (polar angle) of the observer site. Latitude $\theta_{LAT} = \pi/2 - \theta_1$ is often used below: $\sin\theta_1 = \cos\theta_{LAT}$, $\cos\theta_1 = \sin\theta_{LAT}$, $\cot\theta_1 = \tan\theta_{LAT}$.

Comment: Although cos(-x) = cos(x), it happens that $\cos^{-1}(-x) = \pi - \cos^{-1}(x)$, so one cannot "pull out" the minus sign in (10.1). On the other hand, both tan(x) and $\tan^{-1}(x)$ are odd functions of x.

This function $t_{ss}(\theta_t,\theta_1)$ plays an important role in the discussion below, so we want to write a precise expression for it, including the regions in which it is pinned to 12 or 0 hours, meaning the sun is up all the time or down all the time. Here is that expression (see Section 3 (f) and equation (3.2)),

$$t_{ss} = 12 \text{ if: } \underbrace{(\theta_t > 0 \text{ AND } \theta_1 < \theta_t)}_{\text{north pole pin}} \text{ OR } \underbrace{(\theta_t < 0 \text{ AND } \theta_1 > \pi - |\theta_t|)}_{\text{south pole pin}}$$

$$t_{ss} = 0 \text{ if: } \underbrace{(\theta_t > 0 \text{ AND } \theta_1 > \pi - \theta_t)}_{\text{south pole pin}} \text{ OR } \underbrace{(\theta_t < 0 \text{ AND } \theta_1 < |\theta_t|)}_{\text{north pole pin}}$$

$$t_{ss} = \omega^{-1}\cos^{-1}[-\tan\theta_t \cot\theta_1] = \omega^{-1}\cos^{-1}[-\tan\theta_t \tan\theta_{LAT}] \text{ otherwise .} \qquad (10.2)$$

Eq. (10.2) is implemented as $t_{ss}(\theta_t,\text{lat})$ (θ_t radians, lat degrees) by this chunk of Maple code, where th1 = θ_1, tht = θ_t, thLAT = θ_{LAT}, and lat = latitude :

```
tss := proc(theta_t,lat) local thLAT,th1,tht;  # lat in degrees
   if (type(theta_t,numeric) and type(lat,numeric)) then
     thLAT := evalf(lat*Pi/180);
     th1 := evalf(Pi/2) - thLAT;
     tht := evalf(theta_t);
     if ((tht > 0) and (th1 < tht)) then RETURN(12) fi;
     if ((tht < 0) and (th1 > evalf(Pi) + tht)) then RETURN(12) fi;
     if ((tht > 0) and (th1 > evalf(Pi) - tht)) then RETURN(0) fi;
     if ((tht < 0) and (th1 < - tht)) then RETURN(0) fi;
     RETURN(evalf((12/Pi)*arccos(-tan(tht)*tan(thLAT))));
    else 'tss(theta_t,lat)' fi;
end:
```

A 3D plot of this t_{ss} function is rather interesting,

```
plot3d(tss(theta_t,lat),theta_t = -Pi*23.4/180..Pi*23.4/180, lat =
-90..90,axes = boxed, grid = [40,40]);
```

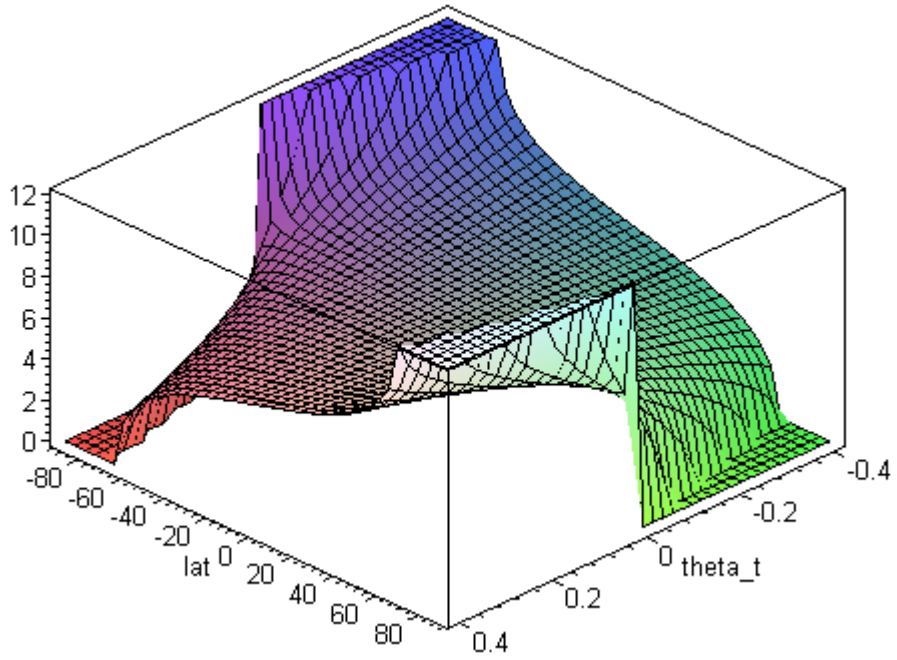

Fig 10.1

This plot shows the regions where t_{ss} is pinned to 12 or 0. When $t_{ss} = 12$, the sun never sets and "day" is a full 24 hours long. When $t_{ss} = 0$ the sun never rises. By doubling the vertical axis, the above plot shows nominal daylight as a function of θ_t= tilt angle and θ_{LAT} = latitude.

Recall equation (5.5) for θ_t, where we now ignore the eccentricity of the earth's orbit,

$$\theta_t(t) \approx \sin^{-1} \{ \sin\theta_{tmax} \sin[\Omega_0 t + \varphi_{per} - \pi/2] \} \quad . \qquad \text{// assumes e = 0} \qquad (5.5)$$

In this equation, t = 0 corresponds to perihelion and $\Omega_0 = 2\pi$ rad/year. The argument may be written

$$[\Omega_0 t + \varphi_{per} - \pi/2] = \Omega_0(\tau + t_{Me}) - \alpha \qquad \text{// (7.2) and (1.9)}$$

$$= \Omega\tau + (\Omega_0 t_{Me} - \alpha) = \Omega\tau \qquad \text{// (4.12)}$$

and our equation above can be expressed in terms of τ as [$\theta_t(t)$ and $\theta_t(\tau)$ are different functions]

$$\theta_t(\tau) \approx \sin^{-1} \{ \sin\theta_{tmax} \sin(\Omega_0\tau) \} \qquad \text{// e = 0, } \tau = 0 \text{ is Me} \qquad (10.3)$$

where $\tau = 0$ is March equinox. Note that $\theta_t = 0$ at $\tau = 0$ as one would expect from Fig 3.5.

For insolation purposes, we want $\tau = 0$ to be the June solstice, the time when θ_t is maximal. With this new time origin, the above becomes

$$\theta_t(\tau) \approx \sin^{-1} \{ \sin\theta_{tmax} \cos[\Omega_0\tau] \} \qquad \text{// e = 0, } \tau = 0 \text{ is Js} \qquad (10.4)$$

or

$$\theta_t(\tau) \approx \sin^{-1} \{ \sin\theta_{tmax} \cos[2\pi (d/365.25)] \} \qquad (10.5)$$

where d is the days elapsed since the June solstice. Using (10.4) for θ_t in (10.2), we obtain a 3D plot of t_{ss} where the θ_t axis is replaced by a days d axis,

```
thmax := 23.4*(Pi/180):
theta_t := (d) -> arcsin(sin(thmax)*cos(2*Pi*d/365.25)):
tss1 := (d,lat) -> tss(theta_t(d),lat):
plot3d(tss1(d,lat),d = -182..182, lat = -90..90,axes = boxed, grid = [40,40]);
```

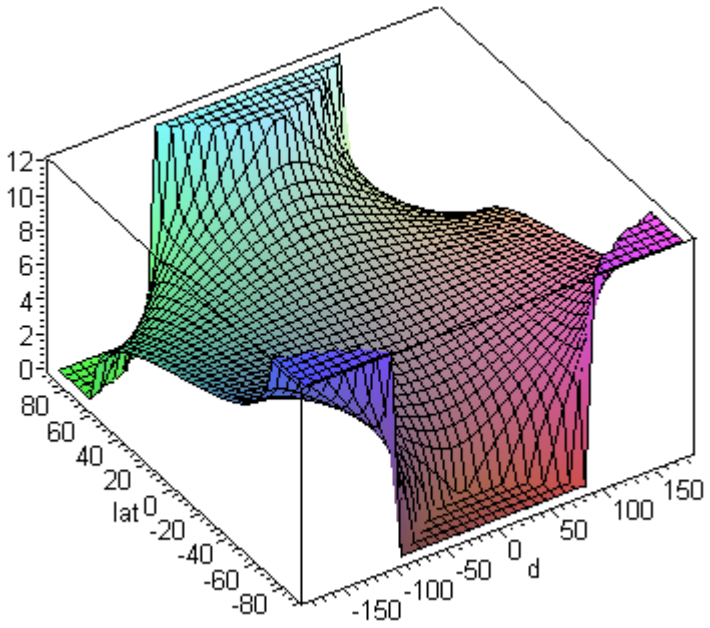

Fig 10.2

Below is a slice of 3D Fig 10.2 taken in mid plot parallel to the left face (June solstice)

```
plot(tss(thmax,lat), lat = -90..90, view = [-09..90,-1..13], axes=boxed);
```

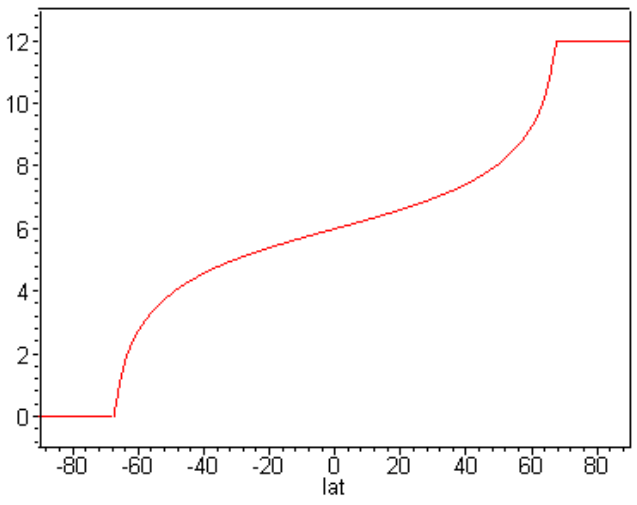

Fig 10.3

The curve is of course continuous but has serious kinks at the pinning points. The plot below gives cross sections of Fig 10.2 parallel to the back face (but doubled in height).

```
plot([seq(2*tss1(d,10*N),N=0..9)],d=-182.625..182.625, daylight=0..24,color = red);
```

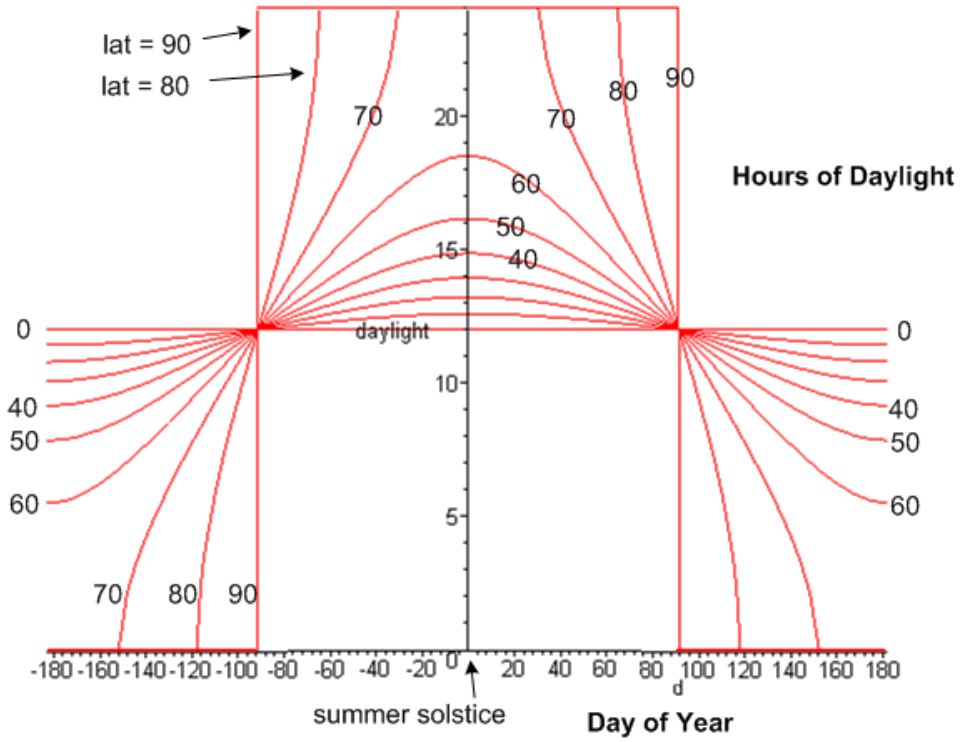

Fig 10.4

The rectangular curve is for latitude = 90^{o} (north pole, back wall of Fig 10.2). This curve is rectangular because at the north pole, the (nominal) sun is either up all day or down all day. The horizontal line for latitude = 0^{o} reminds us that the day is always 12 hours long at the equator. These facts can be visualized by putting an observer on the north pole or equator in Fig 3.13 or 3.14 and remembering that the earth should be shrunk down to a small dot. Only the curves of latitude above the Arctic Circle pin at 24 hours on the top and pin at 0 hours on the bottom.

In the southern hemisphere the above plot is the same but one should negate all latitude labels.

For some external verification of Fig 10.4, here is a web plot showing latitudes 70,50,34,23 and 0 :

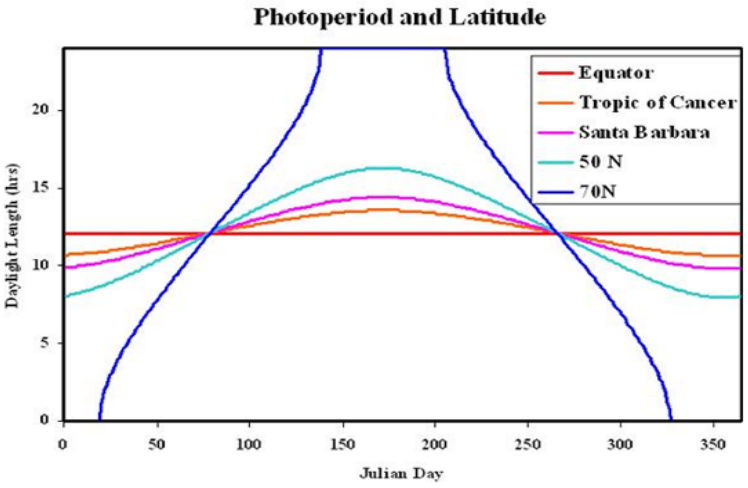

Fig 10.5

http://www.geog.ucsb.edu/ideas/Insolation.html

In the above we have assumed that "day" is twice the sunrise time, where sunrise means the point at which the center of the sun passes through the horizon (same for sunset). The ~ 8 minute adder correction for solar diameter and refraction was discussed in Section 9 (d). These effects and the small time distortion effect of orbital eccentricity are ignored in this entire Section.

(b) Daily Insolation versus latitude and day of year

The Frame S' polar angle θ' of the sun is given by (7.29) where we set $(\varphi-\varphi_b) = -\omega t'$ as in (9.8), where t' is a shifted time which causes noon to occur at t' = 0,

$$\cos\theta' = [\sin\theta_t \cos\theta_1 + \cos\theta_t \sin\theta_1 \cos(\omega t')] \ . \qquad (10.6)$$

The solar power falling on 1 square meter of earth surface is proportional to cosθ'. This is simply because the area presented by 1 square meter of ground to the sun at angle θ' from vertical is only cosθ' square meters. For example, if θ' = π/2 at sunrise, then zero power is delivered to that square meter of ground. Our patch of ground does not care about the azimuth of the sun, only its elevation (π/2-θ'). If we assume a surface solar power flux of S watt/m^2, then the solar energy delivered into 1 square meter of ground during one day (assume the ground is perfectly black and reflects nothing) is given by

$$\text{insolation}/S = 2\int_0^{t_{ss}} \cos\theta' \, dt = 2\int_0^{t_{ss}} [\sin\theta_t \cos\theta_1 + \cos\theta_t \sin\theta_1 \cos(\omega t)] \, dt$$

$$= \sin\theta_t \cos\theta_1 (2t_{ss}) + 2\cos\theta_t \sin\theta_1 \int_0^{t_{ss}} \cos(\omega t) dt$$

$$= \sin\theta_t \cos\theta_1 (2t_{ss}) + 2\cos\theta_t \sin\theta_1 (1/\omega) \sin(\omega t)\Big|_0^{t_{ss}}$$

$$= \sin\theta_t \cos\theta_1 (2t_{ss}) + (2/\omega) \cos\theta_t \sin\theta_1 \sin(\omega t_{ss}) \qquad (10.7)$$

where t_{ss} is given in (10.2). In terms of site latitude $\theta_{LAT} = \pi/2-\theta_1$,

$$\text{insolation} = S\,[\,\sin\theta_t \sin\theta_{LAT}\,(2t_{ss}) + (2/\omega)\cos\theta_t \cos\theta_{LAT} \sin(\omega t_{ss})\,] \quad \text{watts-hrs/m}^2\text{/day} \qquad (10.8)$$

Daily Insolation plotted versus latitude

The following is a plot of this daily insolation versus latitude at three times of the year (S = 1 watt/m^2):

```
insolation := (theta_t,lat) -> sin(theta_t)*sin(lat*c)*2*tss(theta_t,lat) +
(24/Pi)*cos(theta_t)*cos(lat*c)*sin(Pi*tss(theta_t,lat)/12):
plot([seq(insolation(N*thmax, lat),N = -1..1)], lat = -90..90, view =
[-90..90,-1..12], axes=boxed, color = [green,red,blue], thickness=2);
```

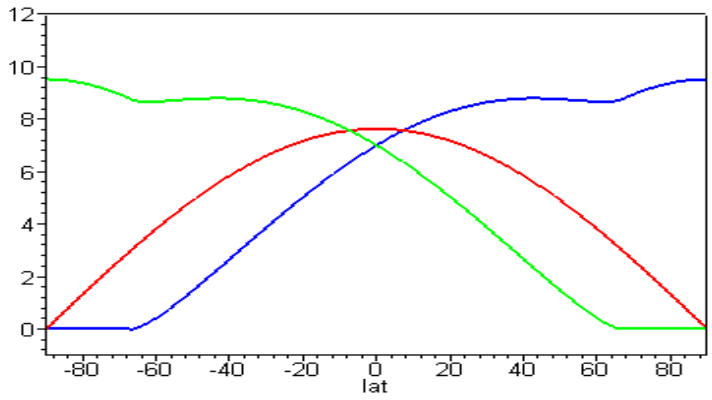

Fig 10.6

where green, red and blue are for December solstice, equinox and June solstice. The kinks in the solstice curves are due to the kinks shown in t_{ss} at the pinning points in Fig 10.3. The blue June curve shows that as one moves north from the equator, insolation peaks around 41^o, then starts to drop, but then rises again in the all-daylight region to have a final peak at the north pole (where the sun is up all the time). The units shown on this graph are watt-hours/m^2/day assuming S = 1 watt/m^2 from the sun.

As was noted in Section 1 (a), the solar flux is in fact 6.9% greater at summer solstice in the southern-hemisphere compared to the northern due to the elliptical earth orbit. The annual average value of S is about 1.367 kW/m^2, so we can then make this more practical version of the above plot where the vertical axis now shows kW-hrs/m^2 per day:

```
plot([1.035*1.367*insolation(-thmax, lat),1.367*insolation(0,
lat),0.965*1.367*insolation(thmax, lat), 2,4,6,8,10,12,14], lat = -90..90, view =
[-90..90,-1..16], axes=normal, color = [green,red,blue, grey$7], thickness=2);
```

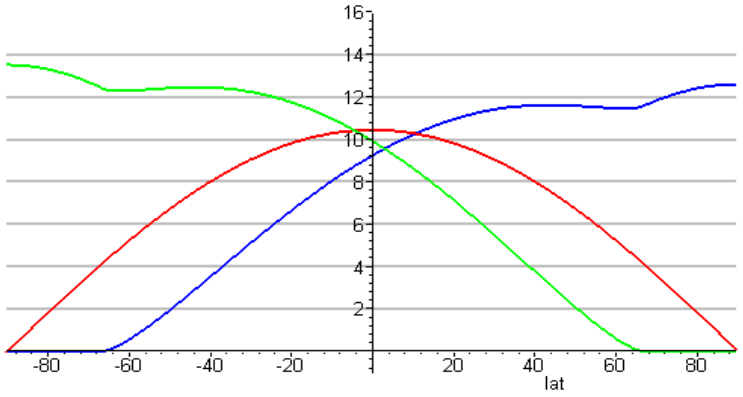

Fig 10.7

which may be compared with this plot found on the web,

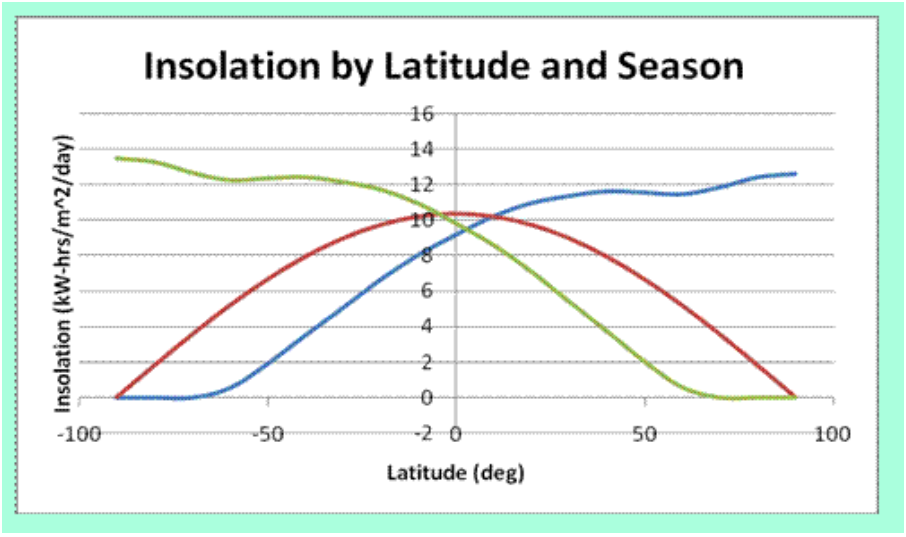

Fig 10.8

http://www.applet-magic.com/insolation.htm

The 3D Daily Insolation function plotted versus latitude and day of year

Here is a 3D plot showing the shape of the insolation function versus latitude and day of year (back to S = 1). Two views of the same plot are shown.

```
insolation1 := (d,lat) -> insolation(theta_t(d),lat):
theta_t := (d) -> arcsin(sin(thmax)*cos(2*Pi*d/365.25)):
plot3d(insolation1(d,lat), d=0..365.25, lat = -90..90, axes=boxed);
```

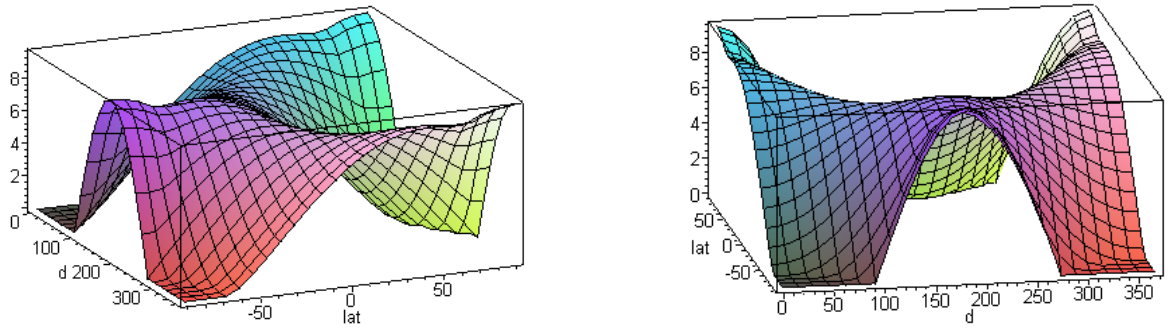

Fig 10.9

The front face of the cube on the left is the blue curve above, while a slice halfway back gives the green curve.

Daily Insolation plotted versus day of year

Slices parallel to the left face of the view on the left above (front face of the view on the right) give daily insolation versus day of year for various latitudes, which we shall now plot. Rather than express the result in watt-hrs/m^2 per day, it is useful to express things in terms of watt-hrs/m^2 per average hour of the day, so the units are then watt-hrs/m^2/hr = watts/m^2. In other words, this is the average power/m^2 during the day and the number is then easily compared with the incident power flux 1367 watts/m^2.

```
with(plots):
p1 := plot([seq((1367/24)*insolation1(d,10*N),N=0..9)], d = -182..182, color = red,
thickness=1, color = [red,blue,green,black,red,blue,green,black,red,blue],
axes=boxed):
p2 := plot([seq(50*N,N=1..12)],x=-180..180,y = 0..600, color=gray):
display(p1,p2);
```

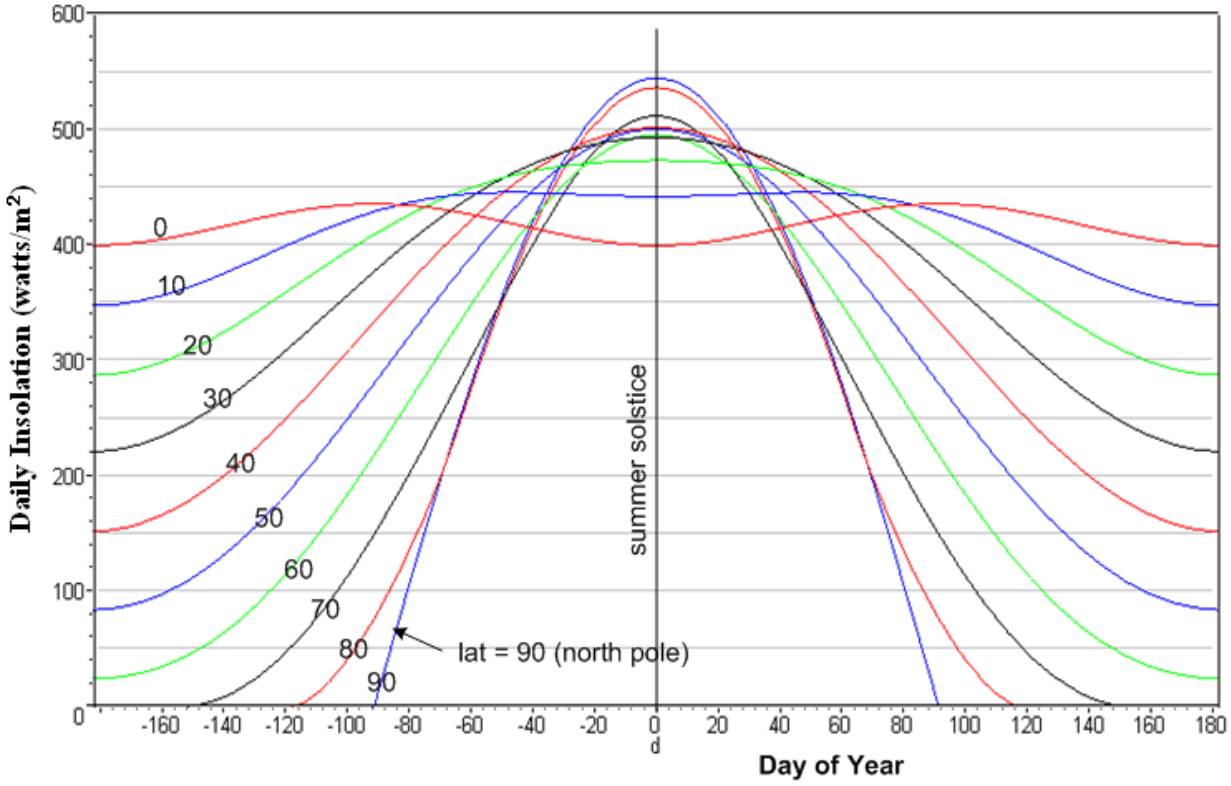

Fig 10.10

An interesting fact here is that within 10^{o} of the equator, daily insolation is not at a maximum at summer solstice. In fact, at the equator insolation is the same at summer and winter solstice and is at its lowest level of the year; it is maximal at the equinoxes. Again, Fig 3.13 and 3.14 show why this is so.

Negate the latitude numbers for the southern hemisphere.

Below is a web plot showing the same information for latitude 0,30,60 and 90. There is some small discrepancy in the vertical scale; the author does not say what value of S was used to make the plot.

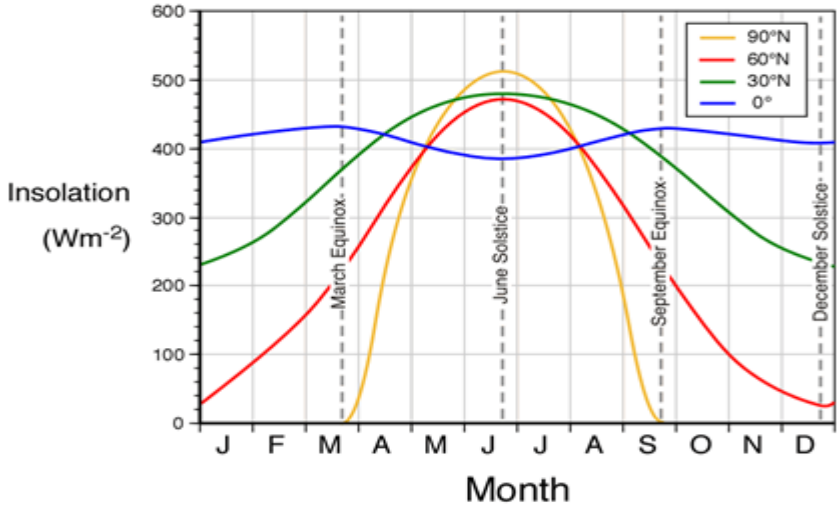

Fig 10.11

http://www.physicalgeography.net/fundamentals/6i.html

(c) Annual Insolation plotted versus latitude

Maple is happy to do some numerical integrations over the year of the daily insolation at selected latitudes. These integrals can be thought of as areas under the curves shown in Fig 10.10. The numbers are in kW-hrs/m^2 per year:

```
for n from 0 to 9 do
   i[n] := (1.367/24)*evalf(Int(insolation1(d,10*n), d = 0.01..365.24));
od;
```

$$i_0 := 152.4575120$$
$$i_1 := 150.3449481$$
$$i_2 := 144.0939449$$
$$i_3 := 133.9646616$$
$$i_4 := 120.4177368$$
$$i_5 := 104.1968319$$
$$i_6 := 86.64789699$$
$$i_7 := 72.10750149$$
$$i_8 := 65.22785914$$
$$i_9 := 63.10828976$$

From this data we can create a normalized plot of annual insolation versus latitude. First we construct a left side and right side sequence of points,

```
> s2 := seq([10*n,i[n]/i[0]],n=0..9);  # right side
```

$$s2 := [0, 1.000000000], [10, .9861432613], [20, .9451416530], [30, .8787016123], [40, .7898445621], [50, .6834483295], [60, .5683412766], [70, .4729678488], [80, .4278428677], [90, .4139401787]$$

```
> s1 := seq([-10*n,i[n]/i[0]],n=0..9); # left side
```

$$s1 := [0, 1.000000000], [-10, .9861432613], [-20, .9451416530], [-30, .8787016123], [-40, .7898445621], [-50, .6834483295], [-60, .5683412766], [-70, .4729678488], [-80, .4278428677], [-90, .4139401787]$$

Then we plot the curve with gridlines,

```
p1 := plot([[s1],[s2]], view = [-90..90,0..1], color=red, thickness=2): # curve
p2 := plot([seq(.1*N,N=1..10)], lat=-90..90,color=gray, view = 0..1):  # hor grid
p3 := PLOT(seq(CURVES([[10*N,0],[10*N,14]]),N=-9..9),COLOR(RGB,.5,.5,.5)): # vert grid
display({p1,p2,p3});
```

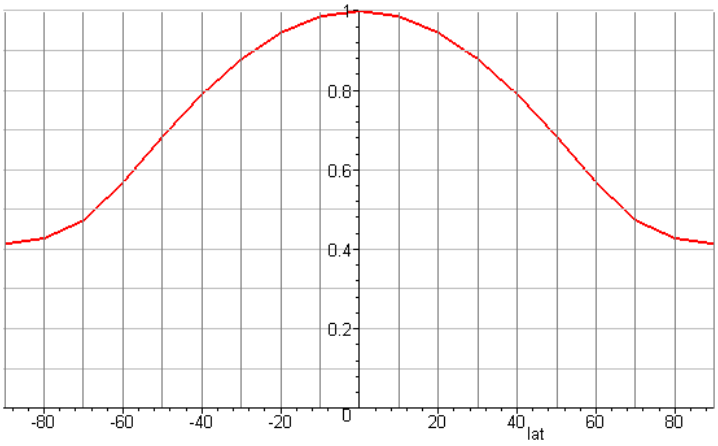

Fig 10.12

The curve peaks at the equator as one might expect. (Mean temperature has a similar shape.)

The above graph may be compared to this web graph which was formed by averaging insolation at the two solstices and the two equinoxes:

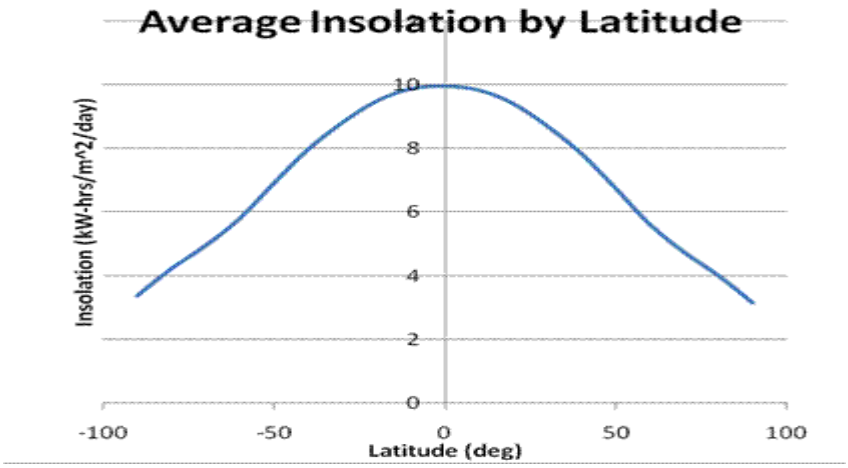

Fig 10.13

http://www.applet-magic.com/insolation.htm

11. The Solar Analemma

(a) The Sun Sphere and the Analemma

In this section the word "ecliptic" means the path of the sun on some surface. On the celestial sphere, the ecliptic is the red circle shown in Fig 3.5. We imagine this red circle is inscribed or burned onto the celestial sphere by the moving sun, and then we can later view the entire circle. In this context, we shall show below that "the solar analemma is the sun's ecliptic on the sun sphere".

What we call "the sun sphere" is a mental construct similar to, and aligned with, the celestial sphere of Section 3. The celestial sphere, enclosing the rate-ω_s rotating earth, is at rest relative to the stars. The sun sphere, being a similar exterior cage affair having lines of longitude and latitude, rotates once per year (rate Ω_0) relative to the distant stars (and the celestial sphere). Thus, the annual paths of the distant stars on the sun sphere are in fact white circles of latitude (declination). The fictitious sun, however, is at rest on the sun sphere! Recall that this fictitious sun executes a uniform annual path around the equator of the celestial sphere, having therefore an ecliptic equal to that equatorial circle. But the sun sphere rotates in the same direction and at the same speed as the fictitious sun, causing that sun to be at rest on it. If we now hop on board the sun sphere as a frame of reference, here is what we see: (1) the fictitious sun at rest at a point on the sun sphere equator; (2) the earth rotating inside the sun sphere at rate $\omega = \omega_s - \Omega_0$, which is to say, one rotation each 24 hours. (3) we also see the *actual* sun following some closed path on the surface of the sun sphere during the year, generally in the neighborhood of the fixed point of the fictitious sun. That closed path is called "the solar analemma"; the path is the actual sun's ecliptic on the sun sphere.

We can and should imagine this analemma to be inscribed on the surface of the sun sphere. We could photograph this inscribed trail from the earth at any time after it was created. In practice, however, the sun leaves no such trail on the sun sphere, so in order to see the analemma we can take a series of 365 multiple-exposure, stroboscopic, heavily filtered photos of the sun. These exposures are taken at the exact same local mean time every day from a rigidly mounted camera on the earth that is aimed generally in the known direction of the fictitious sun at that time of day. The camera film will then contain 365 white dots which trace out the continuous analemma locus. The film is then printed to obtain a photograph. A good representation of the analemma could be obtained by taking a photo perhaps every 10^{th} day. Of course there are cloudy days and snowstorms and other disturbances (earthquakes!), so photographing the analemma is a challenging yet doable task.

In the strobe light of this camera stroboscope, the sun sphere is at rest, so in effect we are taking pictures of a fixed patch on the sun sphere. From a reference frame attached to the earth, the sun sphere rotates around the earth at rate -ω. The sun then appears to be executing a spiral path similar to that shown in Fig 3.7. The strobe camera samples this path once per rotation, and the strobed image is the analemma.

As we shall see, the analemma has roughly the shape of a skinny bowling pin

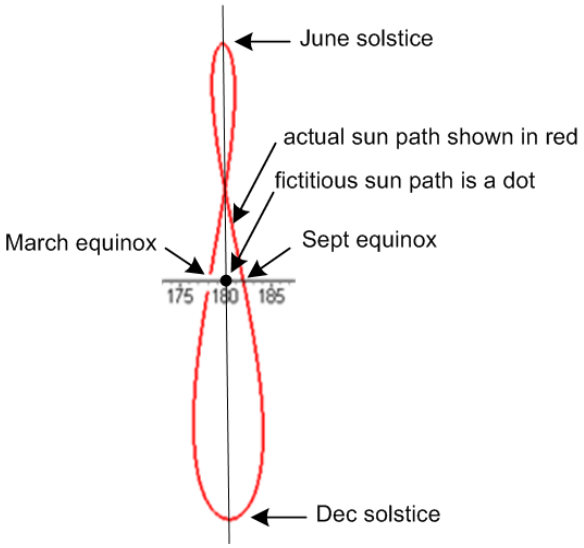

Bowling pin Analemma Fig 11.1

Sometimes analemmas are plotted with the angle axes having different scales, but in the plot above the two scales are the same.

The vertical extent of the analemma is caused by the earth's tilt. Looking at the actual sun ecliptic on the celestial sphere in Fig 3.5 or Fig 6.1, one sees that the sun varies between -23^{o} to 23^{o} relative to the celestial equator, so we expect the angular height of the bowling pin analemma on the sun sphere to be 46^{o}, which is a fairly large angle.

The horizontal extent is due to the azimuthal variation of the actual sun's position from that of the fictitious sun. This difference is the Equation of Time (6.15). Here we plot $\Delta\varphi$ in degrees using the code shown above (6.4) but with a scaling factor $(180/\pi)$ and with n = t_{Me} to diy + t_{Me} with t_{Me} from (4.11),

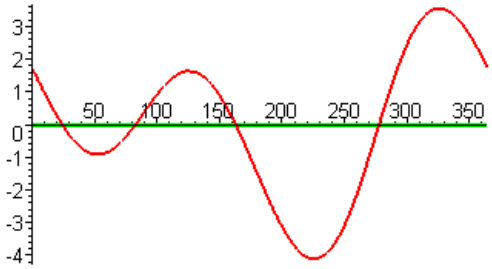

Fig 11.2

The plot shows a peak-to-peak deviation of about 7.5 degrees (green line is the fictitious sun). The left end of this graph is $\tau = 0$, the March equinox, and corresponds to the gap we have intentionally left in the analemma drawing above. The analemma path goes up to the northeast from this gap. The narrower upper part of the bowling pin corresponds to the two smaller bumps on the left of the Equation of Time in the first half of the year, and then the wider bottom part is due to the two larger bumps which end the year. The shape of the equation of time curve results from a combination of the effect of the earth's tilt on the sun's azimuthal speed, and the effect of the earth's orbital eccentricity on that same speed, as was shown in Fig 6.5. Since each pair of bumps is not perfectly symmetric, the analemma is not left/right symmetric though it appears that way above (see Figs 11.18 and 11.26 below).

(b) Qualitative appearance of the inscribed analemma in photos

As just explained, the analemma is aligned vertically along that sun-sphere line of longitude which contains the fictitious sun. In this snapshot, taken from a foggy and snowless north pole, we have turned off the sun, and we are viewing the previously "inscribed" analemma on the sun sphere. We can only see that part of the analemma which lies above the horizon plane, but we show the full analemma anyway (Maple, Stellarium Visio and Irfan)

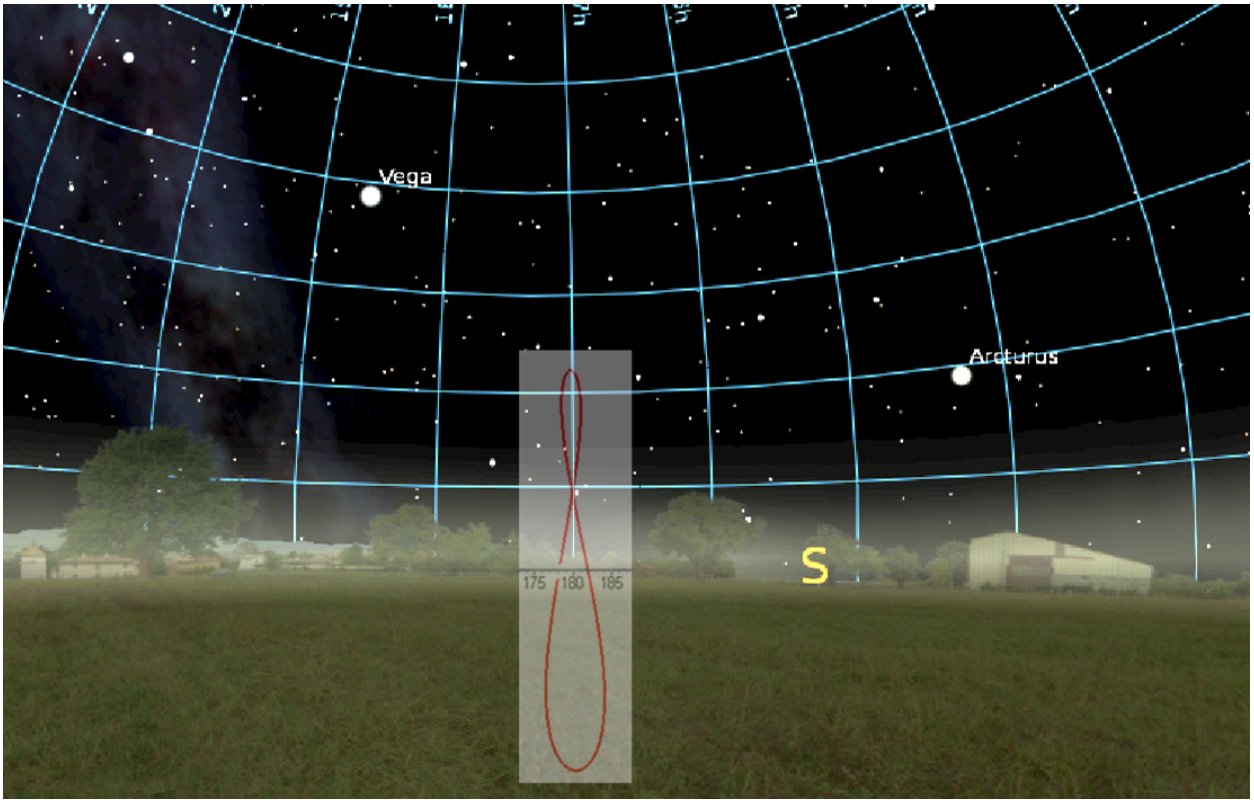

Fig 11.3

The gridlines are those of the sun sphere. Notice that all the lines of longitude meet the horizon plane vertically, but bend toward the center going up since they must meet directly overhead of the viewer. The above picture will look the same regardless of the local mean time of the photo. One could wait an hour, the earth would rotate 15^{o}, and then one could take another photo aiming the camera again at the inscribed analemma. The analemma will look exactly the same as it did in the first photo. In other words, the inscribed analemma just moves in azimuth as the earth rotates.

Now what does this same analemma look like around 8AM local mean time when viewed from 40^{o} north latitude on the earth, instead of from the north pole? The picture below is approximate, but demonstrates the basic facts.

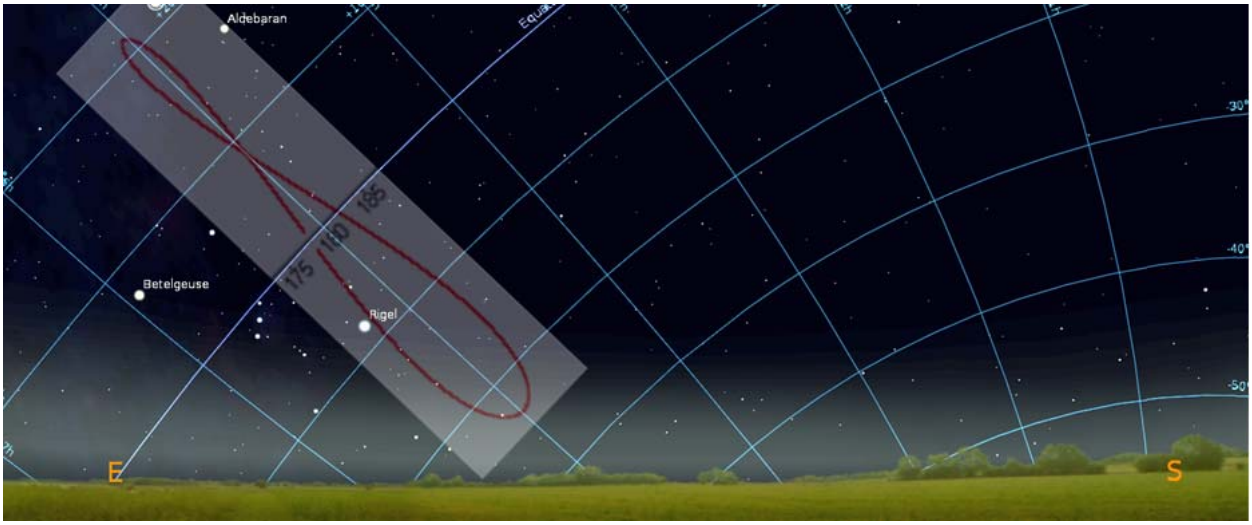

Fig 11.4

For this viewer, the "cage" of the sun sphere has latitude and longitude lines which appear as above. The sun-sphere equator is marked top center (it hits the letter E). The north pole of this cage is at the North star, behind the viewer and up in the sky. The analemma is still lying along its same sun-sphere line of longitude, but that line of longitude is tipped to the left due to the new observer location and the ~8 AM time of day.

If the observer waits 4 hours till noon, the inscribed analemma will move to the right and will become vertical at noon, lining up with the local meridian. At 4 PM in the afternoon the analemma will be off to the right and will be tipped to the right, a mirror image of the above drawing, reflected through the right edge of the picture which is the meridian.

Here is a genuine 34-shot strobed analemma which we will use below in section (g) as a case study (photographer's latitude 44.7^{o} ; shot at 8 AM local mean time; credit and reference given there)

Fig 11.5

For the observer in Fig 11.4, the analemma can never be horizontal because its longitude line is not visible when horizontal. If the viewer moves to the equator, however, then at 6 AM local mean time the analemma will be exactly horizontal,

Fig 11.6

The qualitative images of the imaginary inscribed analemma shown above are those that would appear on the film of a camera. In the following section, we shall compute the exact shape of the analemma in "angle space" and not in "camera film space". In angle space, we shall find that the analemma pattern bends away from the center as we move away from local noon. Later, however, we shall compute the image of the analemma as it appears on film ("screen space") and this bending of the angle-space analemma goes away, and the approximate images above are realized. The exact shape and tilt of the film analemma depends, due to perspective effects, on the exact direction in which the camera is pointed.

(c) Calculation of the analemma in angle space

In this section we develop the equations used in our Maple program to compute the analemma. The math is described here, while the program itself is described in section (e) below. The notion of local mean time LMT was presented above in Section 8 (b).

1. Location of the actual sun and the mean fictitious sun

The location of the **actual sun** for our Frame S' observer at polar angle θ_1 is given by

$\theta' = \cos^{-1}[\sin\theta_t \cos\theta_1 + \cos\theta_t \sin\theta_1 \cos(\varphi_b-\varphi)]$ *(7.29)*
$\varphi' = \tan^{-1}([\sin\theta_t \sin\theta_1 - \cos\theta_t \cos\theta_1 \cos(\varphi_b-\varphi)] / [-\cos\theta_t \sin(\varphi_b-\varphi)])$ *(7.29)*
$\Phi' = \pi + \tan^{-1}([\cos\theta_t \sin(\varphi_b-\varphi)] / [-\sin\theta_t \sin\theta_1 + \cos\theta_t \cos\theta_1 \cos(\varphi_b-\varphi)])$ *(8.3)*

$\theta_t = \sin^{-1}[\sin\theta_{tmax} \sin(\psi-\alpha)]$ *(6.13)*
$\varphi = \tan^{-1}[\cos\theta_{tmax} \tan(\psi-\alpha)]$ *(6.13)*
$\psi = \Omega_0 t + 2e \sin(\Omega_0 t) + (5/4)e^2 \sin(2\Omega_0 t), \quad t = \tau + t_{Me}$ *(6.13), (7.2)*

$\varphi_b = \varphi_{b0} + \omega_s \tau$ with $\varphi_{b0} = \varphi_1 + \varphi_{G0}$. *(7.3),(7.7)* (11.1)

Angles θ',φ' are the spherical angles of the actual sun in Frame S' as in Fig 7.3, while $\Phi' = \pi/2-\varphi'$ as in (8.2). Angles θ_t and φ are the declination and right ascension of the actual sun in Frame S as in Fig 7.1. Angle φ_1 is the east longitude of the observer site relative to Greenwich, and φ_{G0} is the right ascension that Greenwich had at the last March equinox, τ = 0. Angle θ_{tmax} is the famous 23^o tilt (obliquity). Rate $\Omega_0 = 2\pi$ radians per year, and $\omega_s = \omega + \Omega_0$ is the sidereal rotation rate of the earth as in (1.6), where $\omega = 2\pi/24$ radians per hour is the solar rotation rate of the earth. The dimensionless e is the eccentricity of the earth's orbit, while $\alpha = \pi/2 - \varphi_{per}$ where φ_{per} is the 13^o perihelion angle shown in Fig 1.3. Time t_{Me} is the time of March equinox relative to perihelion t = 0 as in (4.12).

For the **fictitious sun**, having e = 0 and $\theta_{tmax} = \theta_t = 0$, these equations reduce to

$\theta'_f = \cos^{-1}[\sin\theta_1 \cos(\varphi_b-\varphi_f)]$
$\varphi'_f = \tan^{-1}([-\cos\theta_1 \cos(\varphi_b-\varphi_f)] / [-\sin(\varphi_b-\varphi_f)])$
$\Phi'_f = \pi + \tan^{-1}([\sin(\varphi_b-\varphi_f)] / [\cos\theta_1 \cos(\varphi_b-\varphi_f)])$. *(8.3)*

$\theta_{t,f} = 0$
$\varphi_f = \Omega_0 t - \alpha = \Omega_0 \tau + k$ *(7.17)*
$k = [\Omega_0 t_{Me} - \alpha]$ *(7.16)*
$\varphi_b = \varphi_{b0} + \omega_s \tau$ with $\varphi_{b0} = \varphi_1 + \varphi_{G0}$. *(7.3),(7.7)*
$(\varphi_b - \varphi_f) = (\varphi_{b0} + \omega_s \tau) - (\Omega_0 \tau + k) = \omega\tau + (\varphi_{b0} - k)$ *(1.6)* (11.2)

The difference $\Delta\varphi \equiv \varphi - \varphi_f$ is then obtained by subtracting φ_f above from φ in (6.13) above, and the result matches (6.15a),

$\Delta\varphi = -\Omega_0 \tau - k + \tan^{-1}[\cos\theta_{tmax} \tan(\psi-\alpha)]$ *(6.15a)* (11.3)

This function is called "the equation of time" and has this characteristic shape in degrees instead of radians (see Fig 6.5 which has t = 0 as its left edge; the figure here has τ = 0 as its left edge),

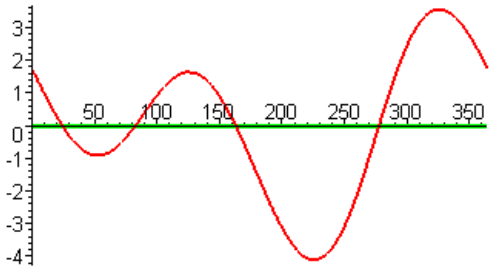

Fig 11.2

According to (11.2) and the fact that $\Delta\varphi \equiv \varphi - \varphi_{\mathbf{f}}$ we get

$$(\varphi_{\mathbf{b}}-\varphi_{\mathbf{f}}) = \omega\tau + (\varphi_{\mathbf{b0}} - k)$$
$$(\varphi_{\mathbf{b}}-\varphi) = (\varphi_{\mathbf{b}}-\varphi_{\mathbf{f}}) - \Delta\varphi = \omega\tau + (\varphi_{\mathbf{b0}} - k) - \Delta\varphi \qquad (11.4)$$

and these phases may be inserted into expressions above as needed.

2. Relationship between local time LMT and master time τ : shooting times $\tau_{\mathbf{N}}$

In this section, $\omega = \pi/12$ rad/year, and time τ is measured in hours.

Recall from Section 8 that :

$$LMT = 12(\Phi'^{\mathbf{NP}}_{\mathbf{f}}/\pi) \qquad (8.9)$$

where this fictitious-sun-tracking North Pole azimuth has the form $\omega\tau$ + constant,

$$\Phi_{\mathbf{f}}'^{\mathbf{NP}} = \{ \omega\tau + \pi + \varphi_{\mathbf{b0}} - k \} \bmod 2\pi \ . \qquad (8.7)$$

Here τ is our "master time" which is 0 at the last March equinox. Then,

$$LMT = (12/\pi)\, \Phi'^{\mathbf{NP}}_{\mathbf{f}} = (12/\pi) \{ \omega\tau + \pi + \varphi_{\mathbf{b0}} - k \} \bmod 2\pi$$
$$= \{ (12/\pi) [\omega\tau + \pi + \varphi_{\mathbf{b0}} - k] \} \bmod [(12/\pi)2\pi]$$
$$= \{ (12/\pi) [(\pi/12)\tau + \pi + \varphi_{\mathbf{b0}} - k] \} \bmod 24$$
$$= \{ \tau + 12 + (12/\pi)(\varphi_{\mathbf{b0}} - k) \} \bmod 24 \qquad (11.5)$$

If $\tau_{\mathbf{N}}$ are the times of analemma daily photo shoots, we can solve (11.5) for $\tau_{\mathbf{N}}$ in terms of day N and the LMT at which those shoots are taken,

$$\{ \tau_{\mathbf{N}} + 12 + (12/\pi)(\varphi_{\mathbf{b0}} - k \} = LMT + 24N, \ N = \text{integer}$$

$$\tau_{\mathbf{N}} = [\, LMT - 12 - (12/\pi)(\varphi_{\mathbf{b0}} - k)] + 24N, \qquad N = 0,1,2....$$

which is to say

$$\tau_N = \tau_0 + 24N, \qquad N = 0,1,2.... \qquad \tau_0 = [\,LMT - 12 - (12/\pi)(\varphi_{b0} - k)] \tag{11.6}$$

In other words, N corresponds to the number of the day of the N^{th} photograph. N = 0 marks a day in the vicinity of the March equinox. Notice that, with $\omega = \pi/12$ rad/hr,

$$\omega\tau_N = \omega\tau_0 + N(2\pi) \quad => \quad \omega\tau_N \bmod 2\pi = \omega\tau_0 \bmod 2\pi$$
$$\sin(\omega\tau_N + a) = \sin(\omega\tau_0 + a) \qquad \cos(\omega\tau_N + a) = \cos(\omega\tau_0 + a) \tag{11.7}$$

3. Location of the actual and fictitious strobed suns in terms of LMT

The phase appearing in the first three equations of (11.1) may be written,

$$(\varphi_b - \varphi)_N = (\omega\tau_N + (\varphi_{b0} - k) - \Delta\varphi(\tau_N)) = (\omega\tau_0 + (\varphi_{b0} - k) - \Delta\varphi(\tau_N)) \qquad // \text{ (11.2) and (11.7)}$$

$$= (\omega[\,LMT - 12 - (12/\pi)(\varphi_{b0} - k)] + (\varphi_{b0} - k) - \Delta\varphi(t_N)) \qquad // \text{ (11.6) and } \omega = \pi/12$$

$$= (\omega[\,LMT - 12] - (\varphi_{b0} - k) + (\varphi_{b0} - k) - \Delta\varphi(\tau_N))$$

$$= (\omega[LMT - 12] - \Delta\varphi_N)\,. \tag{11.8}$$

We then arrive at this strobed version of (11.1) and (11.3), with $\omega = 12/\pi$ and τ in hours,

$$\theta'_N = \cos^{-1}[\sin\theta_{tN}\cos\theta_1 + \cos\theta_{tN}\sin\theta_1\cos(\omega[LMT - 12] - \Delta\varphi_N)]$$
$$\Phi'_N = \pi + \tan^{-1}\left(\frac{[\cos\theta_{tN}\sin(\omega[LMT - 12] - \Delta\varphi_N)]}{[-\sin\theta_{tN}\sin\theta_1 + \cos\theta_{tN}\cos\theta_1\cos(\omega[LMT - 12] - \Delta\varphi_N)\,]}\right)$$

$$\theta_{tN} = \sin^{-1}[\sin\theta_{tmax}\sin(\psi_N - \alpha)]$$
$$\psi_N = \Omega_0 t_N + 2e\sin(\Omega_0 t_N) + (5/4)e^2\sin(2\Omega_0 t_N), \quad t_N = \tau_N(yrs) + t_{Me} \tag{6.13}$$

$$\Delta\varphi_N = -\Omega_0\tau_N(yrs) - k + \tan^{-1}[\cos\theta_{tmax}\tan(\psi_N - \alpha)]$$

$$\tau_N(yrs) = [\tau_0 + 24N] / (diy*24) \qquad N = 0,1,2...364$$
$$\tau_0 = [\,LMT - 12 - (12/\pi)(\varphi_{b0} - k)] \tag{11.9}$$

and for the fictitious sun, this strobed version of (11.2),

$$\theta'_{fN} = \cos^{-1}[\sin\theta_1\cos(\omega[LMT - 12])]$$
$$\Phi'_{fN} = \pi + \tan^{-1}([\sin(\omega[LMT - 12])] / [\cos\theta_1\cos(\omega[LMT - 12])])\,. \tag{11.10}$$

As expected, the strobed fictitious sun position is independent of strobe time τ_N. Its analemma is a dot.

Equations (11.9) lend themselves to a hand calculation of the analemma, but in our Maple code below we shall instead use the continuous-time equations (11.1) and create data arrays by sampling (strobing)

these equations with $\tau = \tau_N$ from (11.9). In that code ω is expressed in radians/year, so the τ_N strobing times appearing there are τ_N(yrs).

4. View of the continuous θ',Φ' data before strobing

One should remember that during the year, the functions θ' and Φ' of (11.1) [the position of the sun as seen from Frame S'] oscillate every day. Here is a typical view of θ' during a year, with a zoomed section below (the dark red areas in the upper image are just an aliasing artifact)

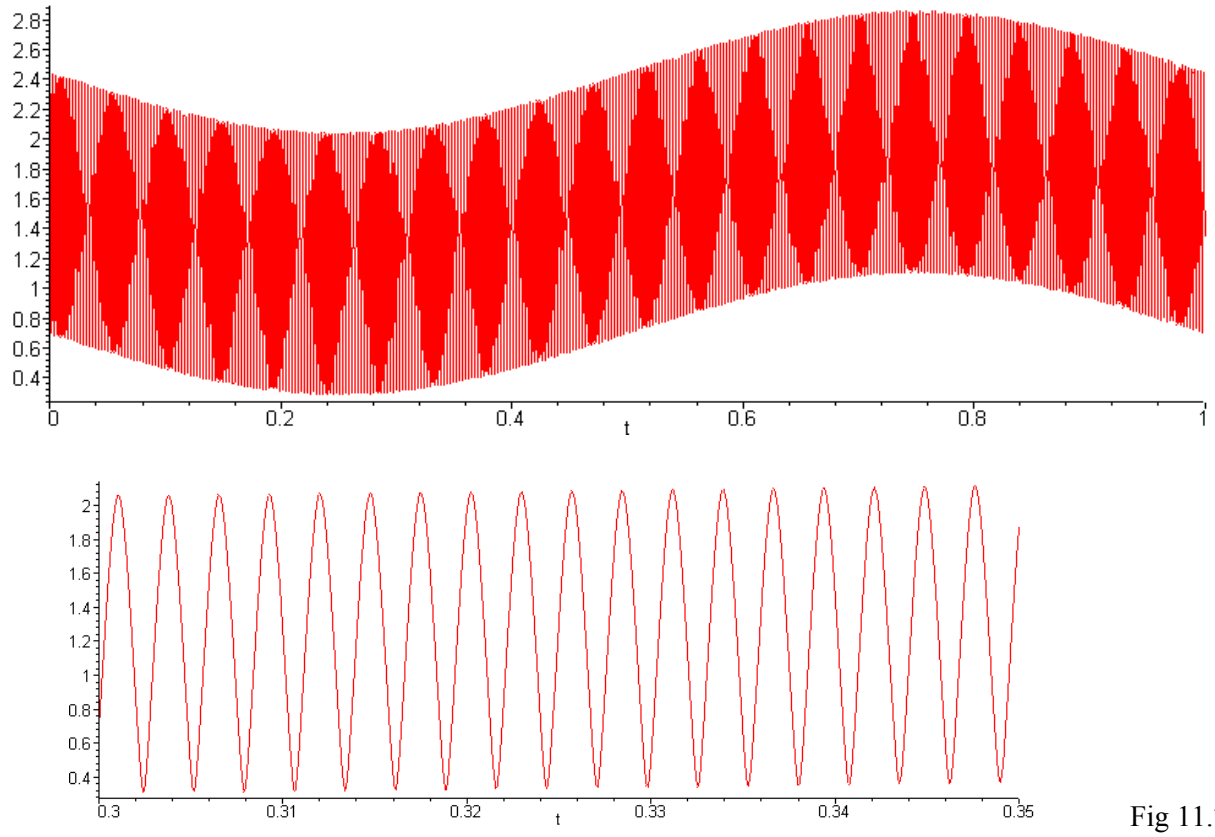

Fig 11.7

The daily strobing picks out a slow sinusoidal curve which tracks the envelope. In these plots, the value θ' = 1.57 = π/2 is that of the points of daily sunrise and sunset. In the first plot, the sun reaches maximum elevation (smallest θ', lowest excursion of the bottom of the envelope) at June solstice located at $\tau = t_{Js} - t_{Me}$ = .4623 - .2084 = .2539, using numbers from (4.11).

Meanwhile, Φ' is even more violent in its activity,

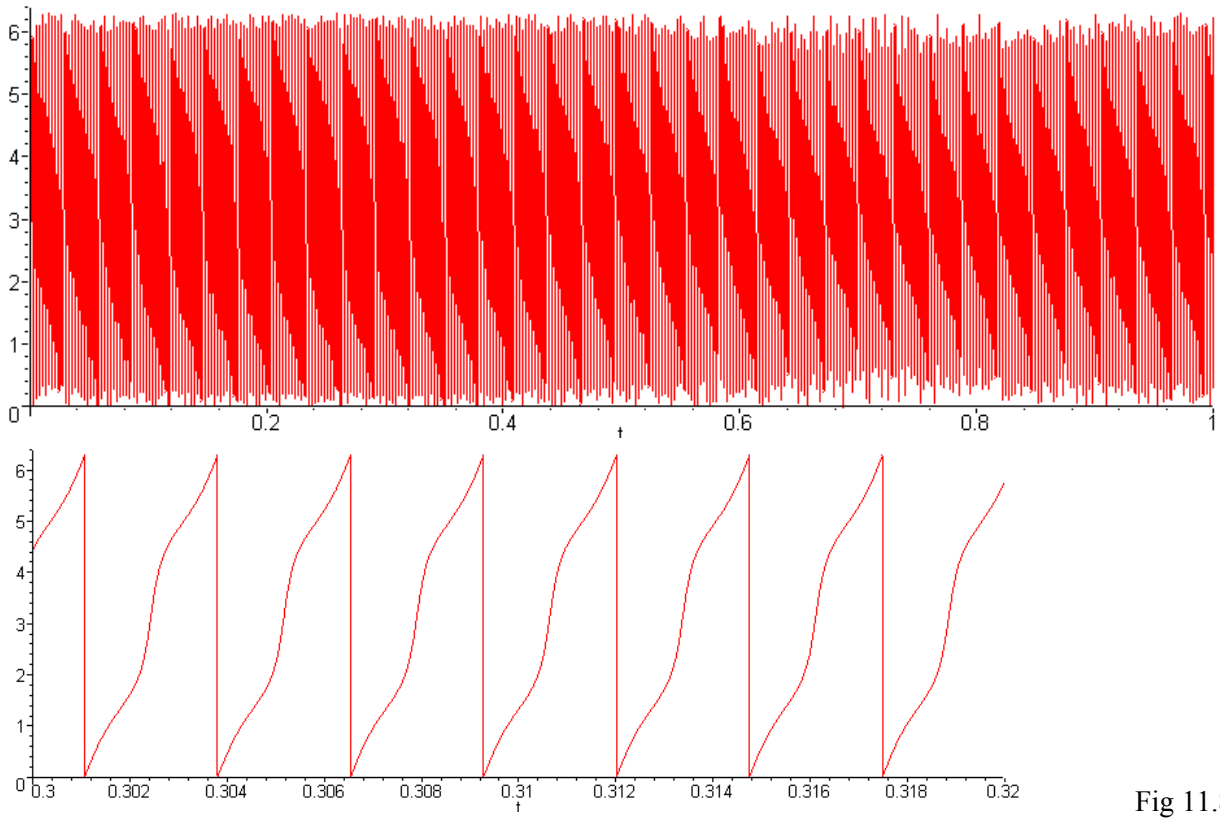

Fig 11.8

During each day, angle Φ' of the observed sun increases from 0 to 2π and then jerks back to 0 again because the value is always shifted to the range (0,2π). The jerk point is Φ' = 0 which is midnight for a northern hemisphere observer, so we don't need to worry about our solar photographer strobing right on those vertical lines.

(d) Calculation of the analemma in film-space

The equations developed in section (c) above are used in our Maple program to compute the angle-space analemma. Here we show a method (installed at the end of the same Maple program) for computing the analemma as it appears on film.

1. Overview

In computer graphics language, one has "the scene" whose points have Cartesian coordinates $\mathbf{r} = x,y,z$ in some Frame S. As viewed by our Frame S' observer, points in the scene have Cartesian coordinates $\mathbf{r}' = x',y',z'$ and spherical coordinates R,θ',φ'. Our analemma observer has a camera which he points in some direction generally not aligned with the axes of Frame S'. That camera then defines a Frame $S_{\mathbf{c}}$ in which point $\mathbf{r}'$ now has coordinates $\mathbf{r_c} = x_{\mathbf{c}}, y_{\mathbf{c}}, z_{\mathbf{c}}$. This Frame $S_{\mathbf{c}}$ is often called "the eye coordinate system" and the transformation from $\mathbf{r}'$ to $\mathbf{r_c}$ is called "the eye transformation", but we shall replace the word eye with the word camera. The unit vector $\hat{\mathbf{z}}_{\mathbf{c}}$ is the direction in which the camera is pointing, $\hat{\mathbf{x}}_{\mathbf{c}}$ is "to the right", and $\hat{\mathbf{y}}_{\mathbf{c}}$ is "up". We can imagine the camera viewfinder providing a "rectangular view" of the scene. This view is a chunk of solid angle bordered by four planes. The intersection of this solid angle with a

plane whose normal is $\hat{\mathbf{z}}_\mathbf{c}$ and which is some arbitrary distance out in front of the camera is a rectangle called "the viewport". Each 3D point in the scene $\mathbf{r_c}= x_\mathbf{c}, y_\mathbf{c}, z_\mathbf{c}$ maps to some 2D point on the viewport, $\mathbf{r_v} = x_\mathbf{v},y_\mathbf{v}$. The final step is to transform these viewport coordinates to coordinates on our piece of film, or to coordinates on a photo printed from this film. This last step is called "the screen transformation" and we end up with $\mathbf{r_s} = x_\mathbf{s}, y_\mathbf{s}$. In the case of a camera, the lens might introduce some distortion in going from the viewport to screen coordinates, but we shall assume this does not happen.

The process just described runs on millions of electronic devices on a daily basis.

We now carry out the steps of the program outlined above.

2. The transformation from Frame S to Frame S'

The first step is already done. Equation (7.14) provides the Cartesian coordinates of points in Frame S',

$$\begin{aligned} x' &= R\cos\theta_\mathbf{t}\sin(\varphi-\varphi_\mathbf{b}) \\ y' &= R\left[\sin\theta_\mathbf{t}\sin\theta_\mathbf{1}-\cos\theta_\mathbf{t}\cos\theta_\mathbf{1}\cos(\varphi-\varphi_\mathbf{b})\right] \\ z' &= R\left[\sin\theta_\mathbf{t}\cos\theta_\mathbf{1}+\cos\theta_\mathbf{t}\sin\theta_\mathbf{1}\cos(\varphi-\varphi_\mathbf{b})\right] \end{aligned} \qquad (7.14)$$

where

$$(\varphi_\mathbf{b}-\varphi) = (\varphi_\mathbf{b}-\varphi_\mathbf{f}) - \Delta\varphi = \omega\tau + (\varphi_\mathbf{b0}- k) - \Delta\varphi\ , \qquad (11.2)$$

and R is the radius of the celestial sphere. These points are of course positions of the sun on that sphere.

3. The transformation from Frame S' to Frame S_c of the camera (eye transformation)

The next step is geared to a northern hemisphere observer, and we recall Fig 7.3 to the stand,

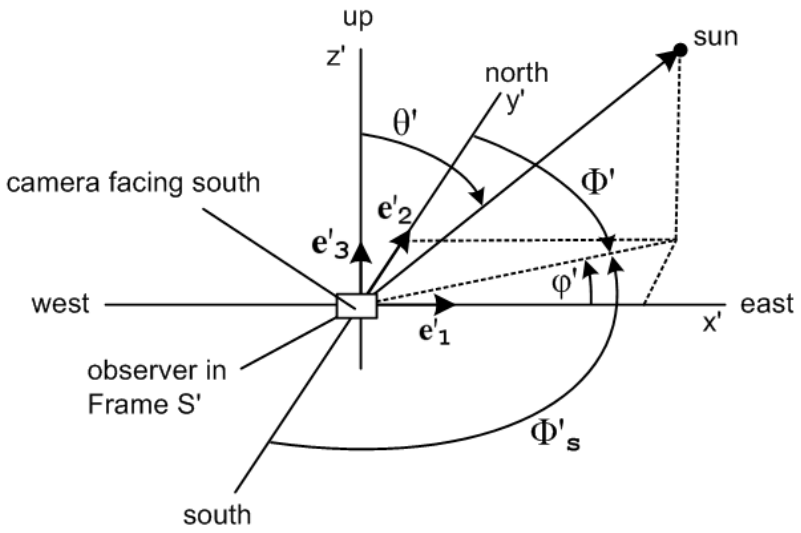

Fig 7.3

For a southern hemisphere observer, we replace do south↔north, east↔west, and $\Phi' \rightarrow \Phi'_\mathbf{s}$.

Imagine a camera at the origin of the above figure which is facing south. For this camera we have

$$\begin{aligned}
&\hat{\mathbf{z}}_{\mathbf{c}} \equiv \text{straight ahead to the south} = -\mathbf{e}'_{\mathbf{2}} = -\hat{\mathbf{y}}' \\
&\hat{\mathbf{y}}_{\mathbf{c}} \equiv \text{up} = \mathbf{e}'_{\mathbf{3}} = \hat{\mathbf{z}}' \\
&\hat{\mathbf{x}}_{\mathbf{c}} \equiv \text{to the right} = \text{west} = -\mathbf{e}'_{\mathbf{1}} = -\hat{\mathbf{x}}' \ . \qquad (11.11)
\end{aligned}$$

Imagine that the point marked "sun" is the location of the fictitious sun at some LMT for the observer. We want this point to appear at the center of the camera image. Rather than rotate the camera, we will move the sun to achieve our goal. We have to do this set of rotations on the sun point to get the sun at camera image-finder center:

$$\mathbf{r}'_{\mathbf{new}} = R_{\mathbf{e}'_{\mathbf{1}}}(\pi/2-\theta'_{\mathbf{f}})\, R_{\mathbf{e}'_{\mathbf{3}}}(-[\pi-\Phi'_{\mathbf{f}}])\, \mathbf{r}'_{\mathbf{fictsun}} \ . \qquad (11.12)$$

For reasons to be given in a moment, let us define these new variables

$$\begin{aligned}
&\alpha_{\mathbf{t}} \equiv \pi/2 - \theta'_{\mathbf{f}} \\
&\alpha_{\mathbf{p}} \equiv \Phi'_{\mathbf{f}} - \pi \qquad (11.13)
\end{aligned}$$

so that the sun transformation (11.12) becomes [$\mathbf{r}'_{\mathbf{new}} = (x'_{\mathbf{new}}, y'_{\mathbf{new}}, z'_{\mathbf{new}})$]

$$\begin{aligned}
&\mathbf{r}'_{\mathbf{new}} = R\, \mathbf{r}'_{\mathbf{fictsun}} \\
&R \equiv R_{\mathbf{1}}(\alpha_{\mathbf{t}})\, R_{\mathbf{3}}(\alpha_{\mathbf{p}}) \ . \qquad (11.14)
\end{aligned}$$

Then, given the usual active rotation matrices,

$$R_{\mathbf{1}}(\theta) = \begin{pmatrix} 1 & 0 & 0 \\ 0 & \cos\theta & -\sin\theta \\ 0 & \sin\theta & \cos\theta \end{pmatrix} \quad R_{\mathbf{2}}(\theta) = \begin{pmatrix} \cos\theta & 0 & \sin\theta \\ 0 & 1 & 0 \\ -\sin\theta & 0 & \cos\theta \end{pmatrix} \quad R_{\mathbf{3}}(\theta) = \begin{pmatrix} \cos\theta & -\sin\theta & 0 \\ \sin\theta & \cos\theta & 0 \\ 0 & 0 & 1 \end{pmatrix}, \qquad (11.15)$$

we find that, with help from Maple,

$$R \equiv R_{\mathbf{1}}(\alpha_{\mathbf{t}})\, R_{\mathbf{3}}(\alpha_{\mathbf{p}}) = \begin{pmatrix} 1 & 0 & 0 \\ 0 & \cos\alpha_{\mathbf{t}} & -\sin\alpha_{\mathbf{t}} \\ 0 & \sin\alpha_{\mathbf{t}} & \cos\alpha_{\mathbf{t}} \end{pmatrix} \begin{pmatrix} \cos\alpha_{\mathbf{p}} & -\sin\alpha_{\mathbf{p}} & 0 \\ \sin\alpha_{\mathbf{p}} & \cos\alpha_{\mathbf{p}} & 0 \\ 0 & 0 & 1 \end{pmatrix} = \begin{pmatrix} \cos\alpha_{\mathbf{p}} & -\sin\alpha_{\mathbf{p}} & 0 \\ \cos\alpha_{\mathbf{t}}\sin\alpha_{\mathbf{p}} & \cos\alpha_{\mathbf{t}}\cos\alpha_{\mathbf{p}} & -\sin\alpha_{\mathbf{t}} \\ \sin\alpha_{\mathbf{t}}\sin\alpha_{\mathbf{p}} & \sin\alpha_{\mathbf{t}}\cos\alpha_{\mathbf{p}} & \cos\alpha_{\mathbf{t}} \end{pmatrix}. \qquad (11.16)$$

Then according to the first line of (11.14) we have

$$\begin{aligned}
&x'_{\mathbf{new}} = \cos\alpha_{\mathbf{p}} x' - \sin\alpha_{\mathbf{p}} y' \\
&y'_{\mathbf{new}} = \cos\alpha_{\mathbf{t}}\sin\alpha_{\mathbf{p}}\, x' + \cos\alpha_{\mathbf{t}}\cos\alpha_{\mathbf{p}} y' - \sin\alpha_{\mathbf{t}}\, z' \\
&z'_{\mathbf{new}} = \sin\alpha_{\mathbf{t}}\sin\alpha_{\mathbf{p}} x' + \sin\alpha_{\mathbf{t}}\cos\alpha_{\mathbf{p}} y' + \cos\alpha_{\mathbf{t}}\, z' \ . \qquad (11.17)
\end{aligned}$$

Now consider this vector $\mathbf{r}'_{\mathbf{new}}$ expanded two ways

$$\mathbf{r'_{new}} = x'_{new}\hat{\mathbf{x}}' + y'_{new}\hat{\mathbf{y}}' + z'_{new}\hat{\mathbf{z}}'$$
$$= x_c\hat{\mathbf{x}}_c + y_c\hat{\mathbf{y}}_c + z_c\hat{\mathbf{z}}_c \qquad (11.18)$$

On the first line we replace the unit vectors as shown in (11.11) to get

$$\mathbf{r'_{new}} = -x'_{new}\hat{\mathbf{x}}_c - y'_{new}\hat{\mathbf{z}}_c + z'_{new}\hat{\mathbf{y}}_c \qquad (11.19)$$

Comparing the last two equations we must have $x_c = -x'_{new}$, $y_c = z'_{new}$ and $z_c = -y'_{new}$. Thus,

$$x_c = -\cos\alpha_p x' + \sin\alpha_p y'$$
$$y_c = \sin\alpha_t\sin\alpha_p x' + \sin\alpha_t\cos\alpha_p y' + \cos\alpha_t z'$$
$$z_c = -\cos\alpha_t\sin\alpha_p x' - \cos\alpha_t\cos\alpha_p y' + \sin\alpha_t z' \qquad (11.20)$$

and this then is the "eye transformation" taking points from Frame S' to Frame S_c of the camera.

Active vs Passive: camera pan and tilt

In the above development we moved the sun to a camera-centered position using rotation R. As shown in Appendix B, the same result is obtained (sun at camera center) if the camera (and its rigidly attached axes) are instead rotated by R^{-1} and the sun is left where it is in the sky. The camera rotation is then

$$R^{-1} = R_3(-\alpha_p)\,R_1(-\alpha_t) = R_{z'}(-\alpha_p)\,R_{x'}(-\alpha_t)\,. \qquad (11.21)$$

Looking at Fig 7.3 just above, and using the right hand rule, this says that the camera is first "tilted up" by angle α_t, and it is then "panned" clockwise by α_p. If we imagine the camera attached to some kind of polar angle mount, it is this mount that is in fact "panned", not the camera itself, but we shall still refer to this as a "pan" action. So α_t and α_p are the camera tilt and pan parameters. It is the equations (11.13) which cause the tilted then panned camera to point to the sun at film center, but we could then imagine adjusting α_t and α_p slightly to make the camera point to some location near the sun, or perhaps to some other location altogether. In the particular case illustrated by Fig 7.3, perhaps $\alpha_t = 50^o$ and $\alpha_p = -120^o$. This model for the operation of the camera platform has implications for the way an analemma appears on film, as discussed in Appendix D.

4. The transformation from Frame S_c to the camera film (viewport transformation)

Since we have only one screen in mind (as opposed to a different screen for each different TV monitor resolution, say) we let the viewport be the screen and then we do the viewport transformation and dispense with the screen transformation. The viewport transformation is easily obtained from this picture,

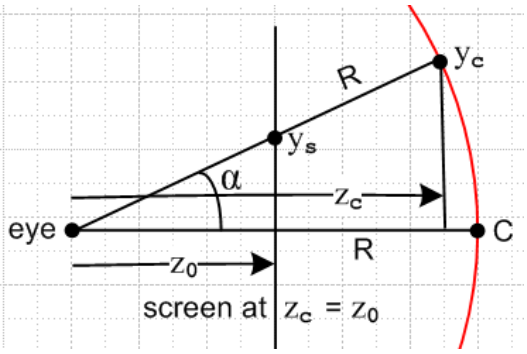

Fig 11.9

where one point of interest $\mathbf{r_c}$ is shown on the celestial sphere of radius R, and where the "viewport" is positioned some arbitrary distance z_0 to the right of the camera marked "eye". The viewport transformation taking us to our screen coordinates is then (by similar triangles $y_c/z_c = y_s/z_0$),

$$x_s = z_0(x_c/z_c)$$
$$y_s = z_0(y_c/z_c)\ . \qquad (11.22)$$

This shows the famous "perspective divide" (by z_c for each point) that used to be very expensive to do in computer hardware, but which has become cheap thanks to Moore's Law. If angle α were 45^0, one would have $y_c = z_c$ and then $y_s = z_0$. In the Maple code we set $z_0 = 1$.

Comments: In the above picture, regardless of the tilt and pan of the camera relative to "south", the camera points to a scene-center point C, distance R away, which lies on a spherical surface (celestial sphere) whose local region is perpendicular to the camera's pointing direction. The picture above is then obtained by "rolling" the camera about its axis so the point $\mathbf{r_c} = (x_c, y_c)$ lies in the plane of paper defined by $x_c = 0$. It is not assumed that the sphere is "flat" in the region of interest, so the screen transformation is accurate even if the angle α is large, as it in fact is in an analemma situation.

5. Putting the pieces together

The Frame S' positions of the sun are given by

$$x' = R\cos\theta_t \sin(\varphi - \varphi_b)$$
$$y' = R\,[\sin\theta_t \sin\theta_1 - \cos\theta_t \cos\theta_1 \cos(\varphi - \varphi_b)\,]$$
$$z' = R\,[\sin\theta_t \cos\theta_1 + \cos\theta_t \sin\theta_1 \cos(\varphi - \varphi_b)] \qquad (7.14)$$

$$(\varphi_b - \varphi) = (\varphi_b - \varphi_f) - \Delta\varphi = \omega\tau + (\varphi_{b0} - k) - \Delta\varphi\ . \qquad (11.2)$$

The camera coordinates of the sun position are

$$x_c = -\cos\alpha_p x' + \sin\alpha_p y'$$
$$y_c = \sin\alpha_t \sin\alpha_p x' + \sin\alpha_t \cos\alpha_p y' + \cos\alpha_t z'$$
$$z_c = -\cos\alpha_t \sin\alpha_p x' - \cos\alpha_t \cos\alpha_p y' + \sin\alpha_t z' \qquad (11.20)$$

and the film coordinates are

$$x_s = z_o(x_c/z_c)$$
$$y_s = z_o(y_c/z_c) \quad . \qquad (11.22)$$

We shall point the camera to the static location of the fictitious sun since this point is roughly at the center of the analemma. Recall that this point is given by (11.10)

$$\theta'_f = \cos^{-1}[\sin\theta_1 \cos(\omega[LMT - 12])]$$
$$\Phi'_f = \pi + \tan^{-1}([\sin(\omega[LMT - 12])] / [\cos\theta_1 \cos(\omega[LMT - 12])]) \qquad (11.10)$$

where $\omega = 2\pi/24$ radians per hour. As noted in (11.13) and the discussion above, the parameters α_t and α_p in (11.20) are the camera tilt and pan parameters where

$$\alpha_t = \pi/2 - \theta'_f \qquad \text{// tilt up to strobe-time elevation of the fictitious sun}$$
$$\alpha_p = \Phi'_f - \pi \qquad \text{// pan clockwise to the strobe-time location of the fictitious sun} \qquad (11.23)$$

The Maple code allows for adjustments to these angles to accommodate a camera which is pointed at some other point near the analemma. As the battery of equations above suggests, the appearance of the analemma on the film will be dependent on the direction in which the camera is pointed.

(e) A tour of Maple code which computes angle-space and screen-space analemmas

The Maple code is freely available from the author upon request. The code appearing below is in screen clips to improve clarity and save time.

In Maple, # is the comment character and % refers to "the last thing computed". A command ending with ; displays its output, one ending with : suppresses its output. The parameters shown here are for our 1999 Ukraine "case study" discussed in section (g) below. In the first block of code, Maple is initialized, a plotting package is activated, and then constants are entered

```
restart; with(plots):
```

General Constants _ θ_{tmax}, e, diy, φ_{per}, Ω_0

```
thtmax := (Pi/180)*23.4399:    # radians
e := 0.016704:                 # eccentricity
diy := 365.256363004:          # days in year
phiper := (Pi/180)*12.878:     # radians see Fig 1
Omega0 := 2*Pi:                # radians per year, earth around sun
```

Observer Site Constants _ φ_1, θ_{LAT}

```
phi1deg := 34.013:             # site east longitude in degrees
thlatdeg := 44.727:            # site latitude in degrees
# LMT will be set below in the code, photographer's local mean time
```

March Equinox Constants

```
MEQhrs := 1:                   # last March equinox at Greenwich, hours
MEQmin := 41:                  # last March equinox at Greenwich, minutes
```

Next, some one-time calculations are carried out,

One Time Computations _ ω, ω_s, φ_1, θ_1, φ_{G0}, φ_{b0}, φ_b

```
omega := 2*Pi*diy:             # radians per year, earth's solar rotation rate
omegas := omega + Omega0:      # radians per year, earth's sidereal rotation rate (1.6)
alpha := Pi/2 - phiper:        # orbital parameter related to phiper(1.9)
phi1 := (Pi/180)*phi1deg:            # radians, site longitude
theta1 := (Pi/180)*(90-thlatdeg):    # radians, site colatitude
phiG0deg := (12*60 - MEQhrs*60 - MEQmin)*15/60:   # degrees, (7.8)
phiG0 := (Pi/180)*phiG0deg:    # radians, longitude of Greenwich at tau = 0
phib0 := phi1 + phiG0:         # radians, site right ascension at tau = 0 (7.7)
phib := phib0 + omegas*tau:    # radians, site right ascension at tau = tau (7.3)
```

A procedure to do the mod 2π operation is specified, with some "noise reduction" installed,

modf(x,y) procedure to map x to the range (0,y) [with noise reduction]

```
modf := proc(xx,yy) local x,y,t; # should have yy > 0
  x := evalf(xx); y := evalf(yy);
  if type(x,numeric) and type(y,numeric) then
     t := x - y*floor(x/y);
     if (y - t) < .000001 then RETURN(0) fi;
     if t < .000001 then RETURN(0) fi;
     RETURN(t);
  else
    'modf'(x,y):
  fi:
end:    # modf(9, 2*Pi); #test
```

and then comes the arctan2Pi routine described in detail in Appendix A,

arctan2Pi(y,x) procedure returns in range (0,2Pi), see Appendix A.

```
arctan2Pi := proc(yy,xx)
   local t,x,y;
   x := evalf(xx); y := evalf(yy);
   if type(x,numeric) and type(y,numeric) then
     if x = 0 and y = 0 then print("arctan2Pi(0,0) error." ); RETURN(0) fi;
     if x = 0 and y > 0 then RETURN(Pi/2) fi;
     if x = 0 and y < 0 then RETURN(3*Pi/2) fi;
     if x > 0 and y = 0 then RETURN(0) fi;
     if x < 0 and y = 0 then RETURN(Pi) fi;
     t := arctan(abs(y/x));
     if x > 0 and y > 0 then RETURN(t) fi;       # I
     if x < 0 and y > 0 then RETURN(Pi-t) fi;    # II
     if x < 0 and y < 0 then RETURN(t+Pi) fi;    # III
     if x > 0 and y < 0 then RETURN(2*Pi-t) fi; # IV
   else
     'arctan2Pi'(y,x);
   fi;
end:
# plot3d(arctan2Pi(y,x),x = -2..2, y = -2..2, axes = boxed);  # test
```

Equation (4.10) is written as a function and then t_{Me} and k area computed from that function,

tt(psi) procedure giving time t in terms of angle psi (4.10); compute tMe and then k

```
tt:=(psi)->(1/Omega0)*(2*arctan(sqrt(1-e)*tan(psi/2)/sqrt(1+e))
-e*sqrt(1-e^2)*sin(psi)/(1+e*cos(psi))):    # (4.10)
tMe := evalf(tt(alpha)):evalf(%*diy):  # time from perihel(t=0)to Mar equinox(tau=0)
k := Omega0 * tMe - alpha:             # (7.16)
```

Equations for the position of the sun in Frame S are then entered (θ and φ with $\theta_t = \pi/2 - \theta$),

Calculate the position of the sun on the Celestial Sphere in Frame S

$\psi = \Omega_0 t + 2e \sin(\Omega_0 t) + (5/4)e^2 \sin(2\Omega_0 t)$ (6.13)

$\theta_t(t) = \sin^{-1}[\sin\theta_{tmax} \sin(\psi-\alpha)]$ (6.13)

$\varphi(t) = \tan^{-1}[\cos\theta_{tmax} \tan(\psi-\alpha)]$ (6.13)

$\varphi_f(t) = \Omega_0 t - \alpha$ (6.14)

$\Delta\varphi(t) \equiv \varphi - \varphi_f$ (6.15a)

```
psi := Omega0*t + 2*e*sin(Omega0*t) + (5/4)*e^2*sin(2*Omega0*t):
thetat := arcsin(sin(thtmax)*sin(psi-alpha)):
phi := arctan2Pi(cos(thtmax)*sin(psi-alpha), cos(psi-alpha)):
phif := Omega0*t - alpha:
dphi := phi - phif:
```

Next, equations for the position of the sun in Frame S' are entered (θ' and φ' with $\Phi' = \pi/2 - \varphi'$),

Calculate the position of the sun on the Celestial Sphere in Frame S'

$\theta' = \cos^{-1}[\sin\theta_t \cos\theta_1 + \cos\theta_t \sin\theta_1 \cos(\varphi-\varphi_b)]$ (7.29)

$\Phi' = \pi + \tan^{-1}([\cos\theta_t \sin(\varphi_b-\varphi)] / [-\sin\theta_t \sin\theta_1 + \cos\theta_t \cos\theta_1 \cos(\varphi_b-\varphi)])$ (8.3)

```
thetap := arccos(sin(thetat)*cos(theta1) +
   cos(thetat)*sin(theta1)*cos(phi-phib)):
top := cos(thetat)*sin(phib-phi):
bot := -sin(thetat)*sin(theta1) + cos(thetat)*cos(theta1)*cos(phib-phi):
Phip := modf(Pi + arctan2Pi(top, bot),2*Pi):
```

The photographer's local mean time LMT is then entered, and the function tstrobe(N) is defined,

Set photographer's local mean time LMT and define the strobe time function as in (11.9)

```
LMT := 8.01773:
tau0 := LMT-12-(12/Pi)*(phib0-k):              # hours, (11.9)
tstrobe := (N) -> (tau0 + 24*N)/(diy*24):      # years, (11.9)
```

The analemma data arrays are then generated, sampling the continuous functions θ' and Φ' using tstrobe,

Compute the analemma angle arrays in degrees by strobing the continuous functions thetap and Phip

```
t := tau + tMe:     # (7.2)
for N from 0 to 364 do
   thetapA[N] := evalf((180/Pi)*eval(thetap,tau=tstrobe(N))):
od:
for N from 0 to 364 do
   PhipA[N] := evalf((180/Pi)*eval(Phip,tau=tstrobe(N))):
od:
```

The first two plots are θ' and Φ' (left edges are τ = 0, March equinox)

Plot the separate functions thetap and Phip

```
p1 := seq([n,thetapA[n]],n=0..364): pointplot([p1]);
p2 := seq([i,PhipA[i]],i=0..364): pointplot([p2], color = blue);
```

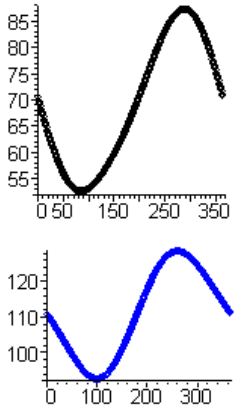

The next plot is the analemma in angle space, where Φ' is the horizontal axis and θ_{EL} = 90-θ' the vertical:

Plot the analemma in angle space. Hor = Phip, Vert = 90-theta' = elevation.
Add e.g. view=[90..270,-70..70] to pointplot before scaling to force axis ranges.

```
p3 := seq([PhipA[i],90-thetapA[i]],i=0..363): pointplot([p3],
scaling=CONSTRAINED,style = LINE, thickness = 2,color = red);
```

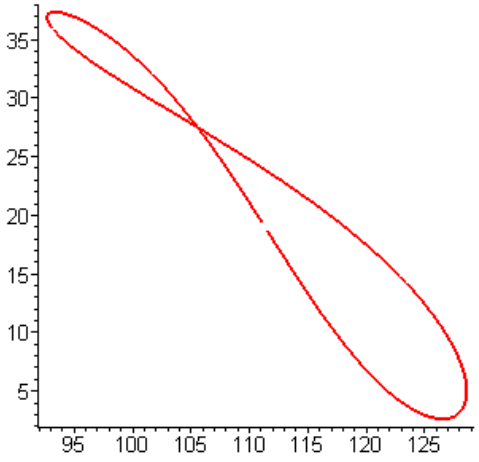

Fig 11.10

The final section of the code computes the analemma in the film "screen space". as summarized in Section 11 d (5). The user can enter tilt and pan offsets to move the camera's pointing direction away from the point of the mean fictitious sun. Since photographers generally don't document the exact point at which their analemma camera was pointed, and since this is sometimes further confused by cropping and/or compositing in a background photo after the fact, some trial and error might be needed to "fit" the analemma computed by the Maple program to a published photo. For Mr. Rumyantsev's photo we use a pan adjust of -6° as indicated by the cross hair location on the plot below.

This block of code allows entry of these offsets and computes the α_t and α_p tilt and pan parameters,

Location of the fictitious sun and the camera tilt and pan angles -- see Section 11 (d) 5

```
tilt_offset := 0:      # degrees, extra tilt up from ficitious sun point
pan_offset := -6:      # degrees, extra pan to right
omegahrs := Pi/12:     # rad/hour solar rotation rate of earth
thetapf := arccos(sin(theta1)*cos(omegahrs*(LMT-12))):   # (11.10)
Phipf := Pi + arctan2Pi(sin(omegahrs*(LMT-12))
,cos(theta1)*cos(omegahrs*(LMT-12))): # (11.10)
at := Pi/2 - thetapf:                 # (11.23)
at := at + (Pi/180)*(tilt_offset):    # add tilt offset
ap := Phipf-Pi:                       # (11.23)
ap := ap + (Pi/180)*(pan_offset):     # add pan offset
```

The final block of code then computes and plots the analemma as it appears in a photo, again as summarized in Section 11 d (5). The viewport distance is set z_0 = 1 unit from the camera :

Compute xp,yp,zp, then camera coordinates, then screen coordinates, then strobe the screen coordinates

```
xp := cos(thetat)*sin(phi-phib):    # (7.14)
yp := sin(thetat)*sin(theta1) - cos(thetat)*cos(theta1)*cos(phi-phib):
zp := sin(thetat)*cos(theta1) + cos(thetat)*sin(theta1)*cos(phi-phib):
xc := -cos(ap)*xp + sin(ap)*yp:     # (11.20)
yc := sin(at)*sin(ap)*xp + sin(at)*cos(ap)*yp + cos(at)*zp:
zc := -cos(at)*sin(ap)*xp - cos(at)*cos(ap)*yp + sin(at)*zp:
xs := xc/zc:  # (11.22)
ys := yc/zc:
for N from 0 to 364 do xsA[N] := eval(xs,tau=tstrobe(N)):od:
for N from 0 to 364 do ysA[N] := eval(ys,tau=tstrobe(N)):od:
p4 := seq([xsA[i],ysA[i]],i=2..364): pointplot([p4], scaling=CONSTRAINED
,style = LINE, thickness = 2,color = blue);
```

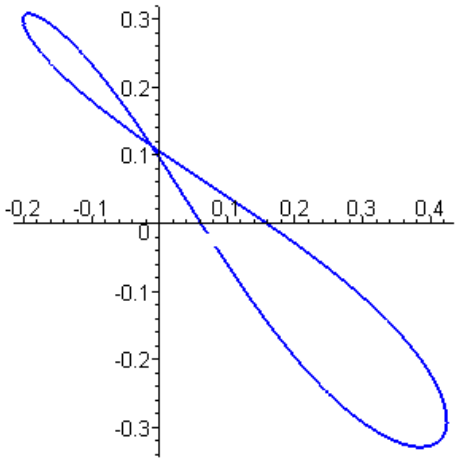

Analemma on the multiple-exposure film Fig 11.11

If this blue screen-space analemma (with no pan offset) is superposed on the red angle-space analemma without altering the aspect ratio of either image, we find

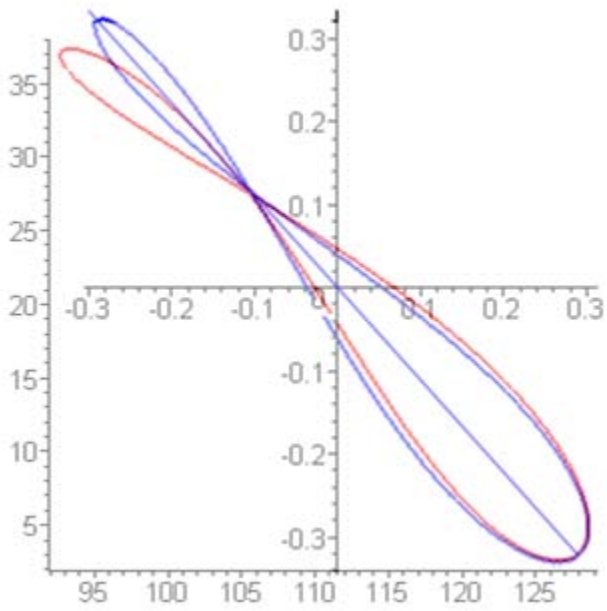

Fig 11.12

The blue screen-space analemma reliably represents the near symmetry of the analemma along its long axis, but the red angle-space analemma is bent as shown.

Here is a very crude explanation of this bending. The drawing below shows a slice of the celestial sphere near the pole for emphasis :

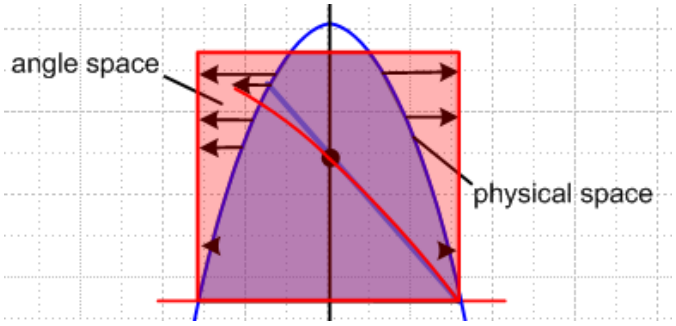

Fig 11.13

The blue region is a patch of physical space (a patch of the sky) on the slice between two blue lines of right ascension. When this region is mapped to angle space (red rectangle), the physical blue region is stretched as indicated by the arrows. In the middle of the blue region is a straight blue line, and this gets warped into the red curve. The blue line represents the nearly-straight analemma photo, while the red curve represents the angle-space analemma.

(f) An Analemma Gallery

1. Analemmas for an observer at the North Pole

These curves are made for the blue, black and red earths discussed in Section 6 (d). The red earth is the real earth, the blue earth's sun has a tilted but circular orbit, while the black earth's sun has an elliptical orbit but no tilt. At the north pole, θ' and Φ' are simply related to θ_t and Δφ as follows,

$$\theta' = \theta = \pi/2-\theta_t \quad \Rightarrow \quad \theta'_{EL} = \pi/2-\theta' = \theta_t \qquad \text{// north pole}$$
$$\Phi' = \pi + \omega\tau - (k-\varphi_{b0}) - \Delta\varphi\ . \qquad \text{// north pole} \qquad (11.24)$$

The first equation θ' = θ is obvious since at the north pole, the polar angle of the sun is the same in Frame S' as in Frame S. It can also be shown from (7.29) with $\theta_1 = 0$. The second equation comes from (8.5) which says $\Phi'^{NP} = \pi + (\varphi_b-\varphi)$, from $\Delta\varphi \equiv \varphi-\varphi_f$, and then from the last line of (11.2). The main idea of this equation is that $\omega\tau_N = \omega\tau_0 \bmod 2\pi$ so under daily strobing, Φ'_N = constant - $\Delta\varphi_N$, so Φ'_N *maps out* the equation of time which gives the horizontal extent of the analemma of Fig 11.14 below.

Blue Earth Analemmas at the North Pole (eccentricity = 0)

When e = 0, (4.12) shows that $t_{Me} = \alpha/\Omega_0$ and then (7.16) says k = 0, so these plots have e = k = 0.

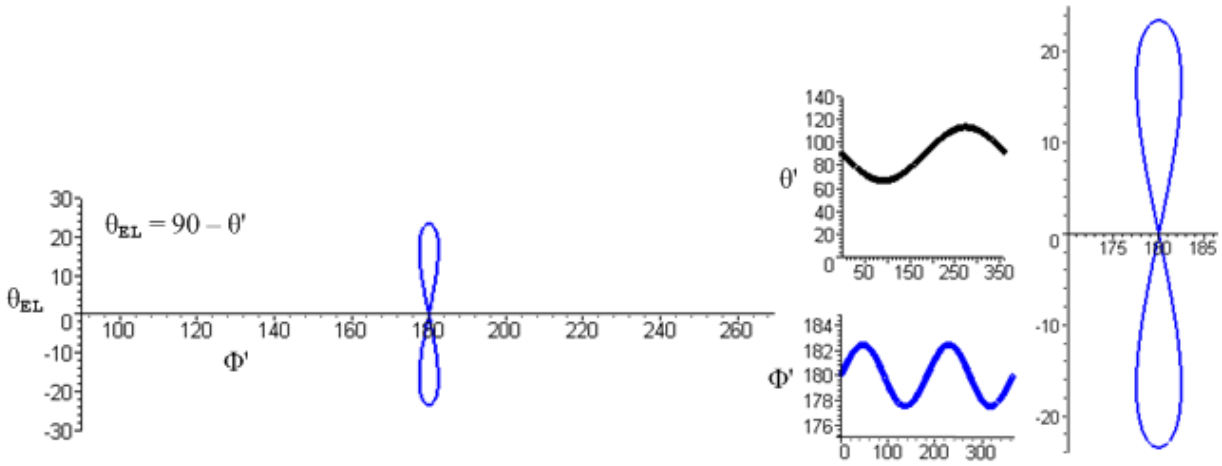

12 noon e = k = 0. Fig 11.14

This is the "prototype analemma" and we have much to say about it that won't be repeated for later analemmas. A blowup is shown on the right (see also labeling in Fig 11.1).

Again, this is the "blue earth" situation of Section 6 (d) and (e). The plots in the middle are θ' and Φ', where the left edge of the plots are at March equinox, τ = 0. For the analemma plot, Φ' is the horizontal axis in degrees, and elevation = $\theta_{EL} = \pi/2 - \theta' = \theta_t$ is plotted vertically in degrees. Both axes are shown with the same scale. Looking south at noon every day for a year, the sun will trace out the blue analemma, but only the top half is visible above the horizon. The topmost point is the day of June solstice (the day elevation is the highest), the bottom is December solstice, and the horizon is the equinox. The path starts

at March equinox on the horizontal axis. It then goes up and to the right because Φ' is moving positive. The days then trace out the "8" pattern like a car on a racetrack of this shape.

This blue earth analemma is symmetric in both directions. Although this seems obvious from the plots shown of θ' and Φ', and although it perhaps seems intuitive, actually showing this symmetry from the analemma equations requires a bit of work, and that work has been relegated to Appendix C.

The analemma is centered in the south at 180^{o} because the photos are taken at noon and the fictitious sun is at $\Phi' = 180^{o}$ every day at noon. The analemma's vertical extent above the horizon is 23^{o}. Its horizontal extent is about 5^{o}.

If we take photos in the morning instead of at noon, the analemma retains its shape but shifts to the left, as is reasonable since it is morning. From (8.6) and (8.7) we know that $\Phi' = \pi + \omega\tau - (k\text{-}\varphi_{b0}) - \Delta\varphi$, so if we do morning shots instead of noon shots, $\omega\tau$ is a smaller number at each $\tau = \tau_N$ and Φ'_N moves to the left. Since $\Delta\varphi$ is a slow function of τ, it does not change much in going to a morning strobe time. Here then is the 9 AM analemma,

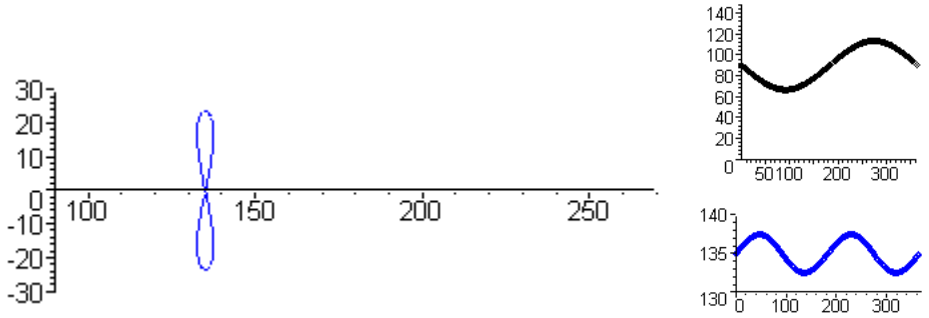

north pole 9 AM e = k = 0. Fig 11.15

Of course the afternoon-shot analemma will be shifted to the right of 180^{o} instead of to the left.

Black Earth Analemmas at the North Pole (tilt = 0)

The black earth has no tilt, so the analemma has no vertical extent. For example, at noon the analemma is a horizontal locus centered at 180^{o}. The width of this locus is about 4^{o} (see black curve in Fig 6.5).

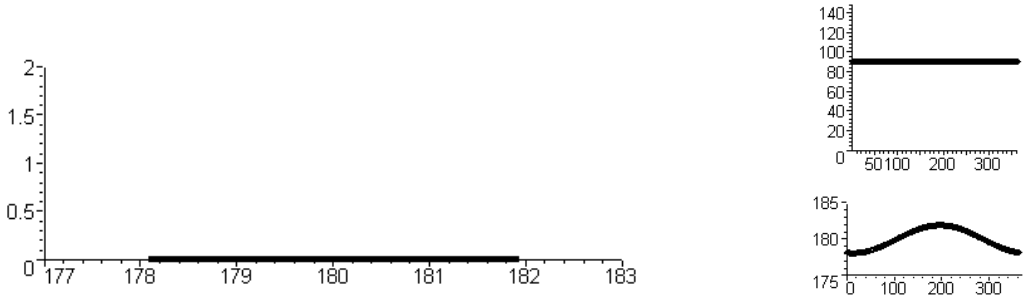

north pole 12 noon $\theta_{tmax} = 0$. Fig 11.16

Morning or afternoon photography again just shifts this locus left or right.

Red Earth Analemmas at the North Pole (actual earth)

We now have the full equation of time and here is the noon analemma (blowup on right)

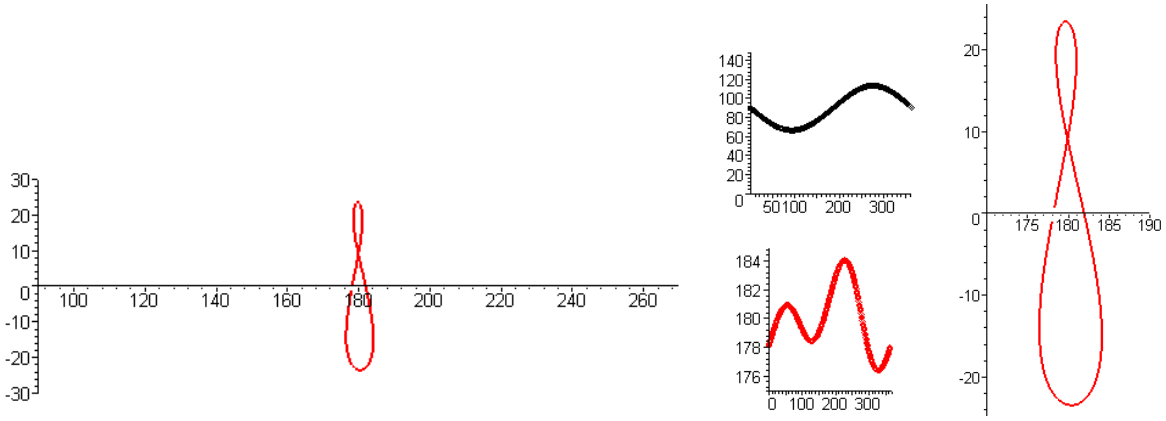

north pole 12 noon actual Fig 11.17

The equation of time (-Δφ) has less amplitude in the summer than in the winter as the red Φ' graph shows, so the analemma is narrower on the top than on the bottom. Again, only the upper part is visible. The vertical extent is still $23^{\mathbf{0}}$ on the visible part. The horizontal extent is now about $7^{\mathbf{o}}$ on the (non-visible) bottom and $2.5^{\mathbf{0}}$ on the top (see red curve Fig 6.5).

Again, morning or afternoon photography again just shifts this locus left or right.

Allowing the horizontal axis to have a different scale from the vertical, the plot on the right above has this appearance, where the left/right asymmetry is more visible,

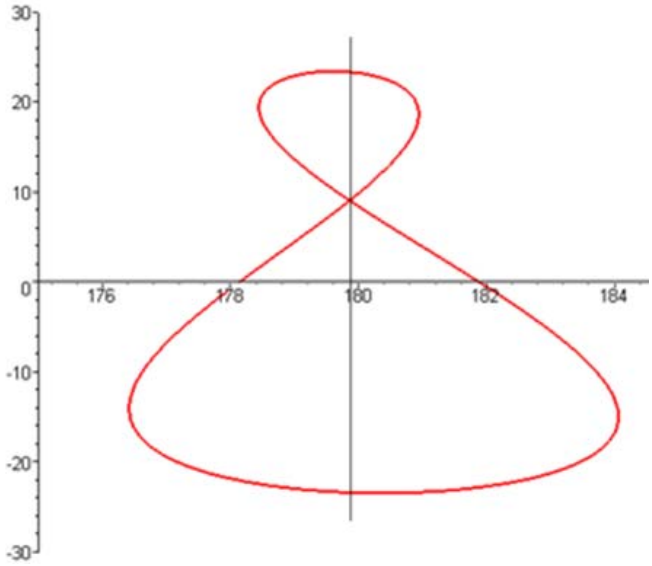

Fig 11.18

2. Analemmas for observers at other latitudes in the northern hemisphere.

Blue Earth Analemmas at the Latitude 70^{o} (eccentricity = 0)

Here is the noon analemma. The upper and lower lobes are different but not too different, and the analemma his lifted almost clear of the horizon:

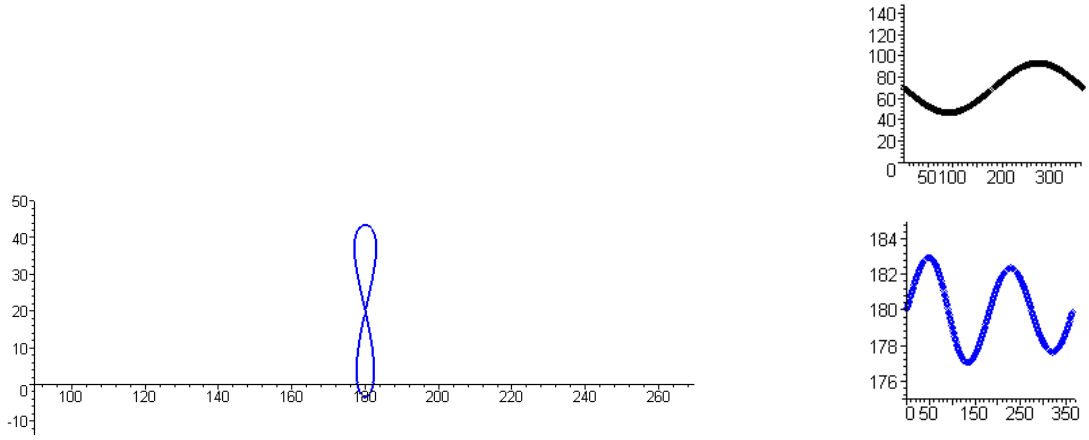

latitude = 70^{o} 12 noon e = k = 0 Fig 11.19

Now a new effect appears. If the photos are shot in the morning or afternoon, the analemma shifts horizontally of course, but now the top tilts away from 180^{o}

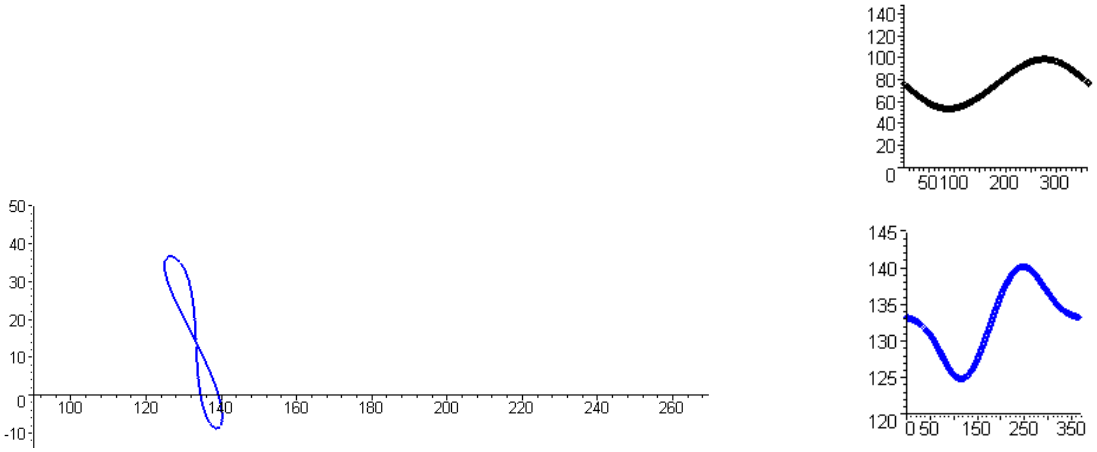

latitude = 70^{o} 9 AM e = k = 0 Fig 11.20

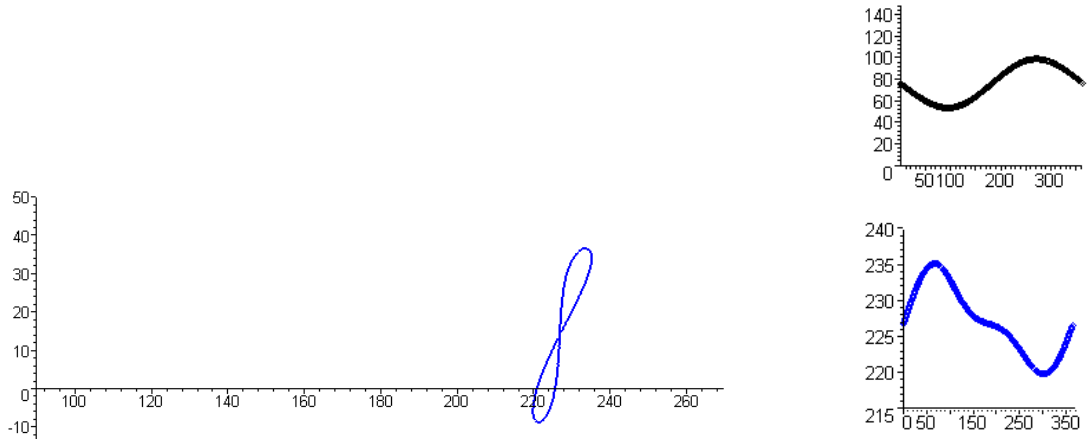

latitude = 70^{o} 3 PM e = k = 0 Fig 11.21

In these last cases, Appendix D Fig D.2 says the tipping angles away from vertical are about ± 15^{o} for the film analemmas, which roughly align with the angle space ones shown above.

Red Earth Analemmas at the Latitude 70^{o} (actual)

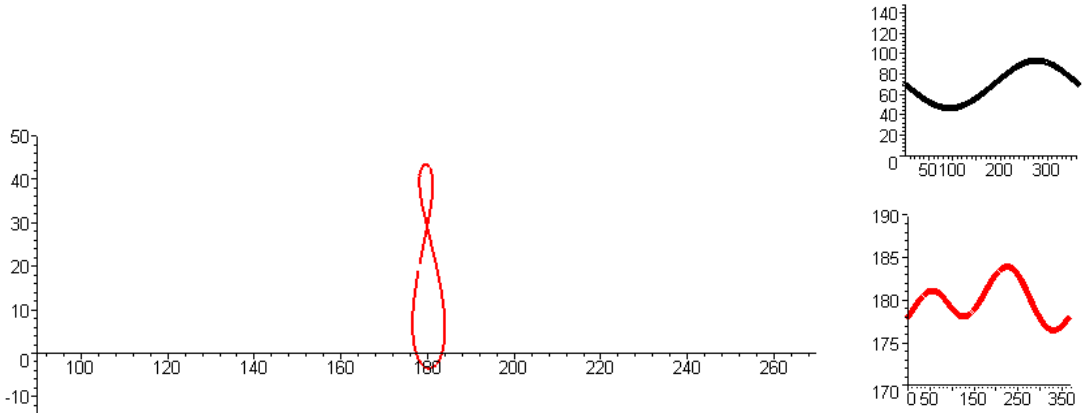

latitude = 70^{o} 12 noon actual Fig 11.22

The analemma now looks like our bowling pin of Fig 11.1, it is more asymmetrical vertically. Morning and afternoon shooting causes horizontal shift and tilt of the top away from 180^{o} just as in the blue case.

Red Earth Analemmas at the Latitude 40^{o} (actual)

The change here is that the analemma is shifted to a higher elevation in the sky,

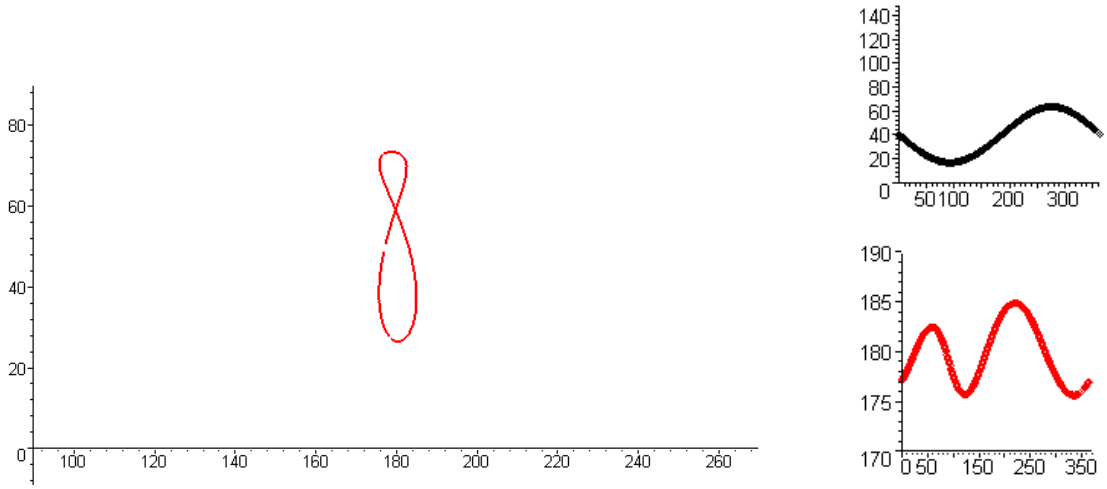

latitude = 40^{o} 12 noon actual Fig 11.23

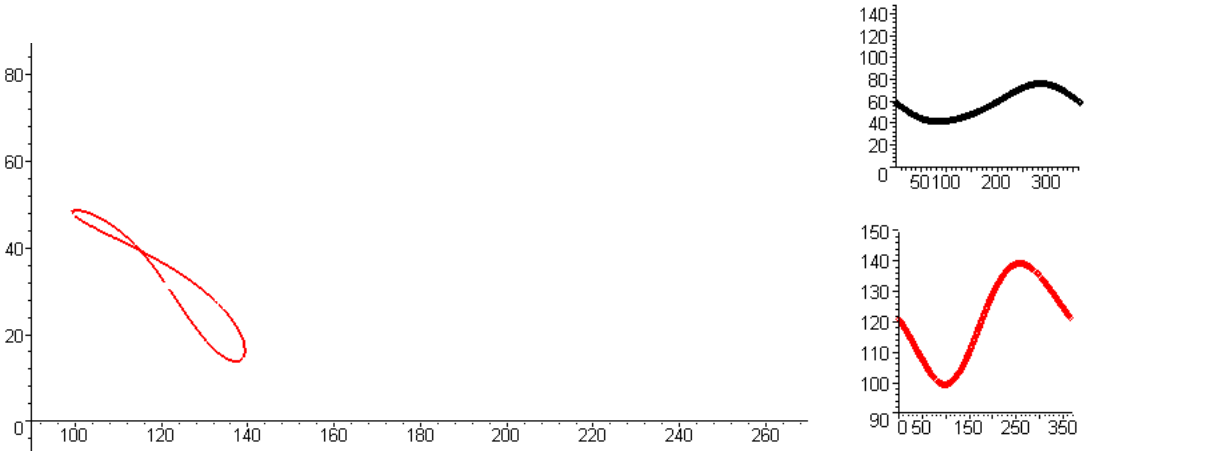

latitude = 40^{o} 9 AM actual Fig 11.24

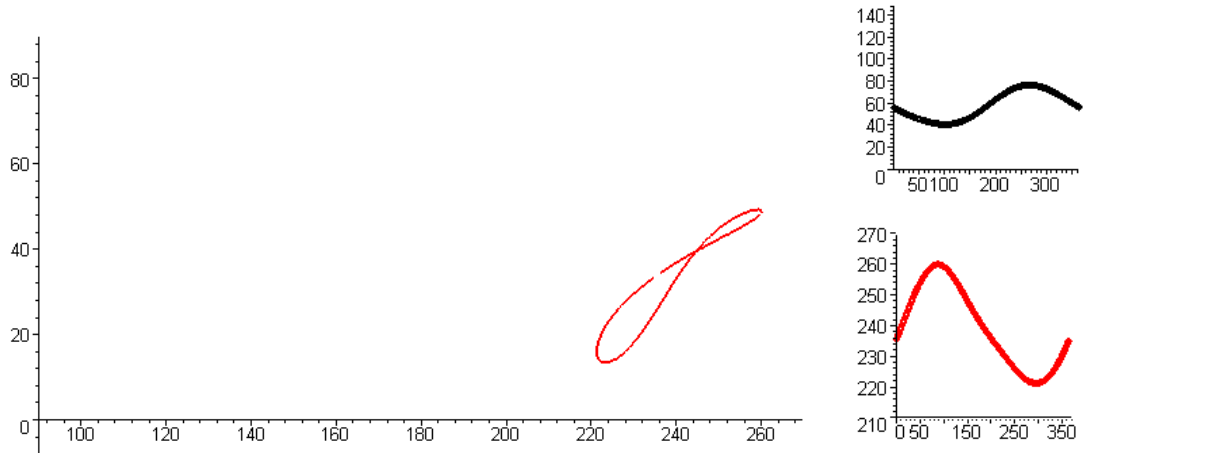

latitude = 40^{o} 3 PM actual Fig 11.25a

Now the angle-space analemmas in morning or afternoon are shifted, tilted, *and* bent away from the $180^{\mathbf{0}}$ line. Figure D.2 gives the *film* analemma tipping angles as $\pm\ 40^{\mathbf{o}}$ away from vertical. Here is the three corresponding film analemmas:

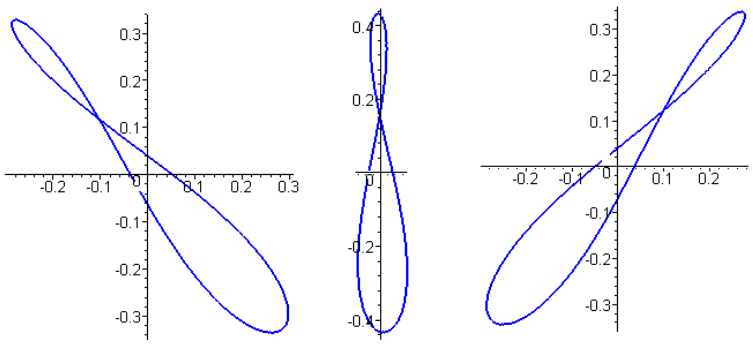

Fig 11.25b

Red Earth Analemma at the Latitude $51.4791^{\mathbf{o}}$

Our computed analemma is on the left. On the right it is superposed on a red analemma which appears on the wiki page http://en.wikipedia.org/wiki/Analemma .

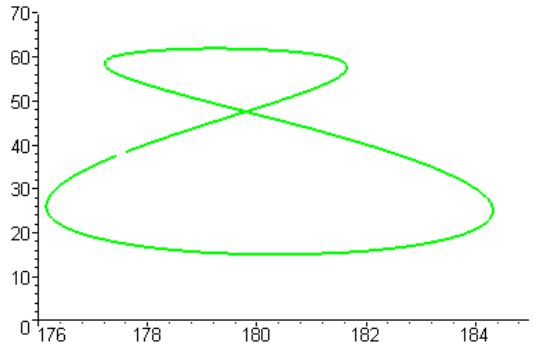

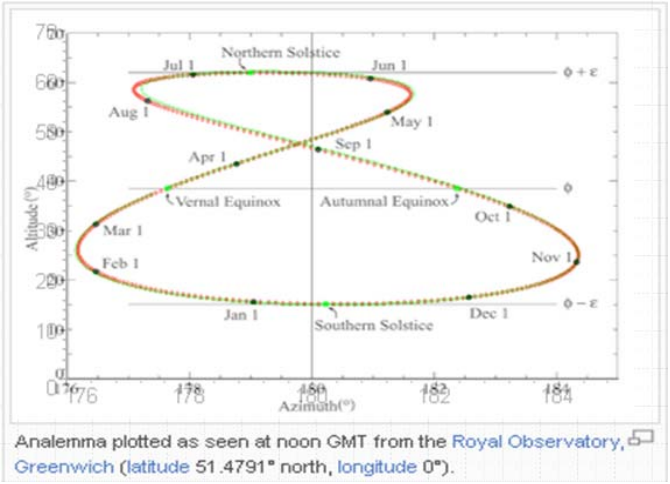

Fig 11.26

Red Earth Analemmas at the Latitude 24.5°

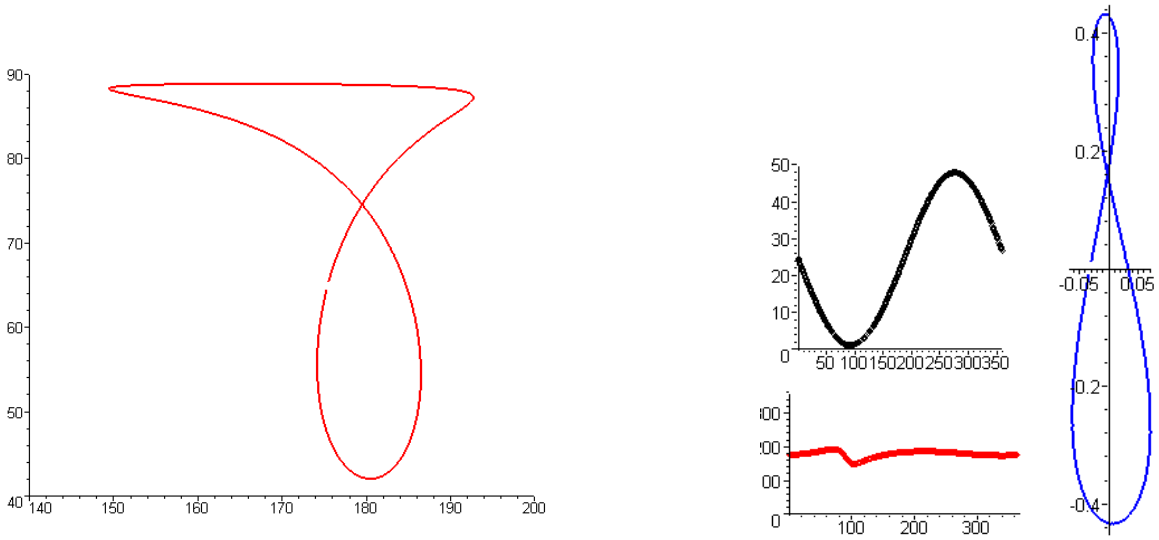

latitude = 24,5° 12 noon actual Fig 11.27

Now the top of the analemma in our (Φ', 90-θ') angle space experiences a horizontal stretching at the top similar to the "Greenland Effect" on a Mercator projection map. The camera film analemma is shown in blue on the right and does not exhibit the angle space distortion. The distortion is worst at noon because that drives the upper end of the analemma closer to 90° elevation.

Red Earth Analemmas at the Latitude 20°

We have entered the tropical zone, and the angle-space analemma pulls apart at the top :

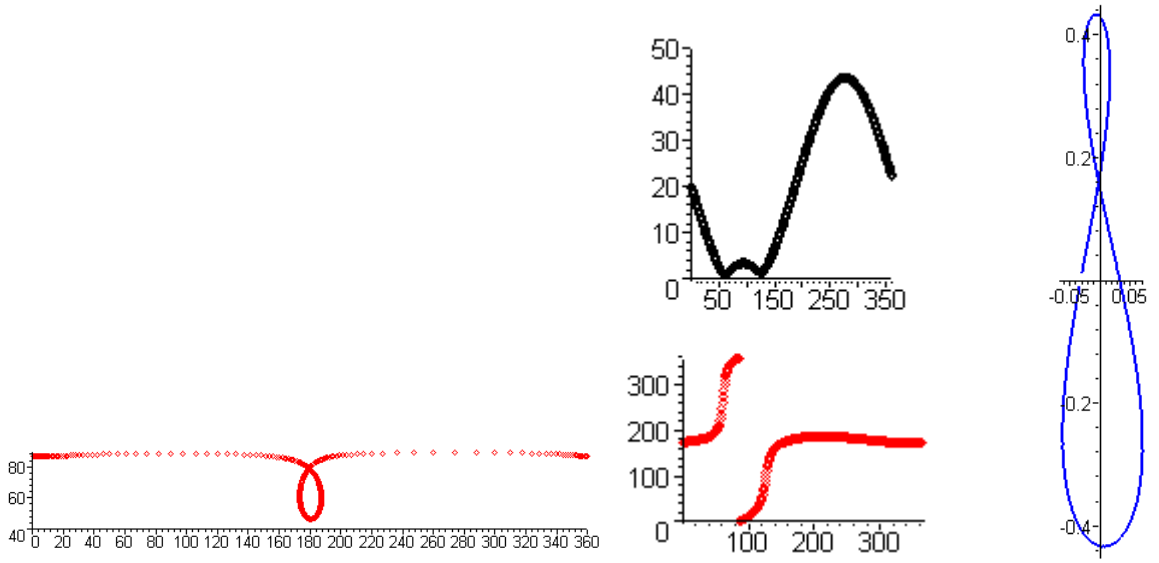

latitude = 20° 12 noon actual Fig 11.28

The above plots are completely accurate in angle space. First look at the black θ' plot on the right. Starting at March equinox, the strobed sun position goes to higher elevation and lower polar angle θ' until it reaches polar angle 0. At that point it goes "over the top", the polar angle starts increasing again, and at

some point the azimuth Φ' crosses our Fig 7.3 discontinuity between 0^o and 360^o. The camera film analemma on the right is normal. Here is the 20^o latitude image from Fig 3.12 showing this over-the-top behavior,

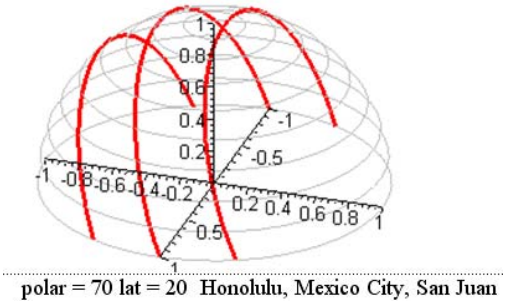

Whenever the "up" z' axis in Frame S' hits the interior of the analemma, this azimuthal discontinuity will be encountered as the year progresses.

Red Earth Analemmas at the Latitude 5^o (actual)

Now the angle-space analemma rips apart at a lower point, things are more dramatic, but the camera film analemma on the right is just fine. We pass through the azimuthal discontinuity three times!

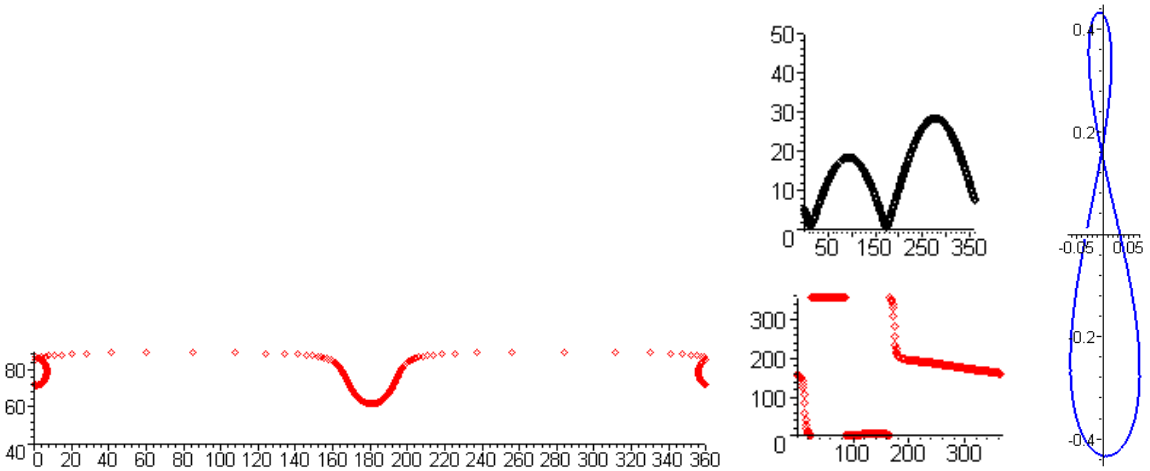

latitude = 20^o 12 noon actual Fig 11.29

Moving to 2 PM, the analemma lays over to the right,

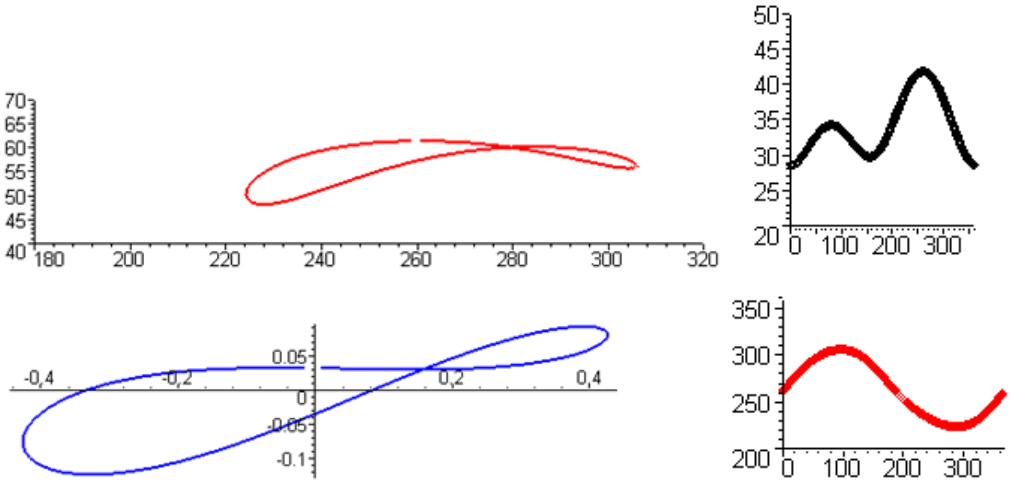

latitude = 20° 2 PM actual Fig 11.30

It might seem strange that this analemma tilts over so far only 2 hours after noon. This is the subject of Appendix D. Fig D.2 says that the blue analemma is in fact tilted 80° to the right from vertical.

(g) Analemma case study from the Crimea (Ukraine)

Mr. Vasilij Rumyantsev, who works at the Crimean Astrophysical Observatory (CrAO) in the town of Nauchny, has a nice analemma picture up on the web at http://vrum.chat.ru/Photo/Astro/analema.htm which is reproduced on the left below (1998-9). His removable but rigidly mounted camera took a shot about every 10 days. Although the strobe sun photos were taken in the early morning, the background picture was taken in the evening. His web page provides an angle-space representation of the analemma, shown on the right below. Probably this was a planning picture he obtained from his own analemma-generating program.

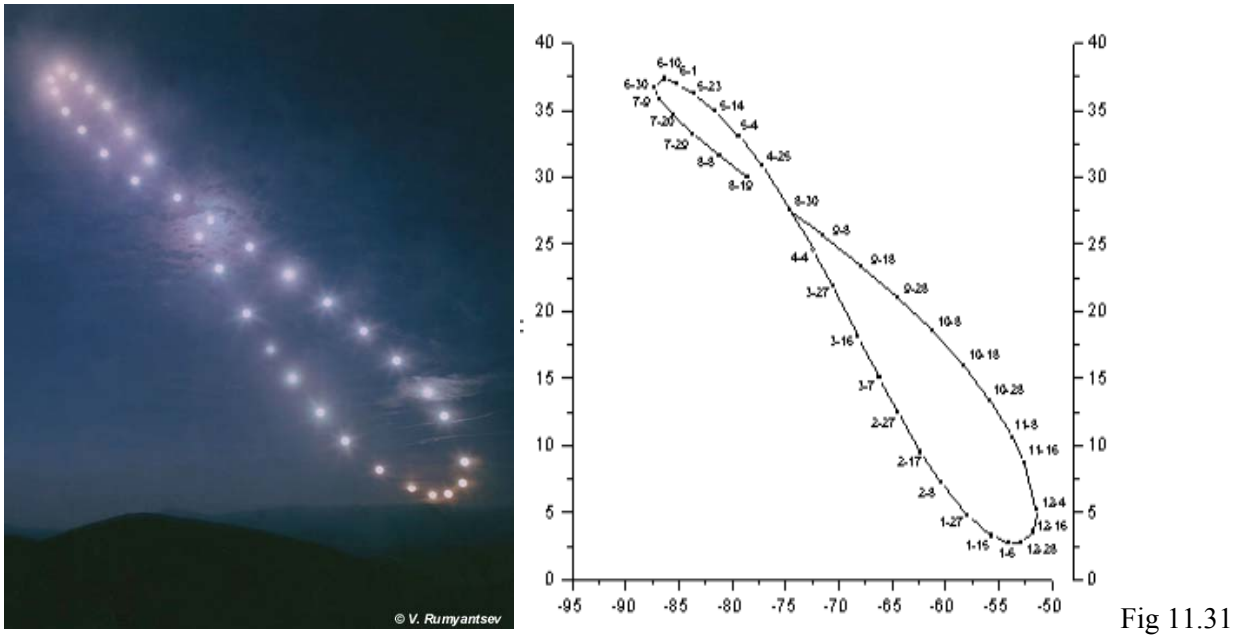

Fig 11.31

His web page provides enough information for us to test out our Maple analemma generating code against his, and to then see how his actual photo compares to our screen space prediction.

Note: As of Dec 2012 the Ukraine seems intent on "terminating" the independent Crimean Astrophysical Observatory, founded 1945, probably for budgetary reasons, see http://www.crao.crimea.ua/ .

The photos were taken close to the observatory's solar telescope which is close to the following coordinates,

Therefore we use,

φ_1 = longitude = 34.000 + 0/60 + 57.1/3600 = 34.016^o
θ_{LAT} = latitude = 44.000 + 43/60 + 36/3600 = 44.727^o .

The analemma was taken Aug 1998 to Aug 1999, so we can use the March 1999 equinox data (source given in Section 7 (b))

Year	Vernal Equinox	Summer Solstice	Autumnal Equinox	Winter Solstice	Perihelion	Aphelion
1998	3/20 19:52	6/21 14:07	9/23 5:39	12/22 1:47	1/03 10:53	7/05 1:47
1999	3/21 1:41	6/21 19:56	9/23 11:28	12/22 7:37	1/03 17:07	7/05 8:01

so we take the GMT of March equinox as 01:41. Mr. Rumyantsev indicates his pictures were taken every 10 days (more or less) at exactly GMT = 05:45. From this we compute his LMT from (8.8),

LMT(t) = [GMT(t) + (φ_1/15)] mod 24 .

= [05:45 + 34.016/15] mod 24 = 5.75+2.26773 = 8.01773 ≈ 8:01 AM .

Finally, the orbital parameters in 1999 were (source given in Section 1 (a))

Year (A.D.)	Eccentricity	Obliquity (degrees)	Long. of Perihel. (degrees)
1997	0.016705	23.4402	282.844
1998	0.016704	23.4400	282.861
1999	0.016704	23.4399	282.878
2000	0.016704	23.4398	282.895

so θ_{tmax} = 23.4399, ε = .016704 and φ_{per} = 12.878^o.

Entering this data into the Maple program, we get the red analemma shown in Fig 11.10 above. If we superpose that red analemma on his data and carefully align the axes, here is the result :

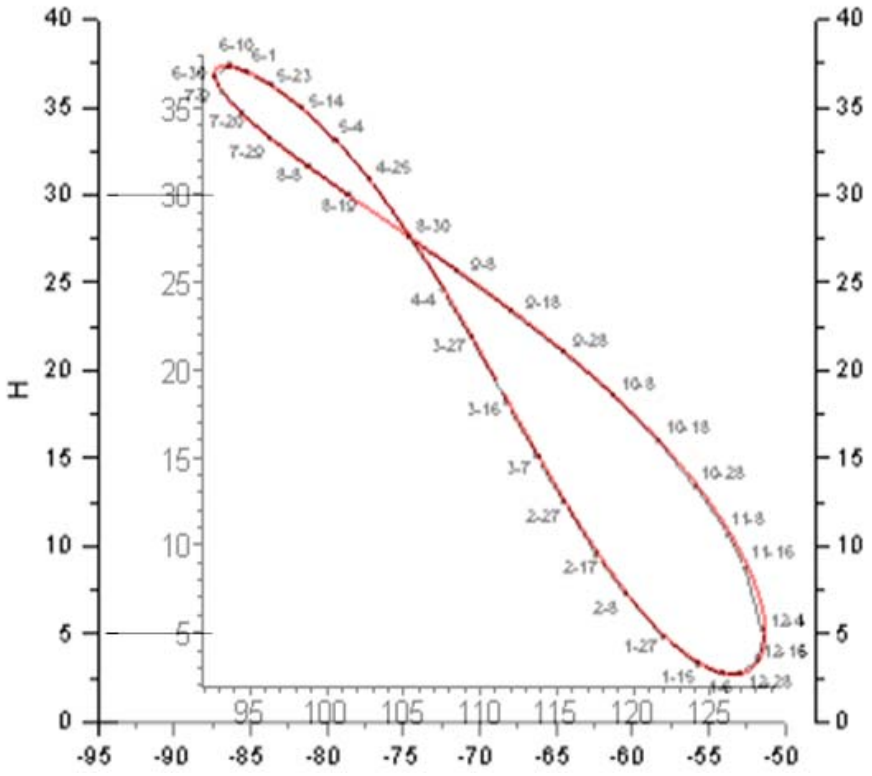

Fig 11.32

The break in our red curve (above 3-16) shows the March equinox which is in agreement with his data. This seems to show that our angle-space Maple program agrees with whatever program he used to generate his planning analemma.

We now superpose our blue screen-space analemma plot of Fig 11.11 on Mr. Rumyantsev's photo without altering the aspect ratio of either image. We had to set our pan adjust to -6^{o} to get things to line up (cross hairs are 6^{o} to the left of the fictitious sun location).

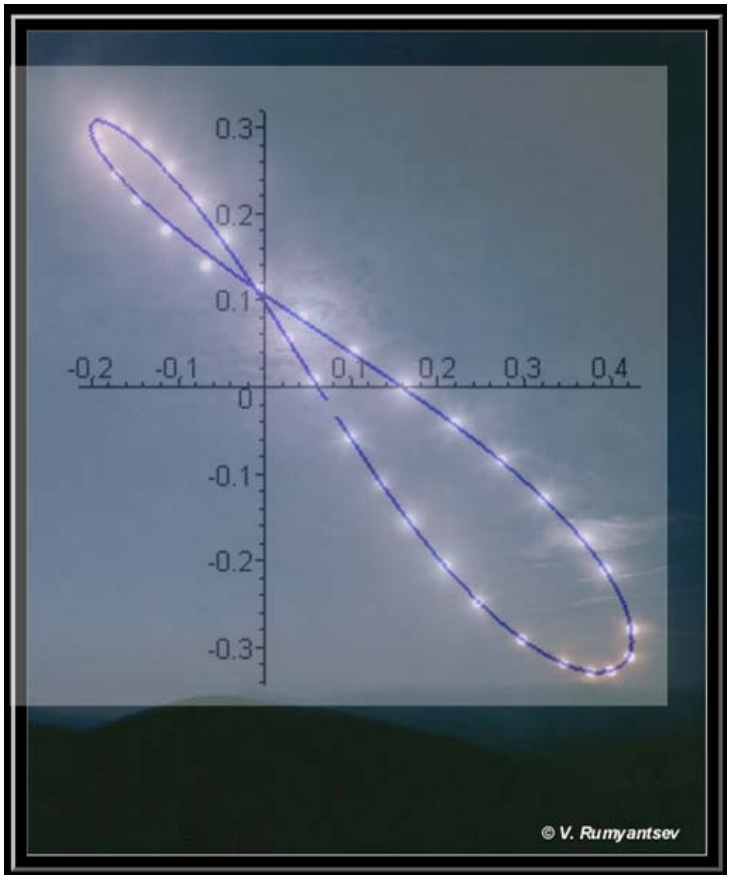

Fig 11.33

The fit is reasonable but unfortunately not perfect in the smaller summer lobe. As shown in the previous figure, our computed angle-space analemma agrees exactly with that of Mr. Rumyantsev, so the photo mismatch is either due an error in our screen space calculation, or to a problem with the camera mount, the former seeming more likely since the winter lobe matches so well.

The first known analemma photograph was taken by Dennis di Cicco in 1978-9, Ref [7] . Since that time, perhaps 10 people have put up analemma photos on the web.

A notable effort is that of Greek photographer Anthony Ayiomamitis who uses multiple cameras to do simultaneous analemma photos during the same year. He does this with cameras mounted in his yard near Athens, each one strobing at a different hour of the day (circa 2002-2004). To add interest, he used Photoshop to composite in photos of various Greek ruins. We did Maple fits to several of his photos with results similar to that shown above. The first link below shows a collection of Mr. Ayiomamitis's analemma photos which demonstrates the effect of time of day, in agreement with our analemma gallery comments above. The second link gives details of his efforts (five web pages) :

http://www.perseus.gr/Astro-Solar-Analemma.htm
http://www.astrosurf.com/luxorion/analemma.htm

Appendix A: A Note on Various Arctangent Functions

When bandying about equations, as we have done freely in this document, one can be cavalier about the meaning of functions like $\tan^{-1}$. But when it comes time to actually compute something, or to make a proper plot of some function, subtle problems arise which can be very annoying. This appendix describes issues involving the arctangent function in various forms. These issues are of course present not only in Maple implementations, but in any calculational method of doing something at the nuts and bolts level.

(a) arctan2Pi(y,x) and comparison with arctan(y/x) and arctan(y,x)

Consider these two equations,

$x = \cos\varphi$
$y = \sin\varphi$

where φ runs through the range $(0,2\pi)$ so that $\mathbf{r} = (x,y)$ moves in a circle. Given x and y, how do we find φ? Consider this picture,

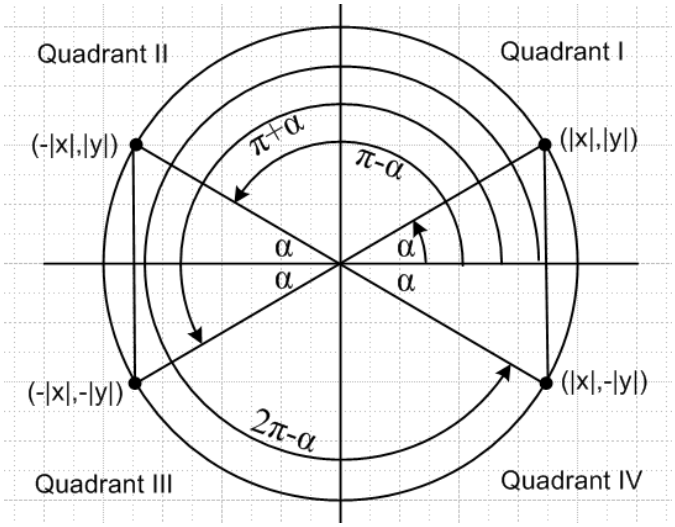

Fig A.1

From the signs of x and y, we can certainly determine the quadrant of (x,y). So here is how we find φ :

If (x,y) is in Quadrant I, then $\varphi = \alpha$ where $\alpha \equiv \tan^{-1}(|y|/|x|)$
If (x,y) is in Quadrant II, then $\varphi = \pi - \alpha$
If (x,y) is in Quadrant III, then $\varphi = \pi + \alpha$
If (x,y) is in Quadrant IV, then $\varphi = 2\pi - \alpha$. (A.1)

This algorithm is implemented in the following Maple function arctan2Pi(y,x), where we put the arguments in order y,x since it reminds us of $\tan^{-1}(y/x)$:

```
arctan2Pi := proc(yy,xx)
   local t,x,y;
   x := evalf(xx); y := evalf(yy);
   if type(x,numeric) and type(y,numeric) then
     if x = 0 and y = 0 then print("arctan2Pi(0,0) error." ); RETURN(0) fi;
     if x = 0 and y > 0 then RETURN(Pi/2) fi;
     if x = 0 and y < 0 then RETURN(3*Pi/2) fi;
     if x > 0 and y = 0 then RETURN(0) fi;
     if x < 0 and y = 0 then RETURN(Pi) fi;
     t := arctan(abs(y/x));
     if x > 0 and y > 0 then RETURN(t) fi;       # I
     if x < 0 and y > 0 then RETURN(Pi-t) fi;    # II
     if x < 0 and y < 0 then RETURN(t+Pi) fi;    # III
     if x > 0 and y < 0 then RETURN(2*Pi-t) fi; # IV
   else
     'arctan2Pi'(y,x);
   fi;
end:
```

Here are two 3D plots of arctan2Pi(y,x), showing its scale invariant shape,

```
plot3d(arctan2Pi(y,x),x=-2..2, y = -2..2, axes = boxed);
plot3d(arctan2Pi(y,x),x = -200..200, y = -200..200, axes = boxed);
```

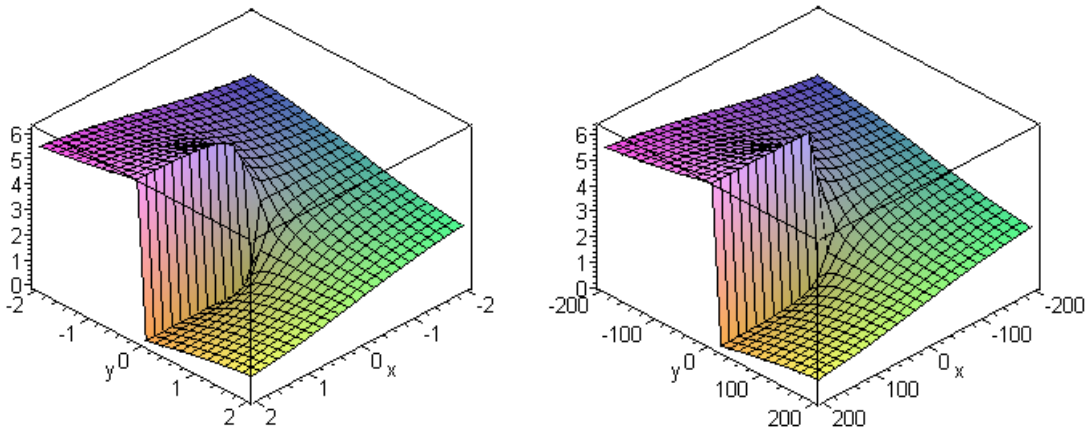

Fig A.2

As one takes a spiral hike around the quadrants going I, II, III, IV the value φ = arctan2Pi(y,x) increases smoothly. When using this function, we stick to the range $0 \le \varphi < 2\pi$ to avoid the discontinuity.

NOTE: All equations below are followed by an implicit "mod 2π". When checking an equation of the form a = b in Maple, one must show that mod(a-b,2π) = 0. In particular notice that π = -π in this world since mod(π - (-π),2π) = mod(2π,2π) = 0.

In general, the function arctan2Pi(y,x) has these properties, as one can show by exhausting all the cases in Fig A.1,

$$\begin{aligned}
&\text{arctan2Pi}(-y,x) = 2\pi - \text{arctan2Pi}(y,x) && \text{// negate y}\\
&\text{arctan2Pi}(y,-x) = \pi - \text{arctan2Pi}(y,x) && \text{// negate x}\\
&\text{arctan2Pi}(-y,-x) = \pi + \text{arctan2Pi}(y,x) && \text{// negate x and y .}
\end{aligned} \qquad (A.2)$$

These rules differ considerably from the principle branch rule that

$$\tan^{-1}(-z) = -\tan^{-1}(z) .$$

To verify (A.2) we run this Maple code [modf(a,b) computes a mod b, see Sec 11 (e)]

```
t1 := modf(arctan2Pi(-y,x) - 2*Pi + arctan2Pi(y,x),2*Pi):
plot3d(t1,x = -2..2, y = -2..2, axes = boxed, view = [-2..2,-2..2,-1..1]):
t2 := modf(arctan2Pi(y,-x)- Pi + arctan2Pi(y,x),2*Pi):
plot3d(t2,x = -2..2, y = -2..2, axes = boxed, view = [-2..2,-2..2,-1..1]):
t3 := modf(arctan2Pi(-y,-x) - Pi - arctan2Pi(y,x),2*Pi):
plot3d(t3,x = -2..2, y = -2..2, axes = boxed, view = [-2..2,-2..2,-1..1]):
```

and all three plots come out looking like this (two views of the same 3D plot)

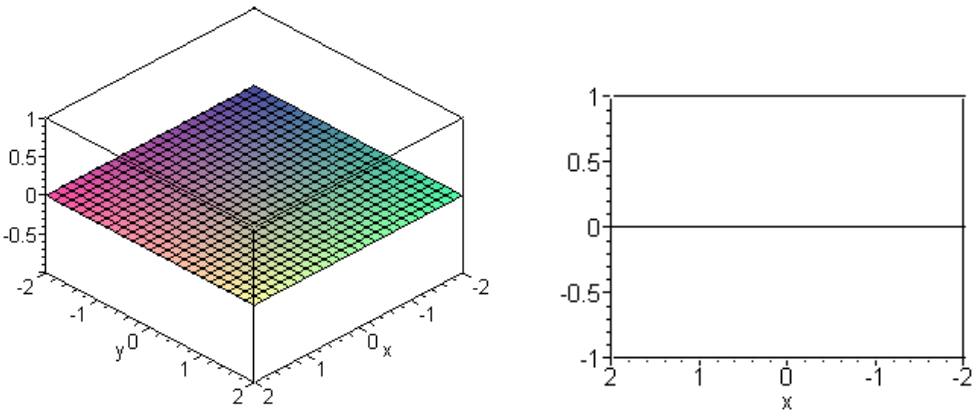

Fig A.3

Rather than write arctan2Pi everywhere, we have adopted this notation,

$$\tan^{-1}([y]/[x]) = \tan^{-1}\left(\frac{[y]}{[x]}\right) \equiv \text{arctan2Pi}(y,x) . \qquad (A.3)$$

One must not "move signs around" carelessly, thinking of $\tan^{-1}(-z) = -\tan^{-1}(z)$. In fact, from (A.2),

$$\begin{aligned}
&\tan^{-1}([-y]/[x]) = 2\pi - \tan^{-1}([y]/[x])\\
&\tan^{-1}([y]/[-x]) = \pi - \tan^{-1}([y]/[x])\\
&\tan^{-1}([-y]/[-x]) = \pi + \tan^{-1}([y]/[x]) .
\end{aligned} \qquad (A.4)$$

Here are some examples of (A.4) :

$$\tan^{-1}([\sin\varphi]/[\cos\varphi]) = \varphi$$
$$\tan^{-1}([-\sin\varphi]/[\cos\varphi]) = 2\pi - \varphi$$
$$\tan^{-1}([\sin\varphi]/[-\cos\varphi]) = \pi - \varphi$$
$$\tan^{-1}([-\sin\varphi]/[-\cos\varphi]) = \pi + \varphi \ . \qquad (A.5)$$

Sometimes we use this abbreviated notation

$$\tan^{-1}(a\tan\beta) \equiv \tan^{-1}([a\sin\beta]/[\cos\beta]) \qquad \text{if } a \geq 0 \qquad (A.6)$$

as in (6.12) and (6.13). Of course if a = 1, then $\tan^{-1}(\tan\beta) = \beta$. Similarly,

$$\tan^{-1}([c]/[ab]) = \tan^{-1}([a^{-1}c]/[b]) \qquad \text{if } a > 0 \qquad (A.7)$$

with corollary

$$\tan^{-1}([ac]/[ab]) = \tan^{-1}([c]/[b]) \qquad \text{if } a > 0 \ . \qquad (A.8)$$

The important fact in such identities is that the quadrant does not change.

The cotangent can be handled similarly. We first define

$$\cot^{-1}([x]/[y]) \equiv \tan^{-1}([y]/[x]) = \text{arctan2Pi}(y,x) \ . \qquad (A.9)$$

We claim that, just as for the regular $\tan^{-1}$ and $\cot^{-1}$ functions,

$$\cot^{-1}([x]/[y]) = \pi/2 - \tan^{-1}([x]/[y]) \ . \qquad (A.10)$$

This can be verified for (x,y) in any quadrant by showing that the following is true,

$$\text{arctan2Pi}(y,x) = \pi/2 - \text{arctan2Pi}(x,y) \ .$$

Testing this claim, we find that the code

```
t4 := modf(arctan2Pi(y,x)-Pi/2 + arctan2Pi(x,y),2*Pi):
plot3d(t4,x = -2..2, y = -2..2, axes = boxed, view = [-2..2,-2..2,-1..1]);
```

produces the same null plot shown in Fig A.3. Combining (A.10) with (A.9) then gives

$$\tan^{-1}([y]/[x]) = \pi/2 - \tan^{-1}([x]/[y]) \ . \qquad (A.11)$$

From (A.11) and (A.4) one may show that

$$\pi/2 - \tan^{-1}([y]/[x]) = \pi + \tan^{-1}([-x]/[-y]) \qquad (A.12)$$

which we once again verify in Maple. We find that this code,

```
t5 := modf(Pi/2-Pi-arctan2Pi(y,x) - arctan2Pi(-x,-y),2*Pi):
plot3d(t5,x = -2..2, y = -2..2, axes = boxed, view = [-2..2,-2..2,-1..1]);
```

produces the usual null plot of Fig A.3.

In the special case (x,y) = (1,y), we know that the normal $\tan^{-1}(y/x) = \tan^{-1}(y)$ lies in $-\pi/2$ to $\pi/2$. For our situation this is Quadrant I or Quadrant IV and we then obtain (don't forget the implicit mod 2π)

$$\tan^{-1}([y]/[1]) = \tan^{-1}(y) \qquad (A.13)$$

then using the second equation of (A.4) we get

$$\tan^{-1}([y]/[-1]) = \pi - \tan^{-1}(y) \; . \qquad (A.14)$$

Other arctan functions in Maple

Maple contains a built-in function arctan(y,x) with two arguments. Here is a plot of this function where the axes are the same as in the left side of Fig A.2 for arctan2Pi(y,x) :

```
plot3d(arctan(y,x), x = -2..2, y = -2..2, axes = boxed);
```

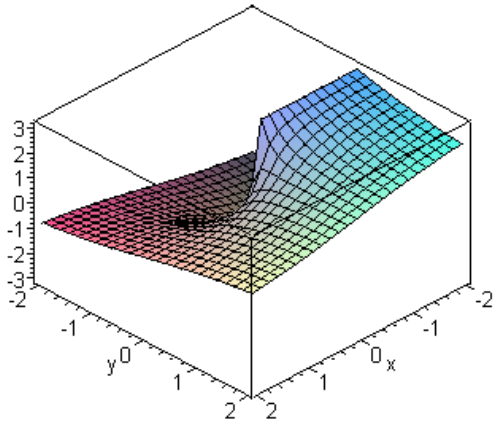

Fig A.4

The output range of this function is $(-\pi,\pi)$ rather than $(0,2\pi)$, which is not what we want for our purposes. It turns out that we can simulate arctan2Pi(y,x) by arctan(-y,-x) + π,

```
plot3d(arctan(-y,-x)+Pi, x = -2..2, y = -2..2, axes = boxed);
```

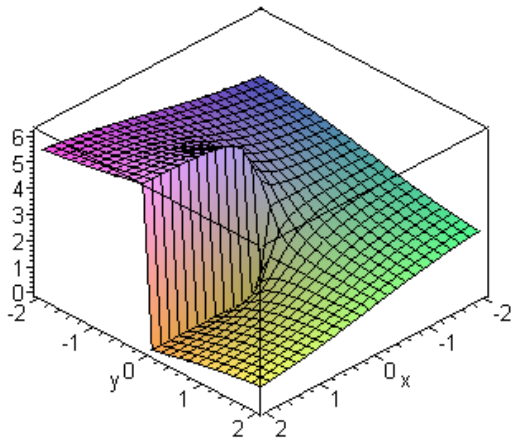

Fig A.5

but it seemed better to write our own clearly defined function arctan2Pi to be sure what it does.

The following three plots using the three arctangent functions demonstrate our motivation in using the arctan2Pi function for our (0,2π) region of interest:

```
plot (arctan(tan(phi)),phi = 0..2*Pi,thickness = 2);
plot (arctan(sin(phi),cos(phi)),phi = 0..2*Pi,thickness = 2);
plot (arctan2Pi(sin(phi),cos(phi)),phi = 0..2*Pi,thickness = 2);
```

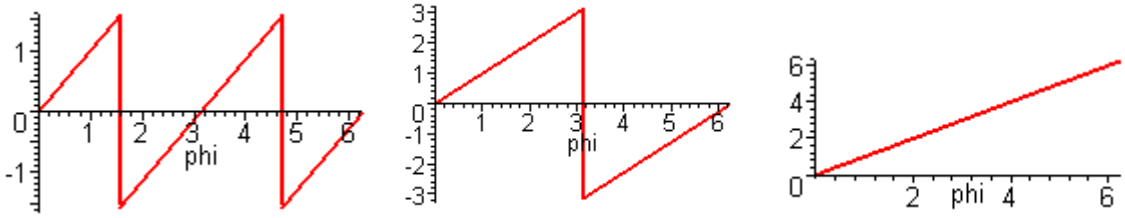

Fig A.6

(b) arctan2Pis(y,x)

First, we demonstrate what this "s" version of arctan2Pi does:

```
plot(arctan2Pi(sin(phi),cos(phi)),phi = 0..6*Pi,thickness = 2);
winit(0):plot(arctan2Pis(sin(phi),cos(phi)),phi = 0..6*Pi,thickness = 2);
```

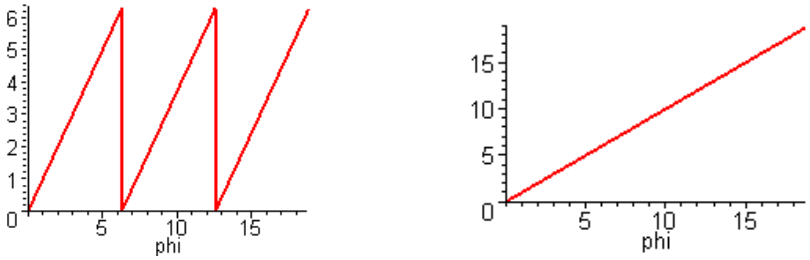

Fig A.7

As a (x,y) vector winds around the origin multiple times, the arctangent increases smoothly so that the result $\tan^{-1}(\tan z) = z$ is realized for z over a larger range than 2π.

Here is the inelegant code for this function :

```
arctan2Pis := proc(yy,xx)
   global quad_last, wind; local x,y,quad_current;
   x := evalf(xx); y := evalf(yy);
   if type(x,numeric) and type(y,numeric) then
     if x = 0 and y = 0 then quad_current := 1;
     elif x > 0 and y >= 0 then quad_current := 1;
     elif x <= 0 and y > 0 then quad_current := 2;
     elif x < 0 and y <= 0 then quad_current := 3;
     elif x >= 0 and y < 0 then quad_current := 4;
     else print ("arctan2Pis illegal quadrant error") ;RETURN(0) fi;
     if quad_last = 4 and quad_current = 1 then wind := wind+1 fi;
     if quad_last = 1 and quad_current = 4 then wind := wind-1 fi;
     quad_last := quad_current;
     RETURN(arctan2Pi(y,x)+wind*2*Pi);
   else 'arctan2Pis'(y,x) ;fi;
end:
```

The function remembers the x,y quadrant of the previous call to the function and compares that with the x,y quadrant of the current call. If the 4→1 boundary is crossed, a winding number "wind" is upticked by 1, and if it crosses the other way it is downticked. Then 2π*wind is added to the arctan2Pi(y,x) result. This function must be initialized before it is used to evaluate a function for some sweep of a variable,

```
winit := proc(w)
   global quad_last, wind;
   quad_last := 0; wind := w;
end;
```

As an illustration of the motivation for using this arctan2Pis function, consider the seemingly simple plot of four curves (as in Fig 6.3) which lie very close together. Here is the code using arctan2Pis :

```
Omega0 := 2*Pi: e := .016708:
thtmax := (Pi/180)*23.4382: phiper := (Pi/180)*13.101:
q := 2*e*sin(Omega0*t) + (5/4)*e^2*sin(2*Omega0*t) :
s := Omega0*t+phiper-Pi/2:
f_red := arctan2Pis(cos(thtmax)*sin(s+q), cos(s+q)):
f_blue := arctan2Pis(cos(thtmax)*sin(s), cos(s)):
f_black := arctan2Pis(sin(s+q), cos(s+q)):
f_green := arctan2Pis(sin(s), cos(s)):
winit(-1): s1 := plot(f_red,t = 0..1, color = red):
winit(-1): s2 := plot(f_blue,t = 0..1, color = blue):
winit(-1): s3 := plot(f_black,t = 0..1, color = black):
winit(-1): s4 := plot(f_green,t = 0..1, color = green):
display([s1,s2,s3,s4,s4]);
```

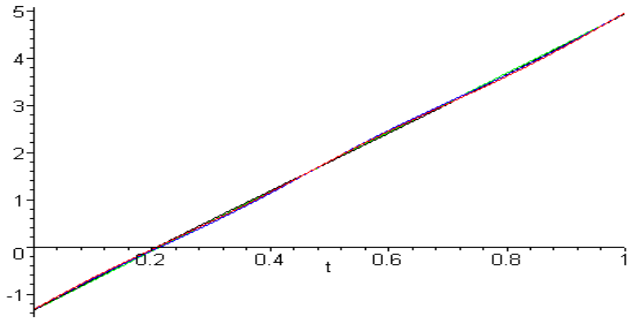

Fig A.8

When these curves are plotted with the other three arctangent functions, we get these annoying results, (the cases are arctan2Pi(y,x), then arctan(y,x), then arctan(y/x))

```
f_red   := arctan2Pi(cos(thtmax)*sin(s+q),cos(s+q)):
f_blue  := arctan2Pi(cos(thtmax)*sin(s),cos(s)):
f_black := arctan2Pi(sin(s+q),cos(s+q)):
f_green := arctan2Pi(sin(s),cos(s)):
plot([f_red,f_blue,f_black,f_green], t = 0.1..0.9, color = [red,blue,black,green]);
```

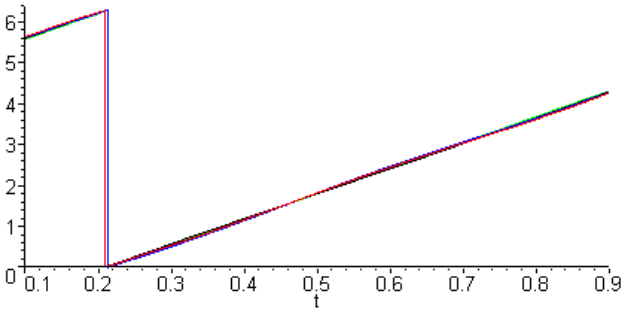

Fig A.9

```
f_red := arctan(cos(thtmax)*sin(s+q), cos(s+q)):
f_blue := arctan(cos(thtmax)*sin(s), cos(s)):
f_black := arctan(sin(s+q), cos(s+q)):
f_green := arctan(sin(s), cos(s)):
plot([f_red,f_blue,f_black,f_green], t = 0.1..0.9, color = [red,blue,black,green]);
```

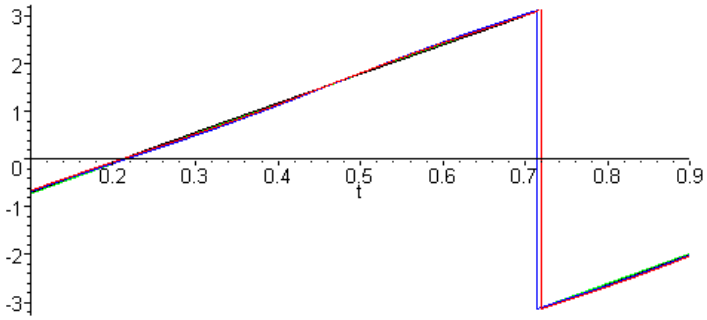

Fig A.10

```
f_red := arctan(cos(thtmax)*sin(s+q)/cos(s+q)):
f_blue := arctan(cos(thtmax)*sin(s)/cos(s)):
f_black := arctan(sin(s+q)/cos(s+q)):
f_green := arctan(sin(s)/cos(s)):
plot([f_red,f_blue,f_black,f_green], t = 0..1, color = [red,blue,black,green]);
```

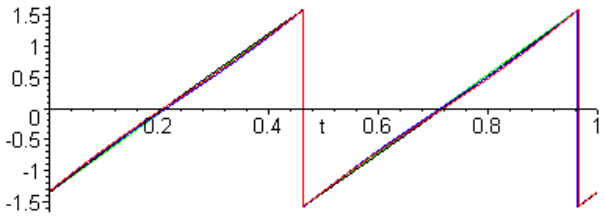

Fig A.1

The following drawing shows how our four different arctangent functions use different branches of the infinitely-branched general arctangent function:

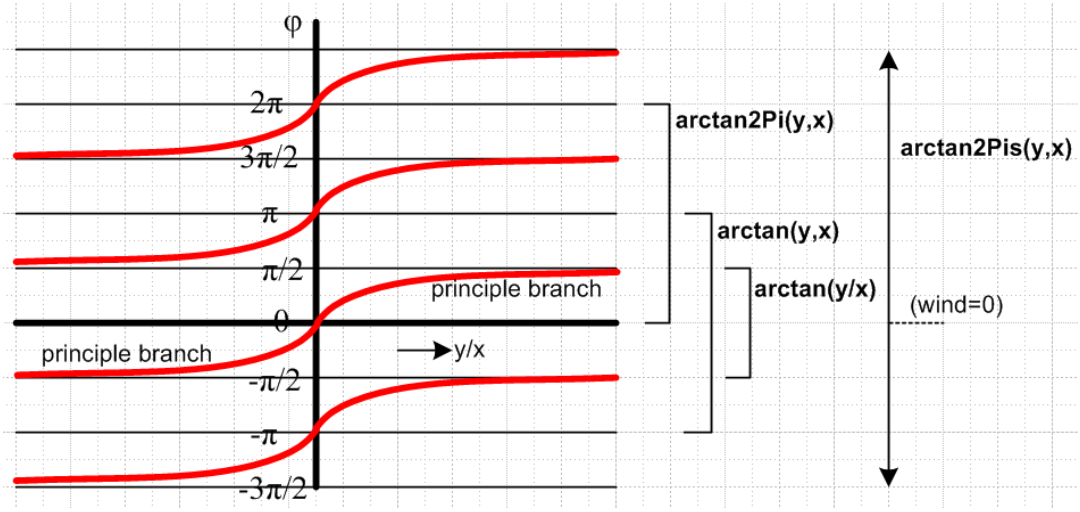

Fig A.12

The normal function $\varphi = \tan^{-1}(z)$ uses only the principle branch and returns φ in $-\pi/2$ to $\pi/2$.

Technical Code Note: The code which generates Fig 6.4 is stated above that figure, and the functions like f_red are defined in terms of the arctan2Pis function. Since this function is designed only for use in a clean "run" from left to right in a plot of a single function, where it internally manages its winding number "wind", it seems odd that there are no "spikes" in the plots like Fig 6.4. There, the plot algorithm evaluates d_red = f_red - f_green which means arctan2Pis is applied first to f_red and then to f_green, and then after the next plot increment arctan2Pis is again applied to f_red and then to f_green. So the use of arctan2Pis *alternates* between the red and green functions, violating the coder's intent. It nevertheless turns out that things really do work even though the red and green functions cross the axis near t = 0.2 (76 days) at different times, and this is regardless of how fine the plotting steps are.

Appendix B: The Active and Passive Views of Vector Rotation

(a) Active view

Let Frame S have orthonormal basis vectors $\mathbf{e_n}$ for n = 1,2,3. Let **V** be some vector in Frame S which has components V_n. Here is the expansion of vector **V** on these basis vectors,

$$\mathbf{V} = \Sigma_n V_n \mathbf{e_n} \qquad \text{where} \qquad V_n = \mathbf{V} \bullet \mathbf{e_n} \; . \qquad \text{(B.1)}$$

Suppose we create a new vector in Frame S, called **V'**, by applying some rotation R to vector **V**,

$$\mathbf{V'} = R\mathbf{V} \qquad \text{meaning} \qquad V'_i = \Sigma_j R_{ij} V_j \; . \qquad \text{(B.2)}$$

We refer to this as " the active rotation of vector **V** into vector **V'**, all in Frame S ". We can expand this new vector **V'** on the same basis vectors $\mathbf{e_n}$ as follows,

$$\mathbf{V'} = \Sigma_n V'_n \mathbf{e_n} \qquad \text{where} \qquad V'_n = \mathbf{V'} \bullet \mathbf{e_n} \qquad \text{(B.3)}$$

where the numbers V'_n are the components of vector **V'** in Frame S.

The interpretation of the numbers V'_n as just described is "the active point of view of a rotation". Here is a simple example of such an active rotation where $R = R_z(\psi)$.

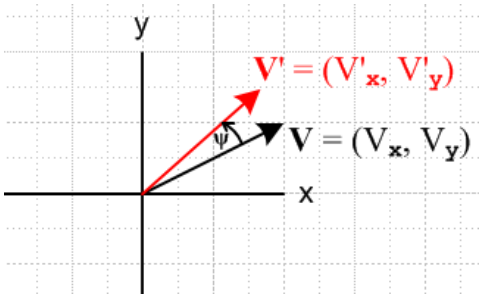

Fig B.1

(b) Passive view

There is another way to interpret the numbers V'_n. Suppose we create a new reference Frame S' which has unit basis vectors $\mathbf{e'_n}$ which are related to those of Frame S as follows:

$$\mathbf{e'_n} = R^{-1}\mathbf{e_n} \qquad n = 1,2,3 \qquad \text{(B.4)}$$

That is to say, these vectors are rotated "backwards" compared to what is shown in (B.2).

The new interpretation of the numbers V'_n is (we claim) that these numbers are the components of the vector **V** when it is *observed* from Frame S'. That is to say, we claim that the expansion of vector **V** in Frame S' looks like this, where V_n' are as given in (B.3).

$\mathbf{V} = \Sigma_n V'_n \mathbf{e}'_n$ where $V'_n = \mathbf{V} \bullet \mathbf{e}'_n$. (B.5)

Dotting both sides of $\mathbf{V} = \Sigma_n V'_n \mathbf{e}'_n$ into $\mathbf{e}'_m$ shows that $V'_n = \mathbf{V} \bullet \mathbf{e}'_m$ (since $\mathbf{e}'_n \bullet \mathbf{e}'_m = \delta_{n,m}$), so basically we want to show that $V'_n = \mathbf{V} \bullet \mathbf{e}'_n$ of (B.5) is the same as $V'_n = \mathbf{V}' \bullet \mathbf{e}_n$ of (B.3) . Proof:

$V'_n = \mathbf{V}' \bullet \mathbf{e}_n$ // from (B.3)

$= [R\mathbf{V}] \bullet [R\mathbf{e}'_n]$ // from (B.2), and (B.4) inverted

$= [RV]^T [R\mathbf{e}'_n]$ // the above just written in matrix notation, T = transpose vector

$= V^T R^T R e'_n$ // rule for applying ^{T} to product of matrices/vectors

$= V^T e'_n$ // $R^T R = 1$ because a rotation is a real orthogonal matrix

$= \mathbf{V} \bullet \mathbf{e}'_n$ // going back to dot product notation

$= V'_n$ // from (B.5)

Thus the numbers V'_n appearing in (B.3) and (B.5) are in fact the same numbers so our claim is verified. Here is a simple example of such a passive rotation. Notice that the vector **V** stays put, and the unit vectors are rotated backwards relative to the active rotation shown in the previous picture,

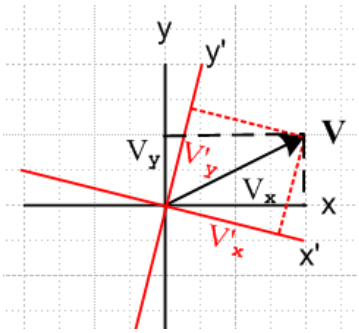

Fig B.2

(c) Summary

The numbers V'_n can be interpreted in two ways, active and passive:

(1) The V'_n are the components of a vector $\mathbf{V}'$ in Frame S (with $\mathbf{e}_n$) obtained from $\mathbf{V}' = R\mathbf{V}$.

(2) The V'_n are components of the vector **V** in Frame S', where $\mathbf{e}'_n = R^{-1}\mathbf{e}_n$ for Frame S'.

Suppose we know that there is some matrix R^{-1} such that the basis vectors of Frame S' are related to those of Frame S in this way

$$\mathbf{e'}_n = R^{-1}\mathbf{e}_n \, .$$

If we want to compute the components of a vector **V** in Frame S', we may use this formula,

$$\mathbf{V'} = R\mathbf{V} \, .$$

The simple rule is that "vectors rotate backwards from the unit vectors". This rule is invoked just after equation (6.1).

Appendix C: Shape of the north pole analemma when e = 0

(a) Parametric equation for the analemma

We assume that the orbit of the earth is circular (e = 0, "blue earth" of Section 6 (d)). When e = 0, we have the following set of facts:

$\varphi' = \Omega_0\tau$ // since circular orbit, φ' as in Fig 3.4 measured from March equinox
$\psi = \Omega_0 t$ // since circular orbit, ψ as in Fig 3.4 measured from perihelion
$\tau = t - t_{Me}$ // valid for any e *(7.2)*
$t_{Me} = \alpha/\Omega_0$ //$\alpha \equiv (\pi/2-\varphi_{per})$ as in (1.9) *(4.12)*
$k = [\Omega_0 t_{Me} - \alpha] = 0$ *(7.17)*
$\varphi' = \psi - \alpha$ // valid for any e *(1.10)*

From the first and last lines we get this e = 0 fact,

$$\psi - \alpha = \Omega_0\tau \; . \qquad \text{(C.1)}$$

The units are taken to be hours for t and τ and t_{Me} and radians per hour for Ω_0.

Now, at the north pole the continuous functions one samples to get the two axes of the analemma have this simple form, as was shown in (11.24),

vertical $= \theta'_{EL} = \theta_t = \sin^{-1}[\sin\theta_{tmax}\ \sin(\Omega_0\tau)]$ // (11.24), (11.1)
horizontal $= \Phi' = \pi + \omega\tau + \varphi_{b0} - \Delta\varphi$ // (11.24)
$\Delta\varphi = -\Omega_0\tau - k + \tan^{-1}[\cos\theta_{tmax}\ \tan(\Omega_0\tau)]$ // (11.3) (C.2)

Using $s = \psi-\alpha = \Omega_0\tau$ from (6.17), one can write $\Delta\varphi$ in the alternate form given in (6.22),

$$\Delta\varphi = \tan^{-1}\left[\frac{(\cos\theta_{tmax} - 1)\tan(\Omega_0\tau)}{1 + \cos\theta_{tmax}\tan^2(\Omega_0\tau)}\right] . \qquad \text{(C.3)}$$

Strobing Φ' at LMT on day N gives

$\Phi'_N = \pi + \omega\tau_N + \varphi_{b0} - \Delta\varphi_N$
$\tau_N = [\tau_0 + 24N];$ *(11.9)*
$\tau_0 = (LMT - 12) - (\varphi_{b0}/\omega)$. // since k = 0, $\omega = \pi/12$ rad/hr *(11.9)*

Since $\omega = \pi/12$, and since Φ'_N is really mod 2π, we can replace $\omega\tau_N \rightarrow \omega\tau_0$ in Φ'_N. That is to say,

$$\omega\tau_N = \omega[\tau_0 + 24N] = \omega\tau_0 + (\pi/12)24N = \omega\tau_0 + 2\pi N \; . \qquad \text{(C.4)}$$

Then

$$\begin{aligned}\Phi'_N &= \pi + \omega\tau_N + \varphi_{b0} - \Delta\varphi_N \\ &= \pi + \omega\tau_0 + \varphi_{b0} - \Delta\varphi_N \\ &= \pi + \omega[(\text{LMT} - 12) - (\varphi_{b0}/\omega)] + \varphi_{b0} - \Delta\varphi_N \\ &= \pi + \omega(\text{LMT} - 12) - \Delta\varphi_N \quad . \end{aligned} \tag{C.5}$$

This result can also be obtained directly from the Φ'_N equation in (11.9) by setting $\theta_1 = 0$.

Strobing θ_t in (C.2) and $\Delta\varphi$ in (C.3) gives, along with (C.5),

$$\begin{aligned}&\theta_{t,N} = \sin^{-1}[\sin\theta_{tmax}\ \sin(\Omega_0\tau_N)] \\ &\Phi'_N = \pi + \omega(\text{LMT} - 12) - \Delta\varphi_N \\ &\Delta\varphi_N = \tan^{-1}\left[\frac{(\cos\theta_{tmax} - 1)\tan(\Omega_0\tau_N)}{1 + \cos\theta_{tmax}\tan^2(\Omega_0\tau_N)}\right] \\ &\tau_N = [\tau_0 + 24N]; \\ &\tau_0 = [\text{LMT} - 12 - (\varphi_{b0}/\omega)] \ . \end{aligned} \tag{C.6}$$

To reduce clutter, we now define these symbols,

$$\begin{aligned}&c \equiv \cos\theta_{tmax} \\ &s \equiv \sin\theta_{tmax} \\ &\beta \equiv \Omega_0\tau_N \\ &x \equiv \Phi'_N - \pi - \omega(\text{LMT} - 12) = -\Delta\varphi_N \\ &y \equiv \theta_{t,N} \quad , \end{aligned} \tag{C.7}$$

so the first three equations in (C.6) may then be written

$$\begin{aligned}&y = \sin^{-1}[s \sin\beta] \\ &x = -\Delta\varphi_N \\ &\Delta\varphi_N = \tan^{-1}\left[\frac{(c - 1)\tan(\beta)}{1 + c\tan^2(\beta)}\right] \ , \end{aligned} \tag{C.8}$$

which we restate one more time as

$$\begin{aligned}&x = -\tan^{-1}\left[\frac{(c - 1)\tan(\beta)}{1 + c\tan^2(\beta)}\right] \\ &y = \sin^{-1}[s \sin\beta] \ . \end{aligned} \tag{C.9}$$

As the parameter β ranges from 0 to 2π (treating β now as a continuous parameter), (x,y) traces out the continuous blue-earth analemma in angle space. Just to make sure we are on track, we can plot this locus (with unequal axis scales each in radians),

```
x := -arctan((c-1)*tan(beta)/(1 + c*tan(beta)^2)):
y := arcsin(s*sin(beta)):
c := cos(N*Pi/180):    s := sin(N*Pi/180):
N := 23.4: plot([x,y,beta=0..2*Pi], color=blue);
```

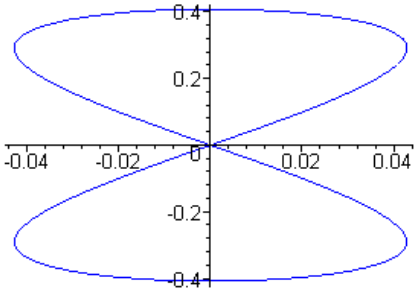

Fig C.1

Plotting for a θ_{tmax} = 10,20...90 shows that the analemmas get larger as θ_{tmax} increases, and also change shape. The triangular analemma is for θ_{tmax} = 90.

```
for N from 10 to 100 by 10 do
   a[N/10] :=
plot([x,y,beta=0..2*Pi],scaling=CONSTRAINED,color=blue):
od:
display(seq(a[M],M=1..4),color=blue,axes = boxed);    # left plot
display(seq(a[M],M=3..9),color=blue,axes = boxed);    # right plot
```

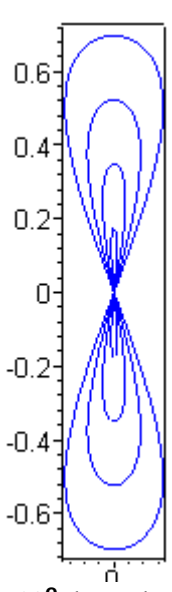

10^0 through 40^0

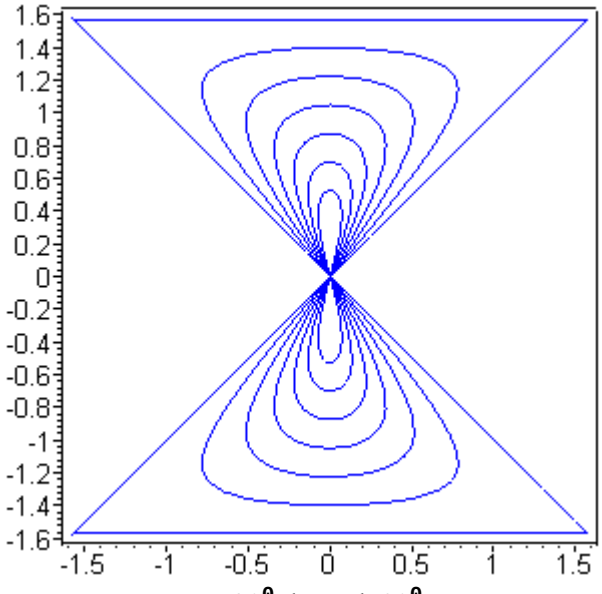

30^0 through 90^0

Fig C.2

(b) Locus of the analemma in angle space: symmetry

The curves above certainly appear to be symmetric in both directions. We can rewrite (C.9) as

$$\tan x = -\left[\frac{(c-1)\tan(\beta)}{1+\text{ctan}^2(\beta)}\right]$$

$$\text{siny} = s\sin\beta\ . \qquad \text{(C.10)}$$

From the second of (C.10) one gets (the goal is to eliminate β),

$$\sin^2\beta = \sin^2 y/s^2$$
$$\cos^2\beta = 1 - \sin^2 y/s^2$$
$$\Rightarrow \tan^2\beta = \sin^2 y/s^2 \,/\, [1 - \sin^2 y/s^2] = \sin^2 y \,/\, [s^2 - \sin^2 y] \,. \qquad \text{(C.11)}$$

The first equation of (C.10) can be squared to yield

$$\tan^2 x = (c\text{-}1)^2 \tan^2\beta \,/\, (1 + c\tan^2\beta)^2 \,. \qquad \text{(C.12)}$$

Using (C.11) in (C.12),

$$\tan^2 x = \{ (c\text{-}1)^2 (\sin^2 y \,/\, [s^2 - \sin^2 y]) \} \,/\, \{1 + c(\sin^2 y \,/\, [s^2 - \sin^2 y]) \}^2$$

Multiply top and bottom by $[s^2 - \sin^2 y]^2$ to get

$$\tan^2 x = \{ (c\text{-}1)^2 \sin^2 y \; [s^2 - \sin^2 y] \} \,/\, \{[s^2 - \sin^2 y] + c(\sin^2 y) \}^2$$

or

$$\tan^2 x = \{ (c\text{-}1)^2 \sin^2 y \; [s^2 - \sin^2 y] \} \,/\, [s^2 - \sin^2 y + c\sin^2 y]^2$$

or

$$\tan^2 x = (c\text{-}1)^2 \sin^2 y \,(s^2 - \sin^2 y) \,/\, [s^2 + (c\text{-}1)\sin^2 y]^2 \,. \qquad \text{(C.13)}$$

Thus β has been eliminated and we have obtained the locus of the analemma. We can verify (C.13) by doing a scanning "implicit plot" in Maple as follows:

```
c := cos(23.4*Pi/180):  s := sin(23.4*Pi/180):
LHS := tan(x)^2:
RHS := (c-1)^2*sin(y)^2*(s^2-sin(y)^2)/((s^2+(c-1)*sin(y)^2)^2):
implicitplot(LHS=RHS, x = -0.05...0.05, y = -0.5..0.5, grid = [40,40]);
```

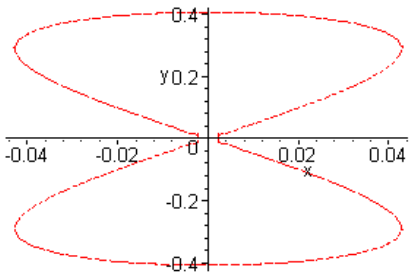

Fig C.3

The locus (C.13) is extremely non-linear in (x,y) space, but does expose the **symmetry** we have been seeking: if x→ –x or y→–y (or both), the locus is unchanged.

(c) How β varies along the analemma

Recall the earlier parametric equation for the analemma,

$$x(\beta) = -\tan^{-1}\left[\frac{(c-1)\tan(\beta)}{1+\text{ctan}^2(\beta)}\right]$$
$$y(\beta) = \sin^{-1}[s\sin\beta] \quad . \qquad (C.9)$$

Using these facts

$\tan(\beta+\pi) = \tan\beta$	$\tan(2\pi-\beta) = -\tan\beta$	$\tan(\pi-\beta) = -\tan(\beta)$
$\sin(\beta+\pi) = -\sin\beta$	$\sin(2\pi-\beta) = -\sin\beta$	$\sin(\pi-\beta) = \sin(\beta)$

one finds

$x(\beta+\pi) = x(\beta)$	$x(2\pi-\beta) = -x(\beta)$	$x(\pi-\beta) = -x(\beta)$
$y(\beta+\pi) = -y(\beta)$	$y(2\pi-\beta) = -y(\beta)$	$y(\pi-\beta) = y(\beta)$

or

$x,y \rightarrow x,-y$	$x,y \rightarrow -x,-y$	$x,y \rightarrow -x,y$
mirror in x=0	invert	mirror in y=0

Here then is the situation with parameter β in (0,2π) for a typical e=0 analemma

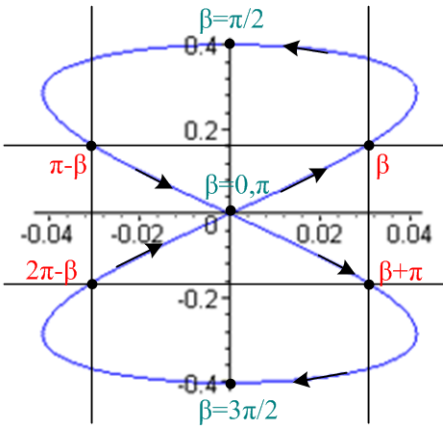

Fig C.4

Note that continuous $\beta = \Omega_{\oplus}\tau = \varphi'$, the azimuth angle of Fig 1.3 and Fig 3.4. Thus,

β=φ'	
0	March equinox
π/2	June solstice
π	September equinox
3π/2	December solstice
2π	March equinox

(d) Limit of analemma shape for small θ_{tmax} : Gerono!

We have seen in Fig C.2 how the analemma approaches a pair of triangles in the limit $\theta_{tmax} \rightarrow 90^0$. In the opposite limit that $\theta_{tmax} \rightarrow 0$, there is also an interesting limiting shape. Recall again,

$$x = -\tan^{-1}\left[\frac{(c-1)\tan(\beta)}{1+c\tan^2(\beta)}\right] \qquad c = \cos\theta_{tmax}$$
$$y = \sin^{-1}[s\sin\beta] \qquad s = \sin\theta_{tmax} \ . \qquad (C.9)$$

When θ_{tmax} is small, s is small, and so y is small. Since $c \rightarrow 1$, x is also small. Looking at (C.13)

$$\tan^2 x = (c-1)^2\sin^2 y\,(s^2 - \sin^2 y) / [s^2 + (c-1)\sin^2 y\,]^2 \qquad (C.13)$$

we then have, for very small θ_{tmax},

$$x^2 \approx (c-1)^2 y^2\,(s^2 - y^2) / [s^2 + (c-1)y^2\,]^2 \ .$$

Now insert $c \approx 1 - s^2/2$ so that $(c-1) \approx -s^2/2$ to get

$$x^2 \approx (s^4/4)y^2\,(s^2 - y^2) / [s^2 - (s^2/2)y^2\,]^2$$

$$x^2 \approx (1/4)y^2\,(s^2 - y^2) / [1 - (1/2)y^2\,]^2$$

$$x^2 \approx y^2\,(s^2 - y^2) / [2 - y^2\,]^2$$

$$x^2 \approx y^2\,(s^2 - y^2)/4$$

$$4x^2 = s^2y^2 - y^4 \ . \qquad \text{// in limit } \theta_{tmax} \rightarrow 0$$

Rescale to new variables

$$Y = (1/s)\,y$$
$$X = (2/s^2)x$$

and the small-θ_{tmax} analemma becomes

$$Y^4 - Y^2 + X^2 = 0 \ .$$

This closed quartic curve is known as the lemniscate of Gerono (not of Bernoulli),

```
implicitplot(Y^4-Y^2+X^2=0, X = -2..2, Y = -2..2, grid = [100,100],
scaling = constrained, thickness = 2, color = red);
```

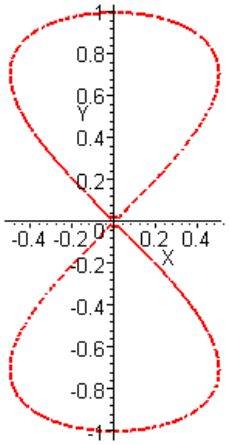

Fig C.5

Wiki shows this curve with the axes swapped,

$$x^4 - y^2 + x^2 = 0$$

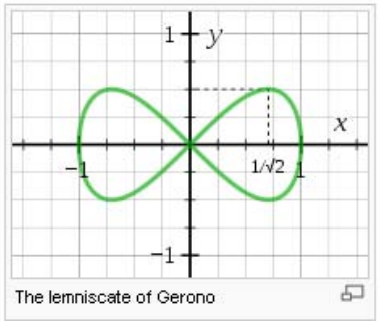

http://en.wikipedia.org/wiki/Lemniscate_of_Gerono

Fig C.6

Appendix D: Calculation of how much the analemma is tipped on film

(a) Calculation of the tip angle from vertical

We shall compute this analemma tip angle as a function of colatitude θ_1 of the observer site, and LMT, the local mean time of the strobe photos.

The plan here is to create a vector $\Delta\mathbf{r}'$ which represents the long direction of an analemma. We make this arrow point from the December solstice end of the analemma to the June solstice end. The arrow is then shrunk in length and mapped into screen space, where it becomes $(\Delta x_s, \Delta y_s)$. We then compute the tip angle of this vector on the film away from vertical as follows

$$\text{tip} \equiv \text{ angle from vertical} = \tan^{-1}(\Delta x_s/\Delta y_s) \ . \qquad \text{(D.1)}$$

For an arrow with $\Delta x_s = 0$, tip = 0^o, a vertical analemma.
For an arrow with $\Delta y_s = \Delta x_s$, tip = $\tan^{-1}(1) = 45^o$, tipped to the right.
For an arrow with $\Delta y_s = -\Delta x_s$, $\tan^{-1}(-1) = -45^o$, tipped to the left.

To simplify matters we shall use the blue earth analemma which has e = 0. As shown in Appendix C (b), this analemma is symmetric both vertically and horizontally. The vertical symmetry implies that $\Delta\varphi_{blue} = 0$ at both solstices, but here is a direct calculation of this claim. We first assemble a few facts,

$\varphi' = \Omega_0\tau$ // since circular orbit, φ' as in Fig 3.4 measured from March equinox
$\psi = \Omega_0 t$ // since circular orbit, ψ as in Fig 3.4 measured from perihelion
$\tau = t - t_{Me}$ *(7.2)*
$t_{Me} = \alpha/\Omega_0$. *(4.12)*

Then from (6.22),

$$\Delta\varphi_{blue}(t) = \tan^{-1}\left[\frac{(\cos\theta_{tmax} - 1)\tan(s)}{1 + \cos\theta_{tmax}\tan^2(s)}\right] = \tan^{-1}\left[\frac{(\cos\theta_{tmax} - 1)\sin(s)\cos(s)}{\cos^2(s) + \cos\theta_{tmax}\sin^2(s)}\right] \qquad \textit{(6.22)}$$

where $s = \psi - \alpha$ since q = 0, see (6.17). But from the facts collected above,

$$s = \psi - \alpha = \Omega_0 t - \alpha = \Omega_0(\tau + t_{Me}) - \alpha = \Omega_0\tau + \Omega_0 t_{Me} - \alpha = \Omega_0\tau + \alpha - \alpha = \Omega_0\tau = \varphi' \ .$$

At the two solstices, as shown in Fig 3.4 we have $s = \varphi' = \pi/2$ and $3\pi/2$. For either value cos(s) = 0 and therefore $\Delta\varphi_{blue}(t) = 0$.

In this case we conclude from (11.8) that,

$(\varphi_b - \varphi)_N = (\omega[\text{LMT} - 12])$. N = day of either solstice strobe time, since $\Delta\varphi_N = 0$ *(11.8)*

Recalling then (7.14) which gives the Frame S' Cartesian coordinates of the sun,

$$x' = R \cos\theta_t \sin(\varphi - \varphi_b)$$
$$y' = R [\sin\theta_t \sin\theta_1 - \cos\theta_t \cos\theta_1 \cos(\varphi - \varphi_b)]$$
$$z' = R [\sin\theta_t \cos\theta_1 + \cos\theta_t \sin\theta_1 \cos(\varphi - \varphi_b)] , \qquad (7.14)$$

we can install (11.8) in three places and then evaluate the result at the two solstices, $\theta_t = \pm \theta_{tmax}$,

$$x' = -R \cos\theta_{tmax} \sin(\omega[\text{LMT} - 12])$$
$$y' = R [\sin\theta_{tmax} \sin\theta_1 - \cos\theta_{tmax} \cos\theta_1 \cos(\omega[\text{LMT} - 12])]$$
$$z' = R [\sin\theta_{tmax} \cos\theta_1 + \cos\theta_{tmax} \sin\theta_1 \cos(\omega[\text{LMT} - 12])] \quad \text{// June solstice} \qquad (D.2)$$

$$x' = -R \cos\theta_{tmax} \sin(\omega[\text{LMT} - 12])$$
$$y' = R [-\sin\theta_{tmax} \sin\theta_1 - \cos\theta_{tmax} \cos\theta_1 \cos(\omega[\text{LMT} - 12])]$$
$$z' = R [-\sin\theta_{tmax} \cos\theta_1 + \cos\theta_{tmax} \sin\theta_1 \cos(\omega[\text{LMT} - 12])] . \quad \text{// Dec solstice} \qquad (D.3)$$

Our difference arrow of interest is then

$$\Delta x' = 0$$
$$\Delta y' = 2 R \sin\theta_{tmax} \sin\theta_1$$
$$\Delta z' = 2 R \sin\theta_{tmax} \cos\theta_1 \qquad (D.4)$$

which is independent of LMT. This may seem strange, but a little pondering with a globe prop and one's right hand to model the Frame S' axes shows it to be true.

Recall next the eye transformation to camera coordinates of (11.20),

$$x_c = -\cos\alpha_p x' + \sin\alpha_p y'$$
$$y_c = \sin\alpha_t \sin\alpha_p x' + \sin\alpha_t \cos\alpha_p y' + \cos\alpha_t z'$$
$$z_c = -\cos\alpha_t \sin\alpha_p x' - \cos\alpha_t \cos\alpha_p y' + \sin\alpha_t z' . \qquad (11.20)$$

Applying this to the vector $\Delta\mathbf{r}'$ of (D.4) gives (matrix transformations are linear so this is allowed)

$$\Delta x_c = -\cos\alpha_p \Delta x' + \sin\alpha_p \Delta y'$$
$$\Delta y_c = \sin\alpha_t \sin\alpha_p \Delta x' + \sin\alpha_t \cos\alpha_p \Delta y' + \cos\alpha_t \Delta z'$$
$$\Delta z_c = -\cos\alpha_t \sin\alpha_p \Delta x' - \cos\alpha_t \cos\alpha_p \Delta y' + \sin\alpha_t \Delta z' \qquad (11.20)$$

or

$$\Delta x_c = \sin\alpha_p 2 R \sin\theta_{tmax} \sin\theta_1$$
$$\Delta y_c = \sin\alpha_t \cos\alpha_p 2 R \sin\theta_{tmax} \sin\theta_1 + \cos\alpha_t 2 R \sin\theta_{tmax} \cos\theta_1$$
$$\Delta z_c = -\cos\alpha_t \cos\alpha_p 2 R \sin\theta_{tmax} \sin\theta_1 + \sin\alpha_t 2 R \sin\theta_{tmax} \cos\theta_1$$

or

$$\Delta x_c = (2R\sin\theta_{tmax}) \sin\alpha_p \sin\theta_1$$
$$\Delta y_c = (2R\sin\theta_{tmax})[\sin\alpha_t \cos\alpha_p \sin\theta_1 + \cos\alpha_t \cos\theta_1]$$
$$\Delta z_c = (2R\sin\theta_{tmax})[-\cos\alpha_t \cos\alpha_p \sin\theta_1 + \sin\alpha_t \cos\theta_1] . \qquad (D.5)$$

Now we scale down our arrow so it is very short, and we imagine that the tail of the arrow is now sitting at the central point of the blue analemma (the fictitious sun location), still pointing to the June solstice end

of the analemma. That central point has $x_c = y_c = 0$ since the camera is pointing right at this point. So we think of this small (differential) arrow as

$$\Delta x_c = \varepsilon \sin\alpha_p \sin\theta_1$$
$$\Delta y_c = \varepsilon [\sin\alpha_t \cos\alpha_p \sin\theta_1 + \cos\alpha_t \cos\theta_1]$$
$$\Delta z_c = \varepsilon [- \cos\alpha_t \cos\alpha_p \sin\theta_1 + \sin\alpha_t \cos\theta_1] \qquad \varepsilon << 1 \quad . \tag{D.6}$$

The reason for this scaling down is the next processing step, the perspective transformation,

$$x_s = z_o(x_c/z_c)$$
$$y_s = z_o(y_c/z_c) \, , \tag{11.22}$$

which is a nonlinear transformation, so we can't just claim $\Delta x_s = z_o(\Delta x_c/\Delta z_c)$. Instead we differentiate (11.22) to get

$$\Delta x_s = z_o(z_c\Delta x_c - x_c\Delta z_c)/z_c^2 = z_o(z_c\Delta x_c)/z_c^2$$
$$\Delta y_s = z_o(z_c\Delta y_c - y_c\Delta z_c)/z_c^2 = z_o(z_c\Delta y_c)/z_c^2 \tag{D.7}$$

where we have used the fact that $x_c = y_c = 0$ for the tail end of our differential arrow. Then the tip angle is given by

$$\text{tip} \equiv \tan^{-1}(\Delta x_s/\Delta y_s) = \tan^{-1}(\Delta x_c/\Delta y_c)$$

$$= \tan^{-1}([\sin\alpha_p \sin\theta_1] / [\sin\alpha_t \cos\alpha_p \sin\theta_1 + \cos\alpha_t \cos\theta_1]) \, . \tag{D.8}$$

[It *happens* that one gets this same result assuming $\Delta x_s = z_o(\Delta x_c/\Delta z_c)$ which was dismissed above.]

From (11.10) and (11.23) we find that

$$\alpha_t = \pi/2 - \theta'_f \qquad \theta'_f = \cos^{-1}[\sin\theta_1 \cos(\omega[\text{LMT} - 12])]$$
$$\alpha_p = \Phi'_f - \pi \qquad \Phi'_f = \pi + \tan^{-1}([\sin(\omega[\text{LMT} - 12])] / [\cos\theta_1 \cos(\omega[\text{LMT} - 12])])$$

which implies that

$$\alpha_t = \sin^{-1}[\sin\theta_1 \cos(\omega[\text{LMT} - 12])]$$
$$\alpha_p = \tan^{-1}([\sin(\omega[\text{LMT} - 12])] / [\cos\theta_1 \cos(\omega[\text{LMT} - 12])]) \quad . \tag{D.9}$$

The final result for the analemma tip angle is then this :

$$\text{tip}(\theta_1, \text{LMT}) = \tan^{-1}([\sin\alpha_p \sin\theta_1] / [\sin\alpha_t \cos\alpha_p \sin\theta_1 + \cos\alpha_t \cos\theta_1])$$
$$\alpha_t = \sin^{-1}[\sin\theta_1 \cos(\omega[\text{LMT} - 12])]$$
$$\alpha_p = \tan^{-1}([\sin(\omega[\text{LMT} - 12])] / [\cos\theta_1 \cos(\omega[\text{LMT} - 12])]) \quad . \tag{D.10}$$

The tip angle is a function of θ_1 and LMT, as one would expect.

We duly enter equations (D.10) into Maple,

```
tip := arctan((sin(ap)*sin(theta1))/(sin(at)*cos(ap)*sin(theta1)+cos(at)*cos(theta1)));
```

$$tip := \arctan\left(\frac{\sin(ap)\sin(\theta 1)}{\sin(at)\cos(ap)\sin(\theta 1)+\cos(at)\cos(\theta 1)}\right)$$

```
at := arcsin(sin(theta1)* cos(omega*(LMT-12)));
```

$$at := \arcsin(\sin(\theta 1)\cos(\omega\,(LMT-12)))$$

```
ap := arctan(sec(theta1)*tan(omega*(LMT-12)));
```

$$ap := \arctan(\sec(\theta 1)\tan(\omega\,(LMT-12)))$$

```
omega := Pi/12:
```

and make a 3D plot of tip(θ_1, LMT)

```
p1 := plot3d(tip, theta1 = 0..Pi/2-.001, LMT = 8..16, grid
= [40,40],axes = boxed):display(p1);
```

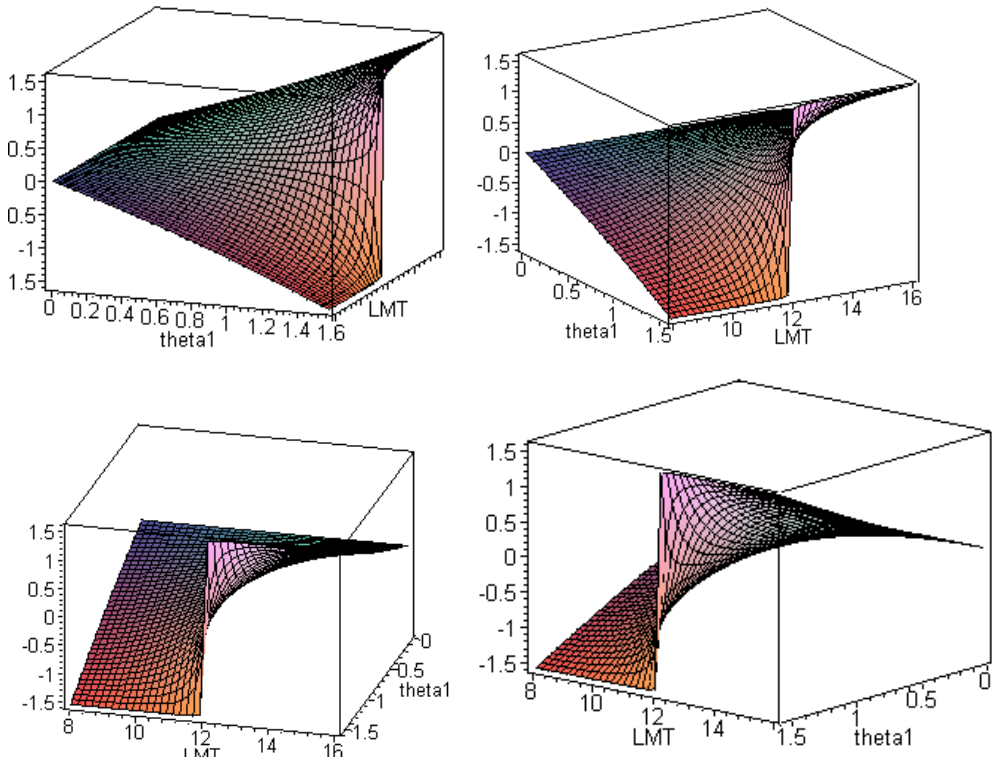

Fig D.1

What the plot shows is that near the equator $\theta_1 = \pi/2 \approx 1.57$, the analemma is vertical at LMT = 12, but as soon as one moves to 12.01 the analemma instantly tips over to its right, tip = $\pi/2$, and at 11.99 it tips to its left, tip = $-\pi/2$. Moving up a bit from the equator, say to latitude 5°, the tip is still fast, but not instantaneous. Probably this situation is clearer in the following plot,

```
plot([seq((180/Pi)*tip,thLAT_deg = [0.001,2,5,10,20,30,40,50,60,70,80,90])], LMT = 6..18,
color = red, thickness = 2, xtickmarks = 12);
```

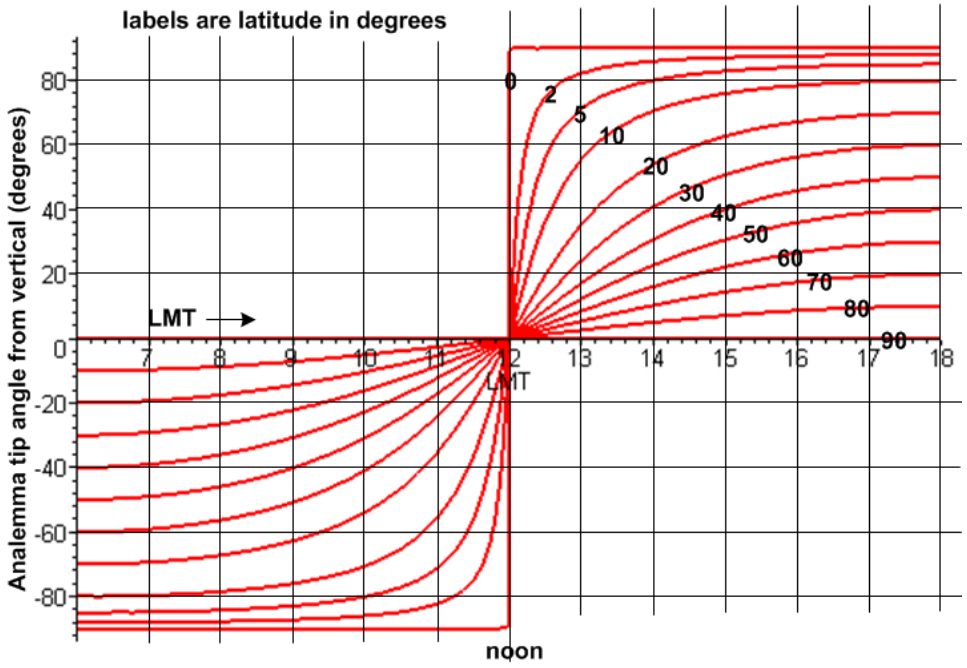

Fig D.2

Again, at the equator the analemma tips over instantly as one moves away from noon. At 2^{o} latitude the tipping over is fairly quick, being perhaps 75^{o} laid over to the right for an LMT = 12:30 PM analemma. We confirm the graph with direct calculation,

```
LMT := 12.5: theta1:= 88*(Pi/180): evalf((180/Pi)*tip);
                                  75.02196197
```

On the other hand, at 40^{o} latitude, the analemma tips 45^{o} to the right at about 4 PM,

```
LMT := 16: theta1:= 50*(Pi/180): evalf((180/Pi)*tip);
                                  45.90468729
```

For the southern hemisphere, just negate the latitude labels in Fig D.2.

(b) Physical explanation of the tip angle behavior

An explanation of the fast tip-over near the equator is as follows. Imagine sitting in a swivel chair looking due south from a site at the equator, camera in hands. At noon the fictitious sun is exactly overhead, so one must tilt the camera up 90^{o} to make it point at the fictitious sun which marks the center of the analemma. There is no need for panning, the analemma appears vertical on the film, since it runs north-south on the celestial sphere (see Fig 11.3). At LMT = 12.001 PM, the fictitious sun has moved a little to the west, so one must swivel that chair 90^{o} to the west in order to point the camera at the new fictitious

sun position. But then the analemma is horizontal on the film since the viewer is pointing up and west but the analemma is still north-south! It "tipped over" instantaneously on the film as we moved away from noon. Similarly at LMT = 11.999 one must instead swivel the chair 90^{o} to the east, so the analemma is horizontal the other way.

In our film projection method, we are only allowed to tilt and then "pan" about the vertical axis to match the polar angles of the fictitious sun; we are not allowed to "roll" the camera about its z_c axis, nor are we allowed to truly pan it about the y_c camera axis.

Now we move say to 2^{o} north latitude. Some fast chair swiveling is still required to track the sun through noon with the camera, but the swiveling is not quite as violent. At 12:30 PM the fictitious sun has moved 7.5^{o} west (15^{o} per hour), and it is 2^{o} to the south. Here is a picture

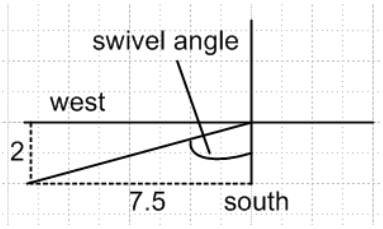

Fig D.3

The swivel angle is then $\tan^{-1}(7.5/2) = 75^{o}$, which is a lot of swivel (though not 90^{o}) so the analemma still being north-south on the celestial sphere is tipped to the right by 75^{o}. It only took a half hour to get it tipped down this great amount. This is in agreement with the above graph and calculation.

One can simulate this perspective effect by making a rectangular viewport with two hands and pretending it is the camera. Find a room with a swivel chair which has parallel lines of some sort running north-south on the ceiling. A directly overhead line is the noon analemma, while a parallel line to the west is the analemma slightly after noon.

References

Various web links appear in-line in this document and most are not repeated here. Links for web pages indicated in-line or below may become invalid, but a search on title or keywords can reveal their new homes.

[1] H. Goldstein, *Classical Mechanics* (Addison-Wesley, Boston, 1950).

[2] I.S. Gradshteyn and I.M. Ryzhik, *Table of Integrals, Series, and Products, 7th Ed.* (Academic Press/ Elsevier, Amsterdam, 2007).

[3] N. Hungerbühler, "Another Design for Sundials" (9p),
http://homeweb2.unifr.ch/hungerbu/pub/sonnenuhr/sundial.ps

[4] Our Fig 6.8 plot of the Equation of Time appears here in the Wikipedia Commons,

http://en.wikipedia.org/wiki/File:Zeitgleichung.png .

The web page also contains the actual code used to generate the plot. It gives two references, one of which is item [3] above. The other reference of Blatter is a dead link, but the "approximation by Blatter" referred to in the code is our equation (4.32). The code uses $\varphi_{\mathbf{per}} = 11.5^{\mathbf{0}}$ ($\alpha = 78.5^{\mathbf{o}}$) and $\theta_{\mathbf{tmax}} = 23.45^{\mathbf{o}}$ which were correct for year 1919.

[5] F.W.J. Olver *et. al*., *NIST Handbook of Mathematical Functions* (National Institute of Standards and Technology, Cambridge University Press, Cambridge, 2010). This excellent reference book is the follow-on to the famous 1964 "Abramowitz and Stegun" handbook.

[6] P. Lucht, *Rotating Frames of Reference* (http://user.xmission.com/~rimrock/ , 2012) . This paper uses names Frame S and S', basis vectors $\mathbf{e_n}$ and $\mathbf{e'_n}$, origin-connecting vector **b**, and other notations which have been utilized in the current paper. Its Appendix A has information on spherical coordinates.

[7] D. di Cicco, "Exposing the Analemma" (Sky and Telescope, June 1979, pp536-540).
D. di Cicco, "Photographing the Analemma" (Sky and Telescope, March 2000, pp135-140).
Dennis di Cicco apparently took the first-ever solar analemma strobe photo. His imaginary club of analemma photographers is slowly increasing its membership.

[8] V. Rumyantsev, http://vrum.chat.ru/Photo/Astro/analema.htm , analemma photo and details.

[9] A. Ayiomamitis, "The Solar Analemma", http://www.astrosurf.com/luxorion/analemma.htm . This is a long description of the analemma adventures of Mr. Ayiomamitis. His photos are displayed on another site, "Solar Image Gallery - Analemma", http://www.perseus.gr/Astro-Solar-Analemma.htm .

[10] NASA, "Determination of Earth's Orbital Parameters", as used in Section 1 and elsewhere.
http://aom.giss.nasa.gov/srorbpar.html . One can obtain actual numbers for e, $\theta_{\mathbf{tmax}}$, and $\varphi_{\mathbf{per}}$.

[11] NASA, "Time and Date of Vernal Equinox", gives times of solstices, equinoxes, perihelion and aphelion for the Earth, http://aom.giss.nasa.gov/srver4x3.html .